Spatio-Temporal Multi- Objective Optimization of Agricultural Best Management Practices

Uribe, N.

DOI
10.4233/uuid:7d0e8676-8323-448a-af4e-9fc6b01b775f

Publication date
2023

Document Version
Final published version

Citation (APA)
Uribe, N. (2023). *Spatio-Temporal Multi- Objective Optimization of Agricultural Best Management Practices*. [Dissertation (TU Delft), Delft University of Technology]. https://doi.org/10.4233/uuid:7d0e8676-8323-448a-af4e-9fc6b01b775f

Spatio-Temporal Multi-Objective Optimization of Agricultural Best Management Practices

Natalia Uribe Rivera

SPATIO-TEMPORAL MULTI-OBJECTIVE OPTIMIZATION OF AGRICULTURAL BEST MANAGEMENT PRACTICES

Natalia Uribe Rivera

Cover design

Marvin Stiefelhagen/ marvin@blish.design /BLISH

SPATIO-TEMPORAL MULTI-OBJECTIVE OPTIMIZATION OF AGRICULTURAL BEST MANAGEMENT PRACTICES

DISSERTATION

Submitted in fulfillment of the requirements of
the Board for Doctorates of Delft University of Technology
and
of the Academic Board of the IHE Delft
Institute for Water Education
for
the Degree of DOCTOR
to be defended in public on
Wednesday, 25 January 2023 at 17:30 hours
in Delft, the Netherlands

by

Natalia URIBE RIVERA

Master of Science in Environmental Science; Specialization
Environmental science and Technology,
IHE Delft Institute for Water Education, the Netherlands
born in Medellín, Colombia

This dissertation has been approved by the
promotor: Prof.dr. D.P. Solomatine and
copromotor: Dr. G.A. Corzo Perez

Composition of the doctoral committee:

Rector Magnificus TU Delft	Chairman
Rector IHE Delft	Vice-Chairman
Prof.dr. D.P. Solomatine	IHE Delft / TU Delft, promotor
Dr. G.A. Corzo Perez	IHE Delft, copromotor

Independent members:

Prof.dr.ir. R. Uijlenhoet	TU Delft
Prof.dr. J.G. Arnold	Agricultural Research Service (ARS), USA
Prof.dr.ir. N.C. van de Giesen	TU Delft
Prof.dr. C.A. Jones	Texas A&M University, USA
Prof.dr.ir. C. Zevenbergen	IHE Delft / TU Delft, reserve member

This research was conducted under the auspices of the Graduate School for Socio-Economic and Natural Sciences of the Environment (SENSE)

Published by IHE Delft Institute for Water Education
www.un-ihe.org
ISBN 978-90-73445-48-2

To my loving family,

To my beloved Jeffrey and Silvio

ACKNOWLEDGMENTS

I want to express my especial gratitude to my promotor, professor Dimitri Solomatine, I thank you for guiding me in the world of optimization, for your critical assessment, for always questioning me (sometimes it was not easy), and for encouraging me during the difficult times of my PhD research journey. Equally important, I want to thank my supervisor Dr. Gerald Corzo for his constant support and advice during my research work, and specially for knowing how to orient my work in such a way that still allowed me to be creative.

My external supervisor Dr. Marcela Quintero and Dr. Srinivasam played an important role in this dissertation and my professional experience. Dr. Marcela Quintero, from CIAT (International Center for Tropical Agriculture) who has been my mentor during my professional experience and encouraged and supporting me to take the challenge of getting enrolled in this hydroinformatics doctoral program. Her past contribution to my professional experience by preparing myself for multidisciplinary work has been indispensable for this work. Thank you, Marcela, for your constant support and for being a role model in my professional career. And, Dr. Srinivasan from Texas A&M university, you introduced me to the world of hydrological modeling and help me master this paradigm of modeling applied to the tropical mountain watersheds. Dr. Srini, you have always had the time within your busy schedule to answer my questions and publication issues. I appreciate your continued support. I thank you both for the advice and support throughout the research period. Equally important, I want to express my sincere gratitude to Dr. Ann van Griensven for her support and directed me in the right path.

The PhD research was made possible by the financial support from the Dutch Organization for internationalization in Education - Nuffic; and Colciencias, Colombia scholarships. I would like to thank University of Antioquia for providing data on the case study and collaboration during the fieldwork and farmers interviews.

I want to thank my new friends, who are part of this valuable and beautiful experience of studying abroad. You made this journey a life experience and not just an academic one: Neiler (parcero), Juanca, Andre (mi guapo), Saffa, Yared, Juli, Pato, Alida, Mauri, Jessica, Pin, Miguel, Vero. Furthemore, special thanks to an amazing designer Marvin Stiefelhagen, who is one of my best Dutch friend and unconditional support.

To my friends “los feitos” in Colombia: Ori, Xime, Jeff, Salo, and Marthis. Feitos, thank you, your messages always made me smile, you can't imagine how important they were in those cold days with low energy. Despite the fact that we are in different places, our friendship always remains, and I hope that it always will. I love you so much!

Also, to a great group of friends “Amigos” Berend, Mohaned, Fer, Peter, Angi and Can thank you for all the beautiful moments shared, for the advice, support, the super parties

that helped to enjoy life, for the interesting talks, and trips made. I love you and may they be many more years of friendship.

Angi and Fer, I have no words to thank you for all the support and love that you have given me at this stage of my life. You are two beautiful women and to be admired. Countless are the beautiful moments that we have lived and which I hope will continue to increase. Thank you for supporting me during my pregnancy and motherhood, without my family by my side, your love and support were crucial. I love you chicas.

To my family, my especial gratitude for your love, encouragement, and support through all my life. A mis padres (Carmen Alicia y Jorge Ivan) quiero darles las gracias por todo el amor que me han brindado, por creer en mi y apoyarme en cada uno de mis proyectos de vida, los amo. My siblings (Enver and Hilda), I thank you for your love and unconditional support. Your presence in my life and even more being at a distance have been vital to achieve this achievement, los amo y admiro mucho mis hermanos. My Teo, my nephew whom I love, thank you for filling me with motivating energy every time I could have my days off. I am grateful to my in-laws, especially Chris, who reminds me that with dedication and the best attitude everything can be achieved. And my primis (Xiomy and Jenni), thanks my “feitas” for always accompanying me in the distance, for the love and support. I admire and love you very much.

Jeffrey, my life partner. Always by my side, supporting me and motivating me to finish. Thank you for your advice, your unconditional love, for allowing me to know other cultures, for all the adventures, and for exploring the world together. And even more thank you because we have built our family with our beloved baby Silvio. This achievement is also yours. Te amo.

SUMMARY

Farmers around the world are facing the need to improve crop yield due to substantial increase in food demand. However, in an effort to meet the global growing food demand, nutrient pollutants in runoff have also increased due to intensified agricultural practices. For this reason, stakeholders and decision-makers have tried to shift from conventional agricultural practices to other types of practices, commonly referred to as best management practices (BMPs). The emphasis of agricultural BMPs (Ag-BMPs) is on environmental protection, which in this research is extended to consider food production, as well as environmental, economic, and social factors as a part of Ag-BMPs.

The selection and allocation of agricultural BMPs at a watershed scale, in practice, is very complex. It is currently acknowledged that in order to design optimal agricultural BMPs scenarios at watershed scale, the problem has to be formulated as a multi-objective optimization problem, which involves conflicting objectives and constraints (Memmah, Lescourret, Yao, & Lavigne, 2015). Despite the increase in the use of optimization to select and allocate agricultural BMPs, research in this area has limitations due to the high number of parameters and high uncertainty inherent to building large models. There are several important gaps related to this topic that have been identified: 1) upscaling process scale (small to large) implementation; 2) inclusion of temporal and dynamic spatial aspects; 3) inclusion of decision-makers' and stakeholders' knowledge to select which BMPs will be optimized. Therefore, there is still a great need to explore various optimization approaches for different types of agricultural optimization problems. The watersheds located in the mountains of the tropical Andes are characterized by shifting cultivation, intensive traditional agriculture, and weather seasonality, and this makes the problem of choosing optimal BMPs especially complex.

The main objective of this dissertation is to develop a modeling framework and methodology to build a spatio-temporal multi-objective optimization model that provides new insights to improve the selection and allocation of agricultural BMPs in a watershed of the Tropical Andes Mountains. This research has the following objectives:

O1. Analyze and determine the impacts on nutrient loss and crop yield from a single agricultural BMP (Ag-BMP) applied to a single crop at the field scale, and upscale its impact assessment to a watershed level.
O2. Analyze variations of spatio-temporal impacts on nutrient loss and crop yield from multiple agricultural management practices (Ag-MP) and determine spatio-temporal critical source areas (ST-CSAs) in the watershed.
O3. Select and parameterize Ag-BMPs scenarios to be used in the optimization model framework that are feasible to implement by stakeholders (local farmers).
O4. Develop a framework and methodology for a spatio-temporal multi-objective optimization model to select and allocate Ag-BMPs for multiple crops.

To achieve these objectives, a methodological approach based on gradually increasing the complexity of the system to be optimized was used. For the first objective (**O1**), we consider the conceptual modeling outline of Ag-BMPs applied in a single crop (potato crop) in the Fuquene watershed. A hydrological model to estimate runoff pollutants and crop yield was built. The model was calibrated with fieldwork data collected from runoff plots installed in the study watershed with current agricultural practices used by farmers. The results revealed that **Ag-BMP impacts obtained at watershed level show important differences from those obtained at farm level**. In the study region, it was found that the Conservation Tillage BMP (CT-BMP) in some areas (farm level) reduces a nitrate (NO_3^--N) losses, however at the watershed level there is a total increase in NO_3^- N loss. Therefore, a detailed spatio-temporal nutrient loss analysis and the application of optimization techniques to determine optimal Ag-BMPs at both farm and watershed levels is suggested.

For the second objective (**O2**), an analysis of the spatial and temporal dynamics of nutrients in runoff resulting from current multiple Ag-BMPs was done. A spatio-temporal critical sources area (ST-CSAs) index was proposed to select the spatial location where the highest pollutant loads occur within the watershed. **The ST-CSAs is a new approach that we propose to select the search space for the optimization problem to achieve a more effective Ag-BMPs** allocation, providing a visual representation of the recurrence and behavior in space and time of the CSAs for an entire simulated period. The results showed that ST-CSAs characteristics and pattern determination are highly relevant to define which and where Ag-BMPs should be implemented.

For a feasible Ag-BMPs scenarios selection and parameterization in the case study region (**O3**), workshops and interviews with local farmers and stakeholders were held. For a realistic and feasible optimization process, farmer and local agricultural information is required. This work aimed at collecting data directly from field plots, whereby the BMP scenarios to be included in the optimization model were selected because they were agricultural practices that did not increase implementation costs, could be implemented by farmers with tools and financial resources they currently had, and were accepted and some proposed by the farmers themselves.

Finally, the modeling framework was developed (**O4**). The optimization framework proposed provides a methodology that allows incorporating a greater number of crops and Ag-BMPs scenarios in the optimization model; as well as contemplating the space and time variations to allocate the optimized Ag-BMPs. The SWAT hydrological model was coupled with the multi-objective optimization algorithm (NSGA-II). Minimization of nitrate (NO_3^-N) losses and maximization crop yields at field level were the objective functions. Pareto-front comparison results between average versus single site (field) values for each objective function were carried out to determine spatial analysis level results to select optimal Ag-BMPs. The main result is an easy-to-follow step-by-step methodology, which can be implemented in any watershed. Additionally, the methodological steps to spatially analyze of the optimization results were provided. The

spatial analysis allows the researcher to define a spatially distributed Pareto-front solution. This means having a Pareto-front solution for each of the different areas with similar spatial variability of the optimization results for each evaluated scenario.

The proposed modeling framework and methodology, results and suggested optimal Ag-BMPs are available for farmers located in the mountains of the Colombian Andes (Latin America), but it is general enough to also be used worldwide after adaptation to local crop conditions. We expect the methodology framework to be accessible and affordable in poorer regions of the world, and it can be a complementary policy instrument for controlling non-point source water pollutants. The proposed framework and methodology can be further improved by contemplating climate change scenarios and analyzing implementation costs of the optimized Ag-BMPs.

SAMENVATTING

Agrariërs wereldwijd staan door de substantiële toename in vraag naar voedsel voor de uitdaging om hun oogstopbrengst te verbeteren. Echter, met het verwezenlijken van dit doel is door de verhoogde agrarische activiteit ook de vervuiling van afvloeiing door voedingsstoffen toegenomen. Om die reden hebben stakeholders en beleidsmakers getracht om te veranderen van conventionele agrarische practices naar andere practices, ook wel bekend onder de term best management practices (BMP). The nadruk van agrarische BMP's (Ag-BMPs) ligt op natuurbescherming; echter, dit onderzoek gaat ook verder en neemt voedselproductie, milieu en socio-economische factoren mee als onderdeel van de Ag-BMPs.

The selectie en toewijzing van agrarische BMP's op stroomgebiedniveau, in de praktijk, is erg complex. Het wordt tegenwoordig erkend dat het ontwerpen en alloceren van optimale agrarische BMP's op stroomgebiedniveau vereist dat het probleem wordt omschreven als een multi-objective optimalisatieprobleem met conflicterende doelen en restricties (Memmah, Lescourret, Yao, & Lavigne, 2015). Ondanks de vooruitgang in benaderingen vanuit optimalisatie om Ag-BMPs te selecteren en te te wijzen, is onderzoek op dit gebied gelimiteerd door het grote aantal parameters en de hoge mate van onzekerheid die inherent is aan omvangrijke modellen. Meerdere significante kloven gerelateerd aan dit onderwerp zijn geïdentificeerd: 1) opschaling van processchalen, van kleinschalig tot grootschalige toepassingen; 2) de toevoeging van temporele en dynamisch-ruimtelijke aspecten; 3) het toevoegen van de kennis van beleidsmakers en stakeholders tijdens BMP-selectie voor optimalisatie. Om deze redenen bestaat er nog steeds de behoefte om verschillende optimalisatieaanpakken te verkennen voor verschillende soorten agrarische optimalisatieproblemen. Dit is voornamelijk het geval in stroomgebieden gelegen in het tropische Andesgebergte, waar verschuivende verbouwing, intensieve traditionele landbouw en de seizoensgebondenheid van het weer predominant zijn.

Het hoofddoel van dit afstudeeronderzoek is het ontwikkelen van een modeleer-raamwerk en methodiek om tijdruimtelijke multi-objective optimalisatiemodellen te ontwikkelen die nieuwe inzichten bieden om de selectie en toewijzing van Ag-BMPs te verbeteren in een stroomgebied van het tropische Andesgebergte. Dit onderzoek heeft de volgende doelen:

O1. Analyse en vaststelling van de impact van een enkele Ag-BMP op voedingsstoffenverlies en oogstopbrengst en de opschaling van deze impact naar een stroomgebied.
O2. Analyse van variaties van tijdruimtelijke invloeden in op voedingsstoffenverlies en oogstopbrengst van meervoudige agrarische management practices (Ag-MP),

en het vaststellen van tijdruimtelijke kritieke brongebieden (ST-CSAs) in een stroomgebied).

O3. Selectie en parametrisering van Ag-BMP scenario's voor gebruik in een optimalisatiemodelraamwerk, welke toegepast kunnen worden door lokale boeren.

O4. Ontwikkeling van een raamwerk en methodologie voor een tijdruimtelijke multi-objective optimalisatiemodel voor de selectie en toewijzing van Ag-BMPs for meerdere gewassen.

Een methodologische aanpak gebaseerd op toenemende complexiteit van het te optimaliseren systeem is gebruikt voor deze doelen. Voor het eerste doel (O1) lichten we het conceptuele modeleer-overzicht van Ag-BMPs toegepast in een enkel gewas (aardappelgewas) in het Fuquene stroomgebied. Een hydrologisch model is ontwikkeld om vervuiling van afvloeiing en oogstopbrengst in te schatten. Het model is gekalibreerd met veldwerkdata verzameld van afvloeiingsvelden in het stroomgebied en met de huidige agrarische practices die gebruikt worden door de landbouwers. De resultaten laten zien dat de Ag-BMP invloeden op stroomgebiedniveau essentieel verschillen van de invloed op boerderijniveau. In het onderzochte gebied is bevonden dat de Conservation Tillage BMP (CT-BMP) in sommige regio's (op boerderijniveau) een nitraat (NO3--N) reductie oplevert; echter op stroomgebiedniveau is een totale toename van NO3--N geconstateerd. Om die reden zijn een gedetailleerde tijdruimtelijke analyse van de voedingsstoffenafname en de toepassing van optimalisatietechnieken vereist om de optimale Ag-BMPs op boerderij- en stroomgebiedniveau te bepalen.

Voor het tweede onderzoeksdoel (O2) is een analyse gedaan naar de ruimtelijke en temporele dynamica van voedingsstoffen in afvloeiing ten gevolge de meerdere huidige Ag-BMPs. Een tijdruimtelijke kritieke brongebieden (STA-CSAs) index is voorgesteld om een ruimtelijke locatie te selecteren waar de hoogste vervuilingsniveaus binnen een stroomgebied aanwezig zijn. De ST-CSAs zijn een nieuwe benadering die wordt voorgesteld voor het zoekgebied van het optimalisatieprobleem om effectiever Ag-BMP toe te wijzen, en om een visuele representatie van de differentie en het gedrag in ruimte en tijd van de CSAs voor een gehele simulatieperiode te bieden. Het resultaat laat zien dat ST-CSAs karakteristieken en patroonbepaling relevant zijn om waar er welke Ag-BMPs toegepast moeten worden.

Voor een haalbare Ag-BMPs scenarioselectie en parametrisering in het onderzoeksgebied (O3), zijn workshops en interviews georganiseerd met lokale landbouwers en stakeholders. Voor een realistisch en haalbaar optimalisatieproces zijn landbouwers en lokale agrarische informatie benodigd. Het veldwerk had als doel om direct data van de landbouwvelden te verzamelen om de BMPs scenario's te selecteren die niet resulteren in operationele kosten. Hiermee kunnen scenario's haalbaar zijn met de huidige middelen van de landbouwers.

Ten slotte is het modeleerraamwerk ontwikkeld (O4). Het voorgestelde optimalisatieraamwerk biedt een methodiek die een significant groter aantal gewassen en Ag-BMPs toestaat in het optimalisatiemodel, en die ruimte- en tijdsvariaties samenvoegt

om de geoptimaliseerde Ag-BMPs toe te wijzen. Een aantal basismodellen tussen het SWAT hydrologisch model en het metaheuristische algoritme NSGA-II zijn gebruikt als optimalisatiemotor. De doelfuncties minimaliseerden nitraat (NO3-N) en maximaliseerden oogstopbrengsten op veldniveau. Een Pareto-front vergelijking tussen de gemiddelde versus de enkele veldwaarden voor iedere doelfunctie zijn uitgevoerd om de ruimtelijke analyseniveaus te bepalen, waarmee de optimale Ag-BMPs geselecteerd kunnen worden. Het resultaat is een eenvoudig te volgen stappenplan methodiek, welke in ieder stroomgebied toegepast kan worden.

Tevens zijn de methodologische stappen beschikbaar gesteld, waarmee de optimalisatieresultaten ruimtelijk geanalyseerd kunnen worden. Daarnaast bevelen de optimalisatieresultaten van de ruimtelijke analyse, uitgevoerd in het onderzoeksgebied, dat een Pareto-front oplossing gedefinieerd dient te worden op een verdeelde manier. Dit betekent dat een Pareto-front oplossing benodigd is, voor ieder van de verschillende gebieden met vergelijkbare ruimtelijke variabiliteit van de optimalisatieresultaten, voor ieder geëvalueerd scenario.

Het voorgestelde modeleerraamwerk en methodologie, de resultaten, en de aanbevolen optimale Ag-BMPs zijn beschikbaar voor de landbouwers in de bergen van de Colombiaanse Andes (te Latijns- Amerika). Echter kunnen deze ook wereldwijd gebruikt worden na aanpassing aan condities van andere gewassen. We verwachten dat het methodologieraamwerk beschikbaar en bereikbaar is in armere gebieden van de wereld. Het kan dienen als complementair beleidsinstrument om non-point bronwatervervuiling te regelen. Echter wordt ook benadrukt dat het voorgestelde raamwerk verbeterd kan worden door klimaatveranderingsscenario’s te raadplegen en door de implementatiekosten van de geoptimaliseerde Ag-BMPs te analyseren.

CONTENTS

1

INTRODUCTION

1.1 MOTIVATION

According to the IPCC 2016 report, an increase in heavy precipitation events could increase the frequency of storm run-off pollution due to changing climatic conditions. This phenomenon tends to be more significant in agricultural systems, considered significant sources of environmental pollution worldwide (Sarkar et al., 2006). Usually, the storm run-off pollution process is more significant in watersheds characterized by intensive traditional agriculture because of the large amounts of fertilizer applied to crops grown on steep slopes. Climate change along the latitudinal gradient can also result in environmental pollution and some loss of biodiversity. Some of the identified causes of this phenomenon include shallow soils with little vegetation, which are susceptible to large precipitation events (Sedano et al., 2013). Thus, there has been a significant increase in the development of watershed plans and actions to help mitigate the effects of agricultural activities on runoff pollution processes. One of the most recommended alternatives includes shifting from conventional agricultural practices to other types of practices, typically termed the agricultural Best Management Practices (BMPs) (Ritter and Shirmohammadi, 2001). Agricultural BMPs aim to meet the projected food demand, reduce environmental pollution, and preserve biodiversity. However, the selection and allocation of agricultural BMPs at a watershed scale is very complex.

It is currently recognized that to design agricultural BMP scenarios for the adoption and promotion at the watershed scale is a multi-objective optimization problem, which involves multiple conflicting objectives and constraints (Memmah et al., 2015). However, agricultural BMP optimization is a very complicated task, involving decision-makers and stakeholders, multiple conflict objectives, temporal and dynamic spatial aspects, and constraints (Liu et al., 2013). Despite the increased use of the optimization approach to select and allocate agricultural BMPs, there are still many gaps in our understanding of this topic. Memmah, Lescourret, Yao, & Lavigne (2015) highlight the most common issues identified to date: (i) defining which optimization algorithm for which problem, (ii) adapting computational techniques that can handle an increasing number of decision variables and dynamics (e.g., hybridization), and (iii) integrating the knowledge of decision-makers and stakeholders into the optimization methods. Therefore, this research area needs to explore how to pose a mathematical optimization problem that is not always trivial due to every problem and case study's particular local features. Also, it is important to explore different optimization approaches for different types of agricultural optimization problems, especially in the watersheds where the complexity of shifting cultivation, intensive traditional agriculture, diverse crops and management practices in a landscape, and weather seasonality are predominant.

1.2 AGRICULTURAL BEST MANAGEMENT PRACTICES (AG-BMP) OPTIMIZATION APPROACHES

1.2.1 Multi-objective optimization of agricultural best management practices

The optimization approach is considered necessary for model-based agricultural BMP's selection and allocation at the watershed level. In the following, we present some examples of studies dealing with agricultural BMPs optimization issues for water management purposes. These studies (described below) considered economic aspects, reducing non-point pollution sources, and some social elements. Table 1.1 presents a brief description of these.

Maringanti, Chaubey, & Popp (2009) investigated an optimization methodology to select and place BMPs in the L'Anguille River watershed located in the Mississippi Delta region. They set 54 different combinations of BMPs for rice and soybean, which are the two crops that predominate in the watershed. This novel approach includes a BMP tool as the best way to link a hydrological model and spatial dynamics of BMPs to be evaluated in the optimization architecture. The model developed a genetic algorithm NSGA-II based multi-objective optimization tool to minimize pollutant (phosphorus, nitrogen, and Sediments) loading and reduce net costs. The results indicated that the optimized BMPs selected and allocated could decrease N, P, and sediments losses by 13%, 32%, and 33%, respectively, from the watershed. Additionally, the highlighted drawbacks in this research were mainly: (i) both objective functions were considered separately by the optimization algorithm, and (ii) the BMPs implementation costs were estimated with a fixed interest rate.

Lehmann, Finger, Klein, Calanca, & Walter (2013) investigated the optimal field BMPs in winter wheat and grain maize crops in two watersheds in Switzerland (Payerne, located in the Western Uster, situated in the Northeast) for two climate change scenarios. The authors developed a bio-economic modeling system coupled with the CropSyst crop growth model and an economic decision model, generating a genetic algorithm to define the optimal field BMPs (schemes for irrigation strategy and nitrogen fertilization) that maximize the farmer's profit margins. The authors argue that 'the computational load was considerable' and could be improved by relaxing the convergence criteria or modifying the Genetic Algorithm (GA) parameter settings.

In order to decrease computing time, parallel computation techniques can be used, as was done in the study "Optimization of Agricultural BMPs Using a Parallel Computing Based Multi-Objective Optimization Algorithm" by Liu, Shen, Yang, & Yang (2013). This research coupled a SWAT model with the ε-NSGA-II multi-objective genetic algorithm to select optimal BMPs for reducing agricultural non-point source pollution. This research considered minimizing total phosphorus load and BMPs implementation costs in the Fairchild Creek watershed in Ontario, Canada. The computational time was

effectively reduced by using 30 processors. The authors mention that the performances are dependent on the number of processers, simulation period, spatial resolution, and several objective functions. On the other hand, this research assessed the uncertainties obtained from the optimization results and suggested that additional studies are needed to improve the spatio-temporal BMPs characterization and BMPs cost estimation to get more reliable optimization results.

Studies focused on achieving better BMP characterization by modifying details on how each BMP is simulated in a SWAT model. One example of this research is the study of Panagopoulos, Makropoulos, & Mimikou (2013). This research integrated a decision support tool (DST) with a SWAT model and a multi-objective evolutionary algorithm to define the selection and locations of agricultural BMPs combinations that ensure good environmental and economic outcomes. The objective functions were formulated to minimize total phosphorus (TP) and nitrate N (NO_3^-N) losses and minimize implementation costs (such as nutrients application, soil, and livestock management). The authors applied their approach in the Arachtos catchment in western Greece with 51 potential agricultural BMPs for corn, alfalfa, and pastureland. The methodology proposed provided a fertilizer application scheme applied to other watersheds with similar agricultural land use at a field scale.

Yet another study, by Babbar-Sebens, Mukhopadhyay, Singh, & Piemonti (2015), did not consider a detailed level of BMPs characterization. It provided only a summary of how the decision variables can be mapped into the model's inputs. Nevertheless, this research focused on incorporating the stakeholder's participation in the simulation-optimization of the BMPs in watersheds. A web-based software tool Watershed REstoration using Spatio-Temporal Optimization of Resources (WRESTORE), was developed based on the Interactive Genetic Algorithm Mixed-Initiative Interaction (IGAMII) coupled with SWAT model. The authors emphasized the importance of IGAMII because this is a novel approach that learned about the problem from human expert feedback to adjust the optimization search process and provided alternative BMPs in the watershed.

There are other examples of research in this field that address the selection and allocation of BMPs in a watershed to minimize the negative impacts of agriculture on reservoirs. A study conducted in the Aharchai river watershed of Iran developed an optimal model for selection and placement of BMPs at minimum cost by linking a coupled watershed-reservoir model (SWAT-SD) with a genetic algorithm at watershed scale (Karamouz et al., 2010). As its primary objective, the model sought to improve reservoir water quality (reduced phosphorous concentration) by applying structural BMPs for non-point sources, e.g., parallel terraces, grade stabilization structures, and permanent pools. The results obtained in this research show that terraces were the most cost-effective BMP option applied in the sub-basins of the watershed. However, they suggest using a probabilistic function to constrain the optimization problem defined for this case study, which could further consider the uncertainties in the solution selected. On the other hand,

other research has shown the importance of investigating the relations between farmers' land tenure security and agriculture production (Singirankabo et al., 2022) and how landowner tenure and attitudes of farming communities can modify the effectiveness of BMP alternatives (Piemonti et al., 2013).

Table 1.1. Summary of the six representative examples of optimizing agricultural BMPs

Reference	Study objectives	Criteria	Method	Level analysis
Lehmann et al. (2013) Case study: Switzerland	Optimal field management practices (schemes) for two climate change scenarios on wheat and maize production	Maximize: 1.Farmer's profit margins 2.Crop yield	Coupled: CropSyst model and Evolutionary algorithm Decision variables: Fertilization (Nitrogen) Irrigation strategy	-Field level (HRU) -Bioeconomic modeling
Liu et al. (2013b) Case study: Canada	Selection of BMPs for reducing agricultural non-point source pollution	Minimize: 1. BMPs costs 2.Total phosphorous	Coupled: ε-NSGA-II (ε dominance archive) and SWAT model Decision variable: Management scheme Fertilization (N and P)	-Field level (151 HRUs) -Slope less 5% -3 BMPs evaluated -Monthly analysis
Panagopoulos et al. (2013) Case study: Grece	Optimal selection and allocation of BMPs on pasture, corn, and alfalfa	Minimize: 1. Total phosphorus 2. Nitrate 3. Implementation cost	Coupled: SWAT model and a DST Decision variables: -Fertilizer timing/reduction -Application scheme	-Field level (259 HRUs) -51 BMPs evaluated -Annual analysis
Rabotyagov et al. (2012) Case study: U.S.A.	An approach for selecting basin configurations, achieving trade-off between costs of BMPs	Minimize: 1. Implementation cost 2. Nutrient's load (N - P)	Coupled: Strength Pareto Evolutionary Algorithm (SPEA2) and SWAT2005GA Decision variables: -Nutrient target reduction	-Subbasin level -23 BMPs evaluated
Babbar-sebens et al. (2015) Case study: U.S.A.	A web-based software tool for participatory optimization of CT	Minimize: 1. Cost-revenue 2. Peak flow 3. Sediments 4. Nitrates	Coupled: -Interactive Genetic Algorithm with Mixed Initiative Interaction (IGAMII) -SWAT model	Subbasin level

1.2.2 Decision-making for agricultural BMPs optimization

One of the objectives of defining optimal BMPs solutions is to be able to support the stakeholders and decision makers in making decisions on watershed management. 'Decision Support Systems' (DSS) is the term used to denote the tools supporting such decisions. Commonly, these systems integrate optimization models, dynamic simulation models, databases and visualization interfaces (Price & Vojinovic, 2011; Pryke, Mostaghim, & Nazemi, 2007; Mendoza, G., Jeuken, A., Matthews, J. H., Stakhiv, E., Kucharski, J., & Gilroy, K., 2018)

One of the recent examples of a DSS for agricultural BMPs at watershed scale is the web-based, interactive optimization tool WRESTORE (Babbar-Sebens et al., 2015). This tool provides stakeholders' with a participatory environment to select the BMPs of their choice within the seven BMPs options available (No-till tillage practice, Strip Cropping, Cover crops, Crop Rotation, Grassed Waterways, Filter Strips, and Wetlands), which can be applied in their sub-basins and throughout the entire watershed. The tool uses the hydrological SWAT model to test the effectiveness of the BMPs, and a meta-heuristic optimization technique to define and allocate the most cost-effective BMP option from the BMPs selected by the users. However, the underlying code and architecture of WRESTORE can be adapted for any other simulation model and other variables.

Nonetheless, most of the examples of decision-making methods for agricultural BMP definition and allocation found in the literature were used independently of the optimization process. Seppelt, Lautenbach, & Volk. (2013) argue that to offer valuable results for stakeholders at the watershed scale, scenario analyses across different scales combined with optimization algorithms, including Pareto-frontiers, will provide efficient and optimal options. This framework allows decision-makers to adjust the criteria weights for each optimization round and adjust these for the next round.

Janssen, van Herwijnen, Stewart, & Aerts (2008) present a heuristic algorithm that allows decision-makers to participate in an interactive session, with the objective of obtaining feedback from decision makers to adjust and generate the land use planning program. Output maps and tables are used as the main interface between stakeholder and algorithm, which is considered an important part of the interactive validation process.

Likewise, Xiao, Bennett, & Armstrong. (2007) present a review of the visual support system for multi-objective spatial decision-making. This review includes a unified conceptual framework which also offers some interactive visual support system alternatives for plotting the near-optimal solutions obtained with evolutionary algorithms. Decision makers can examine and select alternatives that they feel to be more appropriate, using visual tools such as: scatterplot matrix, maps of current and previously viewed alternatives, and parallel coordinate plots (Xiao et al., 2007).

Rabotyagov et al., (2012) developed a support tool which assists users to set the BMPs practices and their implementation costs. This tool integrates the SWAT model with the SPEA2 evolutionary algorithm, and according to the water quality goals to be achieved, it allows the user to define the watershed configuration. It also offers maps with the location of optimal BMPs at the sub-basin level, which is an interesting piece of information to be shared with the decision makers.

The Agricultural Policy/Environmental eXtender (APEX; Williams and Izaurralde, 2006) model helps the user configure BMPs to assess the impact on run-off and water quality in whole farm/small watershed management. Users can consider a group of various structural and non-structural BMPs applicable for heterogeneous farms. In addition, this model includes cost and income accounting and carbon cycling routines. Users can select among three model interfaces, WinAPEX, ArcApex, and iAPEX according to personal preferences. However, the model does not evaluate optimal solutions, and, as a consequence, the users have to define the best option according to the results obtained for each BMPs scenario simulated (Tuppad et al., 2010).

1.3 RESEARCH GAPS IN AG-BMP OPTIMIZATION

The Ag-BPMs optimization research literature review above (numeral 1.2), identified research gaps that this research addresses. These gaps can be divided into two main categories: i) level of the description system and ii) multi-objective optimization techniques.

Regarding methodological studies for different types of agricultural optimization problems, some potentially useful ideas still need in-depth studies to produce a more realistic approach, especially for watersheds located in tropical mountainous regions, where shifting cultivation and intensive traditional agriculture predominate. Therefore, new studies in different areas can contribute to this end by defining characteristics of the problem, which could guide the choice of a suitable optimization approach for a given problem. Besides, adopting certain computational facilities to handle the spatial and temporal dynamics, as well as the large number of decision variables, must be improved.

As discussed above (numeral 1.2.2), one of the main objectives of multi-objective optimization techniques for agricultural BMPs is to offer the stakeholders and decision-makers one or more solutions to solve the problems that concern them. After exploring several decision support systems (DSS), I have concluded that no single methodology or tool that can help all these actors find the best trade-off. However, it is still necessary to consider the importance of including stakeholder participation when designing an optimization strategy. New DSS approaches based on stakeholders/decision-makers reference points and goals can be useful in exploring and improving research methods.

1.4 RESEARCH OBJECTIVES

The general objective of this dissertation is *to develop a modeling framework and methodology to build a spatio-temporal multi-objective optimization model that provides new insights to select and allocate agricultural BMPs in* a *watershed in the tropical Andes mountains*.

To realize this aim, we formulate the following specific objectives:

O1. Analyze and determine the impacts on nutrient losses and crop yield from a single agricultural BMP (Ag-BMP) applied to a single crop at field and watershed level.
O2. Analyze variations of spatio-temporal impacts on nutrient losses and crop yield from multiple agricultural management practices (Ag-MP) to determine spatio-temporal critical source areas (ST-CSAs) in the watershed.
O3. Select and parameterize Ag-BMPs scenarios to be used in the optimization model framework, which are feasible to implement by the local farmers.
O4. Develop a framework and methodology for a spatio-temporal multi-objective optimization model to select and allocate Ag-BMPs for multiple crops.

1.5 RESEARCH QUESTIONS

Based on the research objectives, we formulate the following research questions:

i. What is the impact on nutrient losses and crop yield of a single Ag-BMP applied to a single crop from the field level to the watershed level?
ii. How can we incorporate the spatial and temporal dynamics of the nutrient losses in the runoff to select optimal Ag-BMPs?
iii. How can the agricultural management practices information obtained from the farmers be translated into mathematical representation of modelling variables, constraints and objective functions?
iv. How relevant is it to contemplate temporal and spatial variables in the Ag-BMPs optimization model?

1.6 SCIENTIFIC CONTRIBUTION

Methodology. This research contributes to agricultural BMPs optimization approach by providing a c*oncrete application* of a *spatio-temporal multi-objective optimization framework* for selecting and allocating agricultural BMPs feasible in a *watershed of the Tropical Andes Mountains*. This will be one of the first examples of an in-depth study which will cover the high level of *complexity of shifting cultivation* and *intensive traditional agriculture* presents in this type of watershed and will formulate and solve the corresponding mathematical optimization problem.

Decision-making. This research also contributes with a new approach to promote result based agricultural BMPs as a *complementary policy instrument* for control of *non-point source water pollutants in Colombia*. Likewise, it could be an *assistance tool* for the *local communities* (farmers), which can be used to *adapt the agricultural practices* to cope with unexpected changes that have occurred in recent years.

1.7 OUTLINE

Given the research motivation, questions, objectives, and research approach already presented, this dissertation has been structured in eight chapters (Figure 1.1). The next seven chapters are structured as follows:

Chapter 2 presents the theoretical background of the research and the general methodology description. The chapter defines and explains the three main components of the coupled optimization modeling framework: agricultural BMPs (Ag-BMPs) types, hydrological modeling, and metaheuristic algorithms. Chapter 2, then, explains Ag-BMPs concepts and types of description. It also introduces what hydrological model we used to estimate the runoff nutrient losses and crop yields. And the chapter describes the metaheuristics for optimization problems; and the optimization algorithm description we use. Finally, A general description of the methodology used is presented. In this way the reader will be able to know from the beginning of the thesis the main methodological phases applied to fulfill the objectives of the research.

Chapter 3 contains the description of the study areas. Fuquene and Riogrande II watersheds located in the Colombian Andes, were the two case studies selected for the development of the research. Chapter 3 describes the catchment, climate, land-use, soils, and socio-economic and environmental conditions.

Chapter 4 investigates and analyzes a single Ag-BMP (conservation tillage - CT), and its effects on runoff nutrient losses and crop yield for a single crop (potato-based mixed crop system) at both field and watershed levels. It includes the fieldwork methodological design to collect data of the current agricultural practices (intensive tillage - IT) and experimental runoff plots in the potato crop. And it presents a step-by-step the methodology implemented for the hydrological modeling of the baseline and CT-BMP scenarios.

Chapter 5 presents spatio-temporal analyses of multiple agricultural management practices impacts. Chapter 5 describes the ST-CSAs (spatio-temporal critical sources areas) index for selecting the search space for implementation of the optimization model. And the spatio-temporal runoff nutrient losses in the defined areas are analyzed. It includes the fieldwork methodological design to collect data on the current agricultural practices for the cultivation of potato, tree tomato and kikuyu grass. Finally, the search space to be used in the next general methodology phase corresponding to the implementation of the optimization model is presented.

Chapter 6 describes the proposed spatio-temporal multi-objective optimization modeling framework to select and allocate agricultural BMPs for multiple crops. It provides descriptions of the components of the framework and how they are connected. In this chapter, the selection and parametrization of the Ag-BMPs scenarios to be used in the optimization model are presented. The multi-objective mathematical optimization formulation and parametrization of the Ag-BMPs scenarios are described. It also discusses the insights gained into the Ag-BMP optimization approach by explicitly modeling the spatio-temporal interactions using ST-CSAs to define the optimization search space. Finally, Pareto-front comparison results between the average vs. single sites (HRUs) values for each objective function are presented to select the optimal BMPs.

Finally, **chapter 7** summarizes the results and conclusions of the preceding chapters. This chapter closes with the outlook of the research, recommendations about future research needs and limitations.

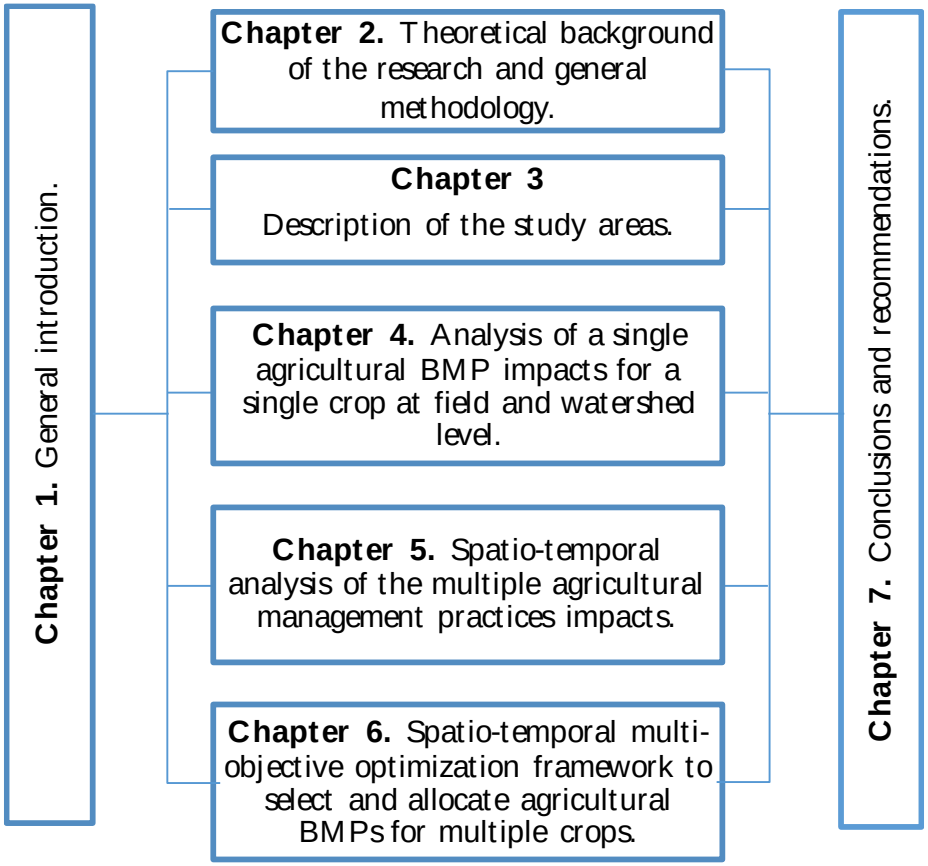

Figure 1.1. Overview of dissertation structure and connections between the chapters.

2

THEORETICAL BACKGROUND AND GENERAL METHODOLOGY

2.1 INTRODUCTION

The goal of this chapter is to present definitions, methods and modeling approaches that will be used in this research. This chapter first presents an overall definition of agricultural best management practices (Ag-BMPs) categories and a brief description of the Ag-BMPs that we will be considering in this research. Second, we explain the two main components (hydrological model and metaheuristic optimization algorithms) of the optimization modeling approach to be used. Particularly, we describe the hydrological model to be used to estimate the pollutants in the runoff water from each of the Ag-BMPs scenarios; and the metaheuristics options (optimization algorithms), especially those that have been implemented for Ag-BMP optimization. Finally, a brief description of the general methodology used to develop the framework is presented. The methodological phases are described, which are developed and presented in the subsequent chapters of the dissertation. Overall, the purpose of this chapter is to provide a brief review of all the concepts mentioned above.

2.2 AGRICULTURAL BEST MANAGEMENT PRACTICES (AG-BMPS)

There is no universal definition available for agricultural BMPs. Today, the emphasis of agricultural BMPs is more focused on environmental protection. For example, Ritter & Shirmohammadi defined agricultural BMPs as a practice or combination of techniques used to minimize or prevent non-point source pollution resulting from agricultural activities (Ritter and Shirmohammadi, 2001). However, the overall philosophy is to identify management techniques to keep pollutants out of the water, be economically feasible to implement for farmers, and offer an optimum production scenario for a specific cropping system and location (Roberts, 2007).

In this research, we felt it necessary to have our own BMPs definition, which considers environmental, economic, and social factors defined in the optimization model. Therefore, the word ‘agricultural BMPs’ is defined by us as a practice or combination of techniques used to protect water quality, prevent soil degradation, reduce soil erosion, and enhance the farm's productive level and the farmer's social well-being.

There are two practice types of BMPs: (i) In-field management practices, which are designed to prevent contaminants from getting into the water in the first place, and (ii) structural BMPs, which include relatively permanent land-shaping or constructed practices. Logan (1990) presented a classification of the agricultural BMPs according to the type, environmental objective, pollutants, and medium impacted (Logan, 1993). Table 2.1 presents the description and classification of the agricultural BMPs according to our research objectives.

While a comprehensive list of agricultural BMPs may exist, what works in one geographic region may not work well in another because of variation in soil

characteristics, geology, topography, climate, and so forth. Nonetheless, we are going to consider only in-field management practices. The main reasons to focus only in this category are (i) Agricultural BMPs designed to be implemented by local farmers on their land, and (ii) not include construction costs of structural options. In this section, the general classification, and characteristics of in-field BMPs are described. And Figure 2.1 graphically shows the Ag-BMPs implementation on a field.

Table 2.1. Description and classification of agricultural BMPs (modified Logan, 1993).

BMP	POLLUTANT TREATED [1]	MEDIUM IMPACTED [2]		
		SURFACE WATER	GROUND WATER	SOIL
Structural				
Buffer zones or filter strips	S	+	+	+
Terraces, hillside ditches	S, P	+	-	+
Grass waterways	S, P	+		+
Subsurface (tile) drains	S, P, N	+/-	+	+
Sediment and water retention basins	S, P, N	+	-	-
Surface drains	N	-	+	+
Irrigation tailwater recovery systems	S, C	+		+
In-Field management				
Conservation tillage	S, N, P	+	-	+
Cover crop and rotation	S	+	+	+
Contour cropping	S	+	-	+
Strip cropping	S	+	-	+
Fertilizer management	N, P	+	+	+
Irrigation management	N, P	+	+	+
Animal waste management	N, P	+	-	+

[1] C, pesticide; S, sediment; P, phosphorus; N, nitrogen; M, heavy metals.
[2] (+), positive impact; and (-), no impact
Source modified: (Logan, 1993)

2.2.1 Conservation tillage

Blevins, R. L., & Frye, W. W. (1993) define conservation tillage as a practice that leaves a percentage of the soil surface covered with green manure or crop residue to reduce run-off and increase infiltration (Ritter and Shirmohammadi, 2001). Over time, the crop residue is degraded, increases soil organic matter, and improves the soil structure and soil biological properties. Therefore, this has a positive effect that allows reducing the run-off, being more relevant during the critical rain periods (Carter and Sanderson, 2001).

The minimum tillage or minimum movement of the soil consists of intervening as little as possible in the soil at the time of cultivation, in such a way that it does not interfere in the natural processes that develop in it (FAO, 2000). Several implements are used in minimum tillage systems to avoid inverting the soil and causing excessive soil erosion (FAO, 2000a, 2015). Minimum tillage involves the amount and distribution of crop/plant residue on the soil surface, limiting soil disturbance to only the amount necessary to incorporate the nutrients and plant the crops (Neitsch et al., 2011). Minimum tillage reduces soil erosion and protects soil moisture due to increased filtration, preserving the soil's structure, increase soil organic matter content, and reducing CO2 losses from the soil. Additionally, the practice allows savings in labor, fuel and heavy machinery costs.

2.2.2 Cover crop and crop rotations

Blevins, R. L., & Frye, W. W. (1993) define cover crops/rotation as a practice that leaves a percentage of the soil surface covered with green manure or crop residue to reduce run-off and increase infiltration (Ritter and Shirmohammadi, 2001). Over time, the crop residue is degraded, increasing soil organic matter, and improving the soil structure and soil biological properties. Therefore, a system with crop rotations and cover crops improves soil productivity and crop yields and reduces run-off and, ideally, losses to insects and diseases (Carter and Sanderson, 2001).

Both crop rotations and cover crops are usually combined in a primary crop cycle. Crop rotation is established sequentially and includes a cover crop in the primary crop cycle that will be used as green manure. Both practices provide potential benefits for organic matter increase due to the addition of green manure sources. Also, soil hydraulic properties can be improved, and there is increased soil protection from the impact of rainfall (Carter and Sanderson, 2001). And, if legumes are used, biological fixation of nitrogen to the soil increases.

A wide range of plants can be used as green manure and/or permanent coverage. These should be plants of rapid initial growth that produce large amounts of biomass with minimum consumption of water, few pests. In addition, green manure and cover crops should not be invasive plants that hinde the growth of successive crops and rotation (FAO and MADS, 2018; Rubiano et al., 2006b; FAO, 2000). According to FAO and MADS (2018) in Colombia, the centeno (*Secale cereale L.*), barley (*Hordeum sativum*), oat (*Avena sativa L.*), nabo forrajero (*Raphanus sativus L.*), vicia (*Vicia atropurpurea*), higuerilla (*Ricinus communis L.*) and some varieties of beans, have been used as green manures in the high altitude tropical regions of the country. In particular, some studies have reported significant environmental and economic benefits of the use of oat as green manure in rotation with potato (oat-potato-potato) compared with the traditional system in the study watershed (Guerrero, 1998) and in other watersheds with similar characteristics (Uribe et al., 2018; Rasouli et al., 2014; Quintero and Comerford, 2013; García et al., 2000).

2.2.3 Contour cropping

Contour farming is a practice that consists of planting along the contours of the terrain. This practice's main objective is to reduce soil erosion, rill erosion, and surface run-off (Tuppad et al., 2010). On the other hand, this practice serves as a barrier to retaining the nutrients in run-off from the crop upslope, providing extra nutrients to the crop and reducing the amount of fertilizer required by the crop.

This practice is being adopted as an alternative to up-and-down-slope farming globally for soil erosion control. Contouring creates furrows perpendicular to the field slope, reducing the runoff velocity, reducing sediment transport, and enhancing the infiltration of the water (Blanco and Lal, 2008). On the other hand, this practice serves as a barrier to retaining the nutrients in a run-off that comes from the crop upstream. In this way, contour planting accompanied by other conservation practices can be added extra nutrients in the crop management, which is vital for crop yield. Contour planting is suggestedin all soils that have a slope. On steeper slopes, the contour lines are essential but not enough, so the combination with terraces, ditches, and live barriers are recommended to discharge runoff from the contour rows. It is an ideal BMP to be used in rolling topography.

2.2.4 Buffer zones and Filter strips

Buffer zones consists of planting with diverse vegetation bands, which act as filters and barriers to collect and remove pollutant nutrients, pesticides, and bacteria from surface run-off. These buffer zones have to be situated at the edge of a field to collect the more significant run-off water from the pollutant source areas (Ritter and Shirmohammadi, 2001). And filter strips are vegetated areas that are situated between surface water bodies and cropland or grazing land. Diversity fencings/bands of vegetation that act as filters and barriers to collect and remove pollutant nutrients, pesticides, and bacteria from surface run-off are planted in these areas. Filter strips are also known as vegetation filter. They are generally situated at the edges of channel segments to protect them from animals that and collect run-off water from the pollutant source areas (Ritter and Shirmohammadi, 2001).

2.2.5 Fertilizer management

Fertilizer management is a practice that fosters the optimization and of fertilizer applications. The International Plant Nutrition Institute (IPNI) summarizes the principles of fertilizer BMPs as the right product, right rate, right time, and the right place. As its primary objective, this approach encourages application of the required amounts of fertilizers needed by the plant at the right time and place. On the other hand, fertilizer loss to the environment and water body is minimized (Roberts, 2007).

The dairy systems in Colombia have a common standard practice of the excessive use of nitrogen fertilizers after each grazing (Rubiano et al., 2006b). This practice allows farmers to appreciate the rapid biomass increase visibly and, consequently, increase the animal load per hectare and graze the pasture more frequently (Correa et al., 2008). However, studies have proven that the excessive use of fertilizers, regarding quantity and frequency, causes changes in the nutritional quality of the pastures, which are not visible to producers (Rodriguez and Soto, 1999; Urbano, 1997; Van Horn et al., 1994) And therefore, it causes adverse effects on productivity, economic and environmental (Hanigan, 2005; Lapierre et al., 2005). In the study area, Rodríguez (1999) showed the importance of adjusting the pastures fertilization schedules for dairy regarding frequency, quantity, and type of fertilizers used. The results showed no significant differences in kikuyu and ryegrass's nutritional components because of the reduction in amount (-10%) and frequency (four cuts every 30 days or two cuts every 60 days without applying N) fertilizer used. The main reason could be the presence of remaining nutrients in the soil (Uribe et al., 2018; Nielsen and Kristensen, 2005).

2.2.6 Living fences

Live fences are those in which a row of trees and shrubs are planting in short distances, and frequent pruning is used to replace conventional barriers. This multipurpose agroforestry practice originated in the need to delimit helps to control the movement of animals and humans, provide firewood or forage, serve as windbreaks, enrich the soil with nutrients, and allow trees or shrubs to be introduced to grazing areas (Blanco and Lal, 2008)(Zhai et al., 2006). At the same time, live fences provide a habitat for wildlife.

For our study, we focused on live tree legume fences used in livestock systems, which have been used in agriculture since ancient times. In more recent times, legumes have become important as high-quality forages for livestock as other feed sources both in cultivated pastures (Broom et al., 2013; Mejia-Diaz et al., 2017). Tree legumes fences in the livestock systems of the high-altitude tropics have multiple environmental and production benefits, including the trees' nutritional quality and nitrogen fixation, as well as counteracting the adverse effects of frost and drought, reducing pests that affect the development of grasses, lower production costs (replacing electric fences), and improving the reproductive performance of animals (Gutteridge and Shelton, 1994; Murgueitio, 2005). In Colombia, options for live fences include hedges with *Leucaena leucocephala*, *Tithonia diversifolia* (commonly known as the "golden button" "botón de Oro"), or *Sambucus peruviana* (widely known as "Tilo") in mountain areas.

In Colombia, the *Tithonia diversifolia* is increasingly being studied and planted in association with improved grasses as one of the best alternatives for silvopastoral systems in the mountains of the high tropics (Mejía-Díaz et al., 2017). When used for forage, it can be harvested up to six times a year after four months of sowing. The plant should be cut before flowering, using leaves and stems two centimeters thick. Reported values of

the dry weight of biomass vary between 16% to 35% depending on planting density, soil type, and environmental conditions (González-castillo et al., 2014; Mejia-Diaz et al., 2017). A study conducted in a farm located in the study area (Municipality of Don Matias) reported an improvement in milk production and quality when 35% of the concentrate in the animals' diet was replaced by *Tithonia diversifolia* forage (Mahecha et al., 2007). In small and medium dairy producers, it has been possible to reduce production costs between 10 and 15 percent due to less use of fertilizers in the grasslands and less concentrated feed (up to 25%) (Zuluaga and Rivera, 2013; Murgueitio et al., 2016). Additionally, after six months of planting the *Tithonia*, the nitrogen, phosphorus, potassium, and calcium content in the soil could be increased by 191, 8, 271, and 70 kg/ha, respectively (González-castillo et al., 2014). In summary, the association of legumes with grasses contributes to environmental, economic, and nutritional improvements in livestock systems, which depend on the established arrangement characteristics implemented in the field.

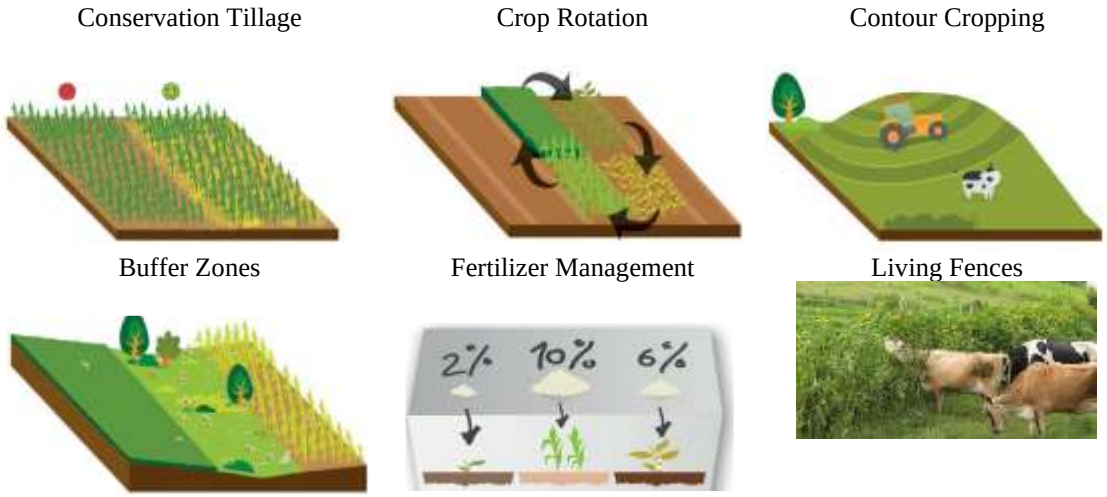

Figure 2.1. Agricultural best management practices (Ag-BMPs) implementation on field.
Source: (INSPIA, 2015)
http://www.inspia-europe.eu/index.php/best-management-practices

2.3 AG-BMP ALLOCATION FOR WATER MANAGEMENT PURPOSES

Agricultural management practices vary widely in terms of scale, geographical location, and purpose. Farmers and decision makers of these real-world systems are faced with the need to select and allocated optimal agricultural-BMPs as alternative management options to reduce nonpoint pollution sources. Agricultural scientists are turning more towards simulation models to identify the optimal selection and location of BMPs. From

a modeling perspective, integrated models using a coupled-component modeling approach are the most widely used modeling type for Ag-BMP optimization problems.

Previous studies have developed several optimization modeling studies of Ag-BMP localization at different scales (field, sub-watershed, and watershed). Among these, the Non-dominated Sorting Genetic Algorithm (NSGA-II) or Genetic Algorithm (GA) has been coupled with the Soil and Water Assessment Tool (SWAT) as optimization engines (Liu et al., 2019; Geng et al., 2019; Dai et al., 2018; Babbar-sebens and Minsker, 2012; Maringanti et al., 2011; Liu et al., 2013; Panagopoulos et al., 2013; García et al., 2000). The SWAT model is commonly used because provides different Ag-BMP types and it is closely connected to GIS (Geographic Information Systems).

2.3.1 Hydrological and water quality modeling

Hydrological models are tools used to represent a watershed's response to climate and/or land use variability, with emphasis on modeling the flow hydrograph at the concentration point of the watershed. Hydrological models are also used as a basis for modeling other processes, such as water quality, erosion, real-time flood forecasting, etc. Hydrological models can be divided 1) according to the conceptualization of the basic processes; can be empirical (metric), conceptual (parametric) or process-based (mechanistic); 2) according to the nature of the basic algorithms, can be deterministic or stochastic; and 3) according to their spatial representation, they can be grouped, distributed or semi-distributed (Solomatine and Wagener, 2011).

The hydrological model used in this research was the Soil and Water Assessment Tool (SWAT) developed by the United States Department of Agriculture – Agricultural Research Service (USDA-ARS) (Arnold et al., 1998). The model is a continuous-time, semi-distributed, process-based river watershed-scale model designed to simulate water management decisions' long-term effects on the water quality and hydrologic response (Neitsch et al., 2011). The model is built on a daily time step at sub-basin and watershed scales. Sub-basins in a simulation are beneficial when different watersheds are dominated by land uses or soils that differ in their properties that may impact the hydrology. These are further subdivided into a series of Hydrological Response Units (HRU), common land areas within the sub-basin composed of unique land cover, soil, and agricultural management practices (Arnold et al., 2012b). The hydrological cycle simulated is based on the water balance equation, including daily precipitation, runoff, evapotranspiration, percolation, and returns flow components (Gassman et al., 2007). Spatial information such as the soil type and characteristics, land use, climate, and topography are necessary inputs. SWAT is a semi-distributed, continuous-time, and process-based watershed-scale model designed to simulate the effects of water management decisions on water quantity and quality (Neitsch et al., 2011). The model's processing units are Hydrological Response Units (HRUs) – small land areas with unique combinations of sub-basin, soil

type, land use, and agricultural management practices (Arnold et al., 1998). The hydrological cycle is based on the water balance equation.

SWAT allows several different physical processes to be simulated in a watershed. A summary of the equations used in the runoff, Nitrate-N loads (NO_3^-N) in runoff, crop yields estimation, and agricultural management practices implementation processes are described below. These equations have been taken from theoretical SWAT documentation version 2009 (The document can be downloading for obtaining detail information (http://swat.tamu.edu/documentation/).

Surface runoff

The Natural Resources Conservation Service Curve Number (CN) method (USDA-SCS, 1972) was used to predict the surface runoff. The model estimates the runoff amounts under varying land use and soil types (Neitsch et al., 2011). The CN equation is shown below.

$$Q_{surf} = \frac{(R_{day} - I_a)^2}{(R_{day} - I_a + S)} \qquad (2.1)$$

where Q_{surf} is the accumulated runoff or rainfall excess (mm H_2O); R_{day} is the rainfall depth for the day (mm H_2O); and I_a is the initial abstractions (mm H_2O) (surface storage as well interception and infiltration before runoff). The initial conception is commonly approximated to 0.2S, and S is the retention parameter (mm H_2O). In this abstraction, S= 25.4 * [(1000/CN) - 10], and CN is the curve number for the day (Neitsch et al., 2011). The CN is a function of the land use, soil permeability, and the soil, as mentioned above, water conditions. Two methods were used to calculate the retention parameter: (1) the soil moisture method, which allows the retention parameter to vary with the soil profile water content; and (2) the plant ET method, which allows the retention parameter to change with the accumulated plant evapotranspiration (Neitsch et al., 2011).

A surface runoff storage feature to lag a portion of the surface runoff release to the main channel is incorporated in SWAT. When surface runoff is calculated using either the CN or the Green-Ampt method, the runoff released to the main channel is calculated with the following equation (Neitsch et al., 2011):

$$Q_{surf} = \left(Q'_{surf} + Q_{stor,i-1}\right)\left[1 - exp\left(\frac{-surlag}{t_{conc}}\right)\right] \qquad (2.2)$$

where, Q_{surf} is the amount of surface runoff discharged to the main channel on the given day (mm H_2O); $Q_{stor,i-1}$ is the surface runoff stored from the previous day (mm H_2O); Q'_{surf} is the amount of surface runoff generated in the sub-basin on a given day (mm H_2O); $surlag$ is the surface runoff lag coefficient, and the t_{conc} is the time of concentration for the sub-basin (hrs). When the concentration-time increases, $surlag$ decreases in value, and more water is held in storage.

Nutrient's transport (Nitrate and Soluble phosphorus)

Nitrate can be transported with surface runoff, percolation, and lateral flow. The nitrate-N concentration in the mobile water must be calculated to determine the amount of nitrate-N moved by the water. The amount of mobile water refers to the amount of water lost by surface runoff (Q_{surf}), lateral flow ($Q_{lat,ly}$) and percolation ($w_{perc,ly}$). The following equation is applied:

$$conc_{NO3,mobile} = \frac{NO3_{ly}\left[1 - exp\left(\frac{-w_{mobile}}{(1-\theta_e).SAT_{ly}}\right)\right]}{w_{mobile}} \qquad (2.3)$$

where $conc_{NO3,mobile}$ is the concentration of nitrate-N in the mobile water for a given layer (kg N/mm H_2O), $NO3_{ly}$ is the amount of nitrate in the layer (g N/ha), θ_e is the fraction of porosity, SAT_{ly} is the saturated water content of the soil layer (mm H_2O), and the $w_{mobile} = Q_{surf} + Q_{lat,ly} + w_{perc,ly}$ is the amount of mobile water in the layer (mm H_2O). The following equations calculate the nitrate-N removed in surface runoff, lateral flow, and percolation:

Nitrate removed in surface runoff → $NO3_{surf} = \beta_{NO3}.conc_{NO3,mobile}.Q_{surf}$ *(2.4)*

Nitrate removed in lateral flow → $NO3_{lat,ly} = \beta_{NO3}.conc_{NO3,mobile}.Q_{lat,ly}$ *(2.5)*

Nitrate removed by percolation → $NO3_{perc,ly} = conc_{NO3,mobile}.w_{perc,ly}$ *(2.6)*

where, β_{NO3} is the nitrate-N percolation coefficient.

The mobility of solution phosphorus is low. Therefore, in the swat model, the surface runoff only interacts partially with the solution P stored in the top 10 mm of soil. The amount of solution P transported in surface runoff is calculated with the following equation:

$$P_{surf} = \frac{P_{solutionsurf} . Q_{surf}}{\rho_b . depth_{surf} . k_{d,surf}} \quad (2.7)$$

where $P_{solutionsurf}$ is the amount of phosphorus in solution in the top 10 mm (kg P/ha), ρ_b is the bulk density of the top 10 mm (Mg/m^3), $depth_{surf}$ is the depth of the surface layer (10 mm), and $k_{d,surf}$ is the phosphorus soil partitioning coefficient (m^3/Mg). This refers to the ratio of the soluble phosphorus concentration in the top 10 mm of soil.

Crop yield

The potential crop yield calculated in SWAT is a function of the harvest index (*HI*) and the plant biomass (*bio*) when the day of harvest/kill operation is performed. The yield calculates will not be added to residue in the soil and are assumed to be lost from the system (i.e., the watershed).

The harvest index (*HI*) is the fraction of the aboveground plant dry biomass removed as dry economic yield. The *HI* will be between 0.0 to 1.0. However, the *HI* may be greater than 1.0 for plants whose roots are harvested (i.e., potatoes, cassava). SWAT calculates the harvest index each day of the plant's growing season using the relationship as:

$$HI = HI_{opt} . \frac{100 . fr_{PHU}}{(100 . fr_{PHU} + exp[11.1 - 10 . fr_{PHU}])} \quad (2.8)$$

where *HI* is the potential harvest index for a given day, HI_{opt} is the potential harvest index for the plant at maturity given ideal growing conditions, and fr_{PHU} is the fraction of potential heat units accumulated for the plant on a given day in the growing season. Then, the potential crop yield is calculated as:

$$yld = bio_{ag} . HI \quad \text{when HI} \leq 1.00 \quad (2.9)$$

$$yld = bio . \left(1 - \frac{1}{(1+HI)}\right) \quad \text{when HI} > 1.00 \quad (2.10)$$

where *yld* is the crop yield (kg ha^{-1}), bio_{ag} is the aboveground biomass on the day of harvest (kg ha^{-1}), *HI* is the harvest index on the day of harvest, and *bio* is the total plant biomass on the day of harvest (kg ha^{-1}). The aboveground biomass is calculated:

$$bio_{ag} = (1 - fr_{root}) . bio \quad (2.11)$$

where fr_{root} is the fraction of total biomass in the roots the day of harvest, and *bio* is the total plant biomass on the day of harvest (kg ha^{-1}).

The actual crop yield is calculated in SWAT adjusting the harvest index predicted with the Eq. 2.8, which is affected by water deficit using the relationship:

$$HI_{act} = (HI - HI_{min}).\frac{\Upsilon_{wu}}{\Upsilon_{wu} + exp[6.13 - 0.833\,.\,\Upsilon_{wu}]} + HI_{min} \qquad (2.12)$$

where $\boldsymbol{HI_{act}}$ is the actual harvest index, *HI* is the potential harvest index on the day o harvest calculated with equation 2.8, HI_{min} is the minimum harvest index allowed for the plant (the harvest index for the plant in drought conditions), and Y_{wu} is the water deficiency factor. The water deficiency factor is calculated:

$$\boldsymbol{\Upsilon_{wu} = 100.\frac{\sum_{i=1}^{m} E_a}{\sum_{i=1}^{m} E_o}} \qquad (2.13)$$

where E_a is the actual evapotranspiration on a given day, E_o is the potential evapotranspiration on a given day, *i* is a day in the plant growing season, and *m* is the day of harvest if the plant is harvested before it reaches maturity or the last day of the growing season if the plant is harvested after it reaches maturity.

Management practices

Fertilizer application: In the fertilizer database, the weight fraction of different types of nutrients and bacteria are defined for each fertilizer/manure applied. The amounts of nutrients added as to the other pools in the soil are calculated as:

$$NO3_{fert} = fert_{minN} * (1 - fert_{NH4}) * fert\_kg \qquad (2.14)$$

where $NO3_{fert}$ is the amount of nitrate (NO_3^-N) added to the soil in the fertilizer (kg N/ha), $fert_{minN}$ is the fraction of mineral N in the fertilizer, $fert_{NH4}$ is the fraction of mineral N in the fertilizer that is ammonium, *fert_kg* is the amount of fertilizer applied to the soil (kg/ha) on a specific ***day*** of the defined management schedule.

Tillage: The tillage operation redistributes residue, nutrients, bacteria, and pesticides in the soil profile. The decision variables to represent the minimum tillage BMP option required are the operation's timing, which in our case won't change, and the type of tillage

operation (*till_id*). The change in the redistribution of nitrate ($NO3_{mixed}$) in the soil is calculated as:

$$NO3_{mixed} = \left(NO3_{total\ mixed} * Depth_{layer}\right)/Deptil \qquad (2.15)$$

where,

$$NO3_{total\ mixed} = \sum_{i=first\ soil\ layer}^{Deptil,\max depth} (NO3_{initial} * Effimix) \qquad (2.16)$$

$Depth_{layer}$ is the depth of each soil layer that is redistributed, *Deptil* depth of soil mixed by the implement, $NO3_{initial}$ is the initial content of nitrate of each soil layer in kg/ha, and *Effimix* is the mixing efficiency of the tillage implement in percentage (%). To calculate the final nitrate content, the $NO3_{mixed}$ is added to the unmixed nitrate for the layer.

Grazing: The simulation of plant biomass removal and manure deposition over a specific period is carried out by the *grazing operation* in the SWAT model. The time during the year at which grazing begins, the amount of biomass removed daily, the amount of the manure deposited daily, the type of manure deposited, and the length of grazing period are the values required. A minimum plant biomass for grazing could be specified. When the plant biomass falls below the amount specified the model will not graze or apply manure in the HRU on that day.

2.3.2 Metaheuristics for agricultural land use optimization

Optimization techniques are considered to be very useful for model-based support-systems designed to define alternatives for a sustainable agriculture sector. Most problems considered in this study do not allow for an analytical representation of the objective function (it is calculated by software), and/or its derivative, efficient gradient-based methods cannot be used. Moreover, the problems considered typically have multiple optima. What is left is the class of optimization techniques that are referred to as "direct methods", "global optimization", or "metaheuristics". In essence, these are methods using randomized search. Metaheuristics optimization approaches are considered the most suitable strategies to solve this type of problems (Ólafsson, 2006). Metaheuristics has been described as "an algorithm designed to solve approximately a wide range of hard optimization problems without deeply adapting to each problem" (Boussaïd et al., 2013).

There are several metaheuristics options available in the literature. However, it is essential to select the most appropriate for the optimization problem to be solved. Groote et al. (2007) propose classification/categories of the study areas in which metaheuristics are applied (Figure 2.2). One of these categories is water resources management, including problems related to agricultural BMP selection and allocation. The criteria

considered in these types of studies are mainly focused on reducing nonpoint pollution sources from farms. However, this approach usually also contemplates environmental, social, and economic aspects as decision variables for the cropping systems evaluated (Figure 2.3). In this way, a better representation of the systems' complexity can be achieved, which lets us offer better solutions for integrated watershed management.

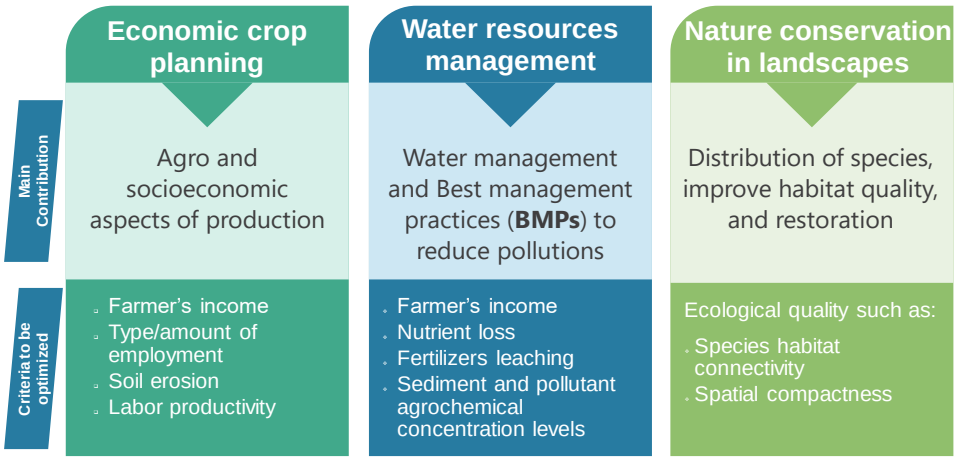

Figure 2.2. Areas of study in which metaheuristic optimization methods have been used.

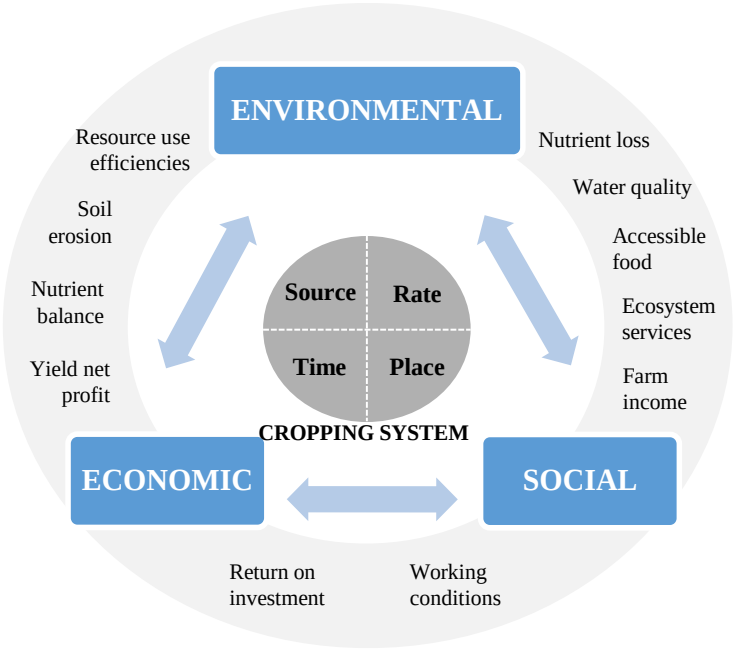

Figure 2.3. Global framework for water resource management of agricultural BMP optimization.

The metaheuristic algorithms can be mainly classified into two categories: i) single solution-based metaheuristics, also called trajectory methods, and ii) population-based metaheuristic (Boussaïd et al., 2013). However, we only highlight and give a global overview of the population-based metaheuristics which have been used in agricultural land-use optimization. The population-based metaheuristics approach is focused on obtaining a set of solutions that seek to identify the preferable regions within a defined research space (Boussaïd et al., 2013; Memmah et al., 2015). Evolutionary Algorithms (EAs) and Swarm Intelligence (SI) are the two most used methods for this research field. EAs are based on Darwin's theory about the evolution of populations as they adapt to the environment. Several optimization algorithms like Genetic Algorithm (GA) and Differential Evolution (DE) are included in this category. A generic form sketch of EAs and SI are shown in Table 2.2.

Several evolutionary algorithms have been developed to solve multi-objective optimization problems. The strength Pareto evolutionary algorithm 2 (SPEA 2) (Zitzler and Thiele, 1999), niched Pareto genetic algorithm (NPGA) (Horn et al., 1994), and non-dominated sorting genetic algorithm II (NSGA-II) (Deb et al., 2002) are some examples. However, the NSGA-II has been widely applied in BMP optimization problems for watershed management and planning studies in recent years (Liu et al., 2019; Geng et al., 2019; Dai et al., 2018; Babbar-Sebens and Minsker, 2012; Maringanti et al., 2011; Liu et al., 2013; Panagopoulos et al., 2013; García et al., 2000).

The NSGA-II improves the nondominated sorting algorithm and reduces the computational complexity of NSGA (Yijie and Gongzhang, 2008). In order to improve diversity, the NSGA-II introduces the crowded-comparison operator and sorts the combination of parents and children's populations. The diversity in solutions is preserved using non-dominated sorting and elitism; therefore, NSGA-II provides a neat spread of solutions, supporting finding the entire Pareto-optimal front (Deb et al., 2002). In summary, the main step-by-step procedure of NSGA-II algorithm is simple. First, a combined population of *2N* dimension (*Rt*) is formed. The offspring population *Qt* is first created by using the parent population (P_t) and these two populations are combined forming (*Rt*). Then, a nondominated sorting is used to sort the population *Rt*. This classification is made using a ranking (fitness) function to identify several fronts (*F1, F2...Fn*). The new population is more significant than *N* and just the best ranked individuals remain; the elitism is ensured. Finally, individuals are not deleted arbitrarily when they have the same ranking (belong to the same front). Instead, they reside in the least crowded region using the crowding-comparation operator (rank and crowded distance) to choose the best solutions needed to fill all population slots, which ensures diversity (Deb et al., 2002). Psedocode of NSGA-II is shown in Table 2.3.

Table 2.2. Evolutionary algorithm (a) and Swarm intelligence (b) form sketch.

	a) EA_S		b) Particle swarm
1	Initial **population**	1	Initial swarm **population**: velocities and positions
2	Evaluated each individual	2	**While** termination condition is not reached, **do**
3	**Repeat**	3	**For each** particle, **do**
4	*Select* parents	4	*Adapt* velocity
5	*Recombine* pairs of parents	5	*Update* the position
6	*Mutate* resulting offspring	6	*Evaluated* the fitness
7	*Evaluate* new individuals	7	Conditions
8	*Select* next-gen. individuals	8	**End**
9	**Until** the condition is satisfied	9	**The end** condition is satisfied

Table 2.3. Non-dominated sorting genetic algorithm II (NSGA-II) form sketch.

	NSGA-II
1	Initialize a randomly distributed **population**
2	Evaluate Objective values of individuals
3	Assign rank (level) to individuals based on nondomination
4	Generate Child population (offspring)
5	*Binary* tournament selection
6	*Crossover* and *Mutation*
7	**For** *i= 1 to g (generations to solve)* **do**
8	**For** *each Parent and Child in population* **do**
9	*Merge* the populations o parents and offspring
10	*Assign* rank (level) to individuals based on *nondominated sorting*
11	*Create* sets o *nondominated* Pareto fronts
12	*Calculate Crowding distance* between points on each front
13	*Select* new parents based on ranks and crowding distance
14	**End**
15	*Select* points on the lower front with high crowding distance
16	*Create* next generation
17	*Binary* tournament selection
18	*Crossover* and *Mutation*
19	**End**

2.4 GENERAL METHODOLOGY FRAMEWORK

Based on the research gaps identified in agricultural BMPs modeling optimization, in this dissertation we present a comprehensive modeling framework for optimal selection and allocation of agricultural BMPs at watershed scale. The methodology has been designed to be developed in five main phases, which are strongly connected to approach the complexity of the problem and to cover the proposed objectives (Figure 2.4).

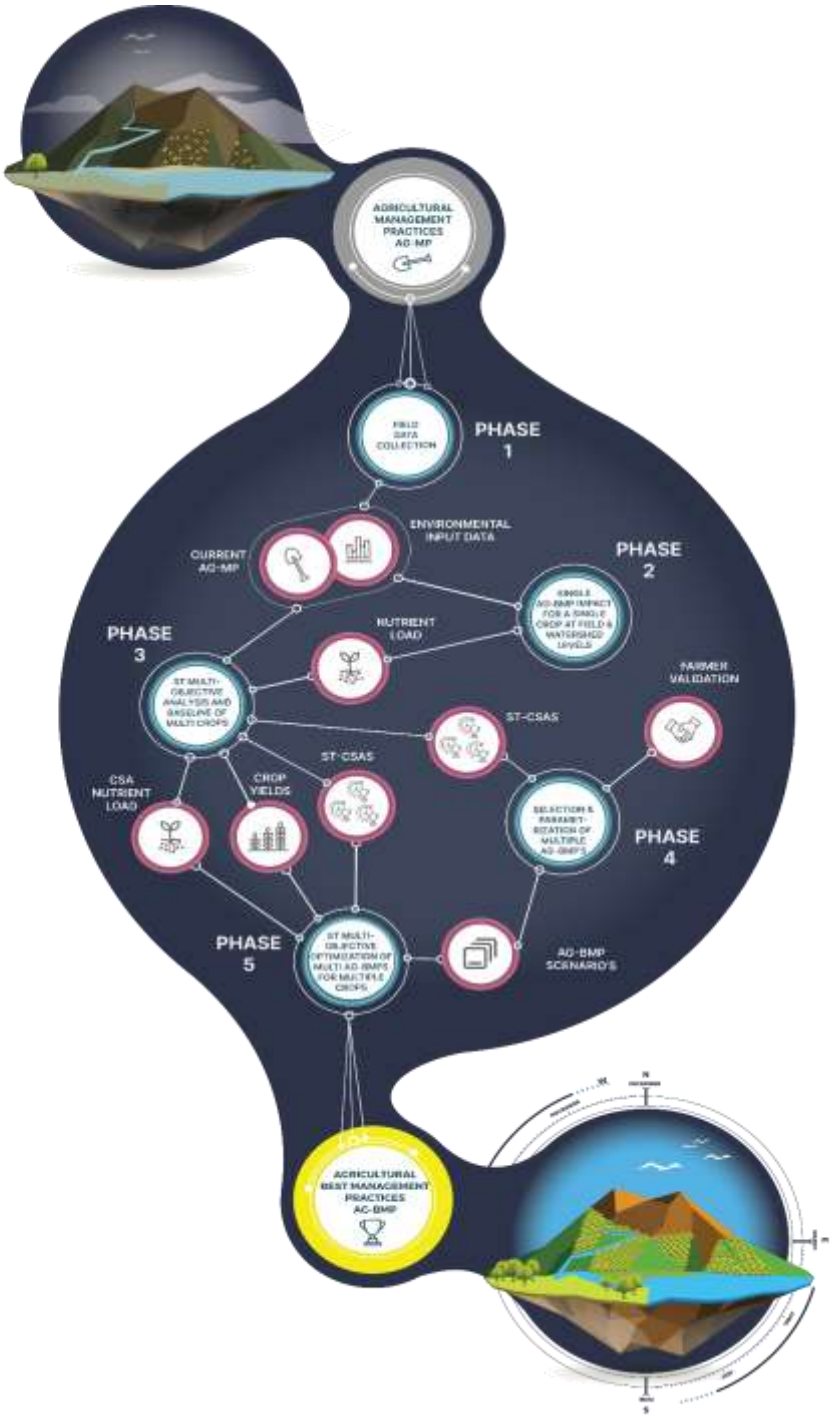

Figure 2.4. Workflow of the general methodology

i. **Problem identification and collection of data in the field:** corresponds to understanding the current situation, the needs and gaps for the objectives, and the case studies. In this phase we identified the data needs as well as field data collection. This dissertation uses data collected in the field during a field campaign to know in detail the current agricultural management practices used by farmers in the study watersheds.

ii. **Analysis of a single agricultural BMP impact for a single crop at field and watershed level:** corresponds to the understanding the impact and effectiveness of implementing one agricultural BMP (Conservation Tillage-CT) to reduce runoff nutrient losses at field and watershed levels. In this phase we explain the conceptual modeling outline of agricultural best management practices applied in a single crop (potato crop) in the Fuquene watershed. In our research we used data collected during a field campaign and complemented with experimental plot data from previous research. The hydrological SWAT model was used to model the hydrology and water quality of the Fuquene watershed.

iii. **Spatio-temporal analysis of the multiple agricultural management practice impacts:** consists of analyzing the spatial and temporal dynamics of nutrients in runoff resulting from current multiple agricultural practices. In this phase we identified the spatio-temporal critical source areas (ST-CSAs) in order to select the areas that contribute with the greates pollutant loads within the watershed. The ST-CSAs is a new approach that we propose to select the search space for the optimization problem for a more effective agricultural BMPs placement. This approach allowed us to identify the temporal and spatial dynamics of the runoff nutrient losses to guide feasible agricultural BMP scenario selection, and for selecting the search spacer for the optimization problem.

   In our research we used data collected during a field research on agricultural management practices for potato, tree tomato, and kikuyu grass (dairy farming) in the Riogrande II watershed. The Nitrate-N (NO_3^-N) and soluble P in runoff and crop yield values for potato, tree tomato, and kikuyu grass at Hydrological Response Units (HRUs) were estimated using the SWAT model. The model was calibrated using observed monthly discharge, nitrate-N (NO_3^-N) and soluble P loads in runoff, and crop yields.

iv. **Selection and parametrization of the BMPs scenarios to be used in the optimization model:** selection and parametrization of the BMPs scenarios simulated by the SWAT hydrological model to estimate the Nitrate-N (NO_3^-N) loads in runoff, and crop yield values for potato, tree tomato, and kikuyu grass at Hydrological Response Units (HRUs) in Riogrande II watershed. In this dissertation fieldwork and interviews with local farmers were taken into account to select feasible BMPs for the watershed studied. The agricultural BMPs were selected because these BMPs do not increase implementation costs, and they can be implemented by farmers with the tools

and wages they currently have, and they were accepted (some were proposed by the farmers themselves).

v. **Spatio-temporal multi-objective optimization framework to select and allocate agricultural BMPs for multiple crops**: The optimization framework proposed is an approach focusing on the minimization of Nitrate (NO_3^-N) losses and maximization crop yields at the field level to select and allocate optimal agricultural BMPs. The objective is to improve water quality without reducing agricultural productivity. The SWAT hydrological model was coupled with the metaheuristic algorithm NSGA-II to create the optimization engine. Pareto-front comparisons of the average vs. single sites (HRUs) values for each objective function were done to determine the spatial analysis level results needed to select the optimal BMPs.

2.5 CONCLUSION

The general objective of this dissertation is to develop a modeling and optimization framework to select and allocate agricultural BMPs (Ag-BMPs). Therefore, we consider it necessary in this chapter to contextualize the reader regarding: i) definition, concept and examples of Ag-BMP; ii) description of the hydrological and water quality model used to estimate the nutrient losses in runoff and crop yields (objective functions of the optimization model); iii) definition and description of the metaheuristics (algorithms) for agricultural land use optimization; and iv) a brief description of the general methodology used in subsequent chapters. In fact, we only focus on the main concepts; we do not consider this to be a literature review needed for a critical analysis.

The optimization framework, to be covered in chapter 6, is mainly based on the results and analysis found in previous chapters 4 and 5. Our methodological approach is based on gradually increasing the level of complexity. This implies increasing the number of crops and BMP scenarios to be optimized, adding the variables of space and time in the analyses, and developing the model-based optimization engine.

3

DESCRIPTION OF THE CASE STUDIES

"La naturaleza sin su biodiversidad es solo un paisaje"

3.1 INTRODUCTION

The methods developed in Chapters 4 to Chapter 6 of this dissertation are applied in two selected case studies with common characteristics. This chapter describes each watershed. The case studies are the Fuquene watershed (Cundinamarca, Colombia) and the Riogrande II watershed (Antioquia, Colombia). These two study areas are of great importance as they are water supply basins for the Fúquene reservoir and the Riogrande II reservoir, which are important sources of drinking water and power generation. Additionally, the upper part of both basins includes the paramo ecosystem, which is the most important source of water and biodiversity in the Andes. Nevertheless, decline in the water quality in the watersheds is a serious environmental problem, especially in the Fuquene reservoir and Riogrande II reservoir, where accelerated eutrophication has been observed. The predominance of livestock and crop production in the middle part, generally with inadequate and low-technology practices, is one of the main causes of deterioration in water quality. Nitrogen and phosphorus runoff from fertilized crops and forage grass operations are assumed to be causing the increase of nutrients in the waterbodies, which, in turn, have increased algae blooms.

Although the research uses the Fuquene and Riogrande II watersheds in Colombia as the main case studies, the goal is to develop general methodologies that are applicable to similar watersheds, with the aim of supporting farmers and public and private entities to implement efficient measures to protect natural resources.

3.2 CASE 1 – FUQUENE WATERSHED

3.2.1 Catchment description

The Fúquene reservoir watershed is located in the northern part of Bogota city (Colombia) (5°28′00″N, 73°45′00″W). The watershed has an area of approximately 784 km^2 (Figure 3.1). The Ubaté River is the main tributary of the Fúquene reservoir with a drainage area of 624.91 km2. The river is born in the municipality of Carmen de Carupa, by the confluence of the Hato and Playa rivers and its main tributaries are the Suta and Lenguazaque rivers. The Fúquene reservoir has an approximate surface area of 30 km^2. The total drainage area of the lake is 991.6 km^2. The study area is characterized by large, rocky outcrops and mixed topography (flat areas, semi-flat, and streams), which varies between 2,520 and 3,786 meters above sea level (m.a.s.l). The lake's water is used and distributed by the municipal water supply companies for human consumption in settlements located downstream of the lake. The water is supplied to more than 500,000 inhabitants of the region (IGAC, 2000).

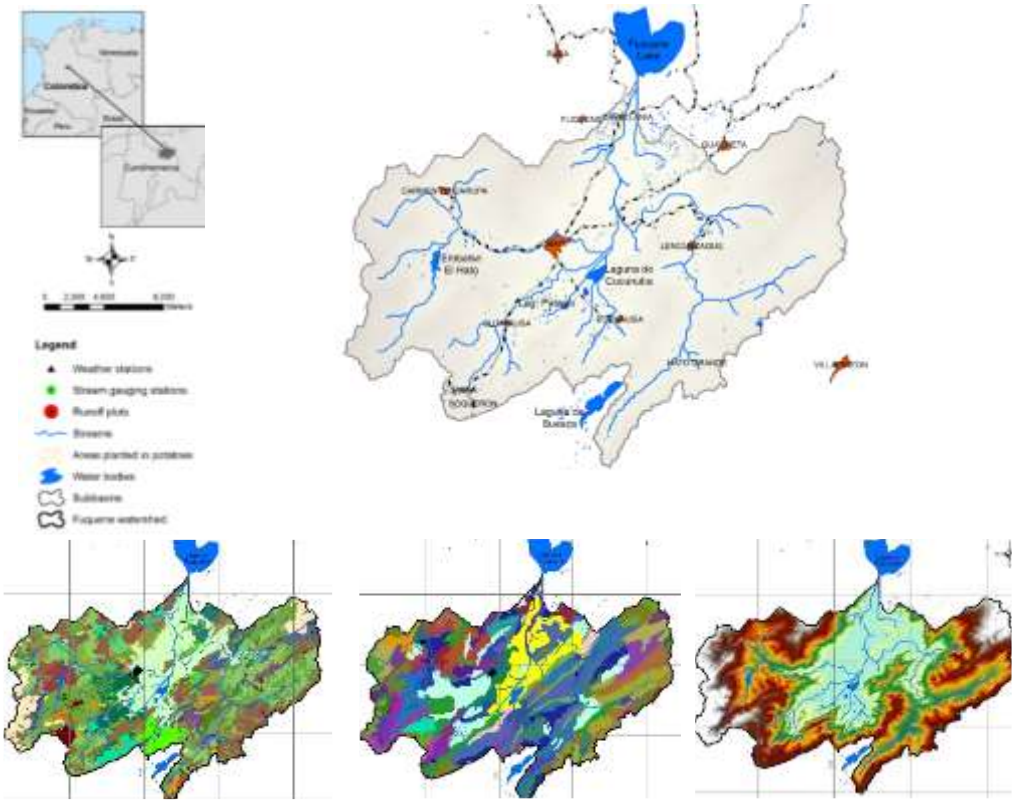

Figure 3.1. Location of the Fuquene watershed in Colombia, stream gauging and weather stations in the watershed, runoff plot's location, and sub-basin delineation are defined in SWAT modeling.

3.2.2 Climate

The weather input data of 46 stations located in the watershed were obtained from public and private institutions and provided by the Regional Environmental Authority of Cundinamarca (CAR). The recorded data were relative humidity, precipitation, temperature (maximum, minimum and average), solar radiation, wind speed and flow gauging. Of these, 18 stations were selected because they had a common period of daily records (2004 to 2013). The lists of stations selected are presented in Table 3.1.

The annual mean precipitation is 777.9 mm with a bimodal behavior in the watershed. The maximum monthly precipitation occurs in April and October with 15% and 16% of the annual total, respectively (Figure 3.2). The minimum precipitation occurs in January (2.3%) and February (3.6%.) (Figure 3.2). During the period December to March the average precipitation is 19% of the annual average. And the rains are distributed throughout the year in 142 days on average. The spatial behavior of rainfall within the basin was obtained from the annual mean isohyets map, obtained from the existing recording stations in the basin (Figure 3.2). In general, the flat area of the watershed

presents low rainfall with annual averages below 100 mm. In the western mountainous area, annual rainfall exceeds 1000 mm. In the rest of the terrain, the values fluctuate between 800 mm to 1200 mm (north of the Fúquene reservoir). Finally, the Saboya sector receives rainfall averaging 2,400 mm per year.

Mean annual temperatures are between 12 °C and 18 °C, without significant variation throughout the year (IDEAM, 2004). And the mean monthly temperature ranges between 12.0 - 13.2°C. Based on the existing records of the monthly temperature values, it is inferred that the temperature varies during the day, reaching maximum temperatures of 21 ° C in the midday hours and minimum temperatures of up to –4 ° C in the early morning. During the first quarter of the year, July, and December frosts often occur in the early morning. In general terms, a bimodal temperature behavior is observed. Towards the eastern part of the basin the lowest values are registered and in the southern part the highest values occur (Figure 3.2).

Table 3.1. Hydro-metereological stations at Fuquene watershed

Name	Latitude (m)	Longitude (m)	Elevation (m)	Precipitation	Temperature
Encanto el	1064300	1020600	3150	X	
Alto de aire	1065500	1028300	2900	X	
Ladera gran	1063400	1022500	2950	X	
Fortuna la	1076000	1054400	2880	X	
Barrancas	1062200	1025740	2720	X	X
Carupa hospi	1083120	1019840	2960	X	
Pino el	1073640	1025580	2575	X	
Hatillo el	1062470	1031590	2885	X	
Espino el	1081440	1038110	2550	X	
Puente el	1084730	1045230	2810	X	
Triangulo el	1078310	1051230	2800	X	
Tres esquina	1087270	1025000	3130	X	
Hato no 1 el	1077060	1017125	2985	X	
Boyera la	1077900	1025200	2610	X	
Carrizal	1067328	1034304	2880	X	X
Novilleros	1080650	1032380	2550	X	X
Sutatausa	1071880	1025020	2700	X	X
Represa el hato	1076689	1019172	2900	X	X

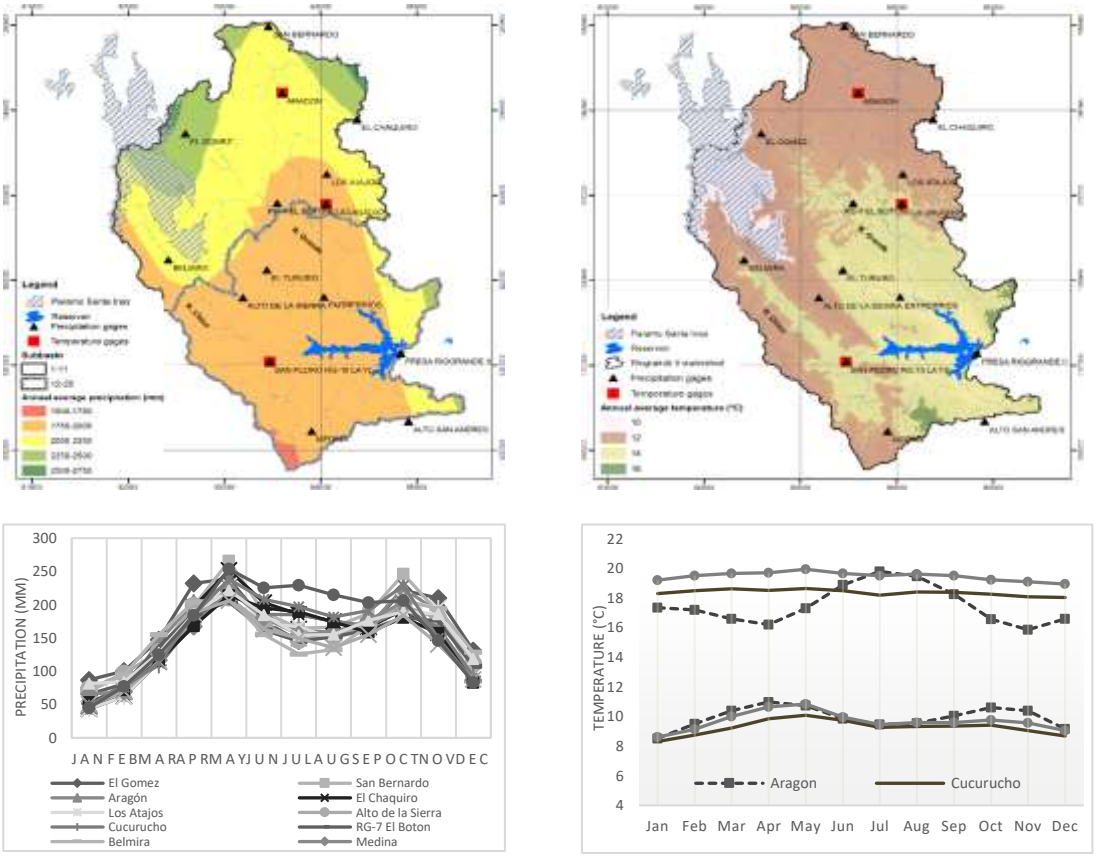

Figure 3.2. Annual average maps (top) and monthly average graphs (below) of precipitation (left) and temperature (right) at Fúquene watershed.

3.2.3 Vegetation cover and soils

The development of agricultural activities in this watershed has become the main economic driver for its inhabitants. Due to the climate and soils of this watershed, monocultures are predominant. The potato crop is considered the most important crop in the watershed. It is worth mentioning that the potato crop has been included in the Food and Nutrition National Plan (PAN) as one of the main crops for the daily diet of millions of consumers, especially in low-income sectors (CAR, 2006). The potato-cultivated area in the Fúquene watershed has an annual average production of 280,000 tons. The distribution by land use in the basin is 15,416 ha of natural pastures, which is equivalent to 19.7%; pastures 10,716 ha (14%); improved pastures with crops 10,520 ha (13.4%); paramo vegetation (4.5%); planted forest 2,938 ha (3.7%); potato 1.3%, among others (Table. 3.2) (Figure 3.3).

The soils that predominate in the basin are mostly entisol sand inceptisols and others in a smaller area such as mollisols, histosols, andisols and alfisols. The soils of the upper

part of the basin are found in the MLVd2 cartographic unit, a nomenclature obtained from the legend of the general study of soils of Cundinamarca (IGAC, 2000). These soils have a type of relief in crestones, with altitudes between 2200 and 3000 meters above sea level, annual temperatures between 12 and 18 ° C, and a humid climate (700 to 1100 mm/year). The taxonomic unit is an association of soils classified as Humic Lithic Eutrudepts, Typic Placudands, Dystric Eutrudepts (IGAC, 2000). On the other hand, the soils of the lower part of the basin are soils Inceptisols, which are found in the cartographic unit MMVe3. These soils have a relief in ridges and altitudes between 1800 and 2600 meters above sea level, with a cold climate (annual temperatures between 12 to 18 ° C) and dry (500 - 1000mm / year). The soil taxonomic units are Typic Haplustepts and Lithic Ustorthents (IGAC, 2000). For both soils, in the upper and lower part of the basin, the parent material is mainly sandy clastic rocks, clayey and carbonate silt, and volcanic ash deposits of variable thickness.

Table 3.2. Fúquene watershed land cover areas

Land Cover	Area (Ha)	Area (%)	Land Cover	Area (Ha)	Area (%)
Grass	15,416.7	19.7	Weedy	2,169.7	2.8
Pastures	10,761.5	13.7	Pastures on the eroded soil	2,074.0	2.6
Pastures and cool weather crops	10,520.0	13.4	Degraded lands	1,448.4	1.8
Potato and other crops	6,685.3	8.5	Savannah herbaceous	1,387.8	1.8
Shrub land	5,847.9	7.5	Reforested eroded lands	1,375.6	1.8
Paramo vegetation	3,539.1	4.5	Secondary forest	1,303.2	1.7
Planted forest	2,938.5	3.7	Potato	1,019.5	1.3
Mosaic of planted forest	2,435.0	3.1	Stubble	932.5	1.2
Pasture crops with natural spaces	2,360.5	3.0			
Watershed total area = 78400 ha					

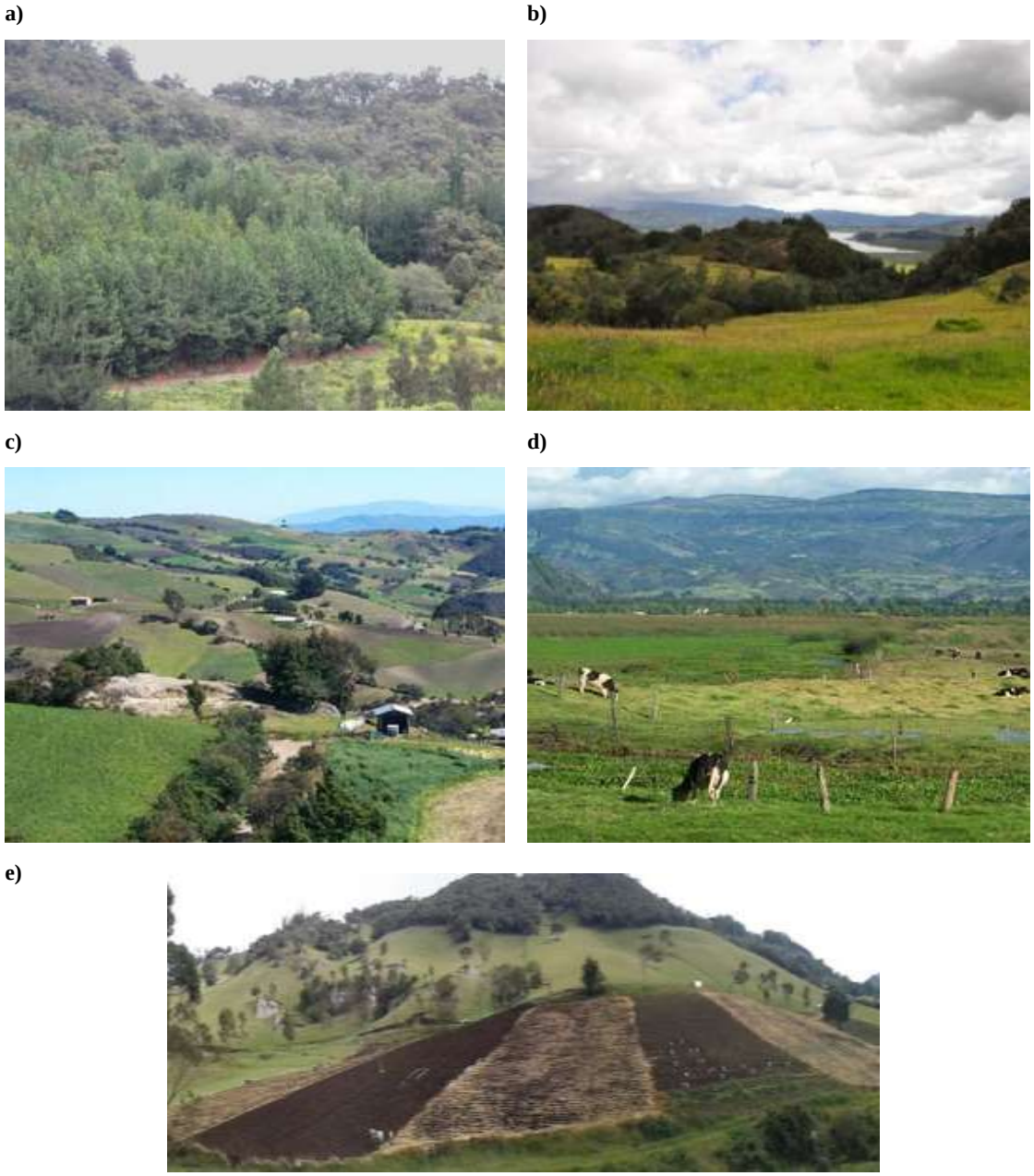

Figure 3.3 Land cover photographic record (a) planted forest, (b) native pasture, (c) pasture and other crops, (d) managed pastures associated with cattle ranching, and (e) potato at Fúquene watershed.

3.2.4 Socio-economic characterization

The total population of the study area is approximately 167,476 inhabitants, according to DANE 1993. Of which 63,262 (37%) are urban residents and 104,214 inhabitants (63%) live in rural areas. Around 66.1% of the population has inadequate housing, and only

28.9% have energy, clean drinking water, and sewerage services. In general, the vast majority of homes, especially in rural areas, are in poor condition (Salazar, 2016).

The agricultural activity development of this watershed has become the main economic alternative of its inhabitants. One of the most typical crops in the basin is the potato, which is a staple in the diet of Colombians. This tuber is included in the Food and Nutrition National Plan (PAN) because it contributes to the daily diet of millions of consumers, especially in low-income sectors (EOT 2000). The potato-cultivated area in the Fúquene watershed is around 16,933 ha, with an annual production of 280,000 tons. Other temporary or semi-annual crops such as wheat, barley, and corn, which are of great economic importance in the watershed, have been disappearing and are being replaced by potato crop. Therefore, potato is first in ranking for the agricultural economy of the region.

In recent years crop production has given way to livestock activities, both with regard to area and intensity of development. Livestock farms produce pigs, poultry, and sheep; however, the trend of agricultural exploitation is towards dairy farming, which is located primarily in the flat or valley area of the lower basin. Dairy production in the area has increased due to the trend to improve the dairy herd with specialized breeds, genetic improvement, and animal feed supplements. The average production is 732,029 liters / day (equivalent to 267 million liters per year) and is increasing about 2.5% annually.

On the other hand, mining activity is of great economic importance in the basin. There are about 268 mines, of which about 98% are coal and only 2% are gravel, according to the INGEOMINAS inventory for 2005. In general, the technological level of coal mining in the basin it is very low, since many operations are manual. The figures for the number of mines and their specific location date back many years. However, export figures are presented, which allows us to infer a link to the foreign market. Mining activity is an important source of employment, although its quality is low, with low remuneration for families. In addition, most of the mines lack safety plans for their workers, being very vulnerable to accidents.

3.2.5 Environmental characterization

This watershed has great environmental and social potential. Water sources and large landscapes make up strategic ecosystems with structural and functional characteristics providing direct benefits for the inhabitants of the region. In the watershed there is a predominance of semi-humid cold climate, which favors the availability of water by interception of air masses. This phenomenon is influenced by vegetation, which serves as an interception trap. For example, within the watershed páramo is a strategic ecosystem due to its high hydrogeological productivity (the Páramo de Rabanal). It is an ecosystem that is also very important for providing protection for wildlife and floristic corridors.

However, the search for productive organic soil motivates the destruction of forest cover in the upper part of the basin. For example, potato cultivation causes strong environmental impacts (high levels of toxicity and nutrient depletion in runoff), and

potato production is moving toward the paramo area. Similarly, the area of improved pasture has grown due to the expansion of dairy activity in the basin. This activity includes the use of agrochemicals to improve pasture production and the use of forage species that are not always compatible with the natural environment, harming the region's soils, water resources, and especially its fauna and flora.

On the other hand, the soils present in the basin are superficial to very superficial and favor the loss of nutrients in runoff. In the rainy season, when the sediment load in the bodies of water increases and they take on a particular color, the negative environmental impacts of this process are more evident. Additionally, the basin has a low water production, which together with the other characteristics mentioned above can cause serious supply problems and even loss of water bodies.

Finally, most of the municipalities in the basin lack wastewater treatment systems. Therefore, the discharges of sewage and the disposal of solid waste in rivers and streams are largely uncontrolled, causing an increase in pollutants in the bodies of water. For example, there are some home-grown potato processing industries that strongly affect water resources due to potato washing because the starch residues in the effluents cause fermentation and the production of abundant foam in thewater.

3.3 CASE 2- RIOGRANDE II WATERSHED

3.3.1 Catchment description

The Riogrande II watershed is located northwest of the city of Medellin (Colombia). The watershed area is 1,034 km^2 and lies between longitudes 75 32' 30'' and 75 26' 10''W, and between latitudes 06 33' 50''and 06 28' 07'' N (Figure 3.4a). The topography varies between 2,229 and 3,314 meters above sea level. Three main tributaries (the Grande and Chico rivers and Las Animas stream) drain into the Riogrande II reservoir. The water from the reservoir is used for electricity generation at the Tasajera hydroelectric power station, and it supplies drinking water via the Manantiales drinking water plant, which currently provides between 30 and 45% of the drinking water to the Valley of Aburrá (Corantioquia and Universidad Nacional de Colombia, 2015).

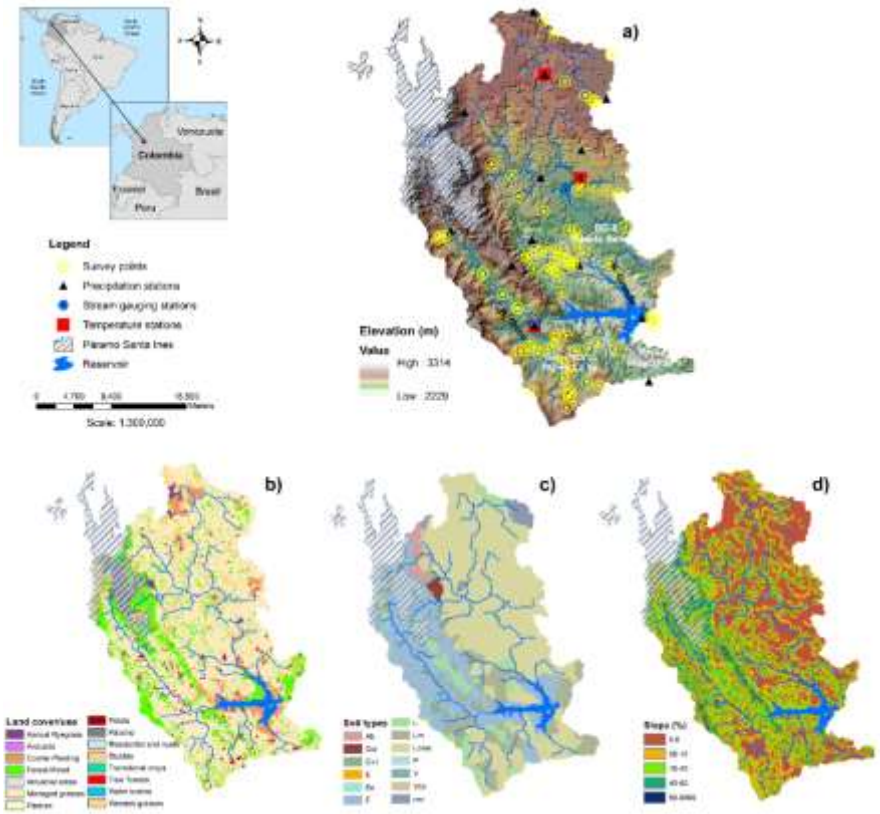

Figure 3.4. Map of the modeled area showing the (a) location of weather stations and survey points, (b) land cover types, (c) soil types, and (d) slopes of the Riogrande watershed

3.3.2 Climate

In general terms, the climate in this area is defined by inter- and intra-annual variations. Intra-annual variation is a phenomenon that is directly related to the particular conditions of the site. In the study area, convective-type precipitation occurs due to the mountain valley effect. Orographic precipitation also takes place due to the mountainous barriers and the variable topography of the area surrounding the plateau.

To characterize the precipitation and temperature of the hydrographic basin, data from 16 weather stations located within the watershed (Figure 3.4b) obtained from Medellin's Public Service Company (EPM) and Institute of Hydrology, Meteorology and Environmental Studies (IDEAM) (Table 3.3) were used. The annual average rainfall is 2,150 mm, with a bimodal regime (Poveda et al., 2014). There are two precipitation peaks throughout the year, the first in April and May with an average of 273 mm and the second in September and October with an average of 255 mm. The minimum of precipitation occurs in January (112 mm). The two dry periods are between December and February, and from mid-June to August (Figure 3.5). The spatial distribution of the mean annual precipitation was estimated from the isohyets at a scale of 1: 25,000, obtained from

Corantioquia. It is highlighted that 41.8% of the territory (53,772.9 ha) receives mean annual rainfall between 1,750 to 2,000 mm, this occurs in the lower middle part of the watershed. In the upper middle part of the watershed an area of 32.4% (41,693.7ha) has mean annual rainfall between 2,000 to 2,250 mm. And a smaller area of the upper part receives mean annual rainfall between 2,250 to 2,500 mm. In general, 74.2% of the territory of the Riogrande II watershed receives between 2,250 mm per year and 1,750 mm.

The mean monthly temperature varies between 9°C and 20°C and the mean annual temperature is around 15.6°C for the study area (Figure 3.5). The paramo area has a mean monthly temperature of 10°CThe upper middle part of the watershed has around 12°C, and the mean monthly temperature in the low area, near the reservoir, is between 14 to 16°C. On the other hand, the mean monthly potential evapotranspiration fluctuates between 70 and 79 mm, with a monthly mean of 76.1mm and an annual mean of 913.2mm. In the highest parts of the basin the mean monthly radiation of 71W/m^2 and in the lowest parts it can reach up to 100 W/m^2.

Table 3.3. Hydro-metereological stations at Riogrande II watershed

Name	Latitude	Longitude	Elevation	Precipitation	Temperature
Aragon	6.783	-75.561	2630	X	X
El Chaquiro	6.755	-75.490	2750	X	
El Gomez	6.739	-75.652	2675	X	
Medina	6.423	-75.532	2620	X	
Belmira	6.605	-75.667	2520	X	
Entrerrios	6.566	-75.521	2285	X	
San Bernardo	6.854	-75.574	2740	X	
Presa Riogrande II	6.506	-75.449	2280	X	
Alto de la sierra	6.565	-75.597	2750	X	
El Tururo	6.594	-75.575	2450	X	
Los Atajos	6.697	-75.519	2575	X	
SanPedro10 LaYe	6.497	-75.571	2340	X	X
Cucurucho	6.664	-75.519	2580	X	X
Rg-7 El Boton	6.666	-75.565	2470	X	
Rg-6 Puente Belmira	6.652	-75.538	2446		
Alto San Andres	6.434	-75.441	2240	X	

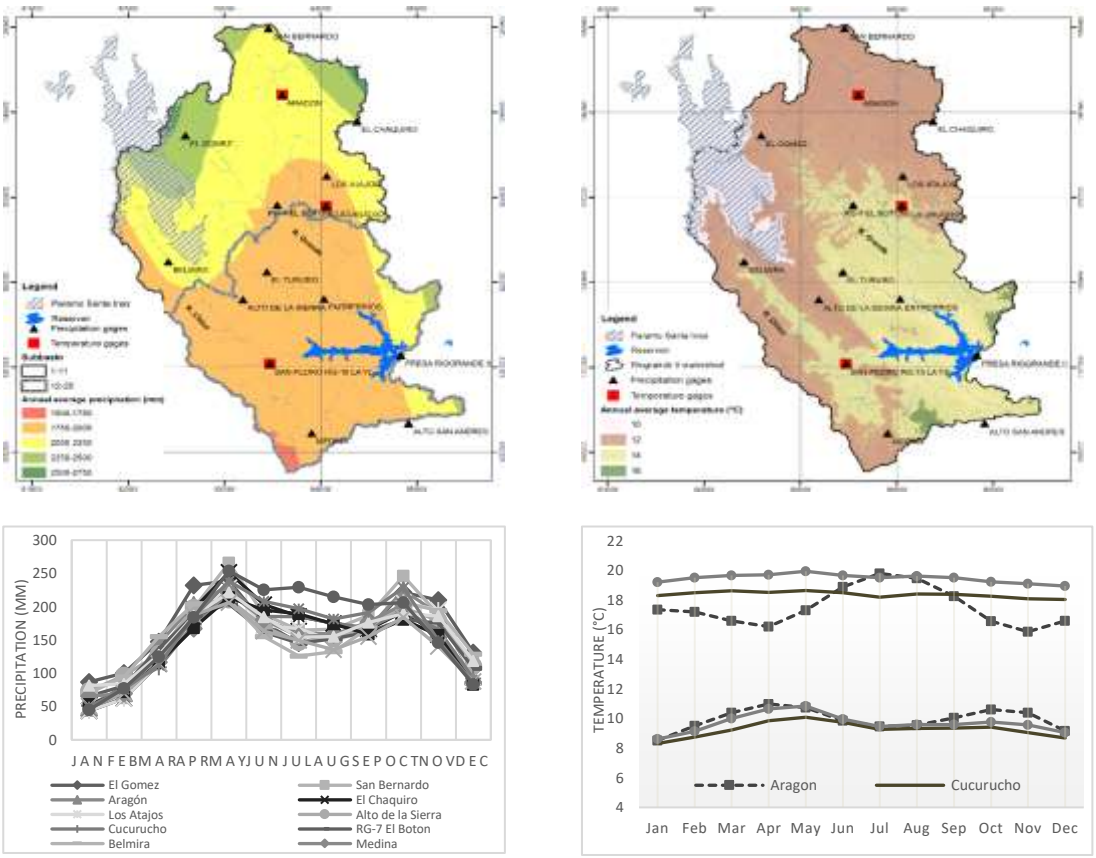

Figure 3.5. Annual average maps (top) and monthly average graphs (below) of precipitation (left) and temperature (right) at Riogrande II watershed.

3.3.3 Vegetation cover and soils

The native vegetation of the basin has been significantly reduced due to human intervention, mainly for grazing. Between 2005 and 2015, the area of natural forest decreased by 7% (CORANTIOQUIA and UNAL, 2015). Some native forests and the moorland (alpine tundra ecosystem or páramo) of Belmira (16% of the basin area) remain undisturbed, mainly in the higher areas. The páramo vegetation is located in the municipality of Belmira, in the páramo that bears the same name. It is short vegetationcomposed of grasslands in association with the *frailejón* (the dominating species of the paramo) located in hilly and flat areas. There are natural intervening forests and oak groves in patches of medium to small areas, located around the Páramo de Belmira. Grazing lands grew by approximately 27% between 2005 and 2015 (Corantioquia and Universidad Nacional de Colombia, 2015). Currently, agriculture and livestock occupy 80% of the total watershed area. Pastures associated with dairy farming, tree tomato (*Solanum betaceum*, also known as tamarillo) and potatoes (*Solanum tuberosum*) are the most prevalent agricultural activities (Table 3.4), followed by coffee and avocado cultivation (Ramírez, 2014) (Figure 3.6).

The soils in the watershed belong to the Andic Dystrudepts, Fluventic Dystrudepts, and Typic Dystrudepts subgroups, which are developed from igneous rock and volcanic ash. These soils are generally characterized by being deficient in nutrients (nitrogen, phosphate, and calcium), low fertility, medium to extreme acidity (pH from 4.5 to 5.6), and medium to high organic matter content. The mineralization is not very significant due to low temperatures. Crops on these soils respond well to organic and chemical fertilization (Corantioquia and Universidad Nacional de Colombia, 2015). In some areas with steep slopes there are soils that are classified as unsuitable soils for agriculture, mainlybecause they are steep and have soils with light to medium textures, including sandy loams, clay loams, and loam.

Table 3.4. Land cover areas at Riogrande II watershed

Land Cover	Area (%)	Land Cover	Area (%)
Annual Ryegrass	1.97	Pasture	0.01
Avocado	0.08	Potato	0.85
Conifer Planting	4.36	Residential and roads	1.05
Forest-Mixed	16.38	Stubble	6.25
Industrial areas	0.00	Tree Tomato	0.34
Managed grasses	58.31	Water bodies	1.33
Transitional crops	0.37	Weedy grasses	5.84
Páramo	2.86		
Watershed total area = 103434.77 ha			

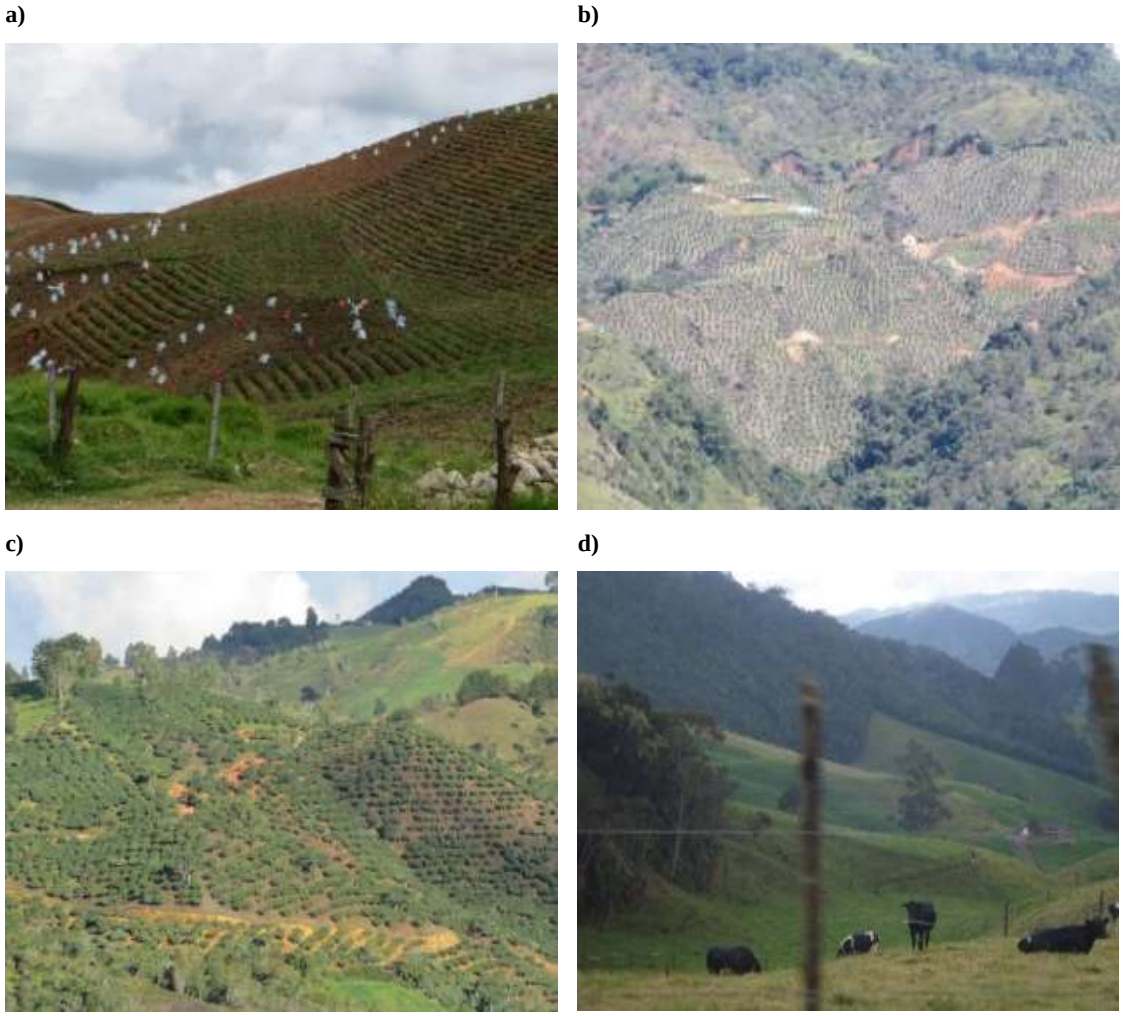

Figure 3.6. Land cover photographic record (a) potato, (b) coffee, (c) tree tomato, and (d) managed pastures associated with cattle ranching at Riogrande II watershed.

3.3.4 Socio-economic characterization

The total population of the Rio Grande watershed is approximately 68,066 inhabitants. The most farms have between 0 and 10 hectares. However, in municipalities such as Santa Rosa de Osos, plots of 10 to 50 hectares predominate. The municipalities with the highest percentage of properties larger than 50 hectares are Belmira and Santa Rosa de Osos. Most of the land in the basin is used for dairy farming, pig farming and other agricultural activities, which are consolidated as the most important economic activities. However, some past analyses suggest that the preferred use for the basin would be commercial forestry for a large part of the territory (Corantioquia and Universidad Nacional de Colombia, 2015).

Dairy is the main economic activity within the basin, mainly focused on breeds suitable for milk production. The predominant breed is Holstein, pastured on kikuyu grass

(*Pennisetum clandestinum*) and ryegrass (*Lolium sp.*) and supplemented with concentrated feed. A large part of the farms use this type of production system to produce high volumes of milk, with some cows reaching a peak production of 56 l day^{-1}, for an approximate average of 20 l cow^{-1} day^{-1}. Most farms have between 10 to 60 milk cows. The milk produced is generally sold to the Cooperativa Lechera de Antioquia (Colanta).

The two most economically important cropping activities in the watershed are potato and tree tomato cultivation. The potato (*Solanum tuberosum ssp. Andigena.*) is currently planted at any time of the year, which causes constant changes in the supply and demand of the product and therefore fluctuations in prices. The five municipalities with the highest percentage of area in the basin represent 68.1% of the total production of the North Subregion of the department, wherethe municipalities of Santa Rosa de Osos and San Pedro de los Milagros represent 59% of the total production. On the other hand, the tree tomato crop (*Cyphomandra betacea Cav. Sendt*) is one of the most productive crops developed in the watershed. Production has grown for the past 25 years, and tree tomatoes are planted and harvested throughout the year, and tree tomato crops occupy almost 60% of the cultivated land in the watershed.

In the basin there are other smaller-scale economic activities such as fish farming and tourism. Tourism has been considered a dynamic factor for the generation of employment, the improvement of road and urban infrastructure, and support for agricultural production. In the basin, it is worth highlighting the tourist developments related to rdairy farming, with the purpose of educating and promoting this activity in urban areas. The production of rainbow trout is another economic alternative. However, the development of this activity is limited by the absence of economic resources to support producers and the lack of clear policies for the sector. The trout are commercialized directly with warehouses in Medellín and neighboring municipalities, and a small part is destined for self-consumption. This activity occurs mainly in the municipalities of Belmira and Entrerríos.

Traditional land use activities in the watershed were home gardens with aromatic plants, vegetables, and grain crops, but they have been mostly replaced by pastures for used for cattle and pig production. Only small plots of products such as beans, corn, vegetables, and fruit remain primarily for self-consumption. This transformation in the economic sphere has generated food dependency in peasant families in Antioquia, who now must buy much of their food in urban centers.

3.3.5 Environmental characterization

Critical parts of the water supply basins, the oak forests, and the Belmira páramo are considered protected areas within the watershed. In the Belmira páramo there are many sources of drinking water that satisfy the basic needs of the human and animal populations in the watershed. However, the páramo system (considered to be above 3000 meters above sea level and covering 9,085 hectares) is threatened, due to expansion of the agricultural frontier towards the páramo area. Even though forest cover has decreased

only slightly (less than 10%), fragmentation throughout the watershed is strong to extreme. Deforestation and inappropriate soil management for agricultural and livestock activities contributes to increased erosion, landslides, and loss of biodiversity in the basin. Mass soil movement has also increased due to the opening of roads for the transport of agricultural products (crops, cattle, pigs, milk) without prior technical studies or drainage infrastructure.

In general, the quality of the water is classified as fair in the middle and lower parts of the watershed. The main causes of water contamination are productive activities in soils low in nutrients where producers use large amounts of chemical inputs, especially in potato crops, tree tomatoes and livestock in general. Also, the bodies of water directly receive discharges of domestic wastewater, agrochemicals, and fertilizers such as porquinaza (manure from pork production). However, in the municipalities located in the upper part of the basin, water quality is often classified as good, and the water is used for domestic supply with minimal purification.

In terms of quantity of water, the water consumption rate in the watershed is high. In many sectors of the watershed the total flow of the streams is being used and therefore deteriorating the water ecosystem. For example, all the water provided by a wetland located 10 meters upstream from the intake is captured in the Santa Bárbara local aqueduct intake. And in the sub-basins directly contributing to the Riogrande II reservoir, the minimum flow of the rives where less than the demand during a period of 2 years.

4

ANALYSIS OF A SINGLE AGRICULTURAL BMP IMPACT FOR A SINGLE CROP AT FIELD AND WATERSHED LEVELS

"Conocer la realidad para proponer"

This chapter is based on Uribe, N., Corzo, G., Quintero, M., van Griensven, A., & Solomatine, D., 2018. Impact of conservation tillage on nitrogen and phosphorus runoff losses in a potato crop system in Fuquene watershed, Colombia. Agricultural Water Management, 209, 62-72

4.1 ABSTRACT

Intensive tillage (IT) in potato crops is considered one of the primary non-point sources (NPS) of local water eutrophication in the Fuquene Lake of Colombia. Therefore, the local government has invested in several programs aiming to increase adoption in the watershed of conservation tillage (CT), a recognized agricultural best management practice (BMP). The complexity of hydrological and geological heterogeneity in the watershed makes the benefit of implementing CT uncertain. In this study, the Soil and Water Assessment Tool (SWAT) was used to assess the impacts of changing IT to CT on nitrogen (N*)* and phosphorus (*P*) losses in surface water runoff from the potato crop in the Fuquene watershed. This is done at field and watershed levels. A two-year study quantified the changes in N and P in surface water runoff for three potato crop cycles under the traditional ITand three CT practices, reduced tillage, green manure, and permanent soil cover, in twelve runoff plots installed in the Fuquene watershed (Quintero and Comerford, 2013). This information was used to build, calibrate and validate the SWAT model. The results suggest that CT for the Fuquene watershed can reduce sediment yield by 26% and surface runoff by 11% compared with IT. The main CT effect on nutrient losses in runoff is an increase in the total losses of N and P (2% to 18% respectively) compared to IT. However, the results at the watershed level showed different patterns from those obtained at the field level. Despite the model uncertainties, the results show a possibility of using hydrological models to assess the effectiveness of various field management practices in agriculture.

4.2 INTRODUCTION

The decline in the water quality in the Fuquene watershed (Colombia) is a severe environmental problem, especially in Lake Fuquene, where an accelerated eutrophication process has been observed (Japan International Cooperation Agency—JICA, 2000). Nitrogen and phosphorus runoff from potato crop fertilization are estimated to be causing the increase of nutrients in the lake, which has, in turn, increased the frequency of algae blooms (Rubiano et al., 2006b). As a result, the biodiversity in the lake is threatened, as well that the drinking water for the local communities. An additional problem has been leakage of a toxic chemical in the treatment process (Hanifzadeh et al., 2017), and also water for agriculture, fisheries and, particularly, for livestock (Quintero and Otero, 2006; Rubiano et al., 2006b). Therefore, the environmental authorities aim to address this problem due to the importance of this water source for the communities, agriculture, and livestock (Rubiano et al., 2006a).

Intensive tillage (IT) is the conventional management practice used by potato farmers in the Fuquene watershed. This practice is characterized by a lack of plant coverage and low crop residue levels in the potato cycle. Because of this, the soil is vulnerable to erosion and nutrient losses in the runoff (Zhang et al., 2014; Carter et al., 2009). Therefore,

research nowadays focuses on agricultural BMPs, which endeavor to use nutrients efficiently, conserve the soil structure and reduce runoff (Quintero and Comerford, 2013; Logan, 1993). In this context, agricultural BMPs that focus on no-tillage and reduced tillage are increasingly being adopted by farmers because they have the potential to reduce water pollution and to develop environmentally-friendly agricultural systems, which at the same time will offer better income to local farmers (Liu et al., 2013; Sedano et al., 2013; Panagopoulos et al., 2011; Soane, 1990). Studies indicated that use of BMPs in potato crops could reduce the loss of nutrients without any adverse effect on the potato yield and quality. However, there may be some influence on potato maturation and the harvest date (Carter and Sanderson, 2001). A study done in 14 potato field trials at various locations across Idaho and Oregon, USA over four years demonstrated that potato farmers following BMPs received a similar yield with less financial investment than when following a maximum yield approach (Hopkins et al., 2007). Also, Zebarth and Rosen (2007) clarified that even when BMPs are developed to optimize tuber yield and reduce losses of nutrients, it is necessary to select the appropriate rate and timing for applying nitrogen-based fertilizers. In this way, it is possible to control potato growth according to the soil properties, water management, climatic conditions, and terrain slope.

In Colombia, the regional environmental authority (Corporacion Autonoma Regional – CAR) in the Fuquene watershed has been investing in adopting conservation tillage (CT) since 1999 for the potato crop production system. In this chapter, CT is defined as any practice of soil cultivation that reduces runoff and increases infiltration by leaving the previous crop residues on the field (Derpsch, 2003). This also increases the soil organic matter near the soil surface, improving the soil structure and biological properties in the potato crop (Carter et al., 2009). Experience has shown that CT provides potential benefits by increasing soil organic matter, improving soil hydraulic properties, and protecting the soil protection from the impact of rainfall (Carter and Sanderson, 2001). Nevertheless, some management effects on soil biological properties' are not measurable in the short term (i.e., less than five years) (Carter, 1992).

The International Center for Tropical Agriculture (CIAT) has been researching the impact of CT on nutrient and soil losses in this crop since 2010 in the Fuquene watershed. Experimental runoff plots were installed, and the IT and CT practices were applied. The specific CT practices adopted in the pilot project included reduced tillage, green manure, and a permanent cover crop before potato sowing. Sediment yield and loss of nitrogen (N) as NH_4^+ and NO_3^-N and phosphorus (P) as PO_4^{3-} in runoff were measured. The results helped to understand the effect of CT at the field level. For example, Quintero and Comerford (2013) investigated CT's impact on soil organic carbon in the potato cropping system in the Fuquene watershed The results indicated that reduced tillage in potato-based crop rotations increased the soil carbon concentration and average C content in the full profile by 50% and 33%, respectively, compared to conventional farming practices. Thus, CT helps to bring these soils back to their original characteristics (high organic matter soils) (Quintero and Comerford, 2013).

Several studies report the effects of CT on pollutant losses by applying hydrological modeling tools. Many of these studies describe the accuracy of pollutant prediction obtained for each case study. However, the results are found to vary significantly and provide essential insights only for particular agricultural watersheds (Park et al., 2014; Amon-Armah et al., 2013; Liu et al., 2013; Bosch et al., 2013; Betrie et al., 2011; Lam et al., 2011). Despite the increased use of modeling tools to assess CT's impact as an agricultural BMP on pollutant losses, there are still knowledge gaps in this topic. One of the most common issues identified to date is evaluating the effectiveness of BMPs at controlling nonpoint source pollution to obtain the necessary information that would help decision-makers develop environmental regulations and manage the agricultural sector. Therefore, the objective of this research is to assess the impact of CT on sediments, nitrogen (N), and phosphorus (P) losses in the runoff for potatoes at field and watershed levels by applying the Soil Water Assessment Tool (SWAT). This chapter will contribute by answering the questions: How do the management practices in a potato-based mixed crop system influencing the runoff and soil nutrients (N and P) losses at the field and watershed levels? What would be the effect of applying CT in current potato systems throughout all the watershed?

4.3 METHODOLOGY

Parameters related to the crop database, soil, and agricultural management practices in the SWAT model were set to represent local cropping systems. Calibration was carried out using data regarding the impact of management practices on soil and nutrient losses and runoff (measured in the field) and streamflow data from gauging stations. Usually, the hydrological model calibration process is challenging forColombian watersheds, where the complexity of shifting cultivation, intensive traditional agriculture, diverse crops and management practices, and weather seasonality must be considered. Also, CT management practices for the potato crop were extrapolated to the whole basin to assess their likely effects at the watershed scale. Additionally, the IT and CT effectiveness at the field and watershed level were evaluated to provide guidelines for the decision-makers and stakeholders who aim to use these agricultural management practices for the potato crop.

4.3.1 Hydrological and water quality model

The watershed model used in this study was the Soil and Water Assessment Tool (SWAT) developed by the United States Department of Agriculture – Agricultural Research Service (USDA-ARS) (Arnold et al., 1998). The input data required for this study were compiled from different sources. These include the Agustin Codazzi Geographic Institute (IGAC), the Institute of Hydrology, Meteorology and Environmental Studies (IDEAM), the Regional Environmental Authority of Cundinamarca (CAR), and the public service

companies (water and electricity supply). The resolution, scale, and sources are shown in Table 4.1.

The weather input data from 46 stations located in the basin were collected by public and private institutions and were provided by CAR (Fig. 3.1 - Chapter 3). The historic recorded daily data included: relative humidity, precipitation, temperature (maximum, minimum, and average), solar radiation, and wind speed. Monthly flow measurements at the Boyera, El Pino, Puente Balsa, and Puente Colorado stations were used to represent the flow in different stream segments. The Puente Colorado station is located near the end of the basin and represents the entire watershed outlet just before the main river reaches the lake (Fig. 3.1 - Chapter 3). The Puente Balsa station has three months of missing records in 2008 and one month in 2013. Likewise, the Puente Colorado station did not record values for 2006, 2008, and 2009. Therefore, these dates were not used to calculate errors in the calibration and validation processes.

Table 4.1. Spatial input data description

Data type	Resolution	Source
Topographic map	30m	CAR
Land use map	1:25.000	IGAC
Soil map	1:100.000	IGAC
Weather	No. of stations: 21	CAR-IDEAM

For this study, the SWAT model was built on a daily time step from 2006 to 2013. The watershed was delineated into 30 sub-basins (Fig. 3.1 - Chapter 3). In the generation of HRUs, the slope classes were always set out in five ranges (0–5%; 5–15%; 15–25%; 25–45%; and >45%). The potential evapotranspiration (PET) was simulated using the Hargreaves method (Hargreaves and Samani, 1985), and the actual evapotranspiration (AET) was calculated based on the methodology developed by Ritchie (1972). The Natural Resources Conservation Service Curve Number (CN) method (USDA-SCS 1972) was used to predict the surface runoff. CN values were determined based on a previous study, where the Colombian Land Cover map categories were associated with SWAT land cover codes (IDEAM et al., 2008).

4.3.2 Agricultural management practices characterization

Agricultural management practices are inputs to the model defined in the management files. The representation of the traditional and conservation agricultural management practices for potato were simulated as scenarios. “IT” is used to represent the baseline (traditional management) scenario, and “CT” represents the conservation practice

scenario considered. 1. Seven HRUs were defined and correspond spatially to the plots installed in the field. These are characterized by being located in sub-basin 12 with a mean slope of 15% to 45%, and soil units MMVe3 and MMVg3, which are Inceptisols classified by IGAC as Typic Haplustepts (IGAC, 2000).

Based on previous results from the experimental runoff plots installed in 2011 by CIAT in the municipality of Ubate, which is located in the watershed, the SWAT parameter values related to management practices were defined (Quintero and Comerford, 2013; Quintero, 2014). The pilot Fuquene project established twelve experimental runoff plots - each with an area of 2,500 m^2 - for assessing two potato-based systems: conventional agriculture with intensive tillage (IT) and conservation agriculture with oat cover crop residues (green manure - GM), and conservation tillage (CT). A total of three crop cycles were planted in September 2011, March 2012, and October 2012. Conventional agriculture with IT is traditionally a rotation between potato (*Solanum tuberosum*) and pasture (*Lolium perenne*) with grazing (Quintero, 2014). The IT operation is carried out by conventional plowing followed by rotovator passes to invert the soil (Figure 4.1).

On the other hand, the CT adopted in the pilot Fuquene project included different management practices such as reduced tillage, green manure, and permanent soil cover. The CT rotation (oats-potato-oats-potato-pasture) involved potatoes with an oat cover crop used as green manure prior to potato planting, and pastures at the end of the rotation cycle (Quintero, 2014) (Figure 4.2). The management practices parameter values obtained from the runoff plots are shown in Table 4.2. The physicochemical characteristics of the soil measured in the field plots were defined in the soil database for the HRUs which correspond to the location of the runoff plots (Table 4.3).

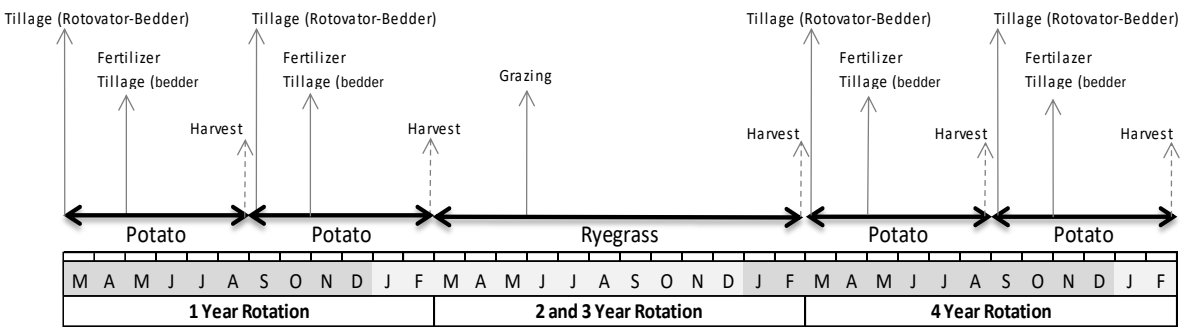

Figure 4.1. Conceptual outline of conventional (IT) potato crop management practices.

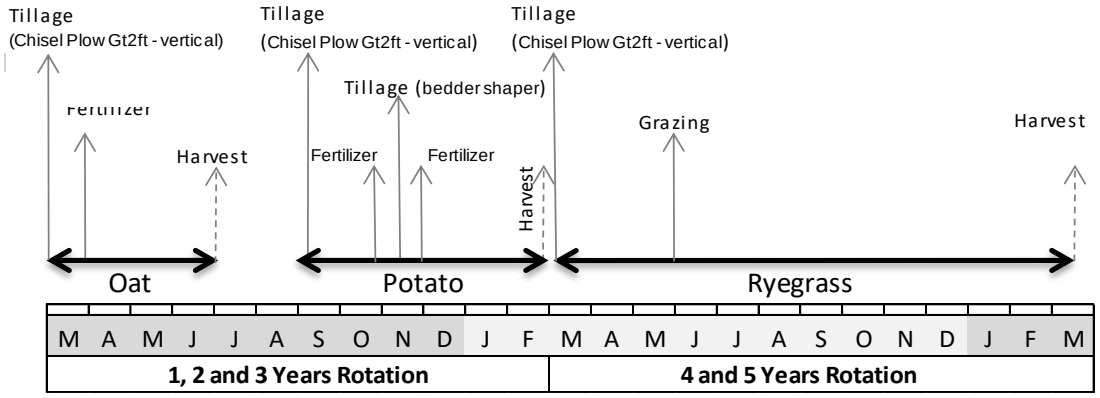

Figure 4.2. Conceptual outline of conservational (CT) potato crop management practices.

Table 4.2. Parameter values defined related management practices per scenario.

Variable name	Definition	Value				
		IT		CT		
Planting		Pota	Pasture	Pota	Oat	Pasture
PLANTID	Plant/land cover code from crop.dat	POTA	RYEG	POTA	OATS	RYEG
HEAT UNITS	PHU: Total heat units required for plant maturity	800	700	800	400	700
BIO_INIT	Initial dry weight biomass (kg/ha)	200		200	18	
CN2	Initial SCS runoff curve number (min 35- max 98)	62	40	62	53	40
Grazing						
MANUREID	Manure code from fert.dat		Beef-Fresh			Urea
GRZ_DAYS	Number of days of grazing		200			200
BIO_EAT	Dry weight plant biomass consumed daily (kg/ha)		30			30
BIO TRMP	Dry weight of biomass trampled daily ((kg/ha)/day)		14			14
MANUREKG	Amount of manure applied -dry weight (kg/ha)		6			6
BIO_MIN	Minimum plant biomass for grazing to occur (kg/ha)		500			500
Tillage						
TILLAGEID	Tillage implementation	Bedder shaper	Rotovator-bedder	Chisel Plow -vertical		Bedder shaper
EFFMIX	Mixing efficiency of tillage operation (fraction)	0.55	0.8	0.3		0.55
DEPTIL	Depth of mixing by tillage operation (mm)	150	100	150		150
BIOMIX	Biological mixing efficiency (fraction)	0.2	0.2	0.2	0.2	0.2
Fertilizer						
FERT_ID	Type of fertilizer/manure applied	13-26-06		13-26-06	Urea	
FRT_KG	Amount of fertilizer/manure applied (kg/ha)	1400(2*700)		1000(2*500)	300	
FRTSURFACE	The fraction of fertilizer applied to the top 10mm	1		1	1	

Table 4.3. Physico-chemical soil parameters are measured in the field plots defined in the selected HRUs.

Type	Depth (cm)	Bulk density (g/cm^3)	Soil available water content (mm/mm)	Hydraulic conductivity (mm/h)	Sand (%)	Silt (%)	Clay (%)	Organic matter (%)	Carbon (%)
IT	0 - 40	1.39	0.140	109.16	32	52	16	3.02	3.05
	40 - 60	1.58	0.160	76.30	33	50	17	1.16	0.57
CT	0 - 20	1.29	0.270	203.14	6	66	28	8.50	3.74
	20 - 40	1.29	0.420	101.07	25	38	37	5.89	2.59

4.3.3 Model calibration and validation

Traditional statistical indicators measuring the proximity of the predictions to the observed values were used to evaluate the performance of SWAT: Nash–Sutcliffe efficiency index (NSE) (Eq. (4.1)), the index of agreement *d* (Eq. (4.2)), the root mean square error (RMSE) (Eq. (4.3)), and the mean absolute error (MAE) (Eq. (4.4)).

$$NSE = 1 - \frac{\sum_{t=1}^{T}(O_i^t - P_i^t)^2}{\sum_{t=1}^{T}(O_i^t - \bar{O})^2} \tag{4.1}$$

$$d = 1 - \frac{\sum_{i=1}^{N}(O_i - P_i)^2}{\sum_{i=1}^{N}(|P_i - \bar{O}| + |O_i - \bar{O}|)^2} \tag{4.2}$$

$$RMSE = \sqrt{\frac{1}{N}\sum_{i=1}^{N}(O_i - P_i)^2} \tag{4.3}$$

$$MAE = \frac{1}{N}\sum_{i=1}^{N}|O_i - P_i| \tag{4.4}$$

where: O_i = measured (observed) data, P_i = modeled data, $\bar{O}$ = mean of measured data, and N is the number of observations during the simulation period. NSE ranges between -∞ and 1.0, with NSE=1 being the optimal value, and values ≤0. 0 indicates that the mean observed value is a better predictor than the simulated values, showing the unacceptable performance (Nash and Sutcliffe, 1970). A computed *d* value of 1 indicates a perfect agreement between the measured and predicted values, and 0 indicates no agreement at all. RMSE and MAE values of 0 indicate a perfect fit.

Global sensitivity analysis was carried out to assess the most sensitive parameters for setting up the model in this watershed. The built-in Latin hypercube one-at-a-time (LH-OAT) technique (Green and van Griensven, 2008; Morris, 1991) was used to determine the model sensitive parameters. The results obtained were used for flow calibration. Manual monthly calibration and validation were conducted using the data from the four-stream gauging stations: Boyera, El Pino, Puente Balsa, and Puente Colorado, compared with the outflows of sub-basins 12, 7, and 2, respectively (Fig. 1). All these comparisons were based on the Nash–Sutcliffe efficiency index (NSE) (Eq. 1). The index of agreement *d*, the root means square error (RMSE), and the mean absolute error (MAE), given by Equations (2) to (4), were used for each gauging station as a reference.

The second step of the calibration process was for losses of sediments and nutrients. The model was calibrated manually using the monthly data from September 2011 to March 2013 for sediments, surface runoff, and concentration of soluble P, and NO_3^--N in the runoff. The mean absolute error (MAE) was used to evaluate the model performance for total accumulated sediment yield and nutrient losses, collected from each runoff plot during the mentioned period. Validation was conducted at the field level with the results obtained in the HRUs where IT and CT practices were applied. . Tables 4.4 and 4.5 provide an overview of the parameters modified in the model calibration and their final calibration values.

4.4 RESULTS AND DISCUSSION

4.4.1 Streamflow model calibration

Sensitivity analysis was performed for streamflow to determine the most influential parameters on the model output. Table 4.4 presents the eleven most sensitive parameters related to streamflow of the 20 evaluated. The parameters were ranked according to the P-value (significance of the sensitivity) from the highest to the lowest, where the highest are the most sensitive parameters (Abbaspour et al., 2015). In general, Revapmn.gw (threshold water depth in the shallow aquifer for return flow by capillary and soil evaporation process), Gwqmn.gw (threshold water depth in the shallow aquifer required for return flow to occur), and Sol_k.sol (saturated hydraulic conductivity into the soil) were the most sensitive. The sensitivity analysis results were included in the streamflow model calibration. Table 4.5 presents the adjusted parameters to improve the efficiency

of the model in the studied watershed for predicting the streamflow, which correspond mainly to runoff and groundwater flow processes.

The simulation period was divided into two without including the first year, which was used as the period to “warm up” the model. The streamflow calibration process was performed for the first period (2006–2010), and the second period (2011–2013) was used for the validation process. The calibration and validation results are summarized in Table 4.6. According to guidelines developed by Moriasi et al. (2007), the monthly streamflow calibration values at the four gauging stations were considered 'good' for the calibration period (NSE values greater than 0.65 and index of agreement (d) values were close to 1), except the Puente Balsa station (NSE = 0.5). The validation model predicted monthly flows at the four stations with NSE= 0.54, 0.32, 0.58, and 0.61, respectively. Only those values obtained at the El Pino station were considered unsatisfactory in the validation period (NSE=0.32). Figure 4.3 shows the hydrographs for the calibration and validation results (the two periods separated by a red line) for each streamflow gauging station.

Table 4.4. Sensitivity analysis ranks results for streamflow model output.

Rank	Parameter[a]	t-value[b]	p-value[c]
1	r_Cn2.mgt	-0.014	0.989
2	r_Sol_awc( ).sol	0.040	0.968
3	v_Gw_revap.gw	-0.391	0.737
4	v_Gw_delay.gw	1.009	0.313
5	v_Shallst.gw	-1.134	0.210
6	v_Rchrg_dp.gw	1.617	0.183
7	v_Gw_spyld.gw	1.877	0.107
8	v_Alpha_bf.gw	-4.381	0.099
9	r_Sol_K( ).sol	-4.348	0.016
10	v_Gwqmn.gw	11.254	0.005
11	v_Revapmn.gw	-11.051	0.000

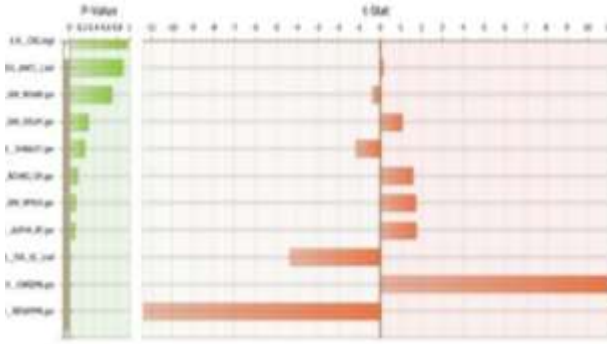

[a] v: parameter value is replaced by a value from the given range; r: parameter value is multiplied by (1 + a given value) (Abbaspour et al., 2007).
[b] *t*-value shows a measure of sensitivity: the larger the *t*-value, are more sensitive.
[c] *p*-value shows the significance of the sensitivity: the smaller the p-value, the less chance of a parameter being by chance assigned as sensitive

Table 4.5. Streamflow, sediment and nutrients parameters, allowable ranges, and final calibration values.

Parameter	Description in SWAT	Range	Model default value	Final value
Streamflow				
ALPHA_BF	Baseflow alpha factor [days].	0 – 1	0.048	0.02
GW_DELAY	Groundwater delay [days].	0 – 500	31	25
GW_REVAP	Groundwater revap coefficient.	0 – 1	0.02	0.02
RCHRG_DP	Deep aquifer percolation fraction.	0 – 1	0.05	0.1
REVAPMN	Threshold water depth in the shallow aquifer for revap [mm].	0 – 500	1	100
GWQMN	Threshold water depth in shallow aquifer for flow [mm].	0 - 5000	0	100
SHALLST	Initial depth of water in the shallow aquifer [mm].	0 - 1000	0.5	100
GW_SPYLD	Specific yield of the shallow aquifer [m^3/m^3].	0 - 0.4	0.003	0.2
GWHT	Initial groundwater height [m].	0 – 40**	1	25
CN2	Initial SCS CN II value.	35 – 98	Specific to HRU	
SOL_K	Saturated hydraulic conductivity [mm/h].	0 - 2000	Specific to soil survey unit	
SOL_AWC	Available water capacity [mm H_20/mm soil].	0 – 1		

Table 4.5. Streamflow, sediment and nutrients parameters, allowable ranges, and final calibration values.

Parameter	Description in SWAT	Range	Model default value	Final value
Sediment				
CN2	SCS runoff curve number for moisture condition II.	35 – 98	Specific to land use	$0.1*CN2_{default}$
USLE_P	USLE equation support practices.	0 – 1	1	0.5
Crop growth				
T_OPT	Optimal temp for plant growth.	Nov-38	22	17
T_BASE	Min temp plant growth.	0 – 18	7	5
HEATUNITS	Total heat units for cover/plant to reach maturity.	0 - 3500	1800	800*
Nutrients				
PHOSKD	Phosphorus soil partitioning coefficient.	100 - 300**	175	200
NPERCO	Nitrogen percolation coefficient.	0 – 1	0.2	1
RSDCO	Residue decomposition coefficient.	0.02 - 0.1	0.05	0.1
SOL_LABP	Initial soluble P concentration in surface soil layer [mg/kg].	0 – 100	0	44
SOL_NO3	Initial NO_3 concentration in soil layer [mg/kg].	0 – 100	0	12
SOL_ORGN	Initial organic N concentration in soil layer [mg/kg].	0 – 100	0	10
SOL_ORGP	Initial organic P concentration in surface soil layer [mg/kg].	0 – 100	0	10
PPERCO_SUB	Phosphorus percolation coefficient.	10 -17.5	10	17
BIO_TARG	Biomass (dry weight) target [metric ton/ha].	4 – 100	0	30
FRT_SURFACE	Fraction of fertilizer applied to top 10mm of soil.	0 – 1	0	1

**The maximum was adjusted for the case study.

Table 4.6. Calibration and validation flow performances at the watershed level.

Station	CALIBRATIO					VALIDATION				
	Flow rate (m_3/s)		NSE	RMSE	MAE	Flow rate (m_3/s)		NSE	RMSE	MAE
	Simulated	Observed				Simulated	Observed			
La Boyera	1.5	1.41	0.78	0.6	0.45	1.6	1.32	0.54	0.59	0.41
El Pino	0.52	0.43	0.61	0.28	0.21	0.42	0.32	0.32	0.2	0.15
Pte. La Balsa	1.58	1.38	0.50	0.79	0.62	2.03	1.45	0.58	0.78	0.66
Pte. Colorado	3.58	3.85	0.68	1.68	1.3	4.6	3.87	0.61	2.26	1.79

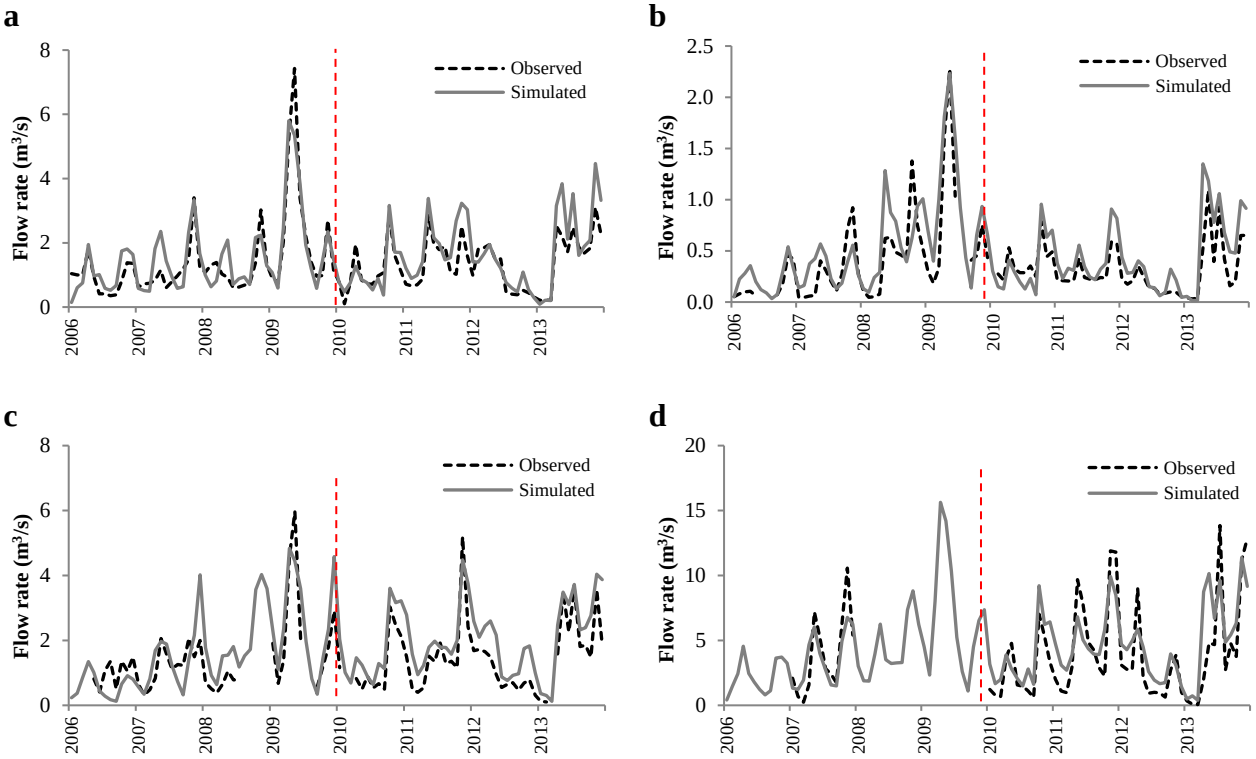

*Figure 4.3. Monthly calibration and validation results for flow (**a**) La Boyera, (**b**) El Pino (**c**) Pte. Balsa, and (**d**) Pte. Colorado.*

Overall, the monthly streamflow predictions were considered acceptable for this project. The baseflow was generally well represented by the model when compared to the observations. However, the peaks for certain times of the simulated period were slightly overpredicted. This is expected, considering that the watershed is under intensive agriculture, and only the potato crop management was considered. Additionally, the calibration and validation were affected by the lack of information on the "El Hato"

reservoir (located upstream) and the dams upstream constructed for irrigation. Similar findings have shown the overprediction of peak flows (Arnold et al., 2012; Harmel et al., 2014; Daggupati et al., 2015; Francesconi et al., 2016), which confirms that there is more significant uncertainty in the calibration process, particularly for scenarios and case studies in which information on upstream water management is not available.

4.4.2 Water quality model calibration

Calibration of nutrient losses in the runoff and sediments was performed for the available experimental period (September 2011 to March 2013) on the runoff plots related to the HRUs selected. Table 4.5 presents the adjusted parameters to improve the efficiency of the model in the studied watershed for the prediction of sediments and nutrients. In general, the calibration of the water quality for the IT management practices (baseline) was done by decreasing the sediment yield, increasing the content of NO_3^--N, and decreasing soluble and organic P yields. Some important parameters are the CN2 defined for potato, which is the model database was increased by 10%, and the USLE_P (ratio of soil loss with a specific support practice) changed from 1 to 0.5 to reduce the sediment yield due to greater aggregate stability of these Inceptisols. In the case of the nutrients in the soil layer, the initial concentrations of NO_3^--N, soluble P, organic N, and P (Sol_no3, Sol_labp, Sol_orgn, and Sol_orgp) were defined according to measurements obtained in the runoff plots.

The measured and simulated total (accumulated) values were compared for (i) the surface runoff, (ii) NO_3^--N, (iii) the soluble P, and (iv) sediment losses at field level (HRU analyzed). The calibration for sediments and nutrients was considered to be acceptable (Moriasi et al., 2007). The results (Table 4.7) showed that the highest absolute errors were calculated for surface runoff, with values of 1.5 and 2.3 l/m^2 for the IT and CT scenarios, respectively. However, the absolute error (Table 4.7) for the other variables was less than zero for each measurement unit. Despite the errors reported, a similar trend was observed for the IT and CT values simulated compared with the field observations (runoff plots measurements). In both cases total runoff and soil losses are reduced in the CT scenario.

In contrast, the nitrogen and phosphorus concentrations in the runoff from the CT plots were higher than the intensive tillage (IT). However, the calibration can probably be further improved if continuous records of water quality parameters were available. Also, several calibration techniques have been developed for a physically-based model like SWAT (Smarzyńska and Miatkowski, 2016; Me et al., 2015; Akhavan et al., 2010; Harmel et al., 2014; Arnold et al., 2012), and these could be suitable depending on the final goal of the modeling.

Table 4.7. Sediment and nutrient losses performance.

Variable**	Measured		Simulated		ε*	
	IT	CT	IT	CT	IT	CT
Runoff water						
Surface runoff (l/m_2)	27.45	26.05	28.97	24.03	1.53	-2.01
NO_3^- in surface runoff (kg N/ha)	0.68	0.72	0.39	0.47	-0.29	-0.25
Soluble P yield (kg P/ha)	0.18	0.20	0.21	0.29	0.03	0.08
Sediments						
Sediment yield (T/ha)	0.62	0.07	0.58	0.31	-0.04	0.25

*** ε**: Absolute error. ** Accumulated total values from September 2011 to March 2013.

4.4.3 The effectiveness of CT-BMP at field level

The effectiveness of CT was first evaluated at the field level with SWAT. The period from September 2011 to February 2012 was selected to simulate the CT and baseline (IT) scenarios. This period was chosen because it corresponds with the potato cultivation phase in both practices. In addition, CT spatial extrapolation was done for the whole potato crop area to estimate the water quality impacts if BMPs were applied by all farmers. Table 4.8 shows the results of IT and CT's direct effects on the average monthly runoff, sediment, and nutrients in the runoff at the field vs. watershed scales.

The CT practice results showed a reduction of sediment yield of 46% and of surface runoff of 27% at the field level (Table 4.8). The simulated sediment loads tended to decrease when surface runoff decreased, and the same trend was found for soil loss, but not as great as for the sediment loads (Figure 4.4). Furthermore, soil loss reduction was almost twice the reduction of runoff during the rainy season. It is noteworthy that the percentage of runoff reduction (27%) is similar to the increase in infiltration obtained for CT, which varies from 429 mm H_2O to 553 mm H_2O (representing a 29% increase). Therefore, when the runoff is minimum and infiltration is maximum, there is a high possibility of water moving through the root zone (Stewart and Lal, 1994). Our study found that the soil–water content increased (approximately 3%), a result similar to previous studies carried out in the same watershed (Quintero, 2009; Quintero and Comerford, 2013: Quintero, 2014). The trend of high infiltration as a consequence of CT practices has been reported by other studies (Deubel et al., 2011; Ram et al., 2018; Villamil and Nafziger, 2015); however, those results varied widely depending on the soil type, cropping system, and management.

Additionally, the mass balances of nitrogen and phosphorus were analyzed to understand the differences between the effects of CT and IT practices on nutrient losses. The mass balances showed that N and P's total losses in the runoff from CT practices

were 17% and 29% greater, respectively, than from IT practices. The total N and total P yields in the runoff at the field level are shown in Figure 4.5. The field-level results agree with the results from the data measured in the runoff plots reported by CIAT (Quintero et al., 2013; Quintero, 2014). The main reason that total N and P losses were greater for CT than IT scenarios is that organic N and soluble P were 50% and 38% greater, respectively, in the CT treatment than in the IT treatment (Table 4.8). This might be attributed to the greater residual cover crop (oat as green manure) in the potato–pasture rotation in the CT scenario.

The average concentration of nitrate N in the runoff was 20% greater (Table 4.8) in the CT practice than in the IT practice. Furthermore, this result was more evident in specific events. The transformation of fresh organic N to mineral N suggests an increase of up to 162 kg N ha^{-1} in the CT practice, compared with 47 kg N ha^{-1} in the IT practice. Mineralization of active nitrogen was up to 248% greater in the CT, compared to IT. The mineralization of nitrogen from fresh plant residue to nitrate N, is about 80%, while active organic nitrogen is 20%. This means that mineralization generates a net increase in the nitrate N due to the N compounds' oxidation, allowing nutrients to be released (Hart et al., 1994). The results for NO_3- leachate from the soil profile suggest an increase of 15%. However, even though there is a high NO_3-N content in the soil, the model shows that it leaches, which prevents its accumulation in the soil profile. Consequently, there is a decrease by 10% of nitrogen uptake in the plants.

Despite the increase of the bulk density of the first soil layer (Table 4.3) and the decrease in surface runoff, soluble phosphorus losses were greater in the field-scale CT scenario than in the IT scenario (Table 4.8). The main reason for the soluble P increment may be that the amount of phosphorus in solution in the top 10 mm of soil increased by 26.88 kg P ha^{-1}, compared to 8.59 kg P ha^{-1} for the IT scenario. The results suggested that the increase of net P in the solution can be attributed mainly to the mineralization of phosphorus from the fresh residue pool and from the active organic pool to the labile pool (P in solution), which increased by up to 178% in the CT, compared to IT. Deubel et al. (2011) reported an increase of soluble P by 24% under conservation tillage in long-term research, along with a trend of high P concentrations in deeper soil layers. In contrast, the implementation of CT can reduce by approximately 33% the organic phosphorus transported with the sediments into the reach (Table 4.8). The transformation of phosphorus between the mineral pool (P in solution) and the "active" mineral pool (P absorbed to the surface of soil particles) decreased by 69.85% in the CT scenario. Additionally, the decrease of the sediment yield (metric tons) for the CT scenario (Table 4.8) has a direct influence on the phosphorus load transported with sediments to the main channel in the surface runoff (Neitsch et al., 2011). Equally important, despite the increased availability of total P and soluble P in this research, the uptake of P by plants was almost the same or even tended to be less for the CT scenario (38.63 and 36.86 kg P ha^{-1} for the IT and CT scenarios, respectively).

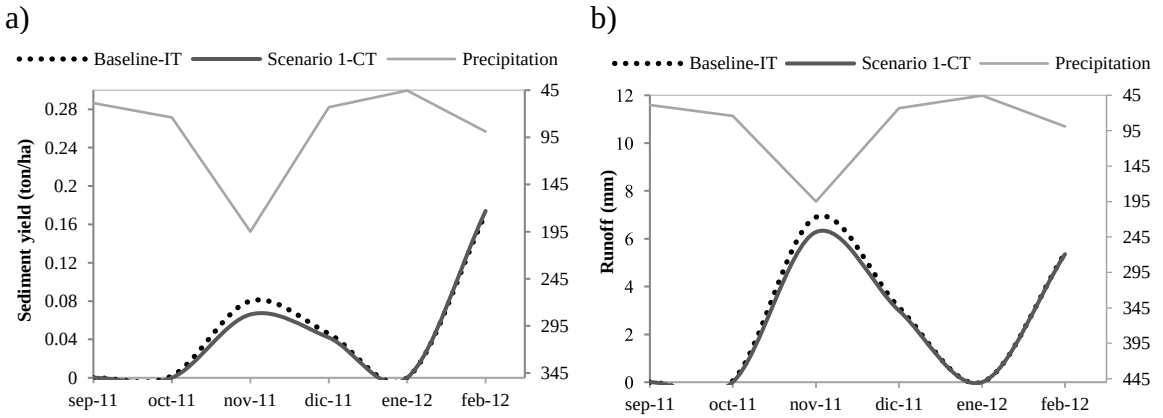

Figure 4.4. Sediment losses (a) and runoff (b) at field level - right vertical axes.

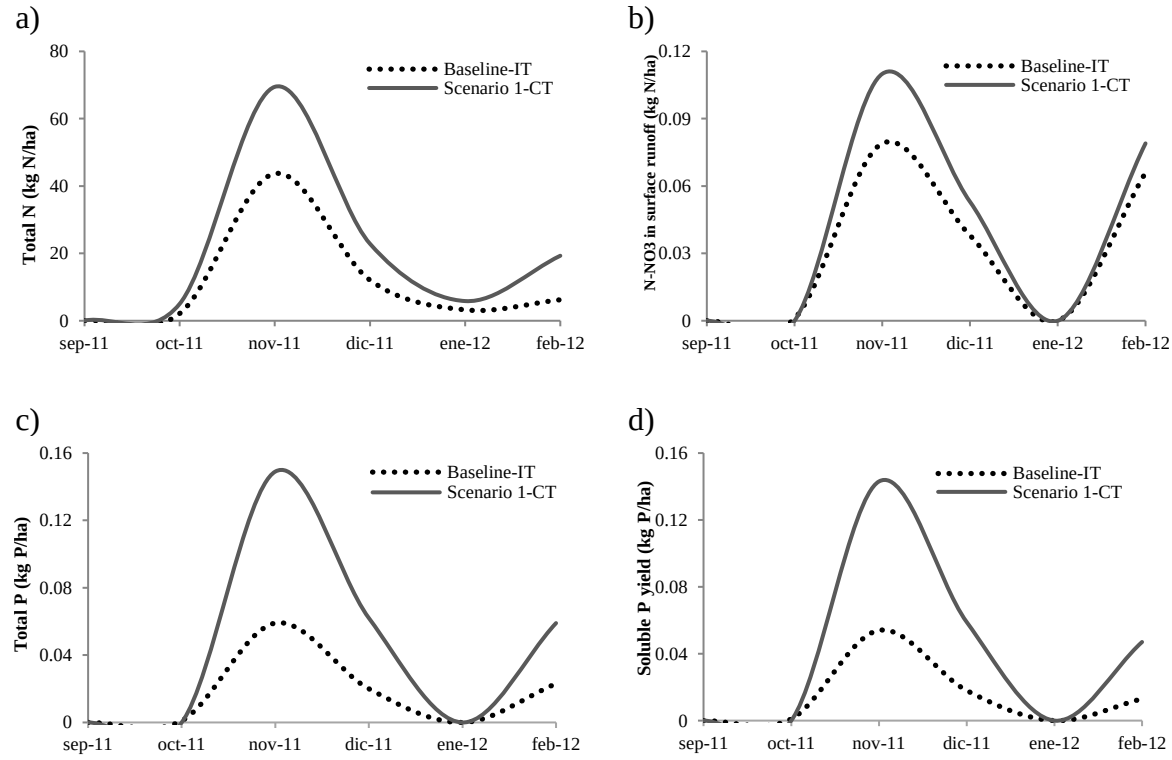

Figure 4.5. Monthly total N (a), total P (b), NO3−-N (c), and soluble P (d) in surface runoff at field level.

4.4.4 The effectiveness of CT-BMP at the watershed level

The CT management practice's extrapolation was performed for the entire potato crop cultivated in the watershed, under different biophysical conditions (HRUs) from those evaluated at the field level. The results suggest that CT at the watershed level reduces the surface runoff and sediment yield by 11% and 26%, respectively. The reduction obtained for the two parameters represents approximately half of the reduction obtained at the field level. Furthermore, the most significant CT decrease compared with IT occurred during the rainy season, when farmers normally perform fertilization tasks to take advantage of the wet soil conditions.

Surface runoff loss could be influenced by the tillage type and the rotation system (e.g., incorporating green manure). However, the SCS runoff curve numbers (CN2) defined per soil type, land use, and management practices in the model inputs were not affected directly by the CT operation. Therefore, the surface runoff increments cannot be attributed mainly to the CT scenario (Maharjan et al., 2018). This is mostly because the precipitation, slope, and soil moisture vary for the other potato crop areas (HRUs) along the watershed. The tillage practices affect the sediment yields. In the model, the P_{USLE} support practice factor (USLE_P) defined in the modified universal soil loss equation (Williams, 1995) is the only parameter related to CT practices that affect the sediment yields. However, soil erosion in the SWAT model is also directly affected by the surface runoff volume, topographic factors, and soil erodibility factors defined in the soil properties.

Total nitrogen loss increased by 2% in the CT scenario at the watershed level (Table 4.8). The losses of nitrate N was significantly higher in CT than IT, with an increase of 17% (Table 4.8). The increment in NO_3^--N was directly affected by the nitrification process, which oxidized the ammonia or ammonium from the inorganic fertilizer applied (0.26 and 4.42 kg N ha^{-1} in the IT and CT scenarios, respectively). Furthermore, no significant differences were shown for organic N losses (Table 4.8). This form of nitrogen is associated with sediment loading, and consequently, organic N losses decrease when the sediment loads are reduced. The amount of organic N transported to the main channel in surface runoff calculated by the model can be adjusted using the nitrogen enrichment ratio (ERORGN) parameter (Neitsch et al., 2011). In our study, the model's default value was used, which is calculated by a logarithmic equation related to sediment concentration developed by Menzel (1980). Therefore, future studies are required to calibrate this parameter for the different types of soils in the watershed and to be able to calibrate the sediment loads for HRUs that are different from those used in the analysis at the field level.

In contrast, total phosphorus losses decreased by 18% in the CT scenario (Table 4.8). This effect is mainly due to the 38% decrease in soluble P loss in the CT scenario's surface runoff compared to the IT scenario (Table 4.8). When each component of the phosphorus mass balance was analyzed, it was interesting to note that the amount of phosphorus that

moved into the "labile" mineral pool (P in solution) from the "active" mineral pool (P sorbed to the surface of soil particles) was -4.97 kg P ha^{-1} in the CT, compared to 3.87 kg P ha^{-1} in the IT scenario. A negative value denotes a net gain in soluble P due to movement to the labile pool from the active pool (Neitsch et al., 2011). However, the amount of soluble P transported in surface runoff also depends on the bulk density of the first soil layer and the phosphorus soil partitioning coefficient (PHOSKD), which is the ratio of the soluble P concentration in the surface soil to the soluble P concentration in surface runoff (Neitsch et al., 2011). For instance, even though the PHOSKD parameter was calibrated (Table 4.5) and the bulk density was measured (Table 4.3) at the field level, the spatial transfer of the CT to a different type of soil affects directly the value calculated for the soluble P (Deubel et al., 2011) at the watershed level.

Furthermore, the principal effect of the CT on loss of organic P was a decrease of 8% compared to the IT scenario (Table 4.8). Unlike organic N loss, the organic P loss showed a direct correlation with the sediment loss. Nevertheless, to verify this impact's consistency over the watershed, the phosphorus enrichment ratio parameter (ERORGGP) calculated as a default by the model needs to be adjusted.

This study indicates that using integrated watershed modeling to assess the impact of CT on nutrient properties requires further spatial calibration to improve confidence in the model. Farm-scale soil physical and chemical data under CT management is necessary to parameterize the inputs. For example, the soil bulk density in SWAT is an input defined manually by the user. The temporal variation of the soil layer's bulk density is not affected by the tillage operation (Arnold et al., 2012a; Maharjan et al., 2018). Although the impact of CT on the soil properties has been studied widely for the management of different crops over short- and long-term durations (Carter and Sanderson, 2001; Deubel et al., 2011; Ram et al., 2018; Quintero and Comerford, 2013; Villamil and Nafziger, 2015; Wang et al., 2015), many gaps still need to be addressed, such as the simulation approach to soil tillage, and especially to the spatial and temporal changes of the soil’s physical and microbial activity. However, we realize that some processes are difficult to characterize accurately in large watersheds due to insufficient data or understanding of the techniques themselves. Furthermore, depending on the research scope, the modeling approach may or may not be a viable alternative.

Table 4.8. IT and CT's direct effects on average monthly runoff, sediment, and nutrients in surface runoff.

Variable	Field-level			Watershed-level		
	IT	CT	Difference (%)	IT	CT	Difference (%)
Surface runoff (l m^2)	32.84	24.03	-26.83	15.91	14.13	-11.19
Sediment yield (ton ha^{-1})	0.58	0.31	-46.55	1.89	1.40	-25.93
Nitrogen losses (kg ha^{-1})						
Total N loss	221.15	258.05	16.69	21.33	21.71	1.78
Organic N	0.08	0.12	50.00	3.36	3.38	0.59
Nitrate surface runoff	0.39	0.47	20.51	0.53	0.62	16.98
Nitrate leached	166.65	191.16	14.71	9.22	9.43	2.28
Nitrate lateral flow	4.00	4.85	21.25	6.03	6.11	1.33
Nitrate groundwater yield	50.03	61.46	22.85	2.17	2.20	1.38
Phosphorus losses (kg ha^{-1})						
Total P loss	0.24	0.31	29.17	0.77	0.63	-18.18
Organic P	0.03	0.02	-33.33	0.49	0.45	-8.16
Soluble P	0.21	0.29	38.10	0.29	0.18	-37.93

4.5 CONCLUSIONS

The objective of this part of the study was to assess the impacts of CT on the runoff quality, as well as soil, nitrogen (N), and phosphorus (P) losses in a potato crop in the Fuquene watershed (Colombia) by applying the SWAT model. The model performance was calibrated and validated at field level for site-specific conditions, and then CT practices were extrapolated to the whole potato crop area in the basin. Despite the modeling uncertainties, the results provide evidence that the model-based approach presented is useful and practical. It can be used to facilitate the development of land-use plans by local decision makers to reduce water pollution in the Fuquene watershed.

The results suggest that CT at the watershed level reduces the sediment yield by 26% and surface runoff by 11% compared with IT, which means an overall reduction of sediment load. The most significant decrease in sediment load due to CT occurs, especially in the rainy season. The main CT effect on nutrient losses in the runoff is that an increase occurs in the total N and P (2% to 18% respectively) compared to the baseline. In addition, the CT simulation results suggest that the loss of NO_3^--N in surface runoff could be increased by 17%. This might be attributed to the nitrification process, which oxidized the ammonia or ammonium from the inorganic fertilizer. However, the results at the watershed level showed different patterns from those obtained at the field level. In fact, the major limitation identified in this study arises from the process of the CT extrapolation practice for all the potato crop areas within the watershed because the model was calibrated for a minimal area (field level), and the initial and calibrated parameter values were the same for other soil types and slopes in the watershed.

This chapter provides important information about the effects of potato management practices on the runoff water quality in an Andean watershed. It thereby provides a potential model for future Andean watershed studies, providing guidelines to decision-makers and stakeholders aiming to use these agricultural management practices for the potato crop. Given the loss of nutrients obtained for the CT practice, the authors suggest that it may be possible to reduce the amounts applied, considering the contribution of the green manure nutrients involved. Adjusting the amounts of fertilizer could help increase conservation agriculture competitiveness in potato crops, compared to conventional management practices. However, it is necessary to assess reduced fertilizer dose trials and their impacts on productivity, erosion, and runoff. Besides, more detailed spatio-temporal models and the application of optimization techniques would help identify and allocate CT-BMP options to reduce the impact of agricultural practices on water pollution. Moreover, using this type of model and methods, it could be possible to simulate several crops in the same watershed, consider climate change scenarios, and define suitable parameters for the different areas in the watershed. Overall, future research that contemplates these points will help mitigate the uncertainty in assessing the implementation of BMPs at the watershed level.

5

SPATIO-TEMPORAL ANALYSIS OF THE MULTIPLE AGRICULTURAL MANAGEMENT PRACTICES IMPACTS

"Paisaje dinamico con diversos terrenos, vida silvestre y clima"

This chapter is based on Uribe, N., Srinivasan, R., Corzo, G., Arango, D., Solomatine, D., 2020. Spatio-temporal critical source areas patterns of runoff pollution from agricultural practices in the Colombian Andes. Ecol. Eng. 149, 105810.
https://doi.org/10.1016/j.ecoleng.2020.105810

5.1 ABSTRACT

Lake Riogrande II, located in the Colombian Andes' central region, has eutrophication due to a progressive increase of runoff pollution from upstream intensive dairy cattle and agricultural activities in the watershed. Public and private entities have invested in adopting the best agricultural management practices (BMP). BMP is a general formulation of recommended criteria and, therefore, does not universally fit all problems. For example, the corrective measures taken so far demonstrate difficulties in selecting and allocating BMPs appropriate for the space-time hydrological variability within the watershed. This research analyses the spatio-temporal dynamics of BMP pollution patterns. The study is built on critical source areas of runoff pollution from agricultural practices in the Colombia Andes. Fieldwork was conducted with farmers' participation to collect spatial data of the current management operations for potato (*Solanum tuberosum*), tree tomato (*Solanum betaceum*), and dairy agriculture. The Soil and Water Assessment Tool (SWAT) model is used to simulate agricultural and hydrological processes. The model was calibrated using observed discharge, nitrate-N (NO_3^-N), and soluble phosphorus (P) concentrations monthly. The origin of pollution at the catchment scale was used applying the critical source areas (CSAs) method. This chapter proposes for this analysis a new spatio-temporal CSA index (ST-CSA) to represent the behavior of the CSAs simultaneously in space and time. For this, several aggregated CSAs were analyzed using monthly and annual time steps. Results indicate that the location of CSAs changes significantly with time using ST-CSA. As expected, the greatest number of CSAs occurs during the rainy months. However, these CSAs are located in the region with the lowest precipitation levels in the agricultural areas within the watershed dominated by potato, tree tomato, and dairy agriculture. These areas vary significantly, from 24.07% of the entire basin area (1034.348 km^2) to a maximum of 61.78%. Despite the model uncertainties, the results highlight the importance of identifying spatio-temporal CSAs to select BMPs with the highest potential for nitrogen and phosphorus losses reduction (such as the adaptation of fertilization schedules) applicable to the study watershed.

5.2 INTRODUCTION

Nowadays, soil resources are under increasing pressure due to its intensification for agriculture, grazing, forestry, and urbanization. It is estimated that by 2050 the demand of a growing population will increase the stress on soils 60% by 2050 (Organización de las Naciones Unidas para la Alimentación y la Agricultura (FAO) and Ministerio de Ambiente y Desarrollo Sostenible (MADS), 2018). These pressures, combined with unsustainable agricultural management practices (soils without vegetation, large amounts of fertilizer applied, and intensive tillage), as well as extreme weather events, are expected to cause significant land degradation (Sedano et al., 2013; Sarkar et al., 2006). The associated external impacts of these practices can lead to degradation of surface water quality, eutrophication of reservoirs, and increased risk of flooding (Giri and Qiu, 2016; Fiener et

al., 2011). Therefore, a detailed understanding of contamination of runoff from agricultural basins to aquatic environments is crucial to designing practices to limit this degradation.

One of the most recommended alternatives to reduce runoff water pollutants within an agricultural watershed is implementing Best Management Practices (BMPs) (Jeon et al., 2018; Ritter and Shirmohammadi, 2001). Nevertheless, the selection and allocation of agricultural BMPs at a watershed scale is very complex in practice. Several studies have shown the importance of focusing on the identification of nutrient losses in Critical Source Areas (CSAs) at a watershed scale to allocate BMPs (Gariz and Talebi, 2016); Giri and Qiu, 2016; Dechmi and Skhiri, 2013; Ghebremichael et al., 2013; Giri et al., 2012; Winchell et al., 2011; Chaubey et al., 2010; Ghebremichael et al., 2010; Tuppad and Srinivasan, 2008). Most of these studies identify and quantify CSAs to evaluate the effectiveness of BMPs that have been previously selected, using models such as the Soil and Water Assessment Tool (SWAT), Water Erosion Prediction (WEPP), and Annualized Agricultural Nonpoint Source (AnnAGNPS). However, research nowadays recognizes that to allocate BMPs at the watershed scale, a detailed understanding of spatio-temporal dynamics of the surface pollutants in runoff is crucial (Uribe et al., 2018; Gao et al., 2017; Giri and Qiu, 2016; Ghebremichael et al., 2013; Fiener et al., 2011).

In various hydrology areas, there is a significant trend to understand the dynamics of each spatial event in time, aiming to analyze spatiotemporal dynamics (Diaz et al., 2019; Laverde-Barajas et al., 2019). These methodologies derive from pattern recognition techniques and are being applied to different fields, providing new alternatives to the generalization of spatial changes on an average time step (Corzo Perez et al., 2011; Li et al., 2013; Cristiano et al., 2017; Amaranto et al., 2019; Laverde-Barajas et al., 2019). Spatiotemporal approaches that do not analyze the dynamics of runoff contaminants at the watershed scale can be found in the literature. For instance, Shen et al. (2015) document changes across space and time in the relationship between water quality and buffer zone-BMPs. The results reveal that the design of a buffer zone-BMPs does not depend only on the land use type, but it also depends on the implementation scale. His conclusion did not take into account the variation of CSA by season or month. Giri et al. (2014) presented an analysis of BMP implementation's spatio-temporal variability based on four targeting methods at the sub-basin level. Temporal and spatial comparisons of ten BMPs' effectiveness with the baseline (without BMPs) were performed for sediment, total nitrogen, and total phosphorus. The results showed significant temporal variability in the defining factors of CSAs, related to the implementation years defined for each of the scenarios evaluated for each BMP. Fiener et al. (2011) studied how spatio-temporal land-use patterns affect surface runoff response. The study focused on the linear landscape structures associated with the spatial organization of fields, and it was found that surface runoff can be reduced by decreasing field size. Therefore, the higher the spatio-temporal variability in hydraulic properties and management intensity, the more significant the impact of field size on surface runoff. These studies focus on the identification of CSAs to evaluate the effectiveness of previously selected BMPs, and in analyzing the results in space and time.

However, there was no direct connection between hydrological events and individual CSA variations. In contrast, in this study, we propose the use of an ST-CSA index for the spatio-temporal dynamics of CSA and its identification. These results will allow us to explore in the future the selection of BMPs that are more aligned with the hydrological spatio-temporal variability in the basin. Hence, the main objectives of this study were to identify spatio-temporal patterns of nitrate-N and soluble P in runoff from the current agricultural practices in the Colombia Andes.

We considered it necessary to define our own CSAs, taking into account space (location) and temporal (time) variability throughout the modeling period. Therefore, the word "spatiotemporal CSAs" is defined in this chapter as dynamic areas in time and space within the watershed. This study will help decision-makers select BMPs that are more in line with local needs and have a higher probability of achieving sustainable agricultural development goals. We apply this approach to watersheds located in the mountains of the tropical Andes, where there are still gaps in addressing this issue. It is the first in-depth study that covers the high level of complexity of shifting cultivation and intensive traditional agriculture, which is currently practiced in this type of watershed. In addition, this work is an essential step towards developing a multi-objective optimization method to select and allocate BMPs at the watershed level. Furthermore, the results provide crucial information about simulation of the spatio-temporal dynamics of the runoff pollutants and further optimization of BMPs.

5.3 METHODOLOGY

5.3.1 Hydrological and water quality model

SWAT model development and input data

The Soil and Water Assessment Tool (SWAT), developed by the United States Department of Agriculture – Agricultural Research Service, was used in this study (Arnold et al., 1998). SWAT is a semi-distributed, continuous-time, and process-based watershed-scale model designed to simulate the effects of water management decisions on water quantity and quality (Neitsch et al., 2011). The model's processing units are Hydrological Response Units (HRUs) – small land areas with unique combinations of sub-basin, soil type, land use, and agricultural management practices (Arnold et al., 1998). The hydrological cycle is based on the water balance equation. A summary of the SWAT equations is presented in the supplementary material online.

The model input data consist of land use/cover type, soil type and properties, topography, weather/climate data, and land management practices (management schedules). A land-use cover map (scale of 1:10,000) was obtained from the regional environmental authority of Antioquia (Corantioquia). A soil map (1:50,000 scale) and physicochemical studies conducted from October 2015 to March 2016 were obtained from the Temporary Union of Environmental Risk Management (UT-GRA). A detailed description of the soil's physical

characteristics defined as model inputs is provided in the appendix A.2. Topography data in a 30-meter resolution Digital Elevation Model (DEM) were obtained from the National University of Antioquia and Corantioquia. The weather data from 16 stations located within the watershed (Figure 3.4-Chapter 3) were obtained from Medellin's Public Service Company (EPM). The historical record daily data included precipitation, temperature (maximum, minimum, and average), relative humidity, solar radiation, and wind speed. Annual and monthly average rainfall and temperature maps are provided in chapter 3 (Figure 3.5-Chapter 3).

Monthly streamflow measurements at the San Pedro Rg-10 La Ye, Rg-6 Puente Belmira, and Presa Riogrande II (located at the outlet of the watershed) stations were used to calibrate and validate the flow in different locations in the watershed (Figure 3.4-Chapter 3). Daily observations of Nitrate-N (NO_3^-N), Total Nitrogen (TN), and soluble phosphorus in the Chico river outlet from 2014 to 2015 were obtained from the Medellin's Public Service Company (EPM). The concentrations were collected during a water quality monitoring campaign (a single measurement per day) performed as part of the project "El estudio de la problemática ambiental de los embalses La Fe, Riogrande II y Porce II, para la gestión integral y adecuada del recurso hídrico" (in Spanish).

For this study, the SWAT model was built on a daily time step from 1996 to 2015. All spatial information was projected to the MAGNA Colombia Bogota Project Reference System (origin Bogotá, False Coordinates N: 1,000,000 m and E: 1,000,000 m, Datum MAGNA (Ellipsoid WGS 84)). The watershed was defined with an area of 103,434.77 ha and delineated into 20 sub-basins representing the main tributaries. The slope classes were defined in five ranges (0-5%; 5-15%; 15-40%; 25-60%; and >60%) and 3060 HRUs were delineated. The actual evapotranspiration (AET) was calculated based on the methodology developed by Ritchie (1972), and the potential evapotranspiration (PET) was simulated using the Hargreaves method (Hargreaves and Samani, 1985). The CN method (USDA-SCS, 1972) was used to predict the surface runoff using the method that varies with soil profile water content to calculate the retention parameter (Eq. 2.1-Chapter 2). The CN values were determined based on Colombian Land Cover Map categories associated with SWAT land cover codes (IDEAM et al., 2008). The CN values defined in the land cover database are presented in the Appendix A.1.

Table 5.1. Spatial input data description

Data type	Resolution	Source
Topographic map	30m	CAR
Land use map	1:25.000	IGAC
Soil map	1:100.000	IGAC
Weather	No. of stations: 21	CAR-IDEAM

Current management practices and characterization

The current agricultural management practices for potato, tree tomato, and kikuyu grass (*Pennisetum clandestinum*) (dairy farming) were defined in the HRU management file (.mgt) and incorporated into the model. Input data for planting, harvesting, fertilizer applications (nutrients), tillage operations, grazing, crop rotation, and scheduled management operations were collected through field surveys and secondary sources. The fieldwork was conducted in January 2016 in partnership with Antioquia University at the Riogrande watershed (Figure 5.1). Since farmers do not use the same schedules, some assumptions were made to unify the current management practices database. These assumptions include that: 1) the planting date in the schedule is the same for each crop, 2) kikuyu grass was selected due to its predominance for dairy farming, 3) transitory crops which may occur in pastures and in addition to potato crop were not considered, and 4) fertilizer application dates and rates are the same for every crop. In general, small-scale farmers apply fertilizers based on estimated quantities needed, and this occurs during the rainy season. The type of fertilizer used changes according to the market price, and the technology for applying the fertilizer also varies (horses, ditches, and spray by sprinklers) within the watershed.

The current agricultural management practice for potatoes is to rotate between potato and pasture. Two potato cycles of six months are carried out, and then kikuyu grass is planted for soil recovery. Tillage operations are carried out by conventional plowing, followed by passes of a bedder shaper to invert the soil. The chemical fertilizer N-P-K (15-15-15 type) is applied simultaneously with the tillage to incorporate it into the soil (Figure 5.2). The kikuyu grass is used for dairy cattle feeding (Holstein cattle). This grass is characterized by its high adaptability, rusticity, load capacity, and excellent ease of handling and response to fertilization. Typically, the animals for grazing are rotated between small sub-areas defined on the farm every 40 days. This way, the grazing is controlled evenly throughout the whole property. The animal load is three per ha day^{-1} of grazing. The dry weight of biomass consumed per animal load is defined as 51 kg ha^{-1} day^{-1}, and the dry weight of manure deposited by 3 animals is ten kg ha^{-1} day^{-1}. The quantities of Potreros mixed fertilizer, urea, and cattle manure applied to grass fields are split into nine applications per year after each grazing (see Figure 5.3). Tree tomato is a semi-permanent crop generally harvested all year (for four to five years after planting). For this study, the harvest operation was defined every five months for five years, which allowed ten harvests per tree. Commonly, urea plus chemical fertilizer N-P-K (13-13-13 type) is applied monthly after the planting date (Figure 5.4). The production of this fruit has been on the rise for the last ten years, and the Riogrande watershed area produces 90% of the total production of the Antioquia region. This tree is also quite demanding in terms of nutritional elements and has a high susceptibility to pests, diseases, and climatic adversity.

The current agricultural management practices for these crop systems were simulated in the model as a baseline. Detailed descriptions of the scheduled operations (planting, grazing, tillage, fertilizer applications, and harvest) are provided in the Appendix A.3. The final values of the management operations' parameters were defined in the HRU management file

(Table 5.2). Moreover, the fertilizer database (.frt) was modified according to the farmers' fertilizer use in our case study (Table 5.3).

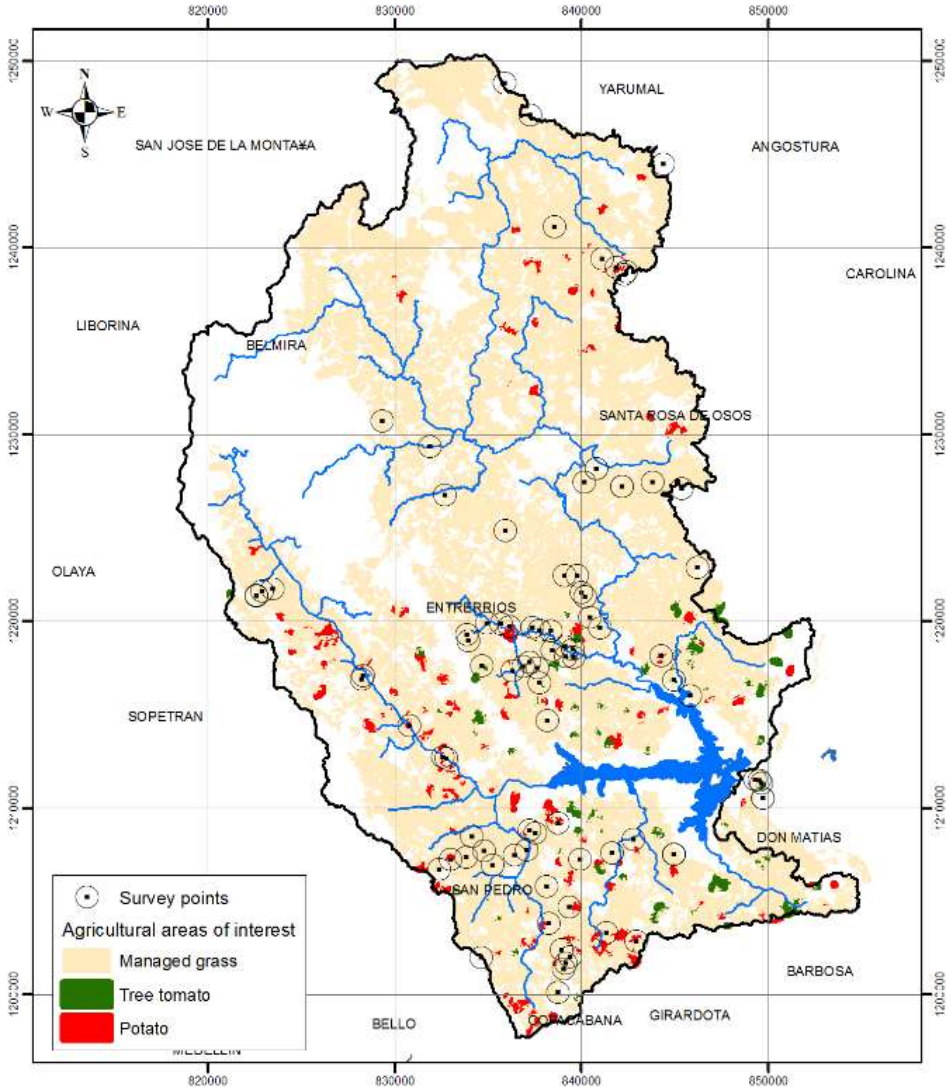

Figure 5.1. Survey points and areas associated with the current potato, tree tomato, and kikuyu grass agricultural management practices.

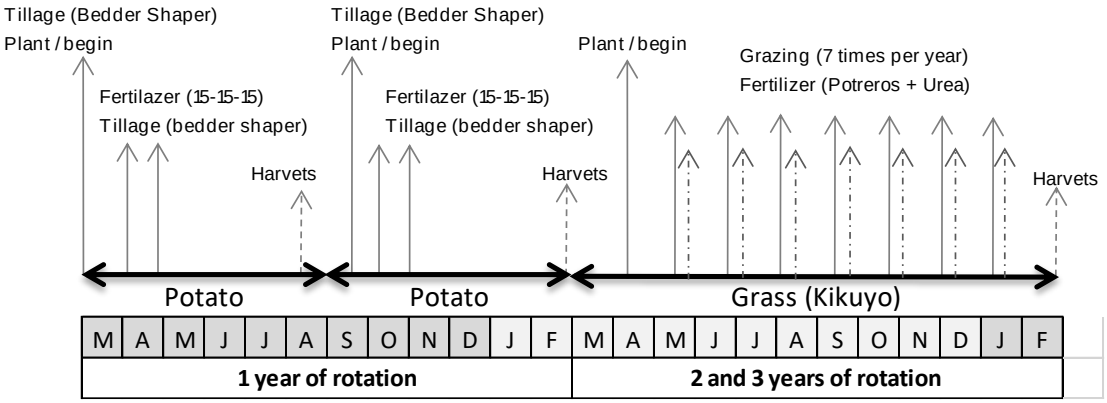

Figure 5.2. Conceptual outline of potato crop management practices.

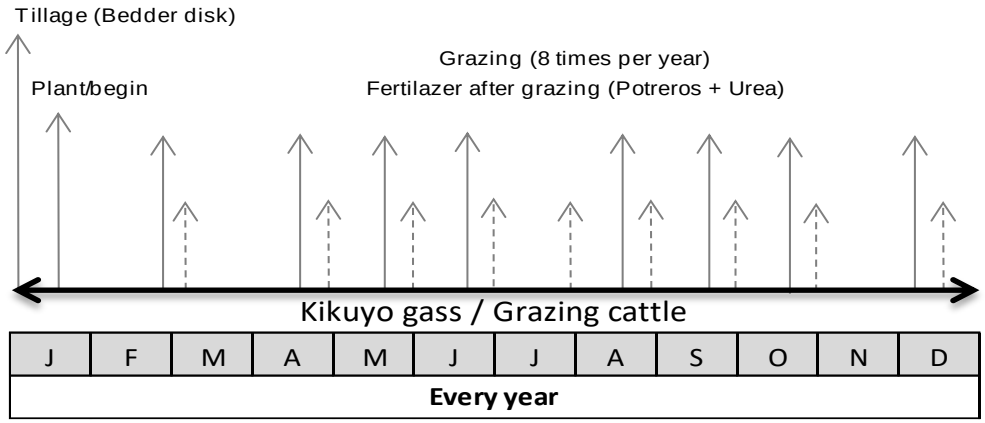

Figure 5.3. Conceptual outline of kikuyu management practices.

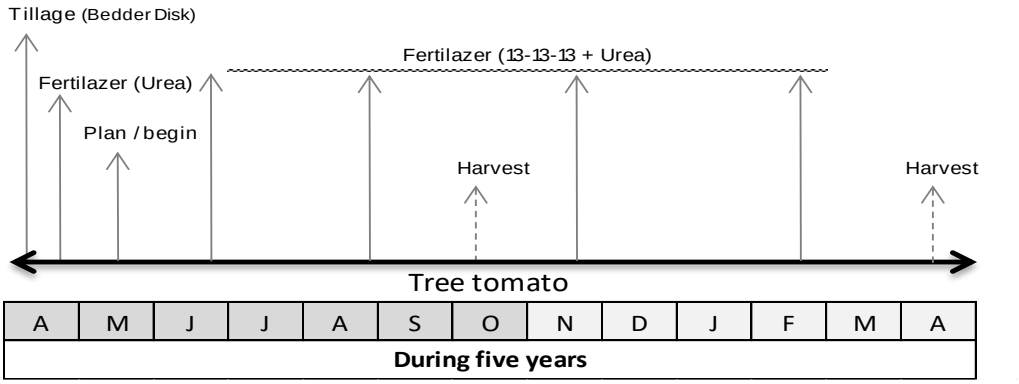

Figure 5.4. Conceptual outline of tree tomato crop management practices.

Table 5.2. The variable name, description, and values defined of the management operations for potato, tree tomato, and kikuyu grass entered in the management file.

Variable Name	Definition	Value defined		
		Potato	Tree Tomato	kikuyu
Planting				
PLANT_ID	Plant/land cover code from crop.dat	POTA	TOMA	PASM
HEAT UNITS	Total heat units required for plant maturity	800	1500	1000
CN2	Initial SCS runoff curve number [35- 98]	62	60	62
Grazing				
GRZ_DAYS	Number days of grazing take place in the HRU			1
BIO_EAT	Dry weight of biomass consumed (kg ha^{-1} day^{-1})			51
BIO_TRMP	Dry weight of biomass trampled (kg ha^{-1} day^{-1})			650
MANURE_KG	Dry weight of manure deposited (kg ha^{-1} day^{-1})			10
Tillage				
TILLAGE_ID	Tillage implementation	Bedder shaper	Bedder Disk	Bedder Disk
Fertilizer				
FERT_ID	Type of fertilizer/manure applied	15-15-15	Urea+ 13-13-13	Urea+ Potreros
FRT_KG	Amount of fertilizer/manure applied (Kg ha^{-1})	700 (2/cycle)	530 (7 per year)	90 (8 per year)
FRT_ SURFACE	Fraction of fertilizer applied to top 10 mm	0.2	0.9	0.9

Table 5.3. Fertilizers selected into the database (.frt file)

Composition (%)	Name				
	15-15-15	13-13-13	Nitromag	Potreros	Urea
Total nitrogen N	15	13	21	31	46
Ammonium nitrate	8.89	6.87	10.3	1.5	
Nitric nitrogen	6.11	3.13	10.7	29.5	
Total phosphorus P_2O_5	15	13		8	
Total potassium KO_2	15	13		8	
Calcium Ca			11		
Magnesium			7.5	3	

5.3.2 Model calibration and validation

The number of parameters included in the calibration process can be reduced by identifying the most sensitive parameters. A global sensitivity analysis was carried out only for flow since it is the only variable with continuously observed records for the simulation period. The built-in Latin hypercube one-at-a-time technique (Green and van Griensven, 2008; Morris, 1991) was used for this purpose. Thirteen parameters were found to influence the streamflow and were thus included in this analysis. The results were used for flow calibration.

Manual flow calibration was performed for the period from 1995 to 2015 using data from the San Pedro Rg-10 La Ye, the Rg-6 Puente Belmira, and the Presa Riogrande II gauging stations, compared with the outflows of sub-basins 17, 9, and 16 (Figure 3.4- Chapter 3). Nash–Sutcliffe modeling efficiency (NSE), root mean square error (RMSE), and time series plots were used to evaluate the model predictions during the calibration and validation periods (Moriasi et al., 2015; Nayeb Yazdi et al., 2019). Second, for potato, tree tomato, and kikuyu grass crops, the harvest yield (ton ha^{-1}) as dry weight was calibrated, comparing the average values simulated with the reference values (measured). An average harvested yield for potato, tree tomato, and kikuyu of 8, 10, and 0.2 to 4 (ton ha^{-1} $harvest^{-1}$), respectively, were reported by the UT-GRA research program (Fedegan and Sena, 2013). The large range of yields for kikuyo is due to the yields varying within between sites. The annual reference values defined to compare the simulated harvest yields during the calibration process were 16, 20, and 1.6 to 32-ton ha^{-1} $year^{-1}$ per crop, respectively. These values were calculated according to the number of harvests per year defined in each operation schedule (2, 2, and 8 times harvested $year^{-1}$, respectively).

Finally, monthly average manual calibrations for nitrate-N (NO_3^--N mg l^{-1}), total nitrogen (TN mg l^{-1}), and soluble phosphorus (PO_4 mg l^{-1}) were performed. Discontinuous sampling daily data collected in a monitoring campaign from 2014 to 2015 by the University of Antioquia, the National University, and EPM (Medellin's Public Service Company) were used. The water samples to estimate nutrient values were extracted with a 5-deep Schindler 5-liter bottle (sub-surface, 10% I_0; 1% I_0; half of the water column; and one meter at the bottom of the aphotic zone) (Ramírez-Restrepo et al., 2015). The NSE, RMSE performance indicators, and time series plots were used to evaluate the model predictions for the period when the concentration data of nitrate-N (NO_3^--N mg l^{-1}), total nitrogen (TN mg l^{-1}), and soluble phosphorus (PO_4 mg l^{-1}) were available.

5.3.3 Identification/characterization of spatio-temporal critical source areas

The targeting technique Load per Unit Area Index (LPUAI) (Tuppad and Srinivasan, 2008; Giri et al., 2012) was computed to identify the CSAs of nitrate-N (NO_3^--N) and soluble P (PO_4) in runoff at the HRU level. Determining runoff CSAs is essential because nutrient loss predictions in the model are positively related to surface runoff (Eq. 2.3 to 2.7- Chapter 2).

SWAT-predicted monthly values were used to apply the LPUAI. The CSAs are based on the monthly average runoff and pollutant load per unit area, which normalizes each HRU for comparison in terms of kg ha^{-1}.

Individual HRUs within the watershed are analyzed in detail to compare their spatial distribution of the pollutants (Tuppad and Srinivasan, 2008). The proposed methodology using the ST-CSA index follows three main steps: 1. Temporal analysis is carried out first, followed by spatial analysis to identify the spatio-temporal CSAs. The threshold values of runoff, NO_3^--N, and PO_4 losses were defined to identify HRUs with higher monthly rates. These values were determined by analyzing the monthly historical records and calculating the 90^{th} percentile of NO_3^--N, and PO_4 losses. 2. A graph per variable was developed to show the defined thresholds and the HURs above these levels. 3. The HRUs above these thresholds were counted for each month and classified for the total simulation period (1995-2015). 4. Subsequently, a spatio-temporal CSA index (ST-CSA) was calculated to define the spatio-temporal CSAs for the region for each variable studied. A value equal to 1 indicates that the HRU examined was above the threshold. And 5. An analysis of how the regions' nutrient losses change based on their index ST-CSA was plotted per monthly time step.

The characterization of the ST-CSAs for NO_3^--N and soluble P was determined by analyzing variance (ANOVA) tests using the R package. A multivariate exploration data analysis was conducted to determine the significance (expressed in probability levels: 1% ($P<0.01$), 5% ($P<0.05$), 10% ($P<0.1$) of surface runoff, vegetation cover, slope, area, precipitation, soil water content, CN, and nitrogen and phosphorus to both NO_3^--N and soluble P losses. These analyses were done separately for the NO_3^--N and soluble P spatio-temporal CSAs identified and the differences were considered significant at $P<0.01$, $P<0.05$, and $P<0.10$. The further post-hoc test was done separately for NO_3^--N and soluble P for each type of soil and sub-basin to identify sub-basins and soil types in groups by having CSAs with the same average of NO_3^--N (kg ha^{-1}) losses and soluble P (kg ha^{-1}) in the watershed.

5.4 RESULTS AND DISCUSSION

5.4.1 Calibration and validation of hydrological model

Streamflow model

The streamflow model sensitivity analysis identified the 13 most influential parameters from the 15 evaluated (Table 5.4). The base flow alpha-factor [1 $days^{-1}$] (alpha-bf), the initial groundwater height [m] (gwht), the soil evaporation compensation factor (esco), the deep aquifer percolation fraction (rchrg_dp), and the USLE soil erodibility factor (usle_k) were found to be the most sensitive parameters affecting groundwater and surface runoff processes. The parameters were ranked according to the significance of the sensitivity (*p*-

value), with the most sensitive parameter ranked first in the list (Abbaspour et al., 2015). Similar findings in previous studies indicate the direct relationship between the surface runoff and both groundwater and aquifer parameters (Uribe et al., 2018; Haghnegahdar and Razavi, 2017; Khorashadi Zadeh et al., 2017; Cho et al., 2017; Romagnoli et al., 2017; Arnold et al., 2012a). In this case study, the input values for the parameters which control the aquifer processes were defined for each sub-basin. For example, the groundwater parameters Gw-delay (groundwater delay time) and alpha-bf (base flow alpha-factor) were calculated using the modified base flow filter program (Arnold and Allen, 1999) developed by Arnold et al. (1995). These values at the three streamflow gauging stations were calculated and applied to the sub-basins upstream. The other necessary parameters to characterize the aquifers of the watershed were defined according to expert knowledge because Guse et al. (2016) highlight the importance of estimating aquifer input values as precisely as possible before the calibration process. If the sensitivity analysis allows a better understanding of model parameters, these can be used for model calibration.

*Table 5.4. Ranking, t-value, and p-value of parameters related to streamflow calculations considered for sensitivity analysis. The first letter before the parameters name indicates the adjusted method in the Sequential Uncertainty Fitting – SUFI-2 algorithm (the letter **v** represents replacing the current parameter value; **r** is multiplying (1 + a given value) to the current parameter value. t-value shows a measure of sensitivity, and p-value indicates the significance of the sensitivity.*

Rank	Parameter[a]	*t*-value[b]	*p*-value[c]
1	v_Alpha_bf.gw	-5.46	0.00
2	v_Gwht( ).gw	-1.06	0.29
3	v_Esco( ).bsn	1.05	0.30
4	v_Rchrg_dp.gw	-0.75	0.45
5	r_Usle_K( ).sol	0.55	0.59
6	v_Gw_revap.gw	0.48	0.63
7	v_Gw_delay.gw	-0.38	0.71
8	v_Gw_spyld.gw	0.22	0.83
9	v_Shallst.gw	0.11	0.91
10	v_Deepst.gw	-0.11	0.91
11	r_Cn2.mgt	0.08	0.94
12	v_Revapmn.gw	0.04	0.97
13	v_Gwqmn.gw	-0.01	0.99

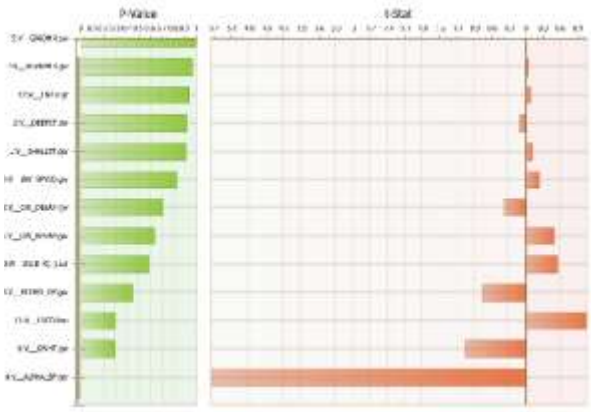

In addition, a manual streamflow calibration using monthly data was performed from 1996 to 2006, and validation from 2007 to 2015. The parameters calibrated to improve the

model's streamflow performance in the Riogrande watershed correspond mainly to groundwater and runoff processes (Table 5.5). The hydrographs and descriptive statistics for the calibration and validation results are shown in Figure 5.5. The NSE values obtained for the three gauging stations were 0.88, 0.85, and 0.93 for the calibration period and 0.86, 0.85, and 0.77 for the validation period. According to the performance rating guidelines developed by Moriasi et al., 2015, the monthly streamflow calibration and validation are considered as 'very good' at the three gauging stations (NSE values>0.75). In particular, the lowest NSE value obtained corresponds to the validation period at Presa station, which is located at the watershed outlet. It is as expected because of missing streamflow observations for this particular station between 2011 and 2015. The graphical results for monthly streamflow predictions matched very well with the observed values at the three available gauging stations of Pte. Belmira, San Pedro, and Presa (Figure 5.5). Linear regression between measured and simulated streamflow was plotted, obtaining an R^2>0.87 for the three gauging stations (Figure 5.5).

Overall, the streamflow acquired by manual calibration at the three gauging stations was satisfactory for this study's objective. Compared to the observed data, the baseflow is well represented by the model, mainly due to the calibration of the majority of inputs required for the groundwater simulation. However, the model slightly underestimated average monthly peak flows at certain times of the simulation period. Closer inspection revealed that this error mainly occurred from May to June and from September to October, which corresponds to the rainy seasons. Notably, the Belmira station, which records the flow values from the upper part of the basin with average rainfall more significant than 2000 mm/year, presents the highest error in the peak flow estimation. Similar studies confirm the uncertainty in the peak flow calibration process (Daggupati et al., 2015; Francesconi et al., 2016; Cho et al., 2017; Romagnoli et al., 2017; Uribe et al., 2018), particularly in watersheds under intensive agriculture with high rainfall and steep slopes.

Table 5.5. Range, default value, and fitted values of calibrated parameters for streamflow, potato, tree tomato, kikuyu.

Parameter	Description in SWAT	Range	Default value	Final value
Streamflow				
SHALLST	Initial depth of water in the shallow aquifer [mm].	0 - 5000	1000	100
DEEPST	Initial depth of water in the deep aquifer [mm].	0 - 10000	1000	2000
GW_DELAY	Groundwater delay [days].	0 – 500	31	2
ALPHA_BF	Baseflow alpha factor [days].	0 – 1	0.048	0.01
GWQMN	Threshold water depth in the shallow aquifer for flow [mm].	0 - 5000	0	5
REVAPMN	Threshold water depth in the shallow aquifer for revap [mm].	0 – 1000	750	100
RCHRG_DP	Deep aquifer percolation fraction.	0 – 1	0.05	0.1
GWHT	Initial groundwater height [m].	0 – 40	1	25
GW_SPYLD	Specific yield of the shallow aquifer [m^3/m^3].	0 - 0.4	0.003	0.3
ESCO	Plant evaporation compensation factor.	0 – 1	0.95	1
CN2	Initial SCS CN II value.	35 – 98	Specific to HRU	$0.1*CN2_{default}$
USLE_K	USLE equation soil erodibility (K) factor.	0 – 0.65	Specific to soil	$0.1*USLE\_K_{default}$

Table 5.5. Range, default value, and fitted values of calibrated parameters for streamflow, potato, tree tomato, kikuyu.

Parameter	Description in SWAT	Range	Default value	
Crop growth			Values for potato, tree tomato, and kikuyu grass, respectively.	
T_OPT	Optimal temp for plant growth.	11 - 38	22, 22, 18	18, 18, 18
T_BASE	Min temp plant growth.	0 – 18	7, 10, 0	3, 4, 3
BIO_E	Biomass/Energy Ratio.	10 – 90	25, 30, 30	40, 45, 30
HVSTI	Harvest index [(kg ha^{-1}) (kg ha^{-1})$^{-1}$].	0.01 – 1.25	0.95, 0.33, 0.9	1.25, 1.25, 0.9
HEATUNITS	Total heat units for cover/plant to reach maturity.	0 - 3500	1800	1400,700,1800
Nutrients				
CDN	Denitrification exponential rate coefficient.	0 - 1	1.4	0.5
SDNCO	Denitrification threshold water content.	0 - 1	1.1	0.5
PHOSKD	Phosphorus soil partitioning coefficient.	100 - 200	175	200
NPERCO	Nitrogen percolation coefficient.	0 – 1	0.2	1
RSDCO	Residue decomposition coefficient	0.02 - 0.1	0.05	0.1

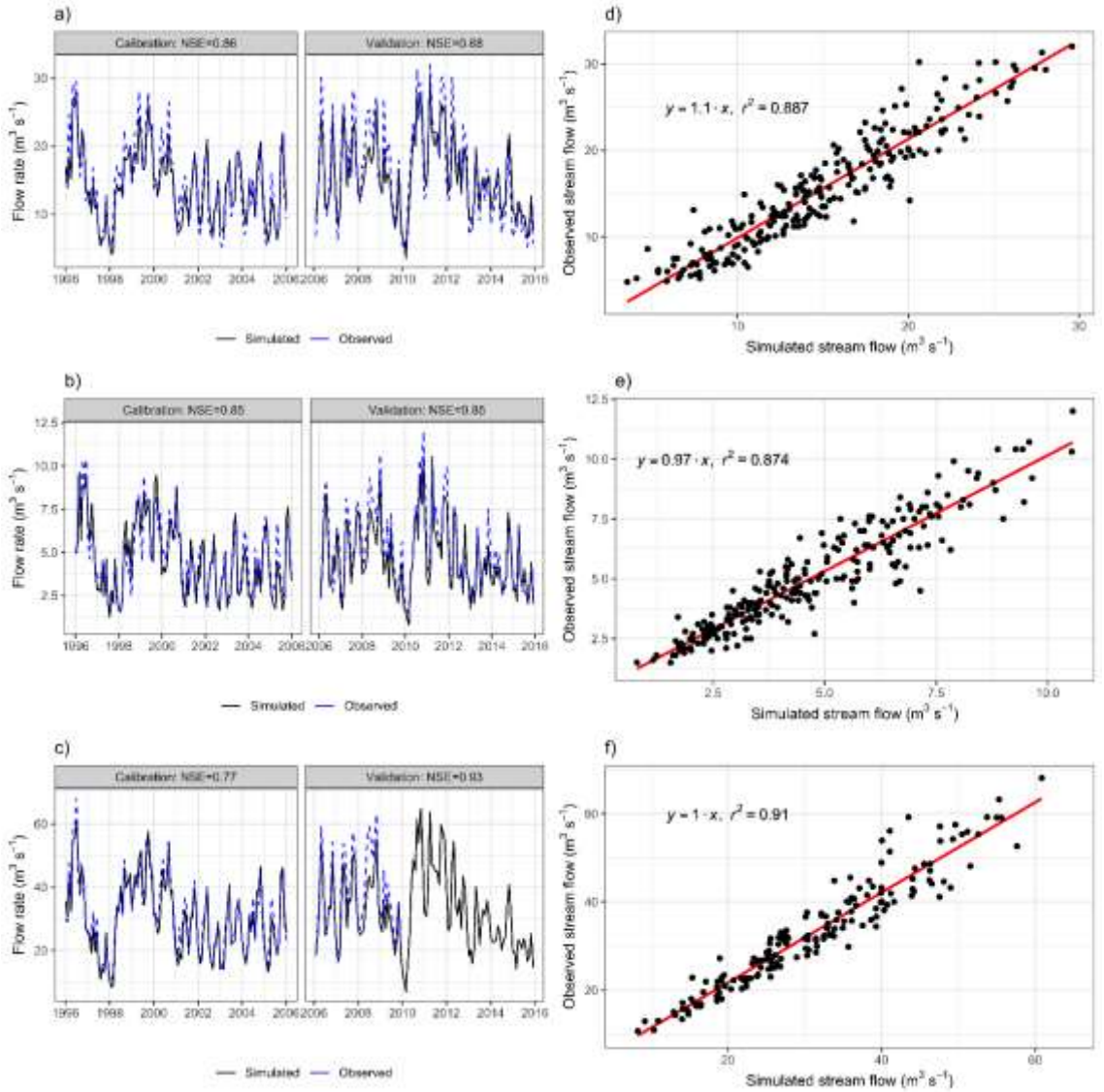

Figure 5.5. Comparison of observed and simulated flow rates (m3 s-1) at the (a) Pte. Belmira, (b) San Pedro, and (c) Presa stations for the calibration and validation period. Scatter plots of observed and simulated flow rates (m3 s-1) for the overall period along the dashed line at the (d) Pte. Belmira, (e) San Pedro, and (f) Presa stations.

Table 5.6. Descriptive statistic of monthly Flow average

Coefficient	Pte. Belmira		San Pedro		Presa	
	Calibration	Validation	Calibration	Validation	Calibration	Validation
NSE	0.88	0.86	0.85	0.85	0.93	0.77
d	0.96	0.95	0.96	0.96	0.98	0.93
RSME	2.08	2.68	0.78	0.89	3.02	3.88
MAE	1.63	2.11	0.61	0.72	2.36	1.89

Crop yield

Crop yield calibration was performed monthly, specifically during the months where harvest operation was implemented in each of the potato, tree tomato, and kikuyu defined grass management operation schedules. A total of five parameters associated with the crop growth cycle were calibrated to improve the crop yield performance of the model in the Riogrande watershed (Table 5.5). Parameters such as optimal and minimum temperature for plant growth (T_opt and T_base, respectively) were adjusted for each crop studied according to the crop's biophysical requirements in the study area. The biomass/energy ratio (Bio_E) and the harvest index ratio with above-ground biomass removed during harvest (Hvsti) were modified based on the authors' experience. The heat unit values required for plant maturity were calculated using the potential heat unit (Phu) program (http://swat.tamu.edu/software/potential-heat-unit-program/). The *heatunit* value was calculated according to the long-term maximum and minimum temperature data and the average number of days that the plant needs to reach maturity (Neitsch et al., 2011). However, it is essential to mention that this parameter's manual calibration was also done for each crop. Some studies have also found that these parameters are the most sensitive in crop calibration for a physically-based model like SWAT (Nair et al., 2011; Sinnathamby et al., 2017; Feng et al., 2017; Uribe et al., 2018). The HRU yields of each harvested crop cycle in each sub-basin were plotted for the simulation period (Figure 5.6). These plots show the simulated values compared to the reference values previously mentioned (8,10 and 0.2 to 4-ton ha^{-1} $cycle^{-1}$, respectively) and the spatial variability obtained.

Potato's annual harvested yields at the HRU level are between 10 to 26-ton ha $year^{-1}$, with an annual average yield of 16-ton ha $year^{-1}$. In terms of spatial distribution, two regions with similar potato harvested yield ranges were identified (Figure 5.6). The HRUs located in sub-basins 2 to 9 (Region 1) presented the highest yield values than the HRUs located in sub-basins 11 to 20 (Region 2). It can be attributed mainly to the spatial distribution of the climatic conditions of the watershed. Region 1 is located at the upper part of the watershed, characterized by having annual average precipitation higher than 2000 mm $year^{-1}$ and an annual average temperature less than 12°C. The tree tomato's annual average harvested yield is 20-ton ha^{-1} $year^{-1}$ with values ranging between 8 to 34-ton ha^{-1} $year^{-1}$. As previously mentioned, tree tomato is present in sub-basins 11 to 20, which corresponds to Region 2. Harvested yield values show less spatial variability in sub-basins 11 and 15 (Figure 5.6). Nevertheless, this is mainly because, for these two sub-basins, the crop area is less than one hectare (corresponding to one HRU) of 356 hectares planted in the watershed. The kikuyu grass is present throughout the watershed except in Sub-basin 8. The planted area corresponds to 58.31% of the total watershed area. The harvested yield values at the HRU level vary between 0.8- and 72-ton ha^{-1} $year^{-1}$(range of yields vary between sites), with an annual average yield of 16-ton ha^{-1} $year^{-1}$. Furthermore, the harvested yields' spatial distribution value is generally constant, except for a few high values obtained in 2014 (Figure 5.6).

Overall, crop yield predictions acquired by manual calibration were satisfactory for the objective of this study. The variability in space and time of the simulated harvest yield was defined per crop in each sub-basin at the HRU level. However, the calibration can be further improved by collecting more field harvest yield values and including them in the model to support the validation. A good description of the agricultural management practices was obtained during fieldwork, but very little information was found on yields. In general, farmers do not regularly record the yield values or do not like to provide this type of information. Furthermore, research on measured harvest yield rates is needed to properly evaluate the model simulation (Sinnathamby et al., 2017).

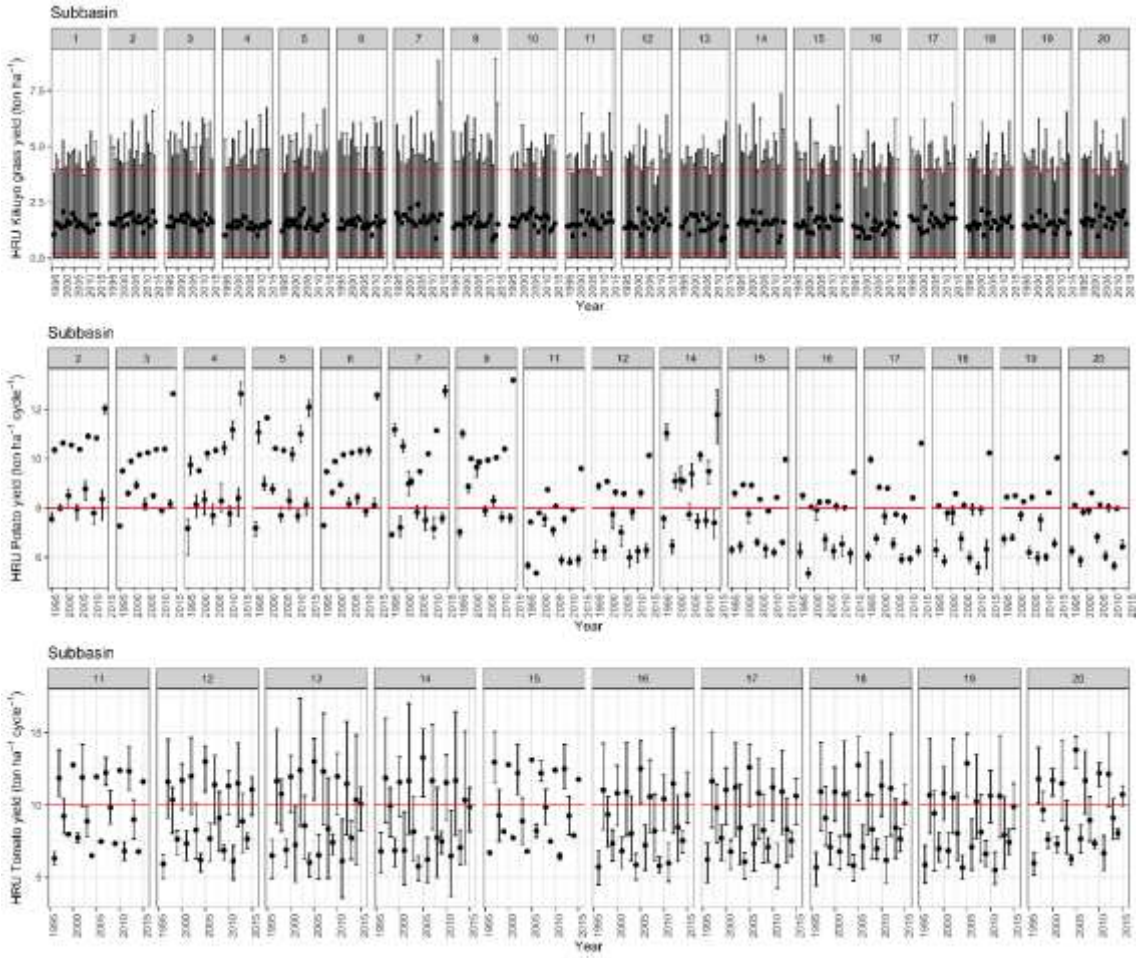

Figure 5.6. Monthly model simulation results for harvested yields (ton ha^{-1} cycle^{-1}) per sub-basin at the hydrological response unity (HRU) level for (a) kikuyu grass, (b) potato, and (c) tree tomato. The reference harvest yield values are shown along the horizontal red line. Error bars represent the standard error of the mean.

Water quality model (nitrogen and phosphorus pollutants)

Model calibration of nutrient losses in the runoff was performed for monthly nitrate N (NO_3^--N), total nitrogen (TN), and mineral phosphorus (PO_4). Sampling quality parameters for the years 2014 and 2015 of the Chico River at the reservoir's entrance were compared with the results obtained in Sub-basin 17. Hydrograph representations of the NO_3^--N (kg month^{-1}), TN (kg month^{-1}), and PO_4 (kg month^{-1}) simulated versus the monthly average discontinuous samples were performed (Figure 5.7). Five parameters were calibrated to improve nutrient loss prediction efficiency in the watershed (Table 5.5). In general, the calibration was done by increasing the coefficients of nitrogen percolation (*nperco*) and phosphorus soil partitioning (*phoskd*) to decrease the nitrate N removed in surface runoff and the amount of soluble P transported in surface runoff. Besides, increasing the rate of the coefficient for denitrification (*cdn)* and the threshold value of nutrient cycling water factor for denitrification to occur (*sdnco)* caused the amount of nitrate available to decrease in the runoff. For NO_3^--N, TN, and PO_4, monthly NSE values were 0.48, 0.32, and 0.33, respectively, which indicates that the results are not satisfactory in terms of extreme values (Moriasi et al., 2007). However, the trends were adjusted appropriately with R^2 values of 0.81, 0.82, and 0.59, respectively. The leading causes of uncertainty in this process could be the following: (1) management operation schedules per crop were defined equally in spatial terms (e.g., same planting and fertilization application dates), (2) uncertainties exist in the observed data (as mentioned earlier, it was only possible to calibrate water quality parameters with grab samples taken discontinuously for two years), and (3) dependence of nutrient yields on hydrologic simulation. Nutrient simulation yields are directly linked to the runoff simulation; Therefore, uncertainties in the runoff estimates are transferred to nutrient load prediction.

Overall, visual inspection of the results shows a relatively good temporal match between simulated and observed values. The most significant uncertainties occur at the extreme event during March 2014 and August 2015 for nitrogen components (Figure 5.7a and 5.7b), and in April and May 2014 for mineral phosphorus (Figure 5.7c). The study carried out by Suescún et al. (2017) allowed us to confirm the direct link between nutrient yields and the precipitation-runoff seasonality at the Riogrande watershed. However, it is worth mentioning that priority was given to represent the nutrient loads simulated with the available information. Consequently, it was possible to adjust the management operation schedule dates so that they were consistent with the reality identified during the nutrient's calibration process. Therefore, we emphasize the need for continuous measurements of water quality parameters for non-point sources in Colombian watersheds. It will help to facilitate a proper calibration of the water quality models.

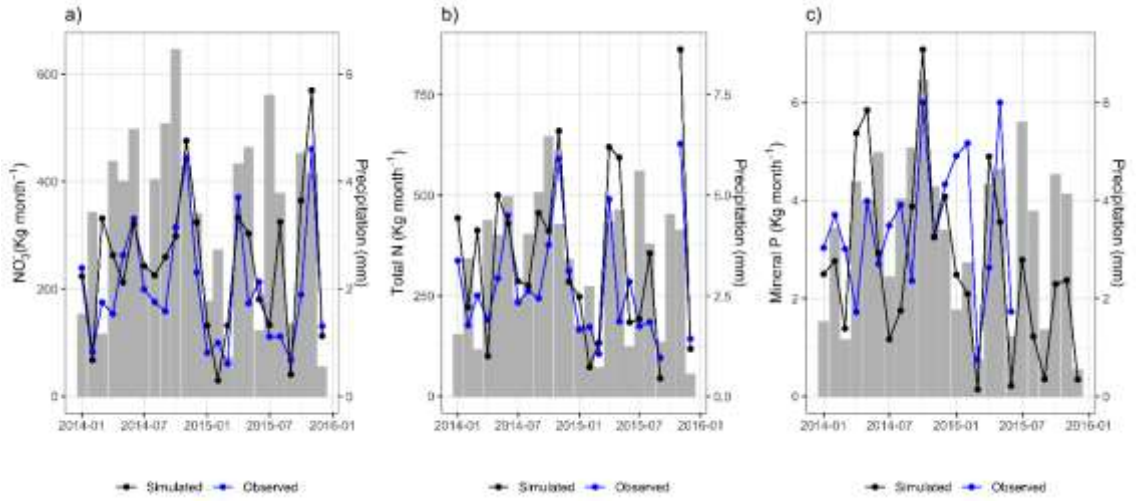

Figure 5.7. Monthly water quality calibration results for (a) NO_3^--N (b) TN, and (c) mineral P load for the period 01/2014 – 12/2015. The gray shaded area is the precipitation (mm). The observed data is represented by the blue dots and the simulated data by the black dots. NO_3^-N: nitrate-nitrogen, Total N: total nitrogen, Mineral P: mineral phosphorus.

5.4.2 Identification of spatio-temporal critical source areas (ST-CSAs)

This section aims to identify the spatio-temporal CSAs at the field (HRU) level in the Riogrande watershed. The LPUAI targeting method was generated for each month of the 21-simulated years, based on pollutant loads of NO_3^--N and soluble P per area, which normalizes each HRU for comparison. Based on a temporal trend analysis of NO_3^--N and soluble P modeling results, the yields varied from 0.0 to 57.0 kg N ha^{-1} and 0.0 to 5.2 kg P ha^{-1}. However, the highest frequency of NO_3^--N in surface runoff and soluble P yield occurred in the range of 0.0 to 10.0 kg N ha^{-1} and 0.0 to 1.0 kg P ha^{-1}. The results indicate that a low percentage of the HRUs contribute to the highest pollutant loads, and these high yields occurred only in specific months of the 1995-2015 simulated period. Threshold values of 1.71 kg N ha^{-1} and 0.18 kg P ha^{-1} for NO_3^--N and PO_4, respectively, were defined as the limits to identify the 10% of the HRUs that generated the most significant monthly load contributions.

Temporal analysis

The monthly temporal analysis of the CSAs for NO_3^--N and soluble P of the entire simulated period shows that the CSAs occur more frequently in 1996, 1999, 2002, 2005, 2008, 2011, 2014 (Figure 5.8). Since the start of the simulated period, a three-year cycle occurs, showing more presence of CSAs. It can be explained by the fact that the rotation between the second harvest cycle of the potato and kikuyu grass occurs every three years, according to the defined management schedules for the crops studied. Additionally, these

years correspond to extreme events of precipitation level related to the La Nina phenomenon. The years 1999 and 2011 have been reported as the heaviest years of precipitation ever recorded in Colombia (Suescún et al., 2017).

On the other hand, the months from April to June and September to October present the highest number of CSAs in most simulated years (Figure 5.8), corresponding to the two periods of rainfall in the study basin. These months also register the highest amount of fertilizer applied for the cultivation of potato and tree tomato. Kikuyu grass is also fertilized in these months, but the cattle rotation allows a more homogeneous distribution of fertilization during the year. The months in which the fertilization of the three crops coincided were also the months with the highest number of CSAs associated with the NO_3^--N and soluble P (e.g., May in Figure 5.8). In contrast, when fertilization occurs only for kikuyu grass, the CSAs decrease (e.g., March in Figure 5.8). Notably, in some months (e.g., January and February), no CSAs were identified since it is the beginning of crop sowing. In conclusion, the temporal variability of CSAs for nutrients in the runoff is associated with rainfall regimes in the study basin. At the same time, it matches the date of the fertilization operations.

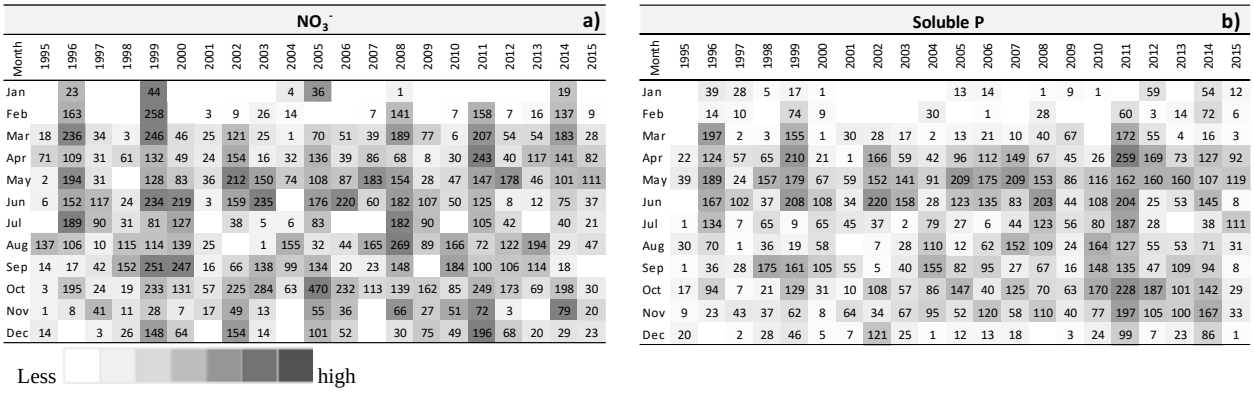

Figure 5.8. Illustration of the CSAs monthly temporal variation over 19 years of simulations (1996-2015) for (a) NO_3^- and (b) soluble P. The grayscale represents the total number of CSAs in each month. NO_3^-N: nitrate-nitrogen, Soluble P: soluble phosphorus.

Spatial analysis

The spatial analysis was performed on an annual and monthly basis. Results showed that the spatial distribution of NO_3^--N and soluble P losses per year was greater in two specific regions of the watershed (Figure 5.9). Fewer CSAs were found in sub-basins 1 to 11 (Region 1) than in sub-basins 12 to 20 (Region 2). Thus, the watershed area with the highest precipitation presents the lowest number of CSAs and vice versa. This result can be attributed to the spatial distribution of rainfall in the study area (Figure 3.5 – Chapter 3). Region 1 is characterized by higher annual average rainfall than Region 2. However,

the results also show a higher variability of CSAs in each sub-basin per year in Region 2, which can be explained by the temporal variability. For instance, Sub-basin 12 has the highest number of CSAs, followed by sub-basins 16 and 17 for nitrate-N and soluble P.

Additionally, some years in the total simulation period were selected for graphical representation of the monthly spatial variability of the CSAs for NO_3^--N and soluble P losses. These years were chosen according to the annual average rainfall (Figure 5.9).). The spatial analysis results monthly show that the trend of the highest recurrence of CSAs per month occurred in sub-basins 4, 5, 7, and 9 (within Region 1), and 12, 15, 17, 19, and 20 (within Region 2) for NO_3^--N and soluble P (Figure 5.9).), which are sub-basins where the three crops grow (POTA, PASM, and TOMA). In contrast, for sub-basins 1, 8, and 10, very few or almost no CSAs were identified for the months analyzed. The area of these sub-basins is dominated by stubble (MESQ), seeded grasses (RYEG), and annual ryegrass (RYEE) crops. In summary, the spatial pattern of the CSAs is related to the spatial variability of precipitation and the crop area's location, which has been previously defined by the different agricultural management operations (e.g., rotation of crops and fertilization). Fewer CSAs were identified in the areas with less crop area.

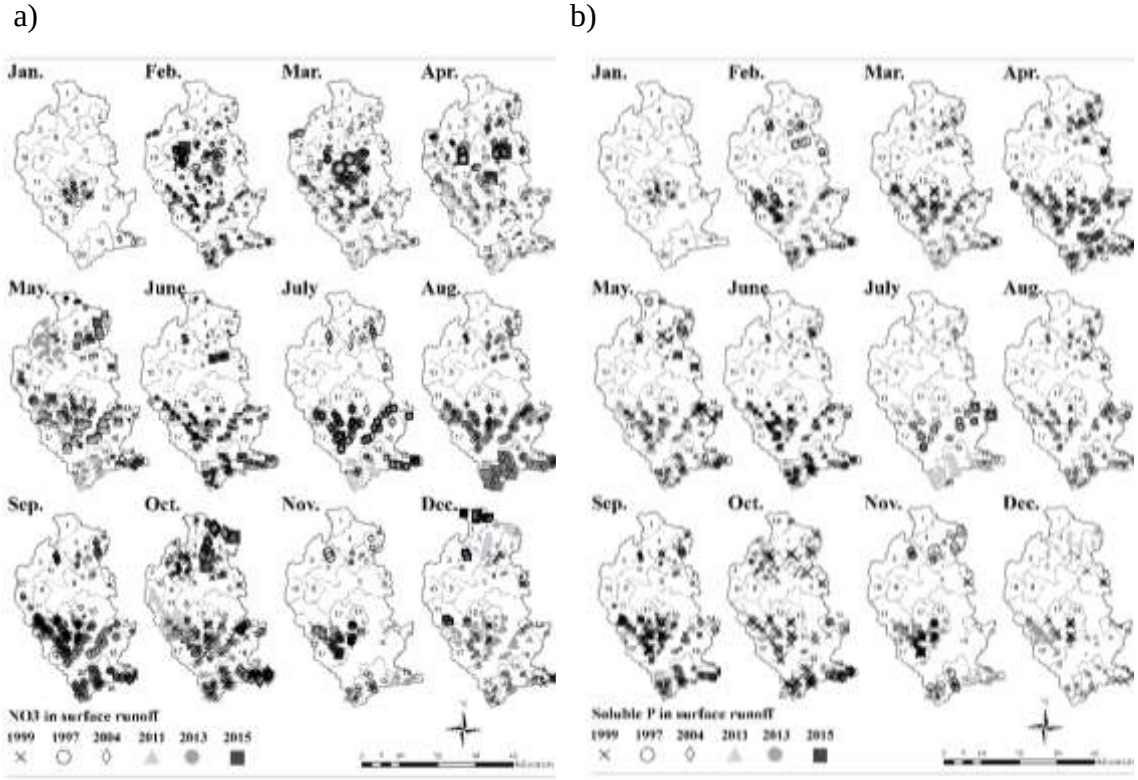

Figure 5.9. Illustration of the CSAs monthly temporal variation over six years of the simulation period for (a)NO_3^- and (b)soluble P. The years presented are selected based on annual average precipitation: 1999 and 2011 (high), 2004 and 2013 (middle), and 1997 and 2015 (low). NO_3^-: nitrate-nitrogen, Soluble P: soluble phosphorus.

Spatio-temporal (ST-CSA) analysis

The CSA temporal analysis showed a recurrence pattern associated with the rainy conditions in the area and the scheduling and quantity of fertilizers applied. For the spatial component, it was possible to identify areas of greater numbers of CSAs, where there is low precipitation, and most of the crops include agricultural management. However, to represent the behavior of the CSAs simultaneously in space and time, the spatio-temporal CSA index (ST-CSA) was applied. A value equal to 1 indicates that the HRU examined in space (location) and time (month-to-month) was always identified as a CSA during the simulated period. The ST-CSA index allows visual analysis of the recurrence and behavior in space and time of the CSAs for the entire simulated period. The ST-CSA index for NO_3^--N and soluble P obtained in the Riogrande watershed is shown in Figure 5.10a and 5.10b. The results allowed us to identify sub-basins with high and medium degrees of CSAs recurrence, which were not detected in the spatial analysis previously performed. For example, Sub-basin 15 has CSAs with the ST-CSA index equal to 1, and sub-basins 3 and 5 have CSAs with values between 0.4 to 0.6 for NO_3^--N (Figure 5.10a). Some areas in the basin, such as sub-basins 1, 5, and 10, do not present any CSAs for soluble P (Figure 5.10b). For both nutrients, sub-basins 4, 12, and 20 obtained an ST-CSA equal to one, which indicates that they were always identified as a CSA during the simulated period. A high percentage of the CSAs identified for NO_3^--N also contains the CSAs for soluble P, but not always. We believe that the ST-CSA index is the most relevant indicator to understand the spatio-temporal dynamics of nutrient loss via runoff at the watershed scale. It is a significant result since, for the first time, we can affirm that an identifiable "large-watershed-scale" exists for CSAs, which can be visually represented in terms of the recurrence in space and time of CSAs within the watershed. This result needs to be extended to the case where the runoff generation method includes topographic effects for slopes greater than 5%, for example, using the methodology proposed by Tessema et al. (2014).

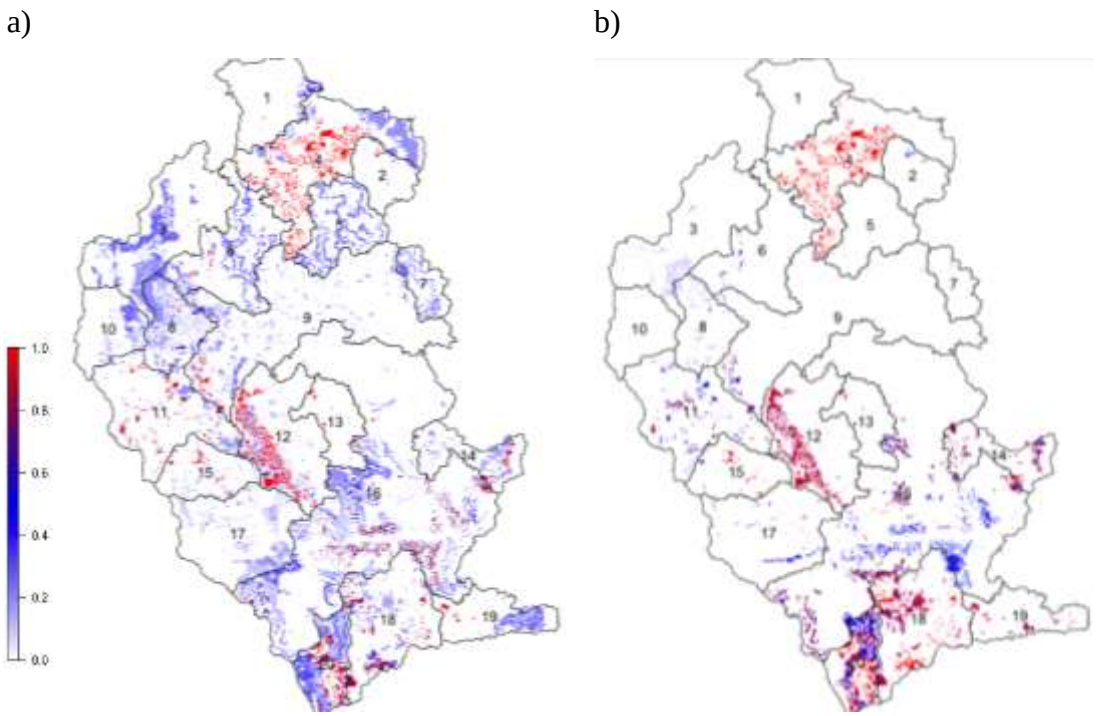

Figure 5.10. Illustration of the spatio-temporal CSA index (ST-CSA) over the 19 years of simulations (1996-2015) for (a) NO_3^- and (b) soluble P. The blue-red color scale represents the recurrence in space and time of the CSAs. A value equal to 1 indicates that the HRU was always identified as a CSA for the entire simulated period.

5.4.3 Spatio-temporal critical source areas characterization

The spatio-temporal CSAs identified were analyzed to describe the general characteristics and common patterns among them. The minimum, maximum, and average monthly values of the area, slope, precipitation, runoff, total N and P applied, and total NO_3^--N and soluble P were analyzed (Table 5.7). The results show that on an annual average, the CSAs correspond to 24.07% of the entire area of the basin (1034.348 km^2), and the maximum and minimum area corresponds to 61.78% and 4.39% in 2005 and 1997, respectively. In terms of monthly averages, the losses of NO_3^--N and soluble P in the runoff of the CSAs varied from 1.17 to 57.75 kg N ha^{-1} and 0.18 to 7.18 kg P ha^{-1}. However, the average production of NO_3^--N was 4.56 kg ha^{-1} and 0.25 kg ha^{-1} for soluble P. The average area of the CSAs was 28 ha, but they ranged from 4,179 ha to 0.02 ha. The range of precipitation varied from 28.50 mm to 508.80 mm, with an average value of 206.68 mm, which generated an average runoff of 28.45 mm. CSAs had an average slope of 25%.

Notably, all the soil types used in the model were defined in the CSAs, which correspond mostly to the Andisol soil type. However, the Cor and Ab soils were not

identified in the CSAs with soluble P. As expected, kikuyu grass (PASM), potato (POTA), and tree tomato (TOMA) provide the highest NO_3^--N and soluble P losses, which are mainly associated with the fertilization operations defined in agricultural calendars for the simulation period. Also, transitional crops (CANT), annual ryegrass (RYEG), weeded grass (RYEE) and managed stubble (MESQ) were associated by providing NO_3^--N in the runoff. The monthly average nitrogen and phosphorus applied (fertilizer + grazing) in the CSAs are 35.0 kg ha^{-1} and 4.8 kg ha^{-1}, respectively. The average amount of NO_3^--N and soluble P generated in runoff is 4.56 kg ha^{-1} and 0.25 kg ha^{-1}, respectively. However, in different CSAs and months, the maximum values of NO_3^--N and soluble P can reach 57.75 kg ha^{-1} and 7.18 kg ha^{-1}, respectively.

Table 5.7. The minimum, maximum, and average values of the area, slope, precipitation, runoff, total N and P applied, and total NO_3^--N and soluble P loads in the spatio-temporal CSAs identified.

Value	Area (ha)	Average slope (mm^{-1})	Precipitation (mm)	Runoff (mm)	N applied (kg N ha^{-1})	P applied (kg P ha^{-1})	NO_3^- (kg ha^{-1})	Soluble P (kg ha^{-1})
					Fertilization			
Min	0.02	0.20	28.50	0.32	0.00	0.00	1.71	0.18
Max	4179.2	87.26	508.80	180.92	166.25	46.20	57.75	7.18
Average	28.09	25.03	206.68	28.45	34.13	4.65	4.56	0.25
					Grazing			
					0.00	0.00		
					1.90	0.40		
					0.87	0.18		
Landuse	CANT	MESQ	PASM*	POTA*	RYEE	RYEG	TOMA*	
Soil	Cor mo*	Ab V*	Cv1* Vco*	Es*	F*	L*	Lm*	Lome*

*For both, NO_3^--N and soluble P. **Average slope steepness (m m^{-1})

Statistical analysis

The ANOVA results obtained from the statistical analysis (Appendix A.4) indicate that the soil water content for Lm and F soil types is significantly correlated with NO_3^-N loss at a significance level of >0.90 (i.e., $p < 0.10$). The surface runoff and Cor soil type are also correlated with the NO_3^--N loss at a significance of $p<0.01$. In contrast, a negative correlation occurs between the Mo soil type and NO_3^--N loss at a significance of $p<0.10$. Also, precipitation ($p<0.05$), CN value, slope, and HRU area ($p<0.01$) are negatively correlated to NO_3^-N loss. On the other hand, the ANOVA results for soluble P (Appendix A.5) indicate that the runoff, precipitation, and soil water content have the highest correlation, with a significance of $p <0.01$. Likewise, the slope, HRU area, and CN value have an negative impact on soluble P loss ($p <0.01$).

A positive correlation between soil content and surface runoff was expected. The amount of NO_3^--N and soluble P losses in surface runoff calculated in the SWAT model is directly related to (1) the nitrate and phosphorus in the available water for the top 10 mm of soil, (2) saturated soil water content (only for nitrate), (3) soil bulk density (only soluble P), and (4) the surface runoff generated on a given day (Eq. 2.4 and 2.7- Chapter 2). The main reason for CN values to have a negative correlation with NO_3^--N and soluble P losses is that the amount of surface runoff is directly proportional to the retention parameter defined according to the CN value, which is based on the type of soil, land use, management, slope, and changes in soil water content. In other words, having a higher CN value increase surface runoff, causing the NO_3^--N also to increase. Also, the precipitation is directly proportional to the amount of mobile water in the soil layer. If rainfall increases, the concentration of nitrate and soluble P in the mobile water decreases since mobile water in this layer increases (Eq. 2.3 and 2.7- Chapter 2). A higher dilution occurs (Yazdi et al., 2019). In particular, the soluble P results suggest that all types of soils presented a negative correlation with a degree of significance of $p < 0.01$. The main reason for this is that the bulk density of the first layer of the soil is inversely proportional to the amount of soluble phosphorus. In our case study, the bulk density of the first soil layer for the different Andisol soils does not vary significantly (Appendix A.5). Therefore, the difference in the correlation of soil type with the soluble P is minor.

Moreover, the results suggest a negative correlation between NO_3^--N and soluble P losses, and slope since changes in slope could slightly change the nitrate and soluble P removed in the surface runoff. For example, if the slope increases by 1%, the reduction could be 0.008 kg ha^{-1} and 0.003 kg ha^{-1} for NO_3^--N and soluble P, respectively (Appendix A.4 and A.5). However, this result was inconsistent with another study's conclusions (Yu et al., 2015), which indicated that the slope has a significant correlation with water quality variables for agricultural lands due to surface runoff variation. The CN method used to calculate surface runoff does not directly consider the slope, and therefore it was necessary to adjust the CN values for soils with a slope higher than 5%. Notably, this is a limitation since the slope average is 25% in the Riogrande watershed. Likewise, the influence of the area of each CSA is inversely proportional to both NO_3^--N and soluble P losses, as expected. The NO_3^--N and soluble P in surface runoff were calculated for each CSA in kg of N or P per hectare. Thus, the results suggest that if the HRU area increases by one ha, the NO_3^--N and soluble P losses decrease by 0.137 kg N ha^{-1} and 0.056 kg P ha^{-1}. There is some indication that by decreasing field sizes, the surface runoff decreases (Fiener et al., 2011; Lam et al., 2011), although in other studies, the opposite has been found (Gao et al., 2017; Zhou et al., 2016). Therefore, the spatial scale used in this modeling approach to identify the spatio-temporal CSAs at the HRU level is the best possible way to represent the characteristics of small farms in the study area spatially.

Finally, the post-hoc test results allowed us to determine the hierarchical importance of the sub-basins' influence and soils on NO_3^--N and soluble P. The CSAs located in sub-basins 9, 13, 19, 6, and 16 with soils Cor, Lome, F, L, and Cv1 have a higher influence

in the generation of NO_3^--N runoff. For soluble P, sub-basins 19, 7, 13, 9, and 2 with soils Vco, L, mo, Cv1, and Lm were the major influencers. Therefore, the CSAs located in these sub-basins were prioritized based on the type of soil and the type of crop (potato, tree tomato, and kikuyu grass for the cattle system) to implement BMPs. Also, depending on the intervention area, other CSAs located in different sub-basins can be selected according to their importance level. The post-hoc test results for sub-basins and soils are presented in Appendix A.6 and A.7.

5.4.4 Importance of the spatio-temporal CSAs to defining BMPs

In general, in practice, identifying non-point source pollution effects on water quality using modeling tools is complex. As shown above, many factors and mechanisms have been identified as triggers of nutrient loss. The spatial and temporal scales (Zhou et al., 2016), agricultural management practices, slope (Yu et al., 2015), and precipitation-runoff conditions (Huang et al., 2015; Gao et al., 2017) influence simulated nutrient losses. In addition, limitations of the hydrological models used to represent these processes introduce uncertainties in simulated results. However, in this study, we focused on understanding and characterizing the spatio-temporal CSAs of non-point source pollution on water quality at a watershed scale. Our methodology provides a visual representation of the recurrence and behavior in space and time of the CSAs through the ST-CSA index, which offers relevant information for decision makers and stakeholders. In this way, areas can be identified for focused intervention. Our analysis clearly shows a strong association between both precipitation seasonality and agricultural management schedules (crops and pastures system) and the spatio-temporal dynamics of the CSAs. Thus, there is evidence, based on the identified spatio-temporal CSAs, of the need to improve fertilizer practices to minimize applications in the rainy months.

Additionally, our results provide insight for land managers in tropical mountain areas, where the implementation of BMPs for the agricultural sector is increasingly promoted. In the case of Colombia, the guide of "*Buenas Prácticas para la Gestión y Uso Sostenible de los suelos de Colombia"* (in Spanish) (Organización de las Naciones Unidas para la Alimentación y la Agricultura (FAO) and Ministerio de Ambiente y Desarrollo Sostenible (MADS), 2018) recommends the identification of priority areas to implement BMPs. The guide offers around 15 BMPs that farmers can use, considering methods of application, economic viability of the products, and social and cultural conditions of the area. However, there is still a clear need to incorporate the temporal and dynamic spatial aspects existing in the agricultural land management-water quality system. Therefore, for selecting appropriate BMPs viable in the future, the spatio-temporal CSAs should be identified to determine the best areas for intervention.

Equally important, as mentioned before, we are currently investigating the agricultural BMPs selection and allocation at the watershed scale using a detailed spatio-temporal multi-objective optimization approach. The results obtained will be used to

describe the spatio-temporal dynamics of the modeled system, which will, in turn, be used as the baseline for the optimization problem. They will also be used to select BMPs incorporated into the optimization problem, which will be more in line with local needs and have a higher probability of being implemented to achieve sustainable agricultural development goals. In this way, we will contribute valuable information that allows the incorporation of the temporal and dynamic spatial aspects into optimization approaches for different types of agricultural optimization problems and the improvement of the integration of relevant models into the optimization process. The results of these ongoing investigations are reported in the next chapter.

5.5 CONCLUSIONS

The highest number of spatio-temporal CSAs were observed during the rainy months, particularly in managed agricultural and pasture systems. However, the most significant actual number of CSAs occurs in the region with the lowest rainfall in the Riogrande watershed. The spatio-temporal CSAs correspond to an average area that is 24.07% of the total watershed (1034.348 km^2). However, in some years, the area reached a maximum value of 61.78%. Also, the NO_3^--N average loss for the CSAs is 4.56 kg ha^{-1} in the surface runoff, while it is 0.25 kg ha^{-1} for soluble P in the surface runoff. The soil water content and runoff significantly influenced both NO_3^--N and soluble P losses, which are variables directly correlated to the amount of NO_3^--N and soluble P loss in surface runoff (kg ha^{-1}) calculated in the model. It is particularly critical in managed agricultural systems where increased runoff nutrient losses are combined with unsustainable fertilizer management practices. In contrast, a negative correlation occurs between precipitation, curve number value, slope, and HRU area with both NO_3^--N and soluble P. Therefore, future research that addresses these points will help mitigate the uncertainty in allocating BMPs at the watershed level.

This approach, which uses modeling tools to identify spatio-temporal CSAs, provides a clear and organized way to define successful agricultural BMPs and develop spatio-temporal multi-objective optimization modes (to be carried out as the next step in this research). It is also important to focus on exploring other methods for calculating runoff at the watershed scale, including approaches that directly consider the influence of steep slopes.

6

SPATIO-TEMPORAL MULTI-OBJECTIVE OPTIMIZATION TO SELECT AND ALLOCATE AGRICULTURAL BMPS FOR MULTIPLE CROPS

"Conocimiento util para los campesinos"

6.1 ABSTRACT

Optimization techniques to select and allocate agricultural BMPs for watershed management require understanding complex space-time hydrological variability within the watershed. Based on chapters 4 and 5, it was possible to assess the difference in the effects of BMPs with and without spatio-temporal analysis. The spatio-temporal analysis for allocating agricultural BMPs (Ag-BMPs), especially in the watersheds where the issue of shifting cultivation, intensive traditional agriculture, diverse crops, and weather seasonality are predominant factors, is quite complex. This chapter proposes a spatio-temporal multi-objective BMP optimization framework, which can be used for selecting and allocating the Ag-BMPs for run-off pollution control at a field scale. The optimization framework is based on spatio-temporal critical sources areas (ST-CSAs) for potential Ag-BMPs spatial location, which represent the behavior of the pollutants simultaneously in space and time within the watershed (Uribe et al., 2020). In the proposed approach, the multi-objective optimization NSGA-II algorithm was integrated with the Soil and Water assessment Tool (SWAT) model. A case study was conducted in the Riogrande II watershed in the Colombian-Andes, which suffers severely from runoff nutrient loss due to the intensive dairy cattle and crop production activities. Five Ag-BMPs selected from previous studies (fertilizer management, minimum tillage, contour planting, filter strips, and living fences) were used in the proposed approach, considering the multiple optimization objectives, which included minimizing Nitrate (NO3-N) load and maximizing crop yields of kikuyu grass (*Pennisetum clandestinum*), potato and tree tomato. An analysis of all degrees of freedom of the optimization problem is used to assess its complexity, and to later narrow down the dimensionality of the problem based on physical spatial and temporal homogeneities. After this, a simplified HRU concept of the hydrological representation is used to find the ST_CSA that can be optimized and the rime frames that are logical for such optimization. Then an NGSA-II algorithm ran over the model and a comparison between the Pareto-optimal front solutions is aggregated. The distribution of solutions was analysed in multiple aggregated (clustered position). The results show that different types of analysis applied (aggregated vs distributed) with different Ag-BMPs scenarios led to significant differences in resulting Pareto-optimal front solutions, optimizing efficiency, and spatial distribution of Ag-BMP scenarios.

Overall, using the HRUs-clusters position units as Ag-BMPs optimization result with the ST-CSAs strategy, had the best Ag-BMP scenarios. Therefore, the Pareto-front solutions must be defined in a distributed way, which means having a Pareto-front solutions for each of the different areas (HRUs grouped in clusters) with similar spatial characteristics for watershed BMP scenarios optimization model.

6.2 INTRODUCTION

Increased water resources pollution around the world has generated pressure on agricultural practices. And, the great increase in food demand, projected by 2050, suggests an increase in intensive agriculture (Alexandratos and Bruinsma, 2012). Agricultural BMPs aim to protect water quality, prevent soil degradation, reduce soil erosion, and enhance farm production and farmers' social well-being (Ritter and Shirmohammadi, 2001). However, the selection and allocation of agricultural BMPs is a very complicated task, involving decision-makers and stakeholders, multiple conflict objectives, temporal and dynamic spatial aspects, and constraints (Liu et al., 2013). Therefore, it is currently recognized that to design agricultural BMP scenarios for the adoption and promotion at the watershed scale; the problem has to be formulated as a multi-objective optimization problem (Memmah et al., 2015).

Many optimization models have been built and implemented in many regions around the world for assessing BMPs effects in protect water quality resources. Despite its well-defined framework the practices are not unique and not all apply to all situations. Previous studies have developed several optimization engines that can be employed for the spatial BMP localization at different scales (field, sub-watershed, and watershed), aiming to achieve the most cost-effectiveness scenario. Among these, the Non-dominated Sorting Genetic Algorithm (NSGA-II) or Genetic Algorithm (GA) has been coupled with the Soil and Water Assessment Tool (SWAT) as optimization engines (Liu et al., 2019; Geng et al., 2019; Dai et al., 2018; Babbar-sebens and Minsker, 2012; Maringanti et al., 2011; Liu et al., 2013; Panagopoulos et al., 2013; García et al., 2000). The SWAT model is commonly used because it can simulate different BMP types, and it is closely connected to GIS (Geographic Information Systems). Other BMP optimization studies have used others metaheuristics search algorithms, such as, Strength Pareto Evolutionary Algorithm (SPEA2) (Rabotyagov et al., 2012) coupled with other NPS pollution models, e.g., WQM-TMDL-N, HSPF, and AGNPS (Barton, 2009; Doody et al., 2012) However, because of the spatio-temporal resolution of these NSP pollution models, they are more frequently used for aggregated but sparse BMP types (e.g., vegetated buffers and constructed wetlands). Those research effort provide a potential base for developing a multi-objective optimization framework for placement of BMPs. Nevertheless, despite the increase of using optimization frameworks to select and allocate agricultural BMPs, research in this area has limitations due to the high number of optimization parameters and the large uncertainty in building large models. Aside from these problems is the high computational demand. There are important gaps related to this topic that have been identified: 1) the inclusion of temporal and dynamic spatial aspects, and 2) the inclusion of the knowledge of decision-makers and stakeholders to select the BMPs to be optimized (Babbar-sebens and Minsker, 2010). Previous research has focused on the spatial scale only and has ignored the temporal scale. In addition, the units used to allocate the BMP options do not always contribute to the most pollution concentration and consequently may not be the best place for their implementation. Thus, there is still a clear need to

explore the impact of different optimization approaches for different types of agricultural optimization problems. This is usually the case of watersheds located in tropical' mountainous regions, where shifting cultivation, intensive traditional agriculture, and weather seasonality are common.

Recent studies proposed different approaches to demonstrate the impact of spatial scale changes on the allocation and effectiveness of BMPs (Geng and Sharpley, 2019; Zhu et al., 2019; Qin et al., 2018). Most of the studies found in the literature focus on one or a few spatial allocation components, like: 1. BMP selection, 2. location determination, and 3. design and sizing. For example, Geng and Sharpley (2019) evaluated different spatial scales (field and watershed) using the number of sub-watersheds and the average sub-watershed size for BMP placement as key indices. They used the critical source areas (CSAs) approach to identify in advance the prioritized location for BMP, which only considered the mean annual TN and TP loads. Yet another focus study is, for instance, the work done by Zhu et al. (2019) considering only topographic characteristics to determine the BMP configuration units as the best way for the location determination. But, the locations identified are optimal only for BMPs focusing to mitigate soil erosion based on the conservation practice factor of the USLE (i.e., USLE_P). Thus, we consider that the three spatial allocation components must be involved in the spatial BMP allocation optimization. Equally important, it is necessary to incorporate into the agricultural BMP optimization problems the temporal scale (e.g. hourly or monthly), and other objective functions as well, such us improving productivity of the crops that may bring economic benefits to the farmers and enhancing the BMP implementation acceptance.

In contrast, in this study, we propose to include the temporal and dynamic spatial aspects, contemplating the three spatial allocation components (BMP selection, location determination, and design-sizing), for selecting and allocating agricultural BMPs feasible in a watershed of the Tropical Colombia-Andes Mountains, as well as measures to improve water quality without offsetting agricultural productivity, and decision-makers' and stakeholders' knowledge into the agricultural BMP optimization model. Hence, the main objectives of this study were to develop a spatio-temporal multi-objective agricultural BMP optimization framework, to select and allocate the optimal BMPs for run-off pollution and agricultural productivity control at a field level. Which, uses the new approach of the spatio-temporal critical sources areas (ST-CSAs) (Uribe et al., 2020) for a more effective agricultural BMPs identification and allocation. The expected results will provide a concrete application of a spatio-temporal multi-objective optimization framework for selecting and allocating feasible agricultural BMPs in a watershed where shifting cultivation, intensive traditional agriculture, and weather seasonality have been typically applied. Also, this study presents a complementary policy instrument for controlling non-point source water pollutants and is an assistance tool for the local communities (farmers), which can be used to adapt the agricultural practices in order to cope with unexpected changes identified in recent years.

This chapter has five sections. Section 6.2 describes the modeling components and integration, including the BMPs description and representation, the multi-objective optimization formulation (decision variables and objective functions), the NSGA-II algorithm overall process, setup and implementation, and the sensitivity analysis of the NSGA-II parameters, as well as the feasible optimal BMP selection method. Section 6.3 presents the results of the modeling-optimization tool. These results include a test of the coupled optimization script/running, the pareto-optimal front solutions derived from the average and single objective site values among the different BMP scenarios, and the comparison between them. Section 6.4 presents the discussion, and the conclusions are drawn in the last section.

6.3 METHODOLOGY

6.3.1 Modelling framework

The spatio-temporal multi-objective optimization framework proposed is an approach focusing on the minimization of nitrate (pollution) and maximization of crop yields at the field level to select and allocate optimal agricultural BMPs (Figure 6.1). It provides multicriteria options for decision makers to improve water quality without offsetting agricultural productivity. In our approach, the optimal BMP placement contemplates the following five main components (Figure 6.1).

1. **Estimation of spatial and temporal dynamics** of nutrients in runoff resulting from current agricultural practices. A Nitrate-N loads (NO_3^-N) in runoff and crop yields estimation model was used.
2. **Location determination** for effective BMPs implementation. Spatio-temporal critical sources areas (ST-CSAs) for potential BMPs spatial location were defined (Chapter 5).
3. **Stakeholders' knowledge** to select Ag-BMPs scenarios. Interviews and workshops with farmers were carried out to select the BMPs scenarios, and the parameterization of these to be incorporated in the hydrological model was done (Chapter 4 and 5).
4. Determination of the **optimal BMPs solutions that** minimized nutrient in runoff and increased crop yields, based on current state of the catchment. An optimization model that used the metaheuristic algorithm (NSGA-II) coupled with the Soil and Water Assessment Tool (SWAT) as an optimization engine was built.
5. Determination of the **spatial analysis level results** to select the optimal BMP. Pareto-front results are compared between the average and single sites (HRUs) values, for each objective function.

The first two components of the proposed multi-objective optimization framework were fully developed in our earlier study (Uribe et al., 2020) and described in chapter 5. The hydrological SWAT model (Soil Water Assessment Tool) was used to model the hydrology, water quality, and crop yields of the Riogrande II watershed (See Uribe et al.,

2020 and Chapter 5 for the case study description). The **modeled period was from 1995 to 2015**. The watershed was defined with **an area of 103,434.77 ha** and **delineated into 20 sub-basins** representing the main tributaries. The slope classes were defined in five ranges (0–5%; 5–15%; 15–40%; 25–60%; and>60%) and **3060 HRUs were delineated**. The current agricultural management practices, based on field data collection and presented in chapter 5, for potato, tree tomato, and kikuyu grass (dairy farming), were setup. The model was calibrated in two phases as described in chapter five, one using observed discharge, and two using nitrate-N (NO_3^-N) losses and crop yields at a monthly scale (Uribe et al., 2020). The Nitrate-N loads (NO_3^-N) in runoff and crop yield values for potato, tree tomato, and kikuyu grass at Hydrological Response Units (HRUs) were estimated in chapter 5.

On the other hand, the spatio-temporal critical source areas (ST-CSAs) were identified in order to select the areas that simultaneously contribute in space and time with the highest pollutant loads within the watershed (Uribe et al., 2020), and a such narrow the space of possible solutions. And, for a more effective agricultural BMPs placement, the ST-CSAs was used as BMP sample (configuration) units which are used as the search space for the optimization problem. This approach allowed us to contemplate the temporal and spatial dynamics of the nutrients in runoff to guide the feasible agricultural BMP scenario selection and the location determination. The following subsections present the detailed description of the other three main components.

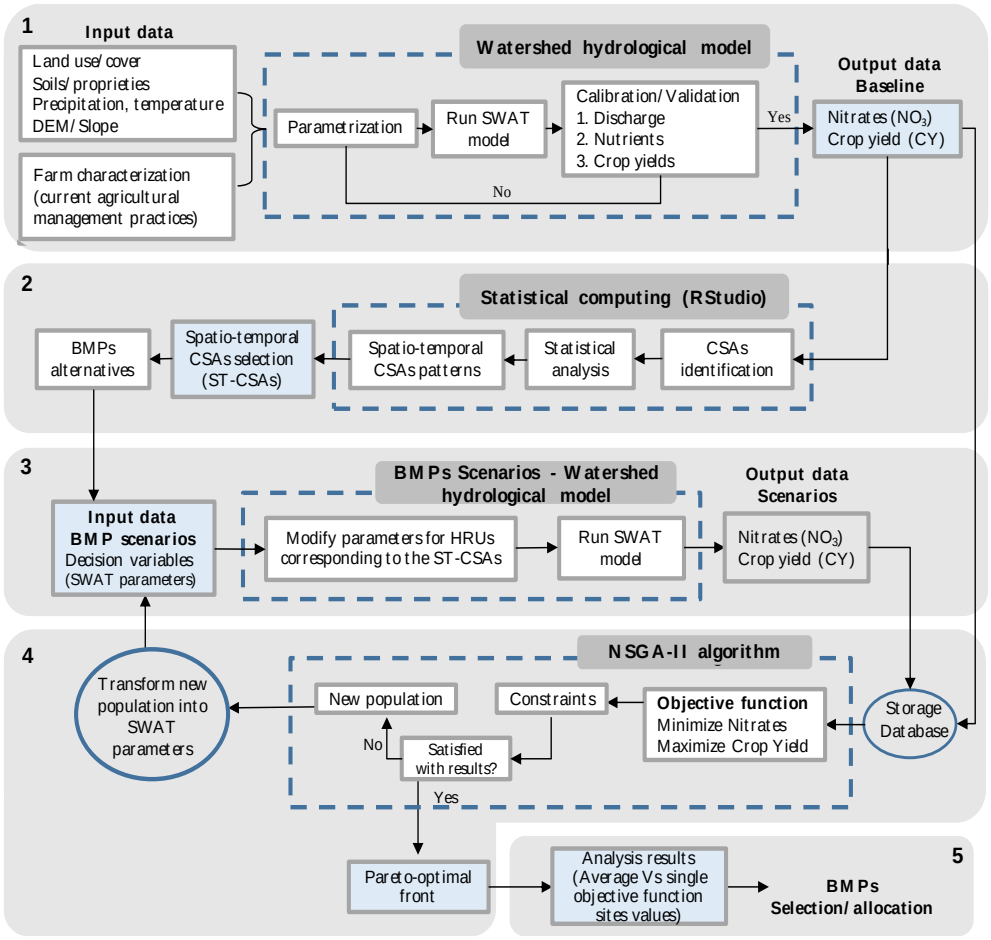

Figure 6.1. Spatio-temporal multi-objective agricultural BMPs coupled-model optimization framework

6.3.2 Human considereations in selection and parametritation of BMP scenarios

A total of five agricultural BMPs types appropriate to the Riogrande II watershed were selected to improve the water quality in runoff and crop yields (Table 6.2), a detailed description of the BPMs is presented in Chapter 2.

Fieldwork and interviews with local farmers were considered to select the feasible BMPs for the watershed studied. A total of **2017 surveys carried out in 123 representatives' farms (48 specialized farms in milk, 40 potato, and 35 tree tomato)** were applied and studied. The detailed data are reported in our previous study (Osorio et al., 2019), which was produced in collaboration with the University of Antioquia. These BMPs were selected because they are agricultural practices that do not increase implementation costs, they can be implemented by farmers with the tools and financial resources they currently have, and they were acceptable to farmers (some were proposed by the farmers themselves). The five BMPs selected are **fertilizer management,**

minimum tillage, contour planting, filter strips, and living fences. A brief description of the selected BMPs and their implementation in the SWAT model is presented below, and Table 6.2 summarized the parametrization of the selected agricultural BMPs to be evaluated in the modeling-optimization framework.

BMP_1) Fertilizer management: This practice has as primary objective to apply the required amount of fertilizers needed by the plant at the right time and place. The BMP_1 was simulated in the SWAT model by reducing the amount of fertilizer applied (Fert_kg) in each of the three crops selected. For this the decision range of reduction between 0 and 5% is set, however, here is good to add that to avoid an unfeasible solution, related to the the information provided by the users, the analysis of the objective function will consider always a baseline formulation related to the reduction in relation to the current.

BMP_2) Minimum Tillage: The minimum tillage or minimum movement of the soil consists of intervening as little as possible into the soil structure at the time of cultivation operation (FAO, 2000; Herrera, 2008). The tillage database (till.dat) in SWAT model was used. The database contains the depth of mixing (Deptil) and the mixing efficiency (Effmix) values. For this case study, we selected the **G*eneric* C*onservation Tillage*, *Chisel Plow* (vertical tillage), *Rotary Hoe* (animal and human-powered implements), and *Generic No-Till Mixing*** (Table 6.1). The tillage implement code from the tillage database (TILL_ID) is changed to implement the BMP_2 in the SWAT model.

Table 6.1. Tillage implements selected from SWAT tillage database (till.dat) to be used in the optimization problem.

Implement	**Tillage Name**	**Till_Id** *Tillage code*	**Effmix** *Mixing efficiency*	**Deptil** *Mixing depth* (mm)	**Random roughness** (mm)
Current baseline					
Bedder Shaper (disk)	BedderS	83	0.55	150	30
Scenarios					
Generic Conservation Tillage	Constill	3	0.25	100	40
Chisel Plow Gt21ft	Chplgt21	2	0.5	125	50
Rotary Hoe	Rothoe	5	0.15	100	15
Generic No-till Mixing	Zerotill	4	0.05	25	10

BMP_3) Filter strips: Filter strips are vegetated areas situated between surface water bodies and cropland to collect and remove pollutant nutrients, pesticides, and bacteria from surface run-off that are planted in these areas (Ritter and Shirmohammadi, 2001). This practice is modeled with a FILTER_RATIO parameter, which represents the ratio

of the field area of the filter strip along a stream**.** Filter strips are simulated in SWAT by modifying/adding an optional schedule Management Operations (.ops) file for each HRU**.**

BMP$_4$) Contour planting: Contour farming is a practice that consists of planting along the contours of the terrains to reduce soil erosion and surface run-off (Tuppad et al., 2010). The BMP$_4$ is simulated by adding a modified CN number which considers the countour effect. In SWAT, contouring is represented in the optional scheduled management operations file (.ops) for each HRU. The BMP$_4$ is modeled with the initial SCS curve number II value (CONT_CN).

BMP$_5$) Living fences: Live fences are those in which a **row of trees (edge rows) and shrubs are planted in short distances**, replacing the traditional fences to be used as grazing areas (Blanco and Lal, 2008, Zhai et al., 2006). This practice in our study is modeled **only for kikuyu grass by decreasing the dry weight of biomass daily consumed per each animal (BIO_EAT)**. The decrease was defined in the range between 0% to -30% (kg ha^{-1}), which is the maximum percentage of forage provided by the *Tithonia diversifoliade* specie (Restrepo et al., 2016).

Table 6.2. Parametrization of the selected agricultural best management practices (BMPs) to be evaluated in the modeling-optimization framework. Kikuyu grass (PASM), potato (POTA), and tree tomato (TOMA) land-covers.

BMP alternative	Parameter in SWAT	Description	Land cover*	Current value	How implemented in SWAT
BMP$_1$ Fertilizer management	FERT_KG	Amount of fertilizer applied to HRU (kg/ha)	PASM POTA TOMA	30 350 725	5% reduction [-0.5 – 0.0]
BMP$_2$ Minimum tillage	TILL_ID	Tillage implements code from tillage database	POTA PASM TOMA	49 83	Changed between [2 - 5]
BMP$_3$ Filter strips	FILTER_RATIO	The ratio of field area to filter strip area	PASM	40	Changed between [30 – 60]
BMP$_4$ Contour cropping	CONT_CN	SCS curve number II value	POTA TOMA	60	10% reduction [-0.1 - 0.0]
BMP$_5$ Living fences	BIO_EAT	Dry weight of biomass consumed daily (kg/ha)	PASM	51	30% reduction [-0.3 – 0.0]

*PASM: Kikuyu grass; POTA: Potato; TOMA: tree tomato

The selected BMPs are spatially matched with the land-cover fields having 4 BMPs (BMP_1, BMP_2, BMP_3, BMP_5) associated to the kikuyu grass, and 3 BMPs (BMP_1, BMP_2, BMP_4) to the potato and tree tomato (Table 6.2). Those are assigned to their respective HRU distributed in a total of 454, 194, and 97 HRUs for kikuyu grass (PASM), potato (POTA), and tree tomato (TOMA), respectively. In this study, we assume that a BMPs can be placed individually for the same land-cover type. Therefore, the number of BMP scenarios tested for kikuyu grass are 4 and 3 for potato and tree tomato land-covers (Table 6.3).

Table 6.3. List of the best management practices (BMP) scenarios to be optimized for kikuyu grass (PASM), potato (POTA), and tree tomato (TOMA) at the Riogrande watershed.

Scenario number	BMP	Land cover	Scenario number	BMP	Land cover
1	BMP_1	PASM	6	BMP_2	POTA
2	BMP_2	PASM	7	BMP_4	POTA
3	BMP_3	PASM	8	BMP_1	TOMA
4	BMP_5	PASM	9	BMP_2	TOMA
5	BMP_1	POTA	10	BMP_4	TOMA

6.3.3 Multi-objective optimization formulation

Objective functions

Government and experts in the region have already promoted BMPs, and in chapter 5 we have seen important issues in the variation of CSA in time. With this, some implementation is expected to take place, but to have an increase in implementation, we need to find the proper approach. Here we follow the optimization approach proposed by Babbar-Sebens et al., 2015, where the base line and the optimal obtained with different Ag-BMPs are maximized. Here we propose a step further, where these results are expected to be used to classify regions where dynamics of the hydrologic responses are captured and at the same time match the Ag-BMP implementation, not withstanding the fact that real life implementation requires decision makers to apply AG-BMPs gradually. Therefore, in the region, two objectives are defined:

1) The maximization of Nitrates loss reduction (***NR***) in the runoff, for each HRU (hydrological responds unit) selected for Ag-BMP implememtation. This done in each HRU by estimating the differences between the baseline calibrated model results (simulation results with the current agricultural management practices) and the different optimized Ag-BMP scenarios results. This concept aims at achieving a plausible

reduction of pollutants in the region, as well as allowing for an easier interpretation of implementation plans.

2) The minimization of the differences from the maximum potential crop yield (***DMCY***), crop's productivity obtained in the BMP scenario reaches the maximum crop yield baseline calibrate model results (potential crop yield values obtained from the simulation results with the current agricultural management practices).

The modeling system used here provides spatial location (explicit-HRUs), and nitrate (NO_3^--N) losses and crop yields on a daily basis; however, as mentioned in chapter 5, calibration and overall parametrization of the BMP scenarios and their objective functions are defined for monthly results. This corresponds to **36 months between January 2013 to December 2015 of the total simulation period (1995-2015)**. This fact and the use of the ST-CSA method, allow us to define an objective function that will target only in certain spatial and temporal areas of pollution (**718 HRUs of the total number of 3640 HRUs set in the SWAT model**). Hence, the number of times a decision variable is applied corresponds to the number of times defined in the baseline management calendars (Uribe et al., 2020) for each of the 718 HRU chosen associated with a land-cover L in the month t. Thereby, an HRU with the land-cover L at time t is defined as $HRU_{L_{(i,t)}}$, where $L \in \{PASM, POTA, TOMA\}$, $i = 1, \dots, N_L$ and N_L is the number of $HRUs$ with the same land-cover $N_L \in \{454,167,97\}$. Thus, the NO_3^--N loads due to a BMP scenario implementation (Table 6.3) in a $HRU_{L_{(i,t)}}$ can be defined as $NO3_{L_{(i,t,scenario)}}$. In the same way, the differences from the maximum crop yields of a BMP implemented scenario in a $HRU_{L_{(i,t)}}$ associated with a land-cover L in the month t is represented as $CY_{L_{(i,t,scenario)}}$.

Therefore, we can define the relative change in the Nitrate-N loads as the difference between the nitrates obtained for a simulated BMP scenario $NO3_{L_{(i,t,scenario)}}$ and the baseline $BNO3_{L_{(i,t,baseline)}}$ in a HRU_{L_i} for a specific time t, as an indicator of environmental benefits. Similarly, we can define the differences from maximum crop yield between the BMP scenario $CY_{L_{(i,t,scenario)}}$ and the maximum crop yield $MCY_{L_{(i,t,baseline)}}$, where the maximum crop yield corresponds to the potential yield value of the current agricultural management. Thus, the function that covers all HRUs for a given land-coverage and time is expressed mathematically as (Eq. (6.1) and (6.2)):

$$\boldsymbol{NR_{L,i}} = \min\left[-\max \sum_{t_i=1}^{t_f=36} \left[NO3_{L_{(i,t,baseline)}} - NO3_{L_{(i,t,scenario)}}\right]\right] \quad (6.1)$$

$$\boldsymbol{DMCY_L} = \min\left[\sum_{t_i=1}^{t_f=36}\left[MCY_{L_{(i,t,baseline)}} - CY_{L_{(i,t,scenario)}}\right]\right] \qquad (6.2)$$

were t_i is the initial time in months in the simulation period, t_f is the final time in months in the simulation period, i is the number of the HRU, N_L is the number of $HRUs$ with the same land-cover at time t, L the land-cover, $NO3_{L_{(i,t,baseline)}}$ is the nitrates load of the HRU for the baseline (simulation results with the current agricultural management practices), $NO3_{L_{(i,t,scenario)}}$ is the nitrates load of the HRU for a simulated Ag-BMP scenario, $MCY_{L_{(i,t,baseline)}}$ is the maximum (potential) crop yield in ton ha^{-1} for the baseline scenario (simulation results with the current agricultural management practices), $CY_{L_{(i,t,scenario)}}$ is the crop yield for a simulated Ag-BMP scenario. Note that these functions are subject to the $NO3_{L_{(i,t)}}$ and $CY_{L_{(i,t)}}$ functions (detailed description of the equations are presented in Chapter 2, which are outputs of the SWAT model and depend on the implementation of a Ag-BMP type or a combination of Ag-BPMs is applied (Table 6.3).

Decision variables and constraints

From the analysis of CSA per BMP, we have divided the problem into 3 regions of possible crop cultivation. In general, 718 HRUs in total, were 454 kikuyu grass (PASM), 167 potato (POTA), and the remaining 97 in tree tomato (TOMA). With this, we divided the optimization problem into three optimization sub-problems for each type of land-cover (Figure 6.2). Hence, the optimization sub-problem for kikuyu grass has a total of 4 decision variables applied to 454 HRUs, not including BMP_4 in this land-cover (Table 6.4). Similarly, BMP_5 does not apply to the potato and tree tomato land-cover, whereby there is a total of three decision variables for potato and tree tomato (Table 6.4). The total number of decision variables is **2608**. This is composed of:

$$\boldsymbol{Kikuyo\ grass} \rightarrow 454\ HRUs * 4\ decision\ variables(X1, X2, X3, X5) = \mathbf{1816}$$

$$\boldsymbol{Potato} \rightarrow 167\ HRUs * 3\ decision\ variables(X1, X2, X4) = \mathbf{501}$$

$$\boldsymbol{Tree\ tomato} \rightarrow 97\ HRUs * 3\ decision\ variables(X1, X2, X4) = \mathbf{291}$$

$$\boldsymbol{Total} = \mathbf{2608}$$

where, $X1$ – amount of fertilizer applied of kgha^{-1} (BMP_1), $X2$ – tillage implemented code (BMP_2), $X3$ – ratio of field area to filter strip area (BMP_3), $X4$ – initial SCS curve number value (BMP_4), and $X5$ – dry weight of biomass consumed daily in Kg ha^{-1} (BMP_5).

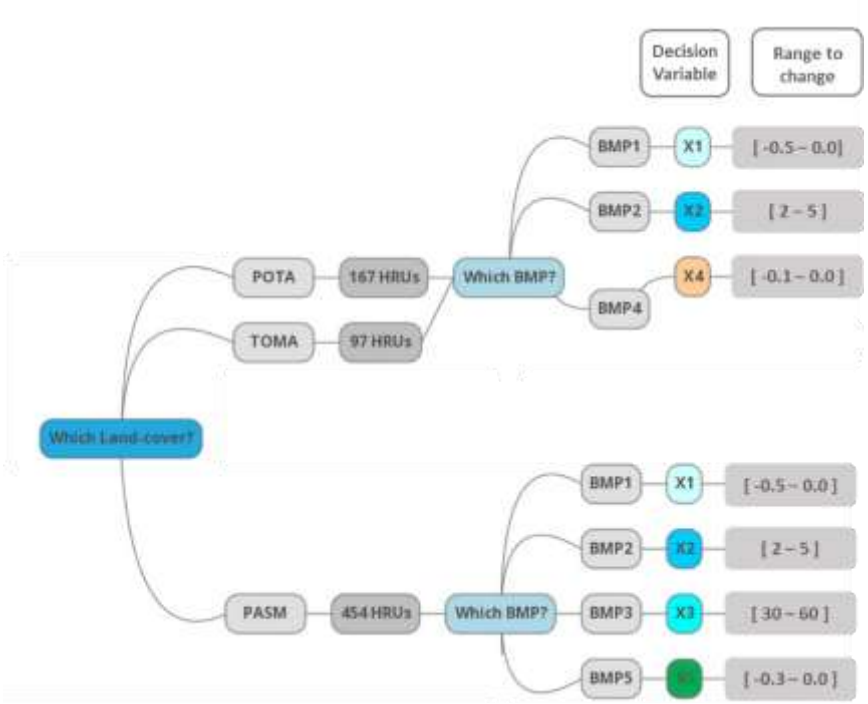

Figure 6.2. The schematic representation of the decision variables for potato (POTA), tree tomato (TOMA), and kikuyu grass (PASM) land-cover types.

Table 6.4. Description of the decision variables, their ranges and constrains.

Land cover	Total HRUs	Number of modified values*	Scenario	Decision variable code	Parameter name	Method	Optimization range
PASM	454	454*10=4540	BMP_1	X1	FRT_KG	Relative	-0.5 -0.0
		454*1=454	BMP_2	X2	TILL_ID	Replace	2 -5
		454*1=454	BMP_3	X3	FILTER_RATIO		30 - 60
		454*8=3632	BMP_5	X6	BIO_EAT	Relative	-0.3 – 0.0
POTA	167	167*4=668	BMP_1	X1	FRT_KG	Relative	-0.5 – 0.0
		167*6=1002	BMP_2	X2	TILL_ID	Replace	2 -5
		167*1=167	BMP_4	X4	CONT_CN	Relative	-0.1 – 0.0
TOMA	97	97*20=1940	BMP_1	X1	FRT_KG	Relative	-0.5 – 0.0
		97*1=97	BMP_2	X2	TILL_ID	Replace	2 -5
		97*1=97	BMP_4	X4	CONT_CN	Relative	-0.1 – 0.0

* Number of modified values = Total HRUs * total number of applications defined in the management calendars during the simulated period.

Optimization engine setup

The Nondominated Sorting Genetic Algorithm (NSGA-II) developed by Deb et al., 2002 was used as the multi-objective optimization algorithm to allocate the five BMPs types selected for the case study watershed. The NSGA-II optimization algorithm in recent years has been widely applied to optimize BMPs placement for pollution reduction in watersheds (Geng et al., 2019; Yang and Best, 2015; Qin et al., 2018; Jeon et al., 2018; Babbar-Sebens et al., 2015; Panagopoulos et al., 2013). The open-source software library[1] for multi-objective calibration of the SWAT model using NSGA-II developed by Ercan and Goodall, 2016, was modified to be used as a optimization engine in our specific spatio-temporal multi-objective BMP optimization modeling-framework.

The NSGA-II/SWAT coupled optimization engine follows the seven main steps.

1. Latin Hypercube technique is used to generate the N vectors of decision variables (parameters sets). (N is the population size.)
2. A module that creates the input file using the parameters generated by the Latin Hypercube is run (step 1). The developed scripts filter the input such that only the HRUs corresponding to the CSAs for each of the three crops to work (kikuyu grass, potato, and tree tomato) are used.
3. A cycle starts with the initial parameters as input to the SWAT model. Total number of iterations (generations) is G.
4. The objective functions are calculated and the results are placed into a file.
5. The NSGA-II algorithm uses the input file and generates N sets of parameters. These parameters and the ranges of each parameter in the model are defined in the NSGA metainformation file (Figure 6.5).
6. A generation of the dominant and nondominant sets of parameters is sorted and used as reference for rejecting parameters of the population. In this step the selected or dominant sets are scaled with distances metrics.
7. With the dominant sets of parameters, a selection crossovers (combination) and mutation (random change) of best samples is done to generate new samples. These parameters are used as input and steps 3 to 7 are executed again. The cycle will last until the number of generations defined in the meta information file of the NSGA-II.

The first four steps result in generating the input data for the NSGA-II algorithm. Therefore, these steps were modified to match our goals and approach, by adding/replacing scripts developed to extract, process, and execute the SWAT model at

[1] Software availability: The software is available free and open source on Github: https://github.com/mehmetbercan/NSGA-II Python for SWAT model.

the HRU unit of analysis level. The developed scripts allow for selecting the HRUs corresponding to the CSAs for each of the three crops to work (kikuyu grass, potato, and tree tomato), defining the objective functions and constraints, and generating/storing the results in the formats of our interest. For further detail on the other three steps corresponds to the NSGA-II algorithm itself, readers are referred to Ercan and Goodall, 2016.

NSGA-II algorithm has several important control parameters that have to be set by the user. To identify the most appropriate values for them, a number of experiments were conducted. The experiment analysis consists of changing the value of the population size (10, 50, 80, 100), crossover probability (0.2, 0.6, 0.8) and the number of generations (5, 10, 50, 80, 100) one-at-a-time. The changes of the Pareto-optimal front obtained for each configuration setup from the ε-NSGA-II optimization with the two objective functions NR (differences from the nitrates load (NO_3^--N) between the baseline model results and the BMP scenarios) and DMCY (differences from the maximum crop yield and the BMP scenarios), were compared. For the particular optimization problem in the Riogrande II watershed, these data were arranged as three individual sub-problems, one for each type of the three land-cover under study (Table 6.4). The detailed description of the NSGA-II/SWAT optimization library is described in the Appendix B.

6.3.4 Comparison between Pareto-optimal front solutions from average vs. single sites values

In this study, the Pareto-optimal solutions for each crop and each BMP scenarios were analyzed at two different levels: 1) Pareto-optimal front solutions from the average sites-HRUs values (per crop). This corresponds to calculating the Pareto-optimal front with the average of the values obtained from the total HRUs used, for each of the objective functions. 2) Pareto-optimal front solution from the single sites-HRUs values (results obtained for each individual HRU), for each of the objective functions. A cluster analysis was used to show the optimization results for each HRUs in a compiled form. The cluster analysis makes it possible to identify HRUs with similar objective function results evaluated among the total HRUs. Additionally, a map of the location of the different clusters in the study watershed is presented.

Furthermore, to determine the main differences between the two levels of result analysis a comparison between the range (minimum and maximum) of the results obtained for each objective function among the different BMP scenarios, was performed. Finally, the most feasible BMP scenarios in the study watershed are presented by the cluster numbers obtained in each of the three studied crops, accompanied by a short description of the spatial characteristics such as the sub-basins, slope, soil, and HRUs area, of the BMP optimized results.

6.4 RESULTS AND DISCUSSION

6.4.1 Benchamark analysis of optimization preliminar results

The optimization algorithm was first run for 10 generations as a benchmark. An analysis of the Pareto-optimal front solutions per each 10 BMP scenarios (Table 6.3) was assessed to know the optimization performance. This analysis was done on each BMP scenario before executing the experimental setup used for the optimization process. In Figure 6.4, results of the HRU benchmark per each land cover was randomly selected.

The benchmark analysis results showed that the Pareto-optimal front solutions for various solutions are quite linear and for the same solution but in another location a nonlinear Pateto is found for objectives DMYC and NR. For example, BMP_1 (Fertilizer management) applied to PASM in the HRU38, a clear non-linear relationship between variables (Figure 6.4a), however, applying the same BMP_1 in a region where there is POTA or where there is TOMA, shows an inverse linear relationship (6.4b 6.4c). The inverse value between DMCY and NR objective functions, for the three crops studied. This shows that a number of formulations could be evaluated to simplify the optimization process, however, more analysis was done.

And the range of possible optimal solutions for the decision variable $X1$ (FRT_KG - the amount of fertilizer applied to HRU) is different for each crop studied (kikuyu grass, potato, and tree tomato) (Figure 6.4a, 6.4b 6.4c). The Pareto-optimal front for scenarios 2, 6, and 9 that corresponds to apply the BMP_2 (Minimum tillage) for kikuyu grass, potato, and tree tomato, respectively, has only four values (Figure 6.4d, 6.4e, and 6.4f). Those four result values correspond to each of the four-tillage type could be selected for the decision variable $X2$ (TILL-ID) in the optimization configuration (Table 6.3). Therefore, it may be concluded that the optimal solutions may be the one or the two values closer to the origin to select the adequate tillage type. Scenario 3 corresponding to the BMP_3 (filter strips) type was applied only to the kikuyu land-cover. As expected, the Pareto-optimal front solutions for the decision variable $X3$ (FILTER-RATIO - the ratio of field area to filter strip area) did not change or moved towards the origin for the objective function Differences from Maximum Crop Yield (DMCY). However, it is very significant for the objective function differences in nitrate loads (NR) by approaching the origin (Figure 6.4g). On the other hand, when the decision variable $X4$ (CONT_CN – SCS - curve number II value) is applied, scenarios 7 and 10 for potato and tree tomato land-cover, respectively; the results obtained indicate a linear regression, for both land-covers (Figure 6.4h, 6.4i). For the BMP_5 (living fences) represented by the decision variable $X5$ (BIO_EAT - Dry weight of biomass consumed daily) and applied only to kikuyu land-cover, the results show a Pareto-optimal front solutions clearer (Figure 6.4j).

Based on the results of the Pareto-optimal front preliminary brenchmark analysis for each BMP scenario, the final setting parameter values for the NSGA-II algorithm that we defined to get the Pareto-optimal front closer to the origin - the better the spread of Pareto-

optimal front solutions for NR and DMCY were: 1) population size of 100; 2) the maximum number of generations of 100; and 3) crossover rate of 0.8 with a uniform crossover-type. Since our parameters do not have a wide range, we used 6 bits for binary crossover and mutations for each variable (parameters), and the mutation probability and the seed for the random number generation were set to 0.5 (Figure 6.5).

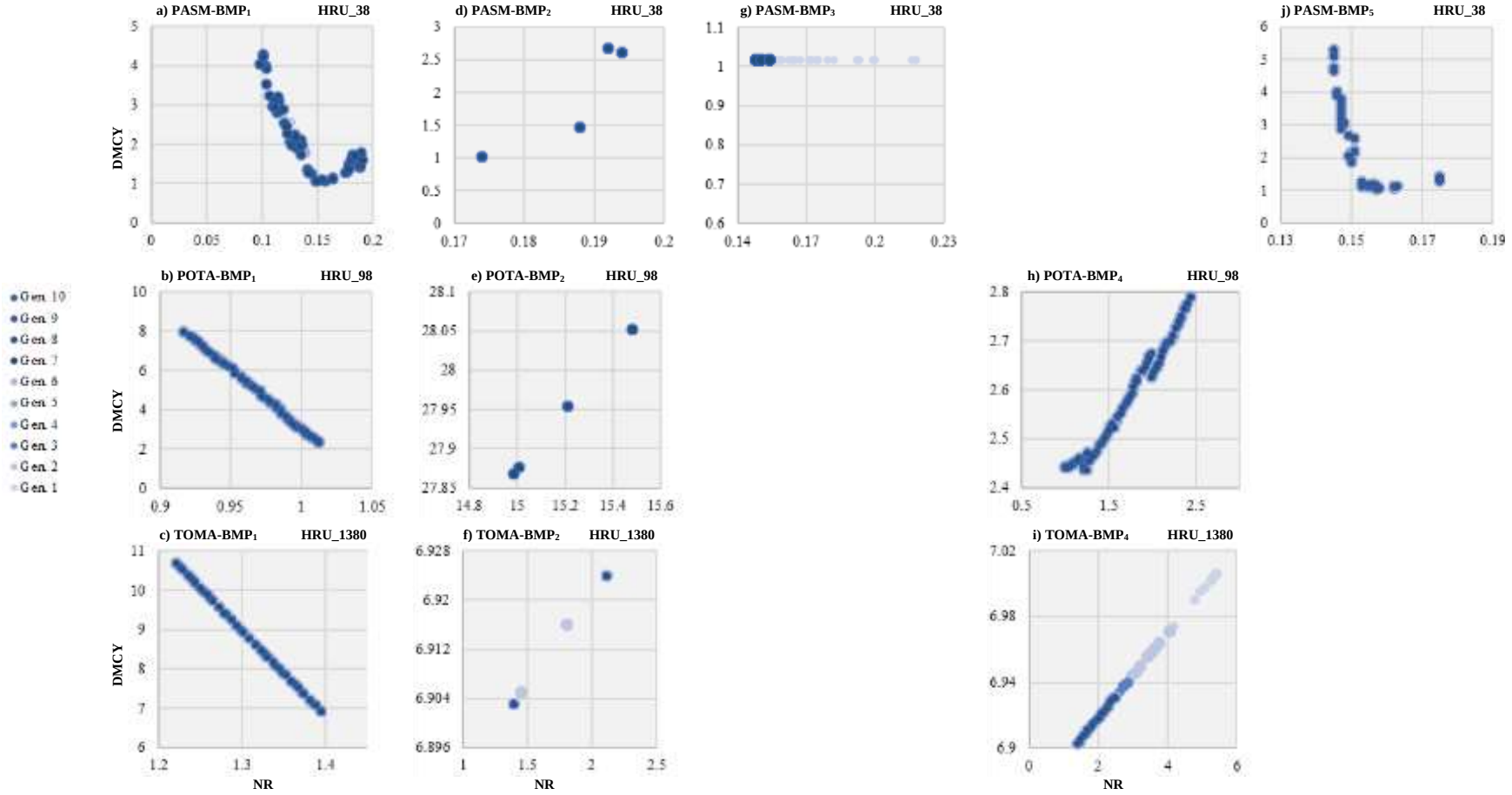

Figure 6.3. Optimization running benchmark analysis of the Pareto-optimal front solutions derived from 10th generation in the NSGA-II/SWAT coupled model: a) PASM-BMP$_1$, b) POTA-BMP$_1$, c) TOMA-BMP$_1$, d) PASM-BMP$_2$, e) POTA-BMP$_2$, f) TOMA-BMP$_2$, g) PASM-BMP$_3$, h) POTA-BMP$_4$, and i) TOMA-BMP$_4$, and j) PASM-BMP$_5$. DMCY: differences from the maximum crop yield, NR: differences from the nitrate.

```
//definition file for nasga2 program
1    PopSize       100    //Population size (an even number)
2    GenNumber     100    //Number of generations (different from 1)
3    CrossPrb      0.8    //Crossover probability (between 0-1)
4    CrossTyp      2      //Crossover type (1=Simple,2=Uniform X-over)
5    Bits          6      //No. of bits assigned to each variable(parameters)
6    MutPrb        0.5    //Mutation prblty proportion range (between 0-1)
7    seed          0.5    //Give seed (between 0-1) for random number generation
8    ObjFunc       6      //1=E; 2=R^2; 3=E, log(E); 4=E, log(E), R^2; 5=E, PB; 6=Nitrate|Yield
9    ObjFuncOpt    0      //0=Do not average; 1=Average OF sites; 2=Average OF
10   ReadMFrmOut   0      //0=normal start; 1= Read last population from output.out
```

Figure 6.4. Final settings parameter for the NSGA-II algorithm used to run the NSGA-II/SWAT library for the Riogrande II watershed BMP optimization model.

6.4.2 Average of the Pareto-optimal front solutions derived from each HRUs optimization results among different BMP scenarios

An average of the Pareto-optimal front solutions from each HRUs optimization results of the 100th generation for the 10 BMP scenarios. The results are described below for each of the three types studied. The average of the Pareto-optimal front solutions obtained for the four BMP scenarios optimized for kikuyu grass (PASM), they are totally different between them (Figure 6.7). The scenario 4 (BMP_5) produced the most non-dominated solutions at almost the entire solution space (Figure. 6.6d). Finally, the average Pareto-optimal front solutions for scenario 1 showed a changing trend (an inversely linear representation between objective functions NR and DMCY) in the solution space with the best optimization efficiency (Figure 6.6a). On the other hand, scenarios 2 and 3 show the least variability in the average Pareto-optimal front solutions space. The values obtained in the average Pareto-optimal front solutions space for scenario 2 (BMP_2) corresponds to each of the four values that the decision variable *X*2-Tillage type [2-5] can be changed (Figure 6.6b). The decision variable *X*2 influences each of the objectives function sites-HRUS in the same proportion, indicating no difference in space and time between the sites-HRUs in the watershed. Similarly, the average Pareto-optimal front solutions for the scenario 3 (BMP_3) gets only one value for the objective function DMCY of 2.4 t ha^{-1} (Figure 6.6c), which is mainly because the decision variable *X*3-Filter ratio influences only the objective function RN when simulating collection and removing of pollutant nutrients from surface run-off, and it doesn't alter the crop yield results.

Figure 6.7 shows the average Pareto-optimal front solutions for the 194 HRUs of the potato crop (POTA) derived from all 100th generations of the three BMPs scenarios. From the visual interpretation, the better convergence and similar diversity in the average Pareto-optimal front were obtained in scenarios 5 and 7. These correspond to the BMP_1 (*X*1-Fertilizer amount) that obtained an inverse regression performance between the two objective functions (Figure 6.7a). And the BMP_4 when the decision variable X*4* (SCS -

curve number II value) is optimized the average Pareto-optimal front solutions correspond to a convex function between the two objective functions (Fiure 6.7c). On the other hand, scenario 6 (BMP_2) shows the least variability in the average Pareto-optimal front solution space (Figure 6.7b), the same result as the kikuyu land-cover.

Finally, the comparison of the average Pareto-optimal front solution derived from the 97 HRUs results among the four BMPs scenarios applied to the tree tomato land-cover (TOMA), shows that the best performances are obtained in scenarios 8 and 10, which correspond to the decision variables $X1$ and $X4$, respectively (Figure 6.8a, 6.8c). The average of the Pareto-optimal front solutions for scenario 10 showed a changing trend (an linear representation between objective functions NR and DMCY) in the solution space with the best optimization efficiency (Figure 6.7c). And, the same as the results obtained for the scenarios 2 and 6 (BMP_2) applied to PASM and POTA, respectively, the values obtained in the average of the Pareto-optimal front solutions space for scenario 9 (BMP_2) corresponds to each of the four values that the decision variable $X2$-Tillage type [2-5] can be changed (Figure 6.8b).

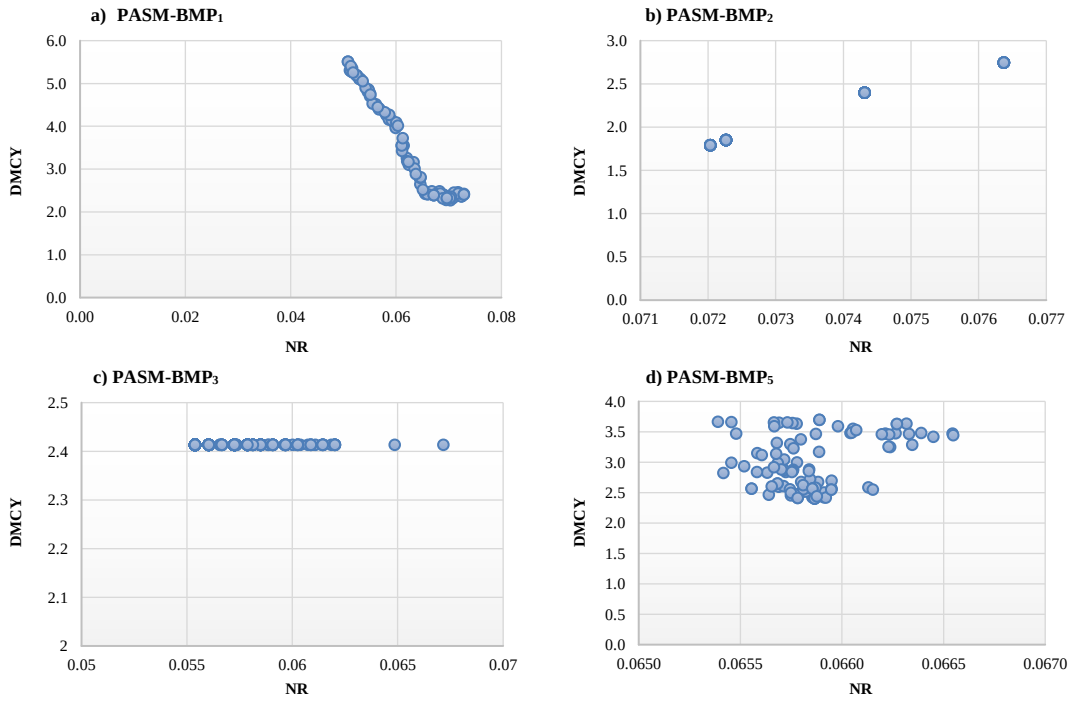

Figure 6.5. Average of the Pareto-optimal front solutions derived from the 454 HRUs of the 100th generation among four BMPs configuration scenarios applied to the kikuyu grass (PASM) land-cover. a) BMP_1, b) BMP_2, c) BMP_3, and d) BMP_5. DMCY: differences from the maximum crop yield, NR: differences from the nitrate.

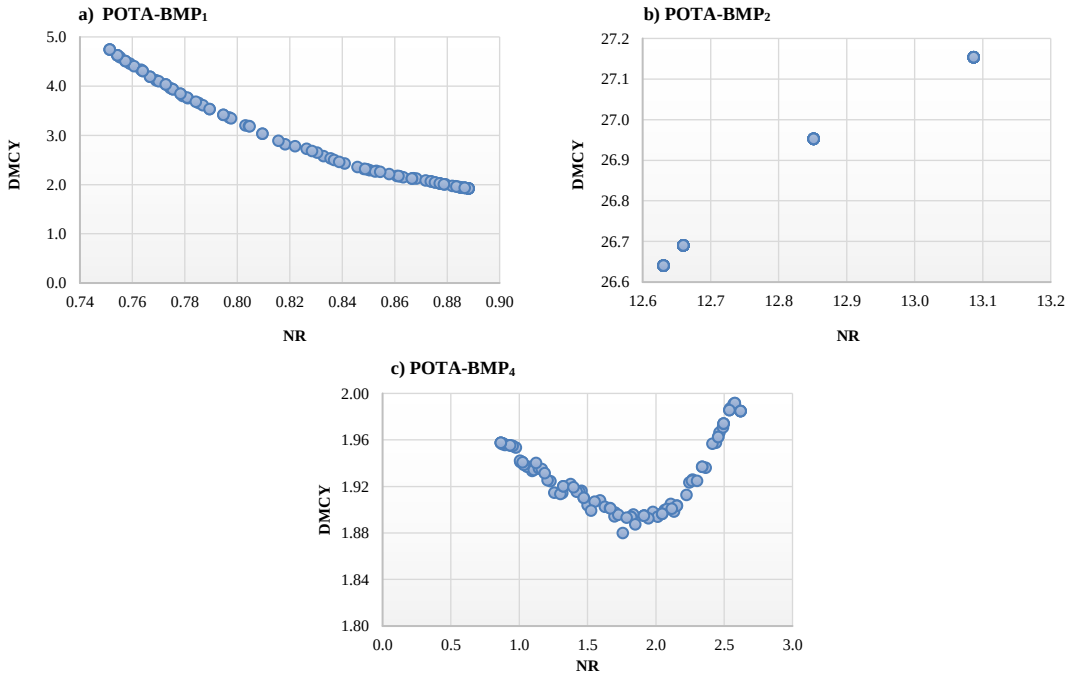

Figure 6.6. Average of the Pareto-optimal front solutions derived from the 194 HRUs of the 100th generation among four BMPs configuration scenarios applied to the potato (POTA) land-cover. a) BMP$_1$, b) BMP$_2$, and c) BMP$_4$. DMCY: differences from the maximum crop yield, NR: nitrate reduction.

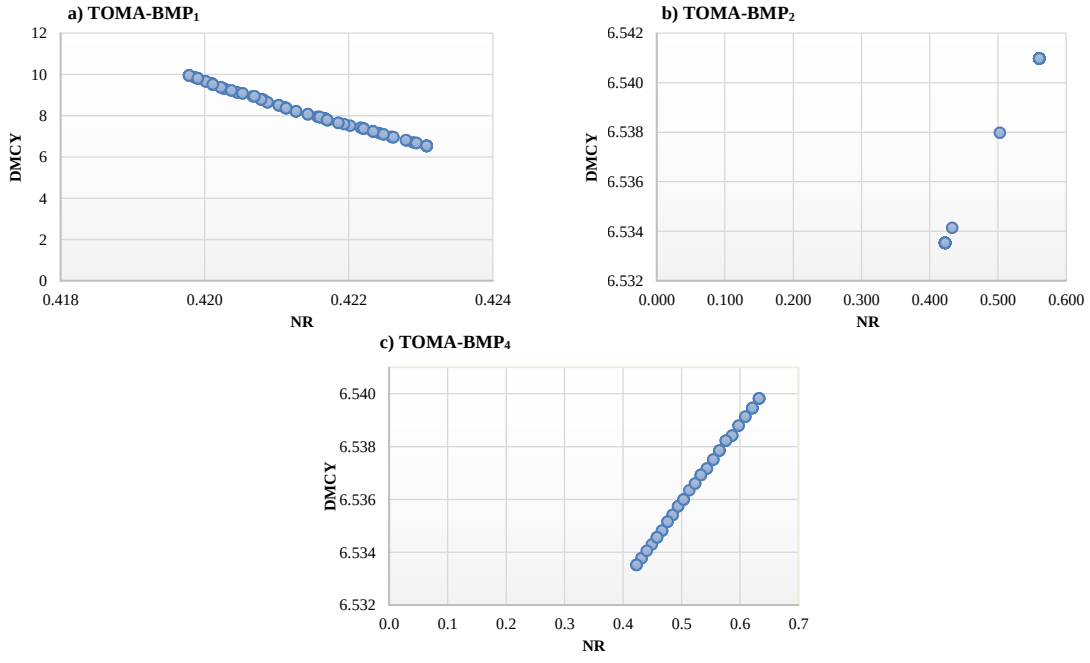

Figure 6.7. Average of the Pareto-optimal front solutions derived from the 97 HRU of the 100th generation among four BMPs configuration scenarios applied to the tree tomato (TOMA) land-cover. a) BMP$_1$, b) BMP$_2$, and c) BMP$_4$. DMCY: differences from the maximum crop yield, NR: nitrate reduction.

6.4.3 Pareto-optimal front solutions derived from the single from the each HRUs optimization results among different BMP scenarios

To identify the single sites-HRUs values among the different BMP scenarios that have a similar optimization result, a cluster analysis (unsupervised classification) was performed for each of the three analyzed crops. For the BMPs scenarios applied to each crop (Table 6.3), the geographical location of the HRUs grouped in clusters is showed in Figure 6.9. Their spatial characteristics, such as sub-basins, area, and total number of HRUs conforming up the cluster, are described below.

Visually it can be observed that the HRUs corresponding to the kikuyu grass coverage (PASM) distributed in four clusters for each of the five applied BMP scenarios, are located in almost the entire basin except for sub-basin 8 (Figure 6.9a). The HRUs that determine cluster 3 are mainly found in the sub-basins located in the north-east region of the watershed, except for scenario 2 (BMP_2) in which the HRU_S that determine cluster 1 predominate in this region (Figure 6.9a). The cluster that groups the largest number of HRUs out of the total HRUs for the kikuyu grass land-cover is cluster 2, and these HRUs are located in most of the watershed area in the four optimized BMP scenarios (Figure 6.9a). The number of HRUs that determine cluster 2 in each BMP scenario corresponds to 68, 67, 63, 63% for scenarios 1 to 4, respectively, with respect to the total HRUs of the kikuyu grass land-cover (454 HRUs). And the area covered by the HRUs grouped in cluster 2 with respect to the total area of the kikuyu grass land-cover (60314.84 ha) in the four BMP scenarios corresponds to approximately 37%. Next is cluster 3 with an average percentage of 33% of the total area in grass, which is the cluster made up only on average by 10% of the 454 total HRUs for kikuyu grass (approximately 45 HRUs in each of the five scenario BMP). And cluster 1 with an average percentage of 22%.

For potato crop, it can be seen visually that the HRUs grouped in the clusters are located mainly in the sub-basins located at the lower part of the watershed and some sub-basins located in the north-east area (sub-basins 2, 4, 5, 6 and 7) (Figure 6.9b). In figure 6.9b, it can be seen that scenarios 5 and 6 that correspond to the BMP_1 and BMP_2 have a similar spatial distribution of the clusters, and the HRUs grouped in cluster 1 are those with a higher percentage of representation area around 50% with respect to the total area planted in potato (cluster 1 has 39% of the 167 total HRUs for potato land-cover). And cluster 2 has 35% of the total HRUs for this land-cover, that corresponds to approximately 30% of the total area of the potato land-cover (874.98 ha). On the other hand, FOR scenario 7 (BMP_4) clusters 3 and 4 present the highest number of HRUs (44% and 25% of the total of 167 HRUs, respectively) and the percentage of coverage covered (55% and 16% of the total area of the potato crop, respectively).

For the tree tomato, the clusters are located in only 8 sub-basins of the total of 20 sub-basins located in the lower part of the watershed (sub-basins 12 to 19) (Figure 6.9c). It can be seen in Figure 6.9c that cluster 3 is the one that contains the highest amount of HRUs (39% of the 97 HRUs for this crop) in the four evaluated scenarios (scenario 8 to

10, Table 6.3), and it represents 59% of the tree tomato land-cover total area. Next, is cluster 2, which is made up of 28 HRUs of the 97 HRUs of the tree tomato land-cover, for the four scenarios. It is highlighted that cluster 1 for scenario 10 (BMP_4) cannot be seen visually in Figure 6.9c because it is made up of only 4 HRUs that represent 0.6% of the area planted in tree tomato in the watershed.

From our previous study (Uribe et al., 2020) the results showed that the spatial distribution of NO_3^--N losses was predominant in two specific regions throughout time within the watershed, the Region 1 conformed by the sub-basins between 1 to 11, and the Region 2 by the sub-basins between 12 to 20. Which are directly attributed to the spatial distribution of precipitation in the study area, where Region 1 is characterized by higher annual average rainfall than Region 2. Therefore, the results of the grouping of the objective sites-HRUs among the different BMP scenarios that have similar optimization results in clusters showed that:

1) for the cultivation of kikuyu grass, the HRUs grouped in cluster 3 predominate in Region 1. And the HRUs grouped in cluster 2 for scenarios 1 to 5 predominate in in Region 2. With the exception of scenario 2, in which the HRUs corresponding to cluster 1 predominate in Region 1.

2) for potato cultivation, most of the HRUs grouped by the four clusters are located in Region 2. Few HRUs from cluster 1 (for scenarios 5 and 6 that correspond to BMP_1 and BMP_2) and cluster 4 for scenario 8 (BMP_4) is located in Region 1.

3) for the tree tomato, all the HRUs grouped in the four clusters are located in Region 2.

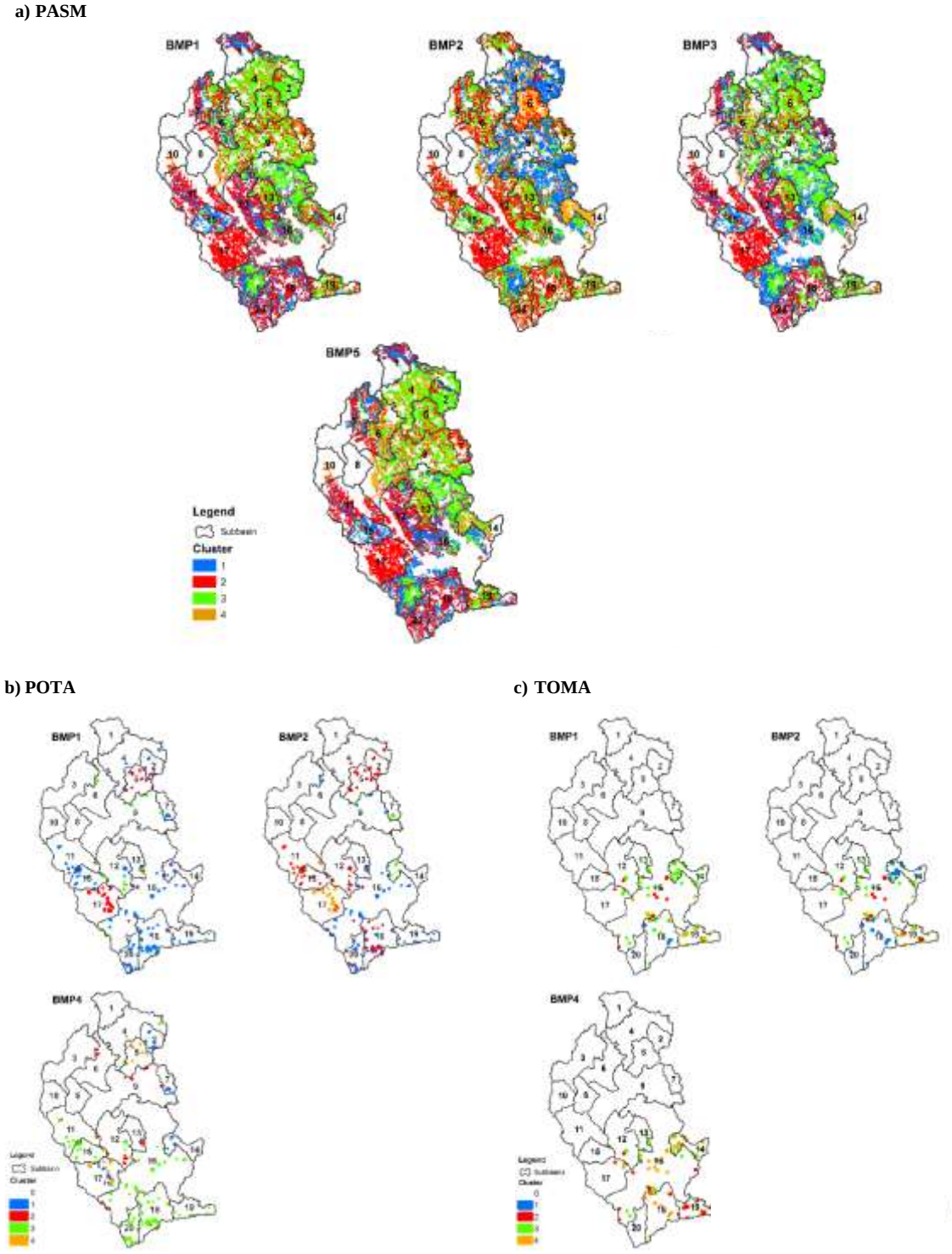

Figure 6.8. Clusters spatial distribution among the BMP scenarios per each land-cover type. a) kikuyu grass (PASM), b) potato (POTA), and tree tomato (TOMA).

One HRU was randomly selected from each of the identified clusters to plot the Pareto-optimal front solutions obtained in each HRU, in this way the differences between the Pareto-optimal front solutions of each cluster can be visually analyzed. The results presented show a higher spatial variability of the objective sites-HRUs (ST-CSAs) optimization results among the different BMP scenarios per each studied crop, which is explained by the Pareto-optimal front solutions of the 100^{th} generation among the BMPs scenarios per each land-cover (Fig. 6.10, 6.11, and 6.12). From de visual interpretation, the convergence and similar diversity in the Pareto-optimal front varies for each of the four clusters of each scenario evaluated and land-cover type, except for the BMP_3 scenario applied to kikuyu grass (*X*3-the ratio of field area to filter strip area) (Fig. 6.10). As we mentioned, the BMP_3 scenario did not change or moved towards the origin for the objective function Differences of the Maximum Crop Yield (DMCY). Furthermore, the convergence and similar diversity in the Pareto-optimal front solutions for the land-cover tree tomato do not change much between clusters. A significant change is only seen for the BMP_1 scenario where cluster 2 shows a different Pareto-optimal front solution from the others (Fig. 6.12).

However, the range of values in which the Pareto-optimal front is located does vary greatly between the clusters for each scenario and type of land-cover evaluated. In common for the kikuyu grass land-cover, cluster 3 groups the sites-HRUs that have the highest range of values for the objective function NR, with the exception of the BMP_2 scenario in which it is cluster 1 that contains only 5% of the total HRUs of this crop. And, cluster 4 presents the largest range of values for the objective function DMCY which corresponds to only 7% of the total HRUs of this crop (Fig. 6.10). For the potato crop, it is cluster 2 that groups the sites-HRUs that have the highest range of values for the objective function (NR), except for the BMP_2 scenario in which it is cluster 1. And for the function objective DMCY cluster 1 groups the sites-HRUs that have the highest range of values, except for the BMP_2 scenario, which corresponds to cluster 3 with 9% of the total HRUs for this land-cover (Fig. 6.11). Finally, for the tree tomato land-cover cluster 1 groups the sites-HRUs (approximately 11% of the total HRUs for this crop) that has the highest value range for NR and cluster 3 for the objective function DMCY with the 39 % of the total HRUs that make up this culture (Fig. 6.12).

These results show the high spatial variability of the optimization results for the evaluated objective functions. Therefore, our approach suggested that it is effective to determine a Pareto-optimal front for the clustered sites-HRUs than to define a single Pareto-optimal front from the average of the each HRU optimization results. Because the optimization results obtained for the average values of the sites-HRUs will not always be the best or ideal solution for certain areas (HRUs).

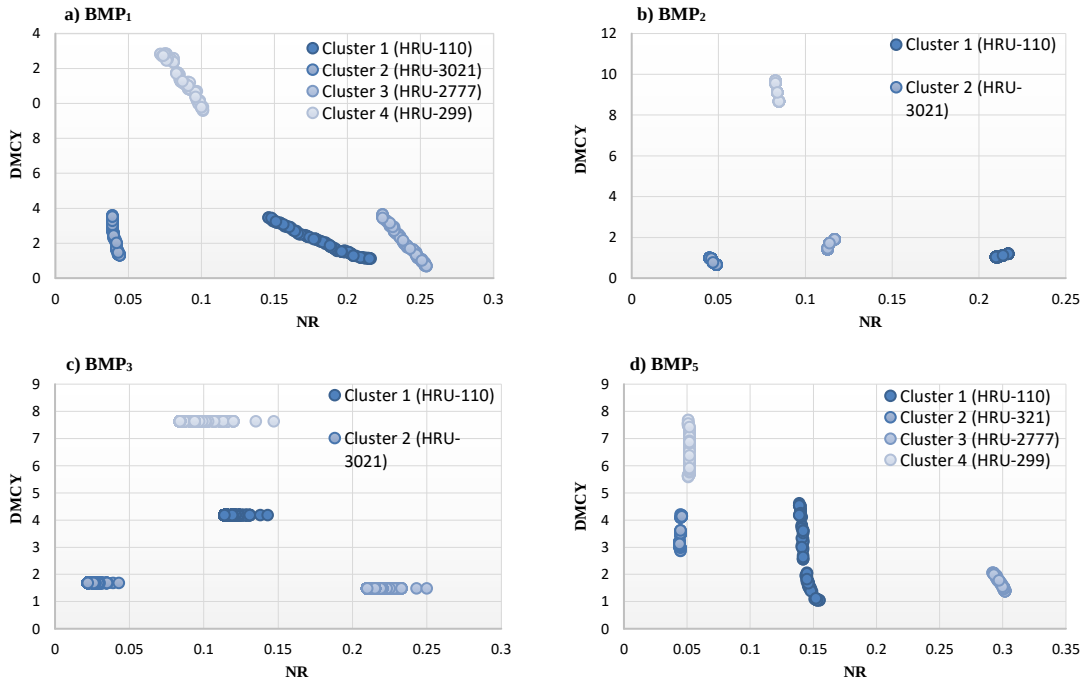

Figure 6.9. Comparing the Pareto-optimal front solutions (100th generations) of one HRU example from each cluster among the BMPs scenarios applied to the kikuyu grass (PASM) land-cover. a) BMP_1, b) BMP_2, c) BMP_3, and d) BMP_5. DMCY: differences from the maximum crop yield, NR: differences from the nitrate reduction.

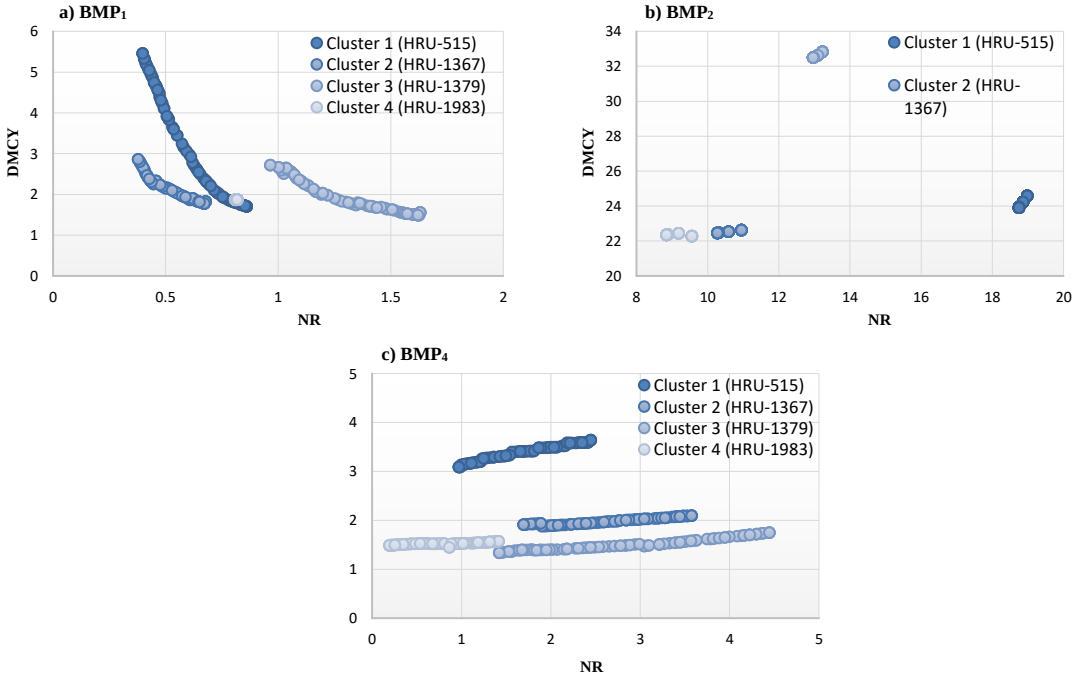

Figure 6.10. Comparing the Pareto-optimal front solutions (100th generations) of one HRU example from each cluster among the BMPs scenarios applied to the potato (POTA) land-cover. a) BMP_1, b) BMP_2, and c) BMP_4. DMCY: differences from the maximum crop yield, NR: differences from the nitrate reduction.

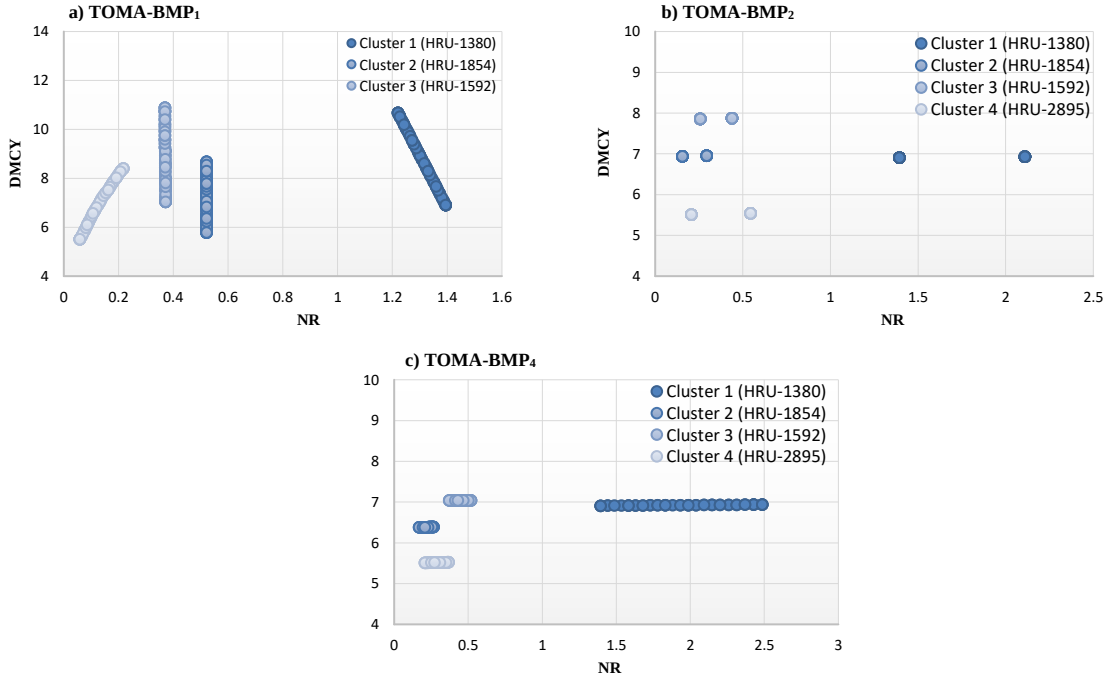

Figure 6.11. Comparing the Pareto-optimal front solutions (100th generations) of one HRU example from each cluster among the BMPs scenarios applied to the tree tomato (TOMA) land-cover. a) BMP$_1$, b) BMP$_2$, and c) BMP$_4$. DMCY: differences from the maximum crop yield, NR: differences from the nitrate reduction.

6.4.4 Comparison between the Pareto-optimal front solutions from average vs. single sites-HRUs values

The comparison between the ranges values results from the optimized solution space for the two objective functions evaluated (NR and DMCY) obtained of the average of the Paretos-optimal front solution of each HRUs (called from now on as Av-HRUs) and the individual objective sites-HRUs grouped by clusters (called from now on as Sin-HRUs) for each scenario are presented per each land-cover type below (Fig. 6.13, 6.14 and 6.15 and Table 6.5, 6.6 and 6.7).

In common, for the four scenarios applied to kikuyu grass, the Av-HRUs range values obtained for the objective function NR optimized corresponds only to 7% percent of the 454 total HRUs optimized, which corresponds to the HRUs grouped in the Cluster 4. Therefore, the NR optimized range values obtained for Av-HRUs does not include the highest values obtained for specific HRUs (Cluster 3 and Cluster 1 only for the BMP2 scenario), which are characterized by having the lowest number of grouped HRUs. It also does not cover the results obtained from the HRUs with the lowest NR optimized values grouped in Cluster 2 (65% of the 454 total HRUs) (Fig. 6.13, Table 6.5). For example, the **Av-HRUs** range values obtained in the BMP$_1$ is 0.05 to 0.07 compared with the 0.02

to 0.03 range values obtained for the HRUs grouped in Cluster 2 (Table 6.5). Therefore, the results indicated that using only the range optimized values obtained from the **Av-HRUs** (similar to the HRUs grouped in Cluster 4) to select the optimal BMP (scenario) to minimized the nitrate rates would not be effective for most HRUs of this crop (Cluster 2).

On the other hand, the comparison results between **Av-HRUs** and **Sin-HRUs** for the objective function DMCY show that the optimized range values obtained for **Av-HRUs** is representative for almost all the HRUs of this crop. Except for the HRUs grouped in cluster 4, which correspond on average to 7% of the total HRUs of the total HRUs, for the four scenarios evaluated (Figure 6.13). The HRUs grouped in Cluster 4 are characterized by being located in Region 1, where there is a lower average temperature in the watershed area (Fig. 6.9). These results indicate that the optimization of the objective function DMCY does not present a high spatial variability compared to the objective function NR. And therefore, to select the Pareto-optimal front and therefore the optimal BMP, the results obtained from **Av-HRUs** could be used.

For the potato land-cover, the optimized NR range values comparison results between the Av-HRUs and the Sin-HRUs showed a similarity with the results obtained and previously explained for the kikuyu grass land-cover (Fig.6.14). Certainly, the range values obtained in both, Av-HRUs and Sin_HRUs, for each of the simulated scenarios are different and correspond only to the potato land-cover (Table 6.5). On the other hand, the optimized DMCY range values comparison results obtained from the Av-HRUs and Sin-HRUs do not vary significantly for the scenario 7 (BMP_4). Although, for the scenarios 5 and 6 (BMP_1 and BMP_2, respectively) the Av-HRUs range results do not include the resulting values of the HRUs grouped in Cluster 4 and Cluster 3, respectively. For example, the optimized DMCY range results for the cluster 4 in the scenario 5 has higher range values than the Av-HRUs results obtained. To emphasize, The HRUs conformed in Cluster 4 corresponds to 2% of the total HRUs of the potato crop.

For the tree tomato crop, the optimized NR range values comparison results between the Av-HRUs and the Sin-HRUs shows that Av-HRUs results generally represent the majority of the HRUs of this land-cover, except for the HRUs grouped in cluster 1 (11% of the total HRUs of this land-cover). The range of values obtained for Cluster 1 is higher than that obtained for Av-HRUs in all the four evaluated scenarios (Fig.6.15, Table 6.6). And the results obtained for the the optimized DMCY range values comparison results between the Av-HRUs and the Sin-HRUs presents that the Av-HRUs range values represent the total HRUs of this land-cover more precise (Fig.6.15). In general, the optimazed NR range values comparison results between the Av-HRUs and the Sin-HRUs present less difference between them compared to the results obtained from the two land-covers already described (Fig.6.15). This result can be explained by the fact that the tree tomato land-cover is conformed of fewer amounts of HRUs (97), grouped in specific areas of the watershed, compared to kikuyu grass land-cover that has a higher amount of HRUs (454) and are distributed throughout the watershed.

Notably, it can be seen in common for the three land-covers that the NR and DMCY range values obtained per cluster show a pattern in all the evaluated scenarios. This pattern may indicate that the optimization range values results do not depend only on the type of BMP applied. This depends on spatial and temporal variables associated with the hydrological dynamics in each one of the HRUs in the watershed. For example, the HRUs grouped in Cluster 2 obtained the minimum NR range values in all the BMP scenarios applied. Those HRUs are located in the watershed in Region 2 that is characterized by lower annual average rainfall (Figure 6.10) and higher average slopes. Therefore, our approach suggests that for the selection of BMPs at the watershed level, it is necessary to perform the respective optimization and analysis to select the Pareto-optimal front at HRU level and not only work with the average values of the HRU results. We suggest grouping HRUs with similar optimization results in clusters to define the optimal-pareto front for each of the defined groups

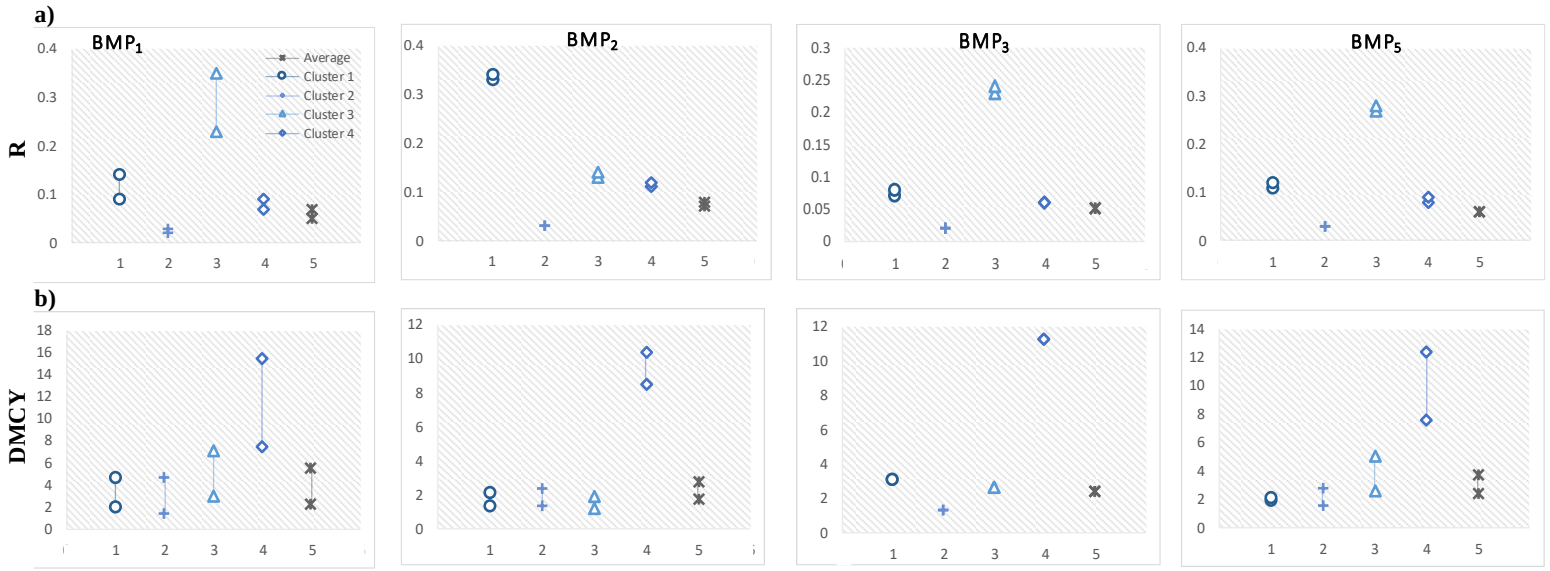

Scenario	BMP		Average		Cluster 1		Cluster 2		Cluster 3		Cluster 4	
			NR	DMCY	NR	DMCY	NR	DMCY	NR	DMCY	NR	DMCY
1	BMP_1	Min	0.05	2.2	0.09	1.9	0.02	1.3	0.23	2.9	0.07	7.4
		Max	0.07	5.5	0.14	4.6	0.03	4.6	0.35	7.1	0.09	15.4
		Total HRUs	454		99		301		17		37	
2	BMP_2	Min	0.07	1.79	0.33	1.34	0.03	1.37	0.13	1.21	0.11	8.54
		Max	0.08	2.75	0.34	2.18	0.03	2.36	0.14	1.89	0.12	10.44
		Total HRUs	454		21		303		102		28	
3	BMP_3	Min	0.05	2.41	0.07	3.17	0.02	1.36	0.23	2.7	0.06	11.3
		Max	0.06		0.08		0.02		0.24		0.06	
		Total HRUs	454		111		284		36		23	
4	BMP_5	Min	0.06	2.4	0.11	1.9	0.03	1.54	0.27	2.57	0.08	7.54
		Max	0.07	3.7	0.12	2.1		2.76	0.28	5.03	0.09	12.4
		Total HRUs	454		97		288		27		42	

Figure 6.12 and Table 6.5. Comparison of the average Pareto-front of each HRU (Av-HRUs) and the individual objective sites-HRUs (Sin-HRUs) ranges values optimized results grouped by clusters for the two objective functions evaluated a) NR and b) DMCY among each scenario applied to kikuyu grass land cover.

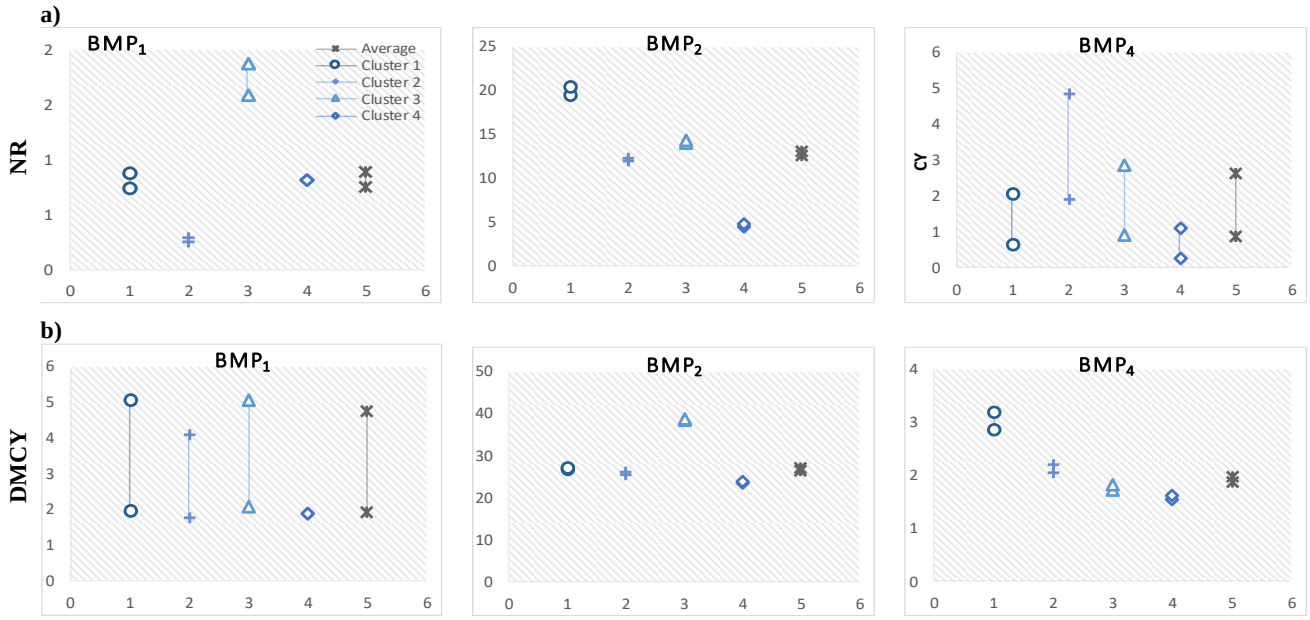

Scenario	BMP		Average		Cluster 1		Cluster 2		Cluster 3		Cluster 4	
			NR	DMCY	NR	DMCY	NR	DMCY	NR	DMCY	NR	DMCY
5	BMP_1	Min	0.75	1.92	0.74	1.95	0.25	1.77	1.60	2.06	0.81	1.87
		Max	0.89	4.74	0.88	5.06	0.29	4.10	1.88	5.06	0.82	1.87
		Total HRUs	167		82		52		32		1	
6	BMP_2	Min	12.6	26.6	19.5	26.8	12.0	25.6	14.0	38.5	4.5	23.5
		Max	13.1	27.2	20.4	27.3	12.3	26.2	14.3	38.7	4.8	24.0
		Total HRUs	167		48		66		15		38	
7	BMP_4	Min	0.87	1.88	0.64	2.88	1.91	2.07	0.90	1.72	0.28	1.54
		Max	2.62	1.99	2.06	3.21	4.83	2.22	2.88	1.84	1.10	1.61
		Total HRUs	167		21		27		75		44	

Figure 6.13 and Table 6.6. Comparison of the average Pareto-front of each HRU (Av-HRUs) and the individual objective sites-HRUs (Sin-HRUs) ranges values optimized results grouped by clusters for the two objective functions evaluated a) NR and b) DMCY among each scenario applied to potato land cover.

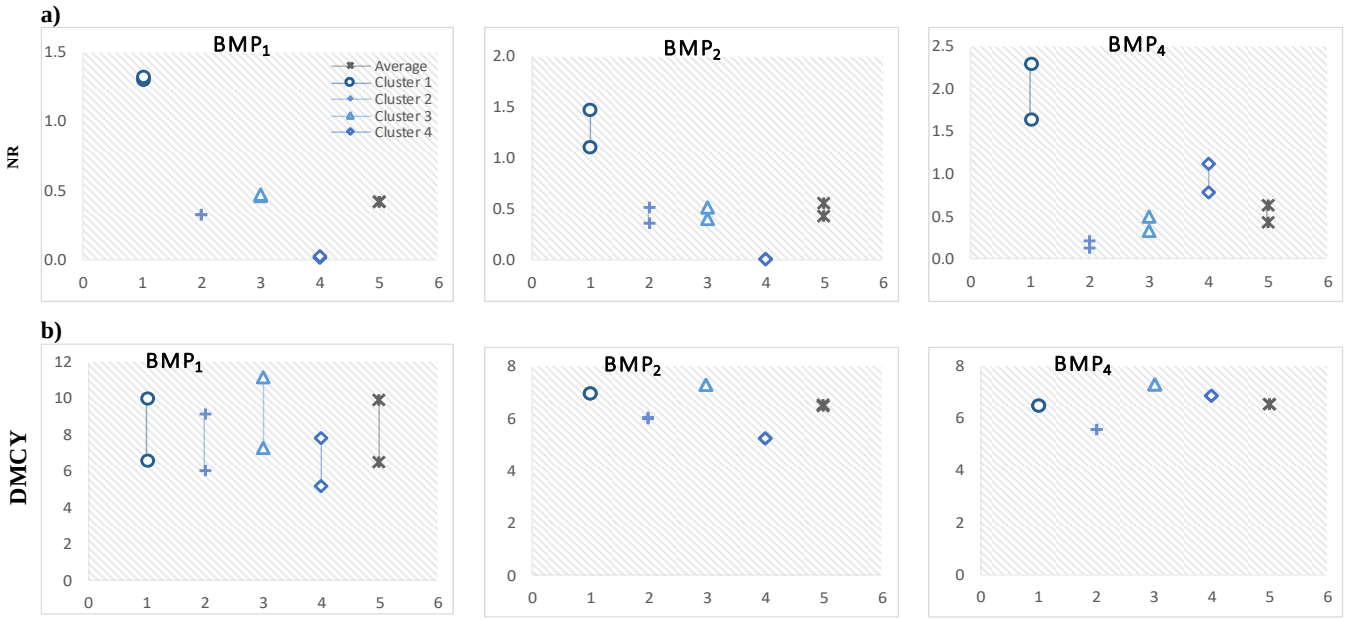

Scenario	BMP		Average		Cluster 1		Cluster 2		Cluster 3		Cluster 4	
			NR	DMCY	NR	DMCY	NR	DMCY	NR	DMCY	NR	DMCY
8	BMP_1	Min	0.42	6.53	1.30	6.63	0.33	6.08	0.46	7.31	0.02	5.22
		Max	0.42	9.94	1.31	10.04	0.33	9.19	0.47	11.21	0.02	7.84
		Total HRUs	97		9		24		45		19	
9	BMP_2	Min	0.42	6.53	1.10	6.98	0.36	6.05	0.40	7.32	0.01	5.25
		Max	0.56	6.54	1.48	6.98	0.51	6.06	0.51	7.33	0.01	5.26
		Total HRUs	97		15		25		38		18	
10	BMP_4	Min	0.42	6.53	1.64	6.47	0.12	5.57	0.32	7.31	0.78	6.87
		Max	0.63	6.54	2.30	6.48	0.21	5.58	0.50	7.32	1.13	6.88
		Total HRUs	97		4		35		33		25	

Figure 6.14 and Table 6.7. Comparison of the average Pareto-front of each HRU (Av-HRUs) and the individual objective sites-HRUs (Sin-HRUs) ranges values optimized results grouped by clusters for the two objective functions evaluated a) NR and b) DMCY among each scenario applied to potato land cover.

6.5 CONCLUSIONS

Understanding and emphasizing the importance of the spatio-temporal allocation of agricultural BMPs has become increasingly important in recent years (Zhu et al., 2019; Geng and Sharpley, 2019; Qin et al., 2018; Yang and Best, 2015; Lescot et al., 2013). This is particularly relevant in tropical Andes mountain agricultural ecosystems, where shifting cultivation, intensive traditional agriculture, and intense precipitation events are predominant. Overall, our research considered all different spatial and temporal allocation components of optimization agricultural BMPs into the optimization framework developed: 1) Ag-BMP type selection, 2) design and sizing of Ag-BMP individual practices, and 3) location determination.

1. Our results highlight the importance of decision-makers' and stakeholders' knowledge to select the BMP type considering willingness from the socio-economic perspective. Mainly, farmers want to improve water quality without reducing agricultural productivity. For example, filter strips is one of the most widely used BMPs used to collect and remove pollutant nutrients from surface run-off (Ritter and Shirmohammadi, 2001). However, this BMP was not accepted by farmers who have less than one hectare cultivated (potato and tree tomato crops). On the contrary, farmers who have the largest area (kikuyu grass for dairy farming) see the implementation of this BMP to be feasible.
2. During the spatial optimization, the NSGA-II model for the Riogrande II watershed was executed to evaluate 10 BMP scenarios for the proposed approach (HRUs located in the ST-CSAs identified). And, the total runtimes was 402 hours (17 days) per each scenario evaluated. Authors like (Qin et al., 2018) found that the computational efficiency can be significantly improving by reducing the simulation time due to the reduction of optimal solutions' search space, instead of using a random approach.
3. The comparison between the average (aggregate) vs. single (distributed) optimization results showed that different analysis results applied with among different BMPs scenarios produced significant differences in Pareto-optimal front solutions, optimizing efficiency, and spatial distribution of BMP scenarios. Generally, the more distributed level analysis was considered, the better the high spatial variability of the optimization results for the evaluated objective functions are shown. Therefore, our approach suggests that the Pareto-front solution must be defined in a distributed way, which means having a Pareto-front solution for each of the different areas (HRUs grouped n clusters) with similar spatial characteristics for the watershed BMP scenarios optimization model. Overall, using the HRUs-clusters position units as Ag-BMP optimization result analysis with the ST-CSAs strategy, the best comprehensive results of Ag-BMP scenarios optimization were obtained.

Also, this study provides a key methodological modeling framework to support the sustainable agriculture plans in Colombia, which aims to propose BMPs to cope with unexpected changes identified in recent years and benefit the farmers. Besides, future research should also focus on exploring the incorporation of BMPs implementation costs as an objective function in the optimization model.

7

CONCLUSIONS AND RECOMMENDATIONS

7.1 SUMMARY

The previous chapter offered insights into the spatio-temporal multi-objective optimization model framework to select and allocate Ag-BMPs for multiple crops and the associated modelling methodology. This concluding chapter summarizes the outcomes of the research questions presented in Chapter 1. Following these research outcomes, the chapter present recommendations on the research process that leads to this dissertation. These are personal reflections of the researcher regarding topics such as model development, how the proposed framework can be indeed incorporated into management practices, and decision makers in sustainable agriculture. And the chapter ends by presenting some limitations to keep in mind for future developments.

7.2 RESEARCH OUTCOMES

The dissertation started by posing four research questions. Below, we discuss how the research outputs address the questions. The research outcomes are formulated with respect to the objectives posed.

The first question was: What are the differences between implementing an Ag-BMP for a crop at farm level versus basin level? And what are the main factors causing these differences? Thus, we proposed our first research objective.

Analyze and determine the impacts on nutrient loss and crop yield from a single agricultural BMP (Ag-BMP) applied to a single crop at field level and watershed level (Objective 1).

A hydrological model (SWAT) was used to assess the impacts of changing IT for CT on nitrogen (N) and phosphorus (P) losses in surface water runoff from the potato crop in the Fuquene watershed. This was done at the field and watershed levels. A two-year study quantified the changes in surface water runoff pollutants for three potato crop cycles under traditional IT practice and CT practice—which included reducing tillage, green manure, and permanent soil cover—at twelve runoff plots installed in the Fuquene watershed (Chapter 4).

The Conservation Tillage BMP's (CT-BMP) objective was the reduction of soil and nutrient loss in runoff. However, CT simulation results at watershed level suggest that total N and P increased (2% and 18% respectively). Also, the concentration of nitrate (NO_3-N) in surface runoff increased by 17% compared to IT. Results at the watershed level showed patterns different from those obtained at field level. These results revealed that CT in some areas (farm level) produces a reduction in nitrate (NO_3^--N) losses reduction. In fact, the greatest limitation identified in this study stems from the process of the CT extrapolation practice for all potato crop areas within the watershed, because the calibrated model was made for a minimal area (field level), and initial and calibrated parameter values are the same for other soil types and average slopes.

The result of the Fuquene watershed modelling show the importance of conducting analyses at farm level (HRUs) and not at watershed level if a lower margin of error is desired when predicting the minimization of impact on water quality. We also concluded that it is necessary to contemplate a detailed spatio-temporal nutrient loss analysis and apply optimization techniques to identify and allocate Ag-BMP options. This approach would help mitigate the uncertainty in assessing the implementation of BMPs at the watershed level. Moreover, by using this type of model and methods, it could be possible to include several crops in the same watershed and define suitable parameters for the different areas in the watershed.

Once we answered the question on the Ag-BMP implementation impact at field level versus watershed levels, we moved on to the second question: How can we determine the spatial and temporal dynamics of nutrient loss in runoff? The second objective has been formulated as follows:

Analyze variations of spatio-temporal impacts on nutrient loss and crop yield from multiple agricultural management practices (Ag-MP) to determine spatio-temporal critical source areas (ST-CSAs) in the watershed (Objective 2).

In Chapter 5, the methodology to develop the new spatio-temporal critical source areas (ST-CSAs) index allows visual representation of the recurrence and behavior in space and time of CSAs. The results show ST-CSAs characteristics and patterns determination is relevant to define which and where Ag-BMPs should be implemented.

The results indicate that there is an essential difference in the aggregation of CSAs in time, and pollution location changes significantly using ST-CSA. As expected, the highest number of spatio-temporal CSAs were observed during rainy months, in the agricultural areas dominated by potato, tree tomato, and dairy agriculture located within the watershed. However, the most significant real number of ST-CSAs occurs in the region with the lowest rainfall in the watershed. Our analysis clearly shows a strong association between both precipitation seasonality and agricultural management schedules (crops and pastures system), and also between spatio-temporal dynamics of CSAs. On the other hand, the ST-CSAs correspond to an average area that is 24.07% of the total watershed (1,034.348 km^2). However, in some years, the area reached a maximum value of 61.78%. The soil water content and runoff significantly influenced both NO_3^--N and soluble P losses, which are variables directly correlated with the amount of NO_3^--N and soluble P loss in surface runoff (kg ha-1) calculated in the model.

Despite the model uncertainties, the results highlight the importance of identifying spatio-temporal CSAs to select BMPs with the highest potential of N and P loss reduction. Additionally, the proposed approach—which uses modeling tools to identify spatio-temporal CSAs—provides a visual representation recommending the identification of priority areas to implement Ag-BMPs (areas for intervention), which is relevant information for decision-makers and stakeholders. And the analysis of the characteristics and spatial and temporal patterns of the ST-CSAs are relevant for the definition of viable BMPs for specific regions identified with similar patterns and nutrient losses in runoff. Besides, it is a clear and organized way to define successful agricultural BMPs and develop spatio-temporal multi-objective optimization models.

Having identified the ST-CSAs for various crops in the watershed, the Ag-BMPs that would be adequate to implement in the study watershed—from all possible types—were determined. And they should be transferred to the model in a manner that they can be represented in the best possible way. Consequently, the third objective was proposed:

Select and parameterize Ag-BMPs scenarios to be used in the optimization model framework that are feasible to implement by local farmers (Objective 3).

In the case of Colombia, the “Best Practices for the Management and Sustainable Use of Colombia’s Soils” guide (Buenas Prácticas para la Gestión y Uso Sostenible de los suelos de Colombia in Spanish) (Organización de las Naciones Unidas para la Alimentación y la Agricultura (FAO) and Ministerio de Ambiente y Desarrollo Sostenible (MADS), 2018) recommends around 15 BMPs that can be used by farmers, according to the benefit and application methods, the economic viability of the products, and the social and cultural conditions of the area. However, the identification of priority areas to implement BMPs is not provided.

Our methodological approach for developing this objective was based on the belief that—to achieve levels of sustainability in the watershed in accordance with the economic and cultural needs of the farmers—their opinion must be considered. Therefore, the results of this research highlight the importance of selecting appropriate BMPs that are viable in the future by: **1. identifying the spatio-temporal CSAs to determine the best areas for intervention; and 2. using the decision-makers' and stakeholders' knowledge to select the feasible BMP type from the socio-economic perspective.** Fieldwork and interviews with local farmers (123 farms' representatives) were considered in the selection of feasible BMPs for the studied watershed. These BMPs were selected because they are agricultural practices that do not increase implementation costs, they can be implemented by farmers with the tools and financial resources they currently have, and they were accepted (and some were proposed) by the farmers themselves. For example, the filter strip is one of the most widely used BMPs to collect and remove pollutant nutrients from surface runoff (Ritter and Shirmohammadi, 2001). However, this BMP was not accepted by farmers who have less than one hectare cultivated (potato and tree tomato crops); on the contrary, farmers who have the largest area (kikuyu grass for dairy farming) view the implementation of this BMP as feasible.

The conclusion lead to the following question: How can we incorporate the spatial and temporal dynamics of nutrient losses in runoff to select optimal Ag-BMPs, thereby allowing for integration of all data and knowledge acquired? Model-based optimization framework would be an answer; therefore, the following objective was formulated:

Develop a framework and methodology for a spatio-temporal multi-objective optimization model to select and allocate Ag-BMPs for multiple crops (Objective 4).

For the third outcome, the modeling framework and methodology were developed. The complexity of the problem was taken into account and the number of crops and Ag-BMPs were increased. The application of the modelling framework showed the importance of defining the optimization search space using ST-CSAs instead of a random approach. It was especially noticeable when it is required to perform the optimization model for several Ag-BMPs and multiple crops at farm level. This approach allows improved computational efficiency by reducing the simulation time due to the reduction of optimal solutions' search space (ST-CSAs).

The methodological steps to analyze the optimization results spatially showed that with inclusion of more spatial data the spatial variability of the optimization results is higher. Therefore, our approach recommends that the optimization procedure should take this into account, and this means having a Pareto-front solution for each of the different areas with similar spatial variability of the optimization results for each of the evaluated scenarios.

This research provides a key methodological modeling framework to support the sustainable agriculture plans in Colombia, which aims to propose Ag-BMPs to cope with unexpected changes identified in recent years and benefit farmers. It would be recommended to consider incorporating it into the Colombian agricultural management practices at various levels.

It can be recommended to explore incorporation of BMPs implementation costs as an objective function in the optimization model. Also, it would be beneficial to develop an assistance tool (e.g., mobile application) for local communities (farmers), which can be used to adapt the agricultural practices to cope with unexpected changes identified in recent years.

7.3 RECOMENDATIONS

Research communities

During the last decades, the connection between research communities developing optimization approaches and land use communities has been increasing with the development of algorithms that tackle the increase of complexity in agriculture optimization problems. The complexity is caused by the type of agricultural management practices, weather variability, and decision-makers' points of view and their competing criteria. However, the more advanced algorithms are not developed specifically for optimization problems in agriculture. Therefore, there are barriers to their wider adoption, and the development of an algorithmic framework that provides a set of guidelines to develop optimization algorithms for agriculture problems would be beneficial.

To help to move in this direction, the present thesis highlights the importance of obtaining knowledge about the following: 1) agricultural practices that farmers currently or traditionally use in their crops, 2) knowing the spatial and temporal dynamics of the objectives of interest (e.g., loss of nutrients in runoff, crop yields, costs), 3) geographical resolution, and 3) know the possibilities and interests of farmers to accept and adopt agricultural BMP (Ag-BMPs) alternatives. This knowledge allows for adequate definition of the optimization problem based on the structure of the issue to be resolved, and adequately constraining its search space. To achieve that, a closer collaboration between modelers, land use researchers, stakeholders, and farmers are needed. This will allow the development/improvement of agriculture optimization algorithms that consider and include the complexity of the selection and allocation of agricultural best management practices. Instead of using a metaheuristic because it is historically and widely used by a research area and its popularity outside the modelling and optimization research community, the choice should be determined by the characteristics of the problems to be solved.

How to handle a large number of decision variables and dynamics?

One of the largest and most important issues to face in agricultural optimization problems involving selection and allocation of Ag-BMPs on a large scale – with more and more emphasis on the local level – is the large number of decision variables involved. The explosion of the number of decision variables depends on the number of crops, the geographic scale, simulation period, units where allocation would take place, and the spatio-temporal and dynamic aspects; and it seems unavoidable. The impact of such large numbers of variables on computation time is severe, and adequate computational facilities to handle a large number of decision variables and dynamics may not be easily found. For example, parallel computing techniques to speed up the evaluation of solutions involving population-based metaheuristics (evolutionary algorithms) is a necessity. However, when temporal and dynamic aspects, local scale, various crops, several Ag-BMPs, as well the optimization goals are contemplated in the optimization problem, computational time demand may still be prohibitively high, even using parallel evolutionary algorithms (Porta et al. 2013; Liu et al. 2013b).

In this dissertation, in order to reduce computing time, the initial search space for the optimization problem (total area of the hydrographic watershed studied) was reduced to the spatio-temporal critical sources area (ST-CSAs), which corresponds to the spatial location where the highest pollutant loads within the watershed are present. For this new search space the optimization problem was divided into three optimization sub-problems for each type of land-cover, which were solved in parallel. The total runtimes were 402 hours (17 days) per each of the 10 scenario evaluated, and the computational time was considerably reduced by using 5 processors. (Qin et al., 2018) found that the computational efficiency can be significantly improved by reducing the simulation time due to the reduction of optimal solutions' search space. Formulation of such constriants is only possible thorough a close collaboration between researchers using land use/agricultural simulation models and the experts in optimization.

How this framework can be incorporated into agricultural management practice?

The goal of agricultural BMPs (Ag-BMPs) optimization is to support decisionmakers and including them in the whole allocation process is crucial. The generated sets of Pareto-optimal solutions represented by spatial configurations and/or Ag-BMPs allocations are to be further analysed by decision makers for selecting the solutions for their actual implementation. Indeed, stakeholders and decisionmakers, who sometimes have competing interests, require tools to help them find trade-offs between their points of views and interests. In the context of Ag-BMPs allocation, the multi-criteria decision-making methods have complemented the optimization process, due to the fact that many competing actors (farmers, governmental institutions, environmental agencies, and economists) are involved, and optimization methods need to consider their priorities and goals.

In relation to that, using, for example, a multi-criteria analysis technique following the approach proposed in the Collaborative Risk Informed Decision Analysis (CRIDA) could be appropriate. Whereby, stakeholders and decision-makers could select one or more BMPs solutions from all the possible options generated by the multi-objective optimization algorithm (Pareto frontier). These could then be considered as new approaches in local watershed management strategies for a specific case study. Likewise, the development and use of a visual assistance tool could be used to adapt agricultural practices to cope with unexpected changes that have emerged in recent years. For example, conversations with the Colombian government are taking place regarding the development of a mobile application as an important and needed assistance tool for local communities (farmers) to analyze the Ag-BMP optimized solutions obtained in the case study of this research.

7.4 LIMITATIONS AND FUTURE DIRECTIONS

There are multiple limitations of the spatio-temporal Ag-BMP optimization framework proposed, which could be addressed when future developments are working on those and released to the community.

As was mentioned before, one of the biggest and most important issues to face in agricultural optimization problems to select and allocate BMPs in a waterhed scale is the large number of decision variables involved, specilly when more and more emphasis on the local level is requiered. One of the main limitations is a challenge to **represent in detail the current agricultural management practices used by farmers**, including the associated spatial and temporal variability. This is especially important for the agricultural dynamics in the tropical Andes (case study of this dissertation) with a variety of crops and livestock activities, which are in many cases combined resulting in mixed crop-livestock systems. In addition, it is possible to find short-cycle crop rotations. All this, associated also with rain seasonality, results in high variation in water pollution and crop yields within a single year.

The approach proposed in this research requires the development of a hydrology model that allows estimating nitrates in runoff and crop productivity at the watershed level, considering the current agricultural practices carried out by farmers. Fieldwork was conducted to collect key information directly from farmers; due to budget limitations a representative sample of the farmers was visited, but not all of them, and some assumptions were made in order to build the current management practices database. Therefore, since farmers do not use exactly the same agricultural management schedules, future research should explore the possibility of incorporating the dynamics of: a) planting date in the agricultural management schedule of each farmer studied, b) incorporate transitory crops which occur mainly in pastures, c) fertilization application dates and rates used by each farmer, and d) technology for applying the fertilizer (horses, ditches, and spray by sprinklers) within the watershed.

Another constraint of the current Ag-BMP optimization is that the evaluation of a practice's **cost-effectiveness, considering that the economic effects of the Ag-BMPs** can change the probability of adoption for an optimized Ag-BMPs alternative. Therefore, implementation cost, land tenure type (owner or rented), and market prices are variables to be considered. However, in some cases, such as in the present investigation, this information could not be collected. The farmers often are not eager to provide the economic information for security reasons. In real life, economic variables such as implementation cost and land tenure change per farmer almost every year, which generates more complexity for the agricultural optimization problem of selecting and allocating BMPs in a watershed. This dissertation proposes that spatially varying economic and sociological data need to be collected and incorporated into the design of Ag-BMPs alternatives. Further investigation is needed to model motivation of adoption by integrating real stakeholder agents into the optimization process.

In addition, changes in runoff, crop yields, as well as the economic consequences, are a few of the **potential effects of climatic change on agriculture**. Therefore, the effectiveness of Ag-BMPs could be beneficial in some areas while other areas may suffer under climate change conditions, indicating the importance of allocating Ag-BMP in specific areas within the watershed under different climate change scenarios. Several studies have focused on understanding the influence of climate change on Ag-BMP performance, and it would be useful to concentrate future research on incorporating climate change-related factors into the proposed optimization framework.

APPENDIX A

A.1 SWAT CROP INPUT PARAMETERS DEFINED IN THE LAND COVER DATABASE

CPNM	RYEG	AVOC	PINA	FRST	PASM	CANT	FESC	PAST	POTA	MESQ	TOMA	WATR	RYEE
CROPNAME	Annual Ryegrass	Avocado	Conifer Planting	Forest-Mixed	Managed grasses	Transitional crops	Páramo	Pasture	Potato	Stubble	Tree Tomato	Water bodies	Weeded grasses
BIO_E	30	20	25	25	55	30	30	35	45	20	55	0	30
HVSTI	0.9	0.1	0.76	0.76	1.25	0.5	0.9	0.9	1.25	0.05	1.25	0	0.9
BLAI	3	3	6.5	3.14	4	3	4	4	4	2.45	4	0	3
FRGRW1	0.2	0.1	0.15	0.05	0.2	0.15	0.15	0.05	0.15	0.05	0.15	0	0.2
LAIMX1	0.32	0.15	0.7	0.05	0.32	0.05	0.01	0.05	0.01	0.05	0.05	0	0.32
FRGRW2	0.45	0.5	0.25	0.4	0.45	0.5	0.5	0.49	0.5	0.4	0.5	0	0.45
LAIMX2	0.95	0.75	0.99	0.95	0.95	0.95	0.95	0.95	0.95	0.95	0.95	0	0.95
DLAI	0.5	0.99	0.99	0.99	0.5	0.6	0.8	0.99	0.6	0.99	0.95	0	0.5
CHTMX	6	15	16.1	20	10	0.5	1.5	0.5	0.6	20	5	0	10
RDMX	1.3	1.5	3.5	3.5	1.3	1.2	2	2	0.6	3.5	2	0	1.3
T_OPT	18	15	15	15	14	18	15	18	14	18	18	0	18
T_BASE	2	7	2	2	1	2	2	7	1	7	4	0	2
CNYLD	0.022	0.0019	0.0015	0.0015	0.022	0.0138	0.0234	0.0234	0.0246	0.0015	0.0235	0	0.022
CPYLD	0.0028	0.0004	0.0003	0.0003	0.0028	0.0017	0.0033	0.0033	0.0023	0.0003	0.0048	0	0.0028
BN1	0.066	0.006	0.006	0.006	0.066	0.0663	0.056	0.06	0.055	0.02	0.0663	0	0.066
BN2	0.0254	0.002	0.002	0.002	0.0254	0.0255	0.021	0.0231	0.02	0.01	0.03	0	0.0254
BN3	0.0147	0.0015	0.0015	0.0015	0.0147	0.0148	0.012	0.0134	0.012	0.008	0.025	0	0.0147
BP1	0.0105	0.0007	0.0007	0.0007	0.0105	0.0053	0.0099	0.0084	0.006	0.0007	0.0053	0	0.0105
BP2	0.004	0.0004	0.0004	0.0004	0.004	0.002	0.0022	0.0032	0.0025	0.0004	0.0035	0	0.004
BP3	0.0024	0.0003	0.0003	0.0003	0.0024	0.0012	0.0019	0.0019	0.0019	0.0003	0.0025	0	0.0024
WSYF	0.9	0.05	0.6	0.01	0.9	0.25	0.9	0.9	0.95	0.01	0.15	0	0.9
USLE_C	0.03	0.001	0.19	0.2	0.15	0.03	0.003	0.5	0.2	0.25	0.03	0	0.15
GSI	0.005	0.007	0.002	0.002	0.005	0.006	0.005	0.005	0.005	0.004	0.008	0	0.005
VPDFR	4	4	4	4	4	4	4	4	4	4	4	0	4
FRGMAX	0.75	0.75	0.75	0.75	0.75	0.75	0.75	0.75	0.75	0.75	0.75	0	0.75
WAVP	6	3	8	8	6	3	8	10	14.8	8	8	0	6
CO2HI	660	660	660	660	660	660	660	660	660	660	660	0	660
BIOEHI	39	20	16	16	39	39	39	36	30	18	39	0	39
RSDCO_PL	0.05	0.05	0.05	0.05	0.05	0.05	0.05	0.05	0.05	0.05	0.05	0	0.05
OV_N	0.14	0.1	0.1	0.1	0.15	0.1	0.1	0.14	0.1	0.1	0.14	0.01	0.15
CN2A	25	25	25	25	25	66	31	25	67	30	50	92	25
CN2B	50	48	45	40	48	77	59	55	77	46	60	92	48
CN2C	74	68	70	65	72	83	72	70	83	63	73	92	72
CN2D	81	74	77	72	79	87	79	77	87	66	87	92	79
FERTFIELD	0	0	0	0	0	1	0	0	1	0	1	0	0
ALAI_MIN	0	0.75	0.75	0.75	0	0	0	0	0	0.75	0	0	0
BIO_LEAF	0	0.3	0.3	0.3	0	0	0	0	0	0.3	0	0	0
MAT_YRS	0	10	50	50	0	0	0	0	0	10	1	0	0
BMX_TREES	0	500	1000	1000	0	0	0	0	0	50	500	0	0
EXT_COEF	0.65	0.65	0.65	0.65	0.65	0.65	0.65	0.65	0.65	0.61	0.65	0	0.65
BM_DIEOFF	0.1	0.1	0.1	0.1	0.1	0.1	0.1	0.1	0.1	0.1	0.1	0.1	0.1

A.2 PHYSICAL CHARACTERISTICS OF THE SOIL TYPES PRESENT IN THE RIOGRANDE II WATERSHED.

SNAM	PERFIL	SOL_Z (mm)	SOL_BD (g/cm3)	SOL_AWC (mm/mm)	SOL_K (mm/hr)	SOL_CBN (%)	CLAY (%)	SILT (%)	SAND (%)	USLE_K
mo	Andisol, Andic Kanhaplohumults	220	0.55	0.41	48.56	3.92	45	48	7	0.20
		340	0.87	0.30	8.07	6.29	60	20	20	0.10
		580	1.33	0.21	8.07	1.14	45	7	48	0.10
		1100	1.48	0.15	8.07	0.39	5	5	90	0.08
Lome	Andisol, Ultic Hapludands	300	0.25	0.81	66.20	13.09	5	90	5	0.34
		470	0.52	0.43	35.07	9.07	5	90	5	0.34
		570	0.62	0.37	35.07	5.60	5	90	5	0.34
		750	1.17	0.21	35.07	2.56	60	20	20	0.10
		1100	1.15	0.22	35.07	0.97	60	20	20	0.13
Vco	Andisol, And.Dystrudepts	400	0.50	0.52	17.23	3.52	45	48	7	0.20
		1100	0.75	0.31	10.32	0.01	13	26	61	0.18
Lm	Andisol, Typ.Melanudadns	300	0.51	0.51	109.60	13.53	15	68	17	0.19
		610	0.42	0.52	25.68	11.40	5	90	5	0.34
		930	0.89	0.32	25.68	3.35	5	90	5	0.34
		1200	0.90	0.32	25.68	3.16	5	90	5	0.34
F	Andisol, Andic Humudepts	230	0.67	0.46	22.30	11.67	18	42	40	0.14
		460	0.80	0.45	22.69	5.52	15	68	17	0.19
		800	1.15	0.22	22.69	1.17	60	20	20	0.12
		1200	1.35	0.21	22.69	0.33	45	7	48	0.11
Cor	Andisol, Typ.Placudands	210	0.42	0.57	51.23	11.69	15	68	17	0.19
		440	0.48	0.57	7.74	6.59	60	20	20	0.10
		640	1.17	0.21	7.74	2.75	60	20	20	0.10
		870	1.15	0.22	7.74	0.83	60	20	20	0.13
		1200	1.14	0.23	7.74	0.13	60	20	20	0.14
Ab	Andisol, Typ.Hapludands	210	0.44	0.50	37.13	10.87	18	42	40	0.14
		410	0.81	0.37	16.26	9.26	45	7	48	0.08
		1000	1.17	0.24	16.26	2.08	45	48	7	0.20
Cv1	Andisol, And.Udifluvents	250	0.23	0.86	57.46	20.25	15	68	17	0.19
		570	0.54	0.59	3.69	5.93	10	25	75	0.12
		670	0.96	0.25	3.69	8.77	45	48	7	0.20
L	Andisol, Typ.Hapludands	200	0.38	0.54	35.30	19.55	15	68	17	0.19
		300	0.83	0.44	1.33	14.45	15	68	17	0.19
		800	1.15	0.22	1.33	0.91	60	20	20	0.13
		1100	1.20	0.24	1.33	0.18	45	48	7	0.26
Es	Andisol, Typ.Hapludands	280	0.36	0.63	44.47	17.81	5	90	5	0.34
		380	0.45	0.56	2.86	9.35	5	90	5	0.34
		900	1.09	0.24	2.86	2.28	45	48	7	0.20
		1200	1.36	0.21	2.86	0.04	45	7	48	0.11
V	Inceptisol, Typ.Dystrudepts	300	0.78	0.44	117.36	2.31	5	5	90	0.06
		720	0.91	0.22	22.45	2.17	5	5	90	0.06
		1080	1.20	0.20	22.45	2.00	10	25	75	0.12
		1800	1.31	0.15	22.45	1.06	5	5	90	0.07
P	Andisol, Lithic Haplundand	140	1.15	0.22	60.35	15.57	25	16	59	0.11
		200	1.13	0.22	72.04	9.59	28	26	46	0.12
		350	1.24	0.20	65.05	3.47	28	32	40	0.12
E	Agua	25	1.72	0.00	260.00	0.00	0	0	0	0.00

A.3 POTATO, KIKUYU GRASS, AND TREE TOMATO OPERATION SCHEDULES

Crop	Operation	Date	Crop	Operation	Date	Crop	Operation	Date
	Tillage	5-Mar		Tillage	5-Jan		Tillage	15-Apr
Potato	Plant	15-Mar		Fertilizer	7-Jan		Fertilizer	15-Apr
	Fertilizer	5-Apr		Fertilizer	8-Jan	Tree	Plant	15-May
	Tillage	5-Apr	Grass	Plant	10-Jan	tomato	Fertilizer	15-Jun
	Fertilizer	25-Apr	(kikuyu)	Grazing	25-Feb		Fertilizer	15-Jun
	Tillage	25-Apr		Fertilizer	4-Mar		Fertilizer	15-Aug
	Harvest /Kill	15-Aug		Fertilizer	5-Mar		Harvest	15-Oct
	Tillage	5-Sep		Grazing	5-Apr		Fertilizer	15-Nov
Potato	Plant	15-Sep		Fertilizer	13-Apr		Fertilizer	15-Nov
	Fertilizer	5-Oct		Fertilizer	14-Apr		Fertilizer	15-Feb
	Tillage	5-Oct		Grazing	15-May		Harvest	15-Apr
	Fertilizer	25-Oct		Fertilizer	23-May		Fertilizer	15-May
	Tillage	25-Oct		Fertilizer	24-May		Fertilizer	15-May
	Harvest /Kill	15-Feb		Fertilizer	3-Jun		Fertilizer	15-Jul
Grass	Plant	15-Apr		Fertilizer	4-Jun		Harvest	15-Aug
(kikuyu)	Grazing	15-May		Grazing	25-Jun		Fertilizer	15-Sep
	Fertilizer	23-May		Fertilizer	3-Jul		Fertilizer	15-Sep
	Fertilizer	24-May		Fertilizer	4-Jul		Fertilizer	15-Nov
	Fertilizer	3-Jun		Grazing	5-Aug		Harvest	15-Feb
	Fertilizer	4-Jun		Fertilizer	13-Aug		Fertilizer	15-Mar
	Grazing	25-Jun		Fertilizer	14-Aug		Fertilizer	15-Mar
	Fertilizer	3-Jul		Grazing	15-Sep		Fertilizer	15-May
	Fertilizer	4-Jul		Fertilizer	23-Sep		Harvest	15-Jul
	Grazing	5-Aug		Fertilizer	24-Sep		Fertilizer	15-Aug
	Fertilizer	13-Aug		Grazing	25-Oct		Fertilizer	15-Aug
	Fertilizer	14-Aug		Fertilizer	27-Oct		Fertilizer	15-Oct
	Grazing	15-Sep		Fertilizer	28-Oct		Harvest	15-Dec
	Fertilizer	23-Sep		Grazing	5-Dec		Fertilizer	15-Jan
	Fertilizer	24-Sep		Fertilizer	13-Dec		Fertilizer	15-Jan
	Grazing	25-Oct		Fertilizer	14-Dec		Fertilizer	15-Mar
	Fertilizer	27-Oct					Harvest	15-May
	Fertilizer	28-Oct					Fertilizer	15-Jun
	Grazing	5-Dec					Fertilizer	15-Jun
	Fertilizer	13-Dec					Fertilizer	15-Aug
	Fertilizer	14-Dec					Harvest	15-Oct
	Harvest /Kill	30-Dec					Fertilizer	15-Nov
							Fertilizer	15-Nov
							Fertilizer	15-Jan
							Harvest	15-Apr
							Fertilizer	15-May
							Fertilizer	15-Jul
							Harvest/Kill	15-Aug

A.4 ANALYSIS OF VARIANCE OF NO3−N LOSSES

Variable	Estimate	Std. Error	t value	p-value	Sig
(Intercept)	2.646	1.360	1.946	0.052	.
Runoff (mm)	0.051	0.002	21.616	0.000	***
Slope (%)	-0.008	0.001	-5.714	0.000	***
Area (km2)	-0.137	0.020	-6.874	0.000	***
Precipitation (mm)	-0.002	0.001	-3.122	0.002	**
Soil water content (mm)	0.011	0.004	-2.544	0.011	*
Daily CN	-0.059	0.008	7.492	0.000	***
Subbasin 2	-1.245	0.308	-4.038	0.000	***
Subbasin 3	-0.493	0.290	-1.703	0.089	.
Subbasin 4	-0.210	0.287	-0.731	0.465	
Subbasin 5	-1.119	0.308	-3.637	0.000	***
Subbasin 6	-0.421	0.293	-1.439	0.150	
Subbasin 7	-0.828	0.310	-2.675	0.007	**
Subbasin 8	0.405	0.589	0.688	0.492	
Subbasin 9	2.107	0.276	7.641	0.000	***
Subbasin 10	-0.119	0.399	-0.299	0.765	
Subbasin 11	-0.121	0.282	-0.430	0.667	
Subbasin 12	-0.404	0.265	-1.521	0.128	
Subbasin 13	1.212	0.314	3.855	0.000	***
Subbasin 14	-0.838	0.282	-2.972	0.003	**
Subbasin 15	-0.359	0.276	-1.305	0.192	
Subbasin 16	-0.072	0.268	-0.268	0.789	
Subbasin 17	-0.892	0.276	-3.228	0.001	**
Subbasin 18	-0.567	0.270	-2.098	0.036	*
Subbasin 19	-0.304	0.272	-1.115	0.265	
Subbasin 20	-0.570	0.278	-2.054	0.040	*
Soil_Cor	4.682	0.623	7.518	0.000	***
Soil_Cv1	-0.013	0.441	-0.030	0.976	
Soil_Es	1.009	0.646	1.562	0.118	
Soil_F	1.043	0.470	2.219	0.027	*
Soil_L	0.424	0.427	0.992	0.321	
Soil_Lm	2.212	0.863	2.562	0.010	*
Soil_Lome	0.399	0.416	0.958	0.338	
Soil_V	0.681	0.595	1.143	0.253	
Soil_Vco	1.060	0.610	1.739	0.082	.
Soil_mo	-1.346	0.543	-2.480	0.013	*

* means the level of significance $p < 0.10$

** means the level of significance $p < 0.05$

*** means the level of significance $p < 0.01$

A.5 ANALYSIS OF VARIANCE OF SOLUBLE P

Variable	Estimate	Std. Error	t value	p-value	Sig
(Intercept)	0.094	0.143	0.655	0.513	
Runoff (mm)	0.008	0.000	35.916	0.000	***
Slope (%)	-0.003	0.000	-16.669	0.000	***
Area (km2)	-0.056	0.007	-8.279	0.000	***
Precipitation (mm)	0.001	0.000	12.275	0.000	***
Soil water content (mm)	0.003	0.000	6.913	0.000	***
Daily CN	-0.021	0.001	-26.841	0.000	***
Subbasin 2	0.768	0.071	10.802	0.000	***
Subbasin 3	0.631	0.073	8.617	0.000	***
Subbasin 4	0.751	0.072	10.364	0.000	***
Subbasin 5	0.650	0.072	8.968	0.000	***
Subbasin 6	0.650	0.074	8.814	0.000	***
Subbasin 7	0.825	0.071	11.621	0.000	***
Subbasin 9	0.845	0.073	11.605	0.000	***
Subbasin 11	0.754	0.071	10.688	0.000	***
Subbasin 12	0.754	0.069	10.856	0.000	***
Subbasin 13	0.796	0.071	11.236	0.000	***
Subbasin 14	0.731	0.070	10.499	0.000	***
Subbasin 15	0.734	0.070	10.472	0.000	***
Subbasin 16	0.739	0.070	10.617	0.000	***
Subbasin 17	0.814	0.070	11.656	0.000	***
Subbasin 18	0.743	0.070	10.694	0.000	***
Subbasin 19	0.778	0.069	11.223	0.000	***
Subbasin 20	0.743	0.070	10.588	0.000	***
Soil_Es	-0.530	0.070	-7.549	0.000	***
Soil_F	-0.249	0.038	-6.602	0.000	***
Soil_L	-0.129	0.023	-5.538	0.000	***
Soil_Lm	-0.685	0.100	-6.883	0.000	***
Soil_Lome	-0.124	0.019	-6.617	0.000	***
Soil_V	-0.433	0.058	-7.424	0.000	***
Soil_Vco	-0.424	0.064	-6.650	0.000	***
Soil_mo	-0.133	0.045	2.990	0.003	***

* means the level of significance $p < 0.10$

** means the level of significance $p < 0.05$

*** means the level of significance $p < 0.01$

A.6 Analysis of variance POSTANOVA of NO3−N losses

Sub-basin	Runoff (kg/ha)	Groups	Soil	Runoff (kg/ha)	Groups
9	7.127	a	Cor	8.926	a
13	5.759	b	Lome	4.783	b
19	4.842	c	F	4.654	bc
6	4.786	c	L	4.477	cd
16	4.747	c	Cv1	4.470	cd
12	4.604	cd	Lm	4.457	d
11	4.577	cde	Vco	4.194	e
20	4.431	def	Es	3.415	f
4	4.365	def	mo	3.388	f
15	4.361	ef	V	3.161	f
18	4.313	ef	Ab	2.753	f
7	4.165	fg			
14	4.126	fg			
2	3.834	gh			
3	3.812	gh			
5	3.810	gh			
17	3.794	gh			
1	3.663	gh			
8	3.596	gh			
10	3.311	h			

A.7 Analysis of variance POSTANOVA of soluble P losses

Sub-basin	Soluble P (kg_ha)	Groups	Soil	Soluble P (kg_ha)	Groups
19	0.550	a	Vco	0.516	a
7	0.540	ab	L	0.497	a
13	0.515	bc	mo	0.492	ab
9	0.507	bcd	Cv1	0.459	bc
2	0.499	bcd	Lm	0.457	bc
12	0.497	cd	Lome	0.448	bcd
4	0.479	cde	F	0.431	bde
17	0.475	de	Es	0.389	cde
14	0.457	e	V	0.388	e
20	0.449	e			
18	0.445	e			
15	0.418	f			
11	0.415	fg			
5	0.396	fgh			
16	0.391	gh			
6	0.372	ghi			
3	0.363	hi			
1	0.254	i			

APPENDIX B

B.1 DESCRIPTION OF THE NSGA-II/SWAT OPTIMIZATION LIBRARY

The NSGA-II/SWAT library design includes three classes: 1) `NSGA2` main class that includes the NSGA-II operations, creating parent population and child., 2) `NSGA2utilities` utility class for lower-level NSGA-II to complete methods required when creating child population and parent population. For example, the `Crossover()` or `Unicross()` and `NonDominatedSorting()` and `CrowdingDistance()` methods, and 3) `SWATutilities` class used for SWAT operations including `CalculateObjectiveFunctions()`(Figure B.1a). Some several scripts and files must be executed (Figure B.1b). First, the batch file `Start_run.bat` is initialized to call the script `ExampleTest.py` that reads the path where the `SWATtxtinoutDirectory` of the SWAT project is saved and imported the classes `NSGA2`, `NSGA2utilities`, and `SWATutilities`. The `NSGA2` class reads in the inputs from the `SWATtxtinoutDirectory` folder, such as `PopulationSize`, `GenerationNumber`, and `Observations`. The initial combined population is created, and the generation loop creates the parent population from the combined population. Second, in the file, a Model is created to store the genes (SWAT model parameter values related to the decision variables – see Table 6.4), transformed into a binary format using a decoding process named `decode()`. Thus, the gene values can be edited, and the child population is used for the `SWATutilities` class method to calculate the objective functions, using the `CalculateObjectiveFunctions()`.

Subsequently, the following scripts and batch files are directly related to the SWAT model, and these are structured and named in the same way as in the SWAT-CUP program (Figure B.1b). The batch file `nsga2_mid.cmd` is used for editing our parameters, extracting the two Python scripts `SWAT_ParameterEdit.py and Extract_hru.py`, and runs the `swat.exe` model engine to create the `model.out` file. The `SWAT_ParameterEdit.py` script changes the SWAT files based on the parameter values previously defined in the `model.in` file. The `swat.exe` model engine is executed to run the SWAT model now with the new parameter values. The `Extract_hru.py` script runs to extract the SWAT model outputs into the `model.out` file. Finally, the parent and child populations are used to create the new combined population for the next generation. Then the `ExampleTest.py` script runs again using the `model.out` file to execute the `CalculateObjectiveFunctions()` method to calculate the objective function values. This process is repeated (loop) until the conditions previously defined in the `NSGA2` class.

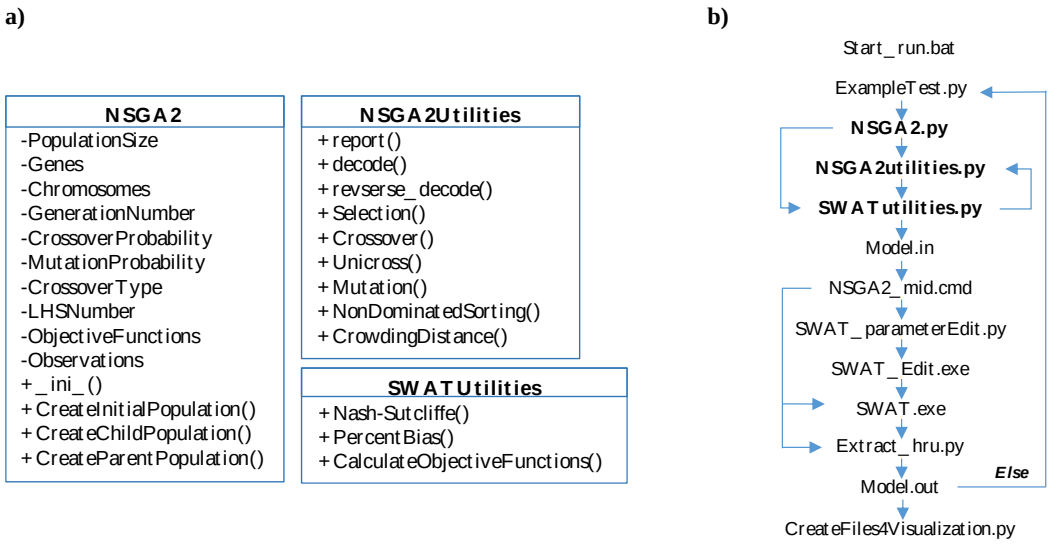

Figura B.1. a) The NSGA-II library classes design and b) Scripts and files connections process flow

The parameters selected to represent the decision variables associated with the BMPs in this study and their acceptable ranges and replacement operations must be defined in the `nsga2_par.def` file. For our study, we have three `nsga2_par.def` files that each corresponds to the optimization problem for each of the land-cover under study (kikuyu grass-PASM, potato-POTA, and tree tomato-TOMA) (Figure B.2). This file's structure must contain as a first letter before the parameter name indicates the adjusted method to use for changing the value of the parameter. The letter **v** represents replacing the current parameter value and **r** are multiplying (1 + a given value) to the current parameter value. The parameter constraints, the file extension, and the minimum and maximum value in which the parameter can change must be defined. The settings parameters for the NSGA-II algorithm must set in the `nsga2_par.def` file. The SURF[2] research cloud service was used to build our virtual research environment.

[2] SURF is the collaborative organization for ICT in Dutch education and research. https://www.surf.nl/en.

```
Method  Name  Constraint       File    Land-cover   Range
    r___FRT_KG{[],3,FERT_ID=55}.mgt_______PASM    -0.5   0
    v___TILL_ID{[],1,6}.mgt_______________PASM       2   5
    v___FILTER_RATIO{[],[],[],4}.ops______PASM      30   60
    r___BIO_EAT{[],9}.mgt_________________PASM    -0.3   0
```

```
Method  Name  Constraint       File    Land-cover   Range
    r___FRT_KG{1,3,FERT_ID=21}.mgt________POTA    -0.5   0
    v___TILL_ID{[],1,6}.mgt_______________POTA       2   5
    v___CONT_P{[],[],[],3}.ops____________POTA     0.6   0.9
    r___CONT_CN{[],[],[],3}.ops___________POTA    -0.1   0
```

```
Method  Name  Constraint       File    Land-cover   Range
    r___FRT_KG{1,3,FERT_ID=23}.mgt________TOMA    -0.5   0
    v___TILL_ID{[],1,6}.mgt_______________TOMA       2   5
    v___CONT_P{[],[],[],3}.ops____________TOMA     0.6   0.9
    r___CONT_CN{[],[],[],3}.ops___________TOMA    -0.1   0
```

Figure B.2. Structure of the optimization parameters (decision variable) to be edited and changed using the NSGA-II/SWAT library for the test case SWAT model.

REFERENCES

Abbaspour, K.C., Rouholahnejad, E., Vaghefi, S., Srinivasan, R., Yang, H., Kløve, B., 2015. A continental-scale hydrology and water quality model for Europe: Calibration and uncertainty of a high-resolution large-scale SWAT model. J. Hydrol. 524, 733–752. https://doi.org/10.1016/j.jhydrol.2015.03.027

Akhavan, S., Abedi-Koupai, J., Mousavi, S.F., Afyuni, M., Eslamian, S.S., Abbaspour, K.C., 2010. Application of SWAT model to investigate nitrate leaching in Hamadan-Bahar Watershed, Iran. Agric. Ecosyst. Environ. 139, 675–688. https://doi.org/10.1016/j.agee.2010.10.015

Alexandratos, N., Bruinsma, J., 2012. World agriculture towards 2030/2050. Land use policy 20, 375. https://doi.org/10.1016/S0264-8377(03)00047-4

Amaranto, A., Munoz-Arriola, F., Solomatine, D.P., Corzo, G., 2019. A Spatially Enhanced Data-Driven Multimodel to Improve Semiseasonal Groundwater Forecasts in the High Plains Aquifer, USA. Water Resour. Res. https://doi.org/10.1029/2018WR024301

Amon-Armah, F., Yiridoe, E.K., Ahmad, N.H.M., Hebb, D., Jamieson, R., Burton, D., Madani, A., 2013. Effect of nutrient management planning on crop yield, nitrate leaching and sediment loading in thomas brook watershed. Environ. Manage. 52, 1177–1191. https://doi.org/10.1007/s00267-013-0148-z

Arnold, .J.G., Srinivasan, R., Muttiah, R.S., Williams, J.R., 1998. Large area hydrologic modeling and assessment part I: Model development. JAWRA J. Am. Water Resour. Assoc. 34, 73–83. https://doi.org/10.1111/j.1752-1688.1998.tb05962.x

Arnold, J.G., Allen, P.M., 1999. Automated methods for estimating baseflow and ground water recharge from streamflow records 1. JAWRA J. Am. Water Resour. Assoc. 35, 411–424.

Arnold, J.G., Allen, P.M., Muttiah, R., Bernhardt, G., 1995. Automated base flow separation and recession analysis techniques. Groundwater 33, 1010–1018.

Arnold, J.G., Moriasi, D.N., Gassman, P.W., Abbaspour, K.C., White, M.J., Srinivasan, R., Santhi, C., Harmel, R.D., Griensven, a. Van, VanLiew, M.W., Kannan, N., Jha, M.K., 2012a. Swat: Model Use, Calibration, and Validation. Asabe. https://doi.org/ISSN 2151-0032

Arnold, J.G., Moriasi, D.N., Gassman, P.W., Abbaspour, K.C., White, M.J., Srinivasan, R., Santhi, C., Harmel, R.D., Griensven, A. Van, VanLiew, M.W., Kannan, N., Jha, M.K., 2012b. Swat: Model Use, Calibration, and Validation. Asabe 55, 1491–1508. https://doi.org/ISSN 2151-0032

Babbar-sebens, M., Minsker, B., 2010. Environmental Modelling & Software A Case-Based Micro Interactive Genetic Algorithm (CBMIGA) for interactive learning and search : Methodology and application to groundwater monitoring design. Environ. Model. Softw. 25, 1176–1187. https://doi.org/10.1016/j.envsoft.2010.03.027

Babbar-sebens, M., Minsker, B.S., 2012. Interactive Genetic Algorithm with Mixed

Initiative Interaction for multi-criteria ground water monitoring design. Appl. Soft Comput. J. 12, 182–195. https://doi.org/10.1016/j.asoc.2011.08.054

Babbar-Sebens, M., Mukhopadhyay, S., Singh, V.B., Piemonti, A.D., 2015. A web-based software tool for participatory optimization of conservation practices in watersheds. Environ. Model. Softw. 69, 111–127. https://doi.org/10.1016/j.envsoft.2015.03.011

Barton, R.R., 2009. Simulation optimization using metamodels, in: IEEE (Ed.), Winter Simulation Conference (WSC). pp. 230–238.

Betrie, G.D., Mohamed, Y.A., Van Griensven, A., Srinivasan, R., 2011. Sediment management modelling in the Blue Nile Basin using SWAT model. Hydrol. Earth Syst. Sci. 15, 807–818. https://doi.org/10.5194/hess-15-807-2011

Blanco, H., Lal, R., 2008. Principles of soil conservation and management. Springer Science & Business Media, New York. https://doi.org/10.1007/978-1-4020-8709-7

Bosch, N.S., Allan, J.D., Selegean, J.P., Scavia, D., 2013. Scenario-testing of agricultural best management practices in Lake Erie watersheds. J. Great Lakes Res. 39, 429–436. https://doi.org/10.1016/j.jglr.2013.06.004

Boussaïd, I., Lepagnot, J., Siarry, P., 2013. A survey on optimization metaheuristics. Inf. Sci. (Ny). 237, 82–117. https://doi.org/10.1016/j.ins.2013.02.041

Broom, D.M., Galindo, F.A., Murgueitio, E., 2013. Sustainable , efficient livestock production with high biodiversity and good welfare for animals. Proc. R. Soc. Biol. Sci. 280, 2013–2025.

CAR, C. autónoma R. de C., 2006. Diagnóstico prospectiva y formulación de la cuenca hidrográfica de los ríos Ubaté y Suárez. Bogota.

Carter, M.R., 1992. Influence of reduced tillage systems on organic matter, microbial biomass, macro-aggregate distribution and structural stability of the surface soil in a humid climate. Soil Tillage Res. 23, 361–372. https://doi.org/10.1016/0167-1987(92)90081-L

Carter, M.R., Noronha, C., Peters, R.D., Kimpinski, J., 2009. Influence of conservation tillage and crop rotation on the resilience of an intensive long-term potato cropping system: Restoration of soil biological properties after the potato phase. Agric. Ecosyst. Environ. 133, 32–39. https://doi.org/10.1016/j.agee.2009.04.017

Carter, M.R., Sanderson, J.B., 2001. Influence of conservation tillage and rotation length on potato productivity, tuber disease and soil quality parameters on a fine sandy loam in eastern Canada. Soil Tillage Res. 63, 1–13. https://doi.org/10.1016/S0167-1987(01)00224-0

Chaubey, I., Chiang, L., Gitau, M.W., Mohamed, S., 2010. Effectiveness of best management practices in improving water quality in a pasture-dominated watershed. J. Soil Water Conserv. 65, 424–437. https://doi.org/10.2489/jswc.65.6.424

Cho, J., Her, Y., Bosch, D., 2017. Sensitivity of Simulated Conservation Practice Effectiveness to Representation of Field and In-Stream Processes in the Little River Watershed. Environ. Model. Assess. 22, 159–173. https://doi.org/10.1007/s10666-016-9530-6

CORANTIOQUIA, C.A.R. del C. de A., UNAL, U.N. de C.S.M., 2015. Actualización y

ajuste Plan de Ordenación y Manejo de la Cuenca de los Ríos Grande y Chico. Medellin.

Correa, C.H.J., Pabón, R.M.L., Carulla, F.J.E., 2008. Valor nutricional del pasto kikuyu (Pennisetum clandestinum Hoechst Ex Chiov.) para la producción de leche en Colombia (Una revisión): I - Composición química y digestibilidad ruminal y posruminal. Livest. Res. Rural Dev. 20.

Cristiano, E., ten Veldhuis, M. C., & Van De Giesen, N. (2017). Spatial and temporal variability of rainfall and their effects on hydrological response in urban areas–a review. Hydrology and Earth System Sciences, 21(7), 3859-3878.

Daggupati, P., Yen, H., White, M.J., Srinivasan, R., Arnold, J.G., Keitzer, C.S., Sowa, S.P., 2015. Impact of model development, calibration and validation decisions on hydrological simulations in West Lake Erie Basin. Hydrol. Process. 29, 5307–5320. https://doi.org/10.1002/hyp.10536

Dai, C., Qin, X.S., Tan, Q., Guo, H.C., 2018. Optimizing best management practices for nutrient pollution control in a lake watershed under uncertainty. Ecol. Indic. 92, 288–300. https://doi.org/10.1016/j.ecolind.2017.05.016

Deb, K., Pratap, A., Agarwal, S., Meyarivan, T., 2002. A fast and elitist multiobjective genetic algorithm: NSGA-II. IEEE Trans. Evol. Comput. 6, 182–197. https://doi.org/10.1109/4235.996017

Dechmi, F., Skhiri, A., 2013. Evaluation of best management practices under intensive irrigation using SWAT model. Agric. Water Manag. 123, 55–64. https://doi.org/10.1016/j.agwat.2013.03.016

Derpsch, R., 2003. Conservation Tillage, No-Tillage and Related Technologies BT - Conservation Agriculture: Environment, Farmers Experiences, Innovations, Socio-economy, Policy, in: García-Torres, L., Benites, J., Martínez-Vilela, A., Holgado-Cabrera, A. (Eds.), . Springer Netherlands, Dordrecht, pp. 181–190. https://doi.org/10.1007/978-94-017-1143-2_23

Deubel, A., Hofmann, B., Orzessek, D., 2011. Soil & Tillage Research Long-term effects of tillage on stratification and plant availability of phosphate and potassium in a loess chernozem. Soil Tillage Res. 117, 85–92. https://doi.org/10.1016/j.still.2011.09.001

Diaz, V., Corzo Perez, G.A., Van Lanen, H.A.J., Solomatine, D., Varouchakis, E.A., 2019. Characterisation of the dynamics of past droughts. Sci. Total Environ. https://doi.org/10.1016/j.scitotenv.2019.134588

Doody, D.G., Archbold, M., Foy, R.H., Flynn, R., 2012. Approaches to the implementation of the Water Framework Directive: Targeting mitigation measures at critical source areas of diffuse phosphorus in Irish catchments. J. Environ. Manage. 93, 225–234. https://doi.org/10.1016/j.jenvman.2011.09.002

Ercan, M.B., Goodall, J.L., 2016. Design and implementation of a general software library for using NSGA-II with SWAT for multi-objective model calibration. Environ. Model. Softw. 84, 112–120. https://doi.org/10.1016/j.envsoft.2016.06.017

FAO, 2000. Manejo del suelo en pequeñas fincas. Estrategias y métodos de introducción, tecnologías y equipos. Boletín de Tierras y Aguas de la FAO 8, Roma.

FAO, MADS, 2018. Guía de buenas prácticas para la gestión y uso sostenible de los

suelos en áreas rurales. Bogotá, D.C.

FEDEGAN, SENA, 2013. Costos modales en ganadería de leche, Trópico alto de Colombia: Ventana a la competitividad ganadera. Bogotá, D.C.

Feng, Q., Chaubey, I., Engel, B., Cibin, R., Sudheer, K.P., Volenec, J., 2017. Marginal land suitability for switchgrass, Miscanthus and hybrid poplar in the Upper Mississippi River Basin (UMRB). Environ. Model. Softw. 93, 356–365. https://doi.org/10.1016/j.envsoft.2017.03.027

Fiener, P., Auerswald, K., Van Oost, K., 2011. Spatio-temporal patterns in land use and management affecting surface runoff response of agricultural catchments-A review. Earth-Science Rev. 106, 92–104. https://doi.org/10.1016/j.earscirev.2011.01.004

Food and Agriculture Organization (FAO), 2000. Manual de prácticas integradas de manejo y conservación de suelos. Boletín Tie- rras y Aguas la FAO 8.

Francesconi, W., Srinivasan, R., Pérez-Miñana, E., Willcock, S.P., Quintero, M., 2016. Using the Soil and Water Assessment Tool (SWAT) to model ecosystem services: A systematic review. J. Hydrol. 535, 625–636. https://doi.org/10.1016/j.jhydrol.2016.01.034

García, M., Treto, E., Alvarez, M., 2000. Los abonos verdes: una alternativa para la economía del nitrógeno en el cultivo de la papa. I. Estudio comparativo de diferentes especies. Cultiv. Trop. 21, 5–11.

Gariz, A.Z., Talebi, A., 2016. Identification of critical sediment source areas across the Gharesou watershed , Northeastern Iran , using hydrological modeling. Environ. Resour. Res. 4, 1–26.

Gassman, P.P.W., Reyes, M.M.R., Green, C.C.H., Arnold, J.J.G., 2007. The Soil and Water Assessment Tool : historical development, applications, and future research directions. Trans. ASAE 50, 1211–1250. https://doi.org/10.1.1.88.6554

Geng, R., Sharpley, A.N., 2019. A novel spatial optimization model for achieve the trad-offs placement of best management practices for agricultural non-point source pollution control at multi-spatial scales. J. Clean. Prod. 234, 1023–1032. https://doi.org/10.1016/j.jclepro.2019.06.277

Geng, R., Yin, P., Sharpley, A.N., 2019. A coupled model system to optimize the best management practices for nonpoint source pollution control. J. Clean. Prod. 220, 581–592. https://doi.org/10.1016/j.jclepro.2019.02.127

Ghebremichael, L.T., Veith, T.L., Hamlett, J.M., 2013. Integrated watershed- and farm-scale modeling framework for targeting critical source areas while maintaining farm economic viability. J. Environ. Manage. 114, 381–394. https://doi.org/10.1016/j.jenvman.2012.10.034

Ghebremichael, L.T., Veith, T.L., Watzin, M.C., 2010. Determination of critical source areas for phosphorus loss: Lake Champlain basin, Vermont. Am. Soc. Agric. Biol. Eng. 53, 1595–1604.

Giri, S., Nejadhashemi, A.P., Woznicki, S., Zhang, Z., 2014. Analysis of best management practice effectiveness and spatiotemporal variability based on different targeting strategies. Hydrol. Process. 28, 431–445. https://doi.org/10.1002/hyp.9577

Giri, S., Nejadhashemi, A.P., Woznicki, S.A., 2012. Evaluation of targeting methods for implementation of best management practices in the Saginaw River Watershed. J. Environ. Manage. 103, 24–40. https://doi.org/10.1016/j.jenvman.2012.02.033

Giri, S., Qiu, Z., 2016. Understanding the relationship of land uses and water quality in Twenty First Century: A review. J. Environ. Manage. 173, 41–48. https://doi.org/10.1016/j.jenvman.2016.02.029

González-castillo, J.C., Hahn von-Hessberg, C.M., Narváez-solarte, W., 2014. Botanical characteristics of Tithonia diversifolia (Asterales: Asteraceae) and its use in animal diet. Bol. Cient. Mus. Hist. Nat. U. Caldas 18, 45–58.

Green, C.H., van Griensven, A., 2008. Autocalibration in hydrologic modeling: Using SWAT2005 in small-scale watersheds. Environ. Model. Softw. 23, 422–434. https://doi.org/10.1016/j.envsoft.2007.06.002

Guerrero, R., 1998. Fertilización de cultivos en clima frío. Monómeros Colombo Venezolanos S.A. (E.M.A.), Bogotá, D.C.

Guse, B., Pfannerstill, M., Gafurov, A., Fohrer, N., Gupta, H., 2016. Demasking the integrated information of discharge: Advancing sensitivity analysis to consider different hydrological components and their rates of change. Water Resour. Res. 52, 8724–8743. https://doi.org/10.1002/2016WR018894

Gutteridge, R.C., Shelton, H.M., 1994. The role of forage tree legumes in cropping and grazing systems. FAO 1–7.

Haghnegahdar, A., Razavi, S., 2017. Insights into sensitivity analysis of Earth and environmental systems models: On the impact of parameter perturbation scale. Environ. Model. Softw. 95, 115–131. https://doi.org/10.1016/j.envsoft.2017.03.031

Hanifzadeh, M., Nabati, Z., Longka, P., Malakul, P., Apul, D., Kim, D.S., 2017. Life cycle assessment of superheated steam drying technology as a novel cow manure management method. J. Environ. Manage. 199, 83–90. https://doi.org/10.1016/j.jenvman.2017.05.018

Hanigan, M.D., 2005. Quantitative aspects of ruminant predicting animal performance. Anim. Sci. 80, 23–32. https://doi.org/10.1079/asc40920023

Hargreaves, G.H., Samani, Z.A., 1985. Reference crop evapotranspiration from temperature. Appl. Eng. Agric. 1, 96–99.

Harmel, R.D., Smith, P.K., Migliaccio, K.W., Chaubey, I., Douglas-Mankin, K.R., Benham, B., Shukla, S., Muñoz-Carpena, R., Robson, B.J., 2014. Evaluating, interpreting, and communicating performance of hydrologic/water quality models considering intended use: A review and recommendations. Environ. Model. Softw. 57, 40–51. https://doi.org/10.1016/j.envsoft.2014.02.013

Hart, S.C., Stark, J.M., Davidson, E.A., Firestone, M.K., 1994. Nitrogen mineralization, immobilization, and nitrification. Methods of Soil Analysis: Part 2 -Microbiological and Biochemical Properties:985-1018., Soil Science Society of America.

Hopkins, B., Horneck, D., Pavek, M., 2007. Evaluation of potato production best management practices. … J. Potato … 19–27.

Huang, J., Huang, Y., Pontius, R.G., Zhang, Z., 2015. Geographically weighted

regression to measure spatial variations in correlations between water pollution versus land use in a coastal watershed. Ocean Coast. Manag. 103, 14–24. https://doi.org/10.1016/j.ocecoaman.2014.10.007

IDEAM, 2004. Climatic Data. Tausa municipality Station. Instituto de Hidrología Meteorología y Estudios Ambientales. Bogota.

IDEAM, IGAC, CORMAGDALENA, 2008. Mapa de Cobertura de la Tierra Cuenca Magdalena-Cauca: Metodología CORINE Land Cover adaptada para Colombia a escala 1:100.000. Instituto de Hidrología, Meteorología y Estudios Ambientales, Instituto Geográfico Agustín Codazzi y Corporación Autónoma Regio. Bogotá, D.C.

IGAC, I.G.A.C., 2000. "Estudio General de Suelos y Zonificación de Tierras del Departamento de Cundinamarca." Bogota.

INSPIA, 2015. European index for sustainable productive agriculture - INSPIA.

Japanese International Cooperation Agency—JICA, 2000. "Estudio Sobre Plan de Mejoramiento Ambiental Regional Para la Cuenca de la Laguna de Fuquene."

Jeon, D.J., Ki, S.J., Cha, Y.K., Park, Y., Kim, J.H., 2018. New methodology of evaluation of best management practices performances for an agricultural watershed according to the climate change scenarios: A hybrid use of deterministic and decision support models. Ecol. Eng. 119, 73–83. https://doi.org/10.1016/j.ecoleng.2018.05.006

Karamouz, M., Taheriyoun, M., Baghvand, A., Tavakolifar, H., Emami, F., 2010. Optimization of watershed control strategies for reservoir eutrophication management. J. Irrig. Drain. Eng. 136, 847–861. https://doi.org/10.1061/(ASCE)IR.1943-4774.0000261

Khorashadi Zadeh, F., Nossent, J., Sarrazin, F., Pianosi, F., van Griensven, A., Wagener, T., Bauwens, W., 2017. Comparison of variance-based and moment-independent global sensitivity analysis approaches by application to the SWAT model. Environ. Model. Softw. 91, 210–222. https://doi.org/10.1016/j.envsoft.2017.02.001

Lam, Q.D., Schmalz, B., Fohrer, N., 2011. The impact of agricultural Best Management Practices on water quality in a North German lowland catchment. Environ. Monit. Assess. 183, 351–379. https://doi.org/10.1007/s10661-011-1926-9

Lapierre, H., Berthiaume, R., Raggio, G., Thivierge, M.C., Doepel, L., Pacheco, D., Dubreuil, P., Lobley, G.E., 2005. The route of absorbed nitrogen into milk protein. Anim. Sci. 80, 11–22. https://doi.org/10.1079/asc41330011

Laverde-Barajas, M., Corzo, G., Bhattacharya, B., Uijlenhoet, R., Solomatine, D.P., 2019. Spatiotemporal Analysis of Extreme Rainfall Events Using an Object-Based Approach, in: Spatiotemporal Analysis of Extreme Hydrological Events. https://doi.org/10.1016/b978-0-12-811689-0.00005-7

Lehmann, N., Finger, R., Klein, T., Calanca, P., Walter, A., 2013. Adapting crop management practices to climate change: Modeling optimal solutions at the field scale. Agric. Syst. 117, 55–65. https://doi.org/10.1016/j.agsy.2012.12.011

Lescot, J.M., Bordenave, P., Petit, K., Leccia, O., 2013. A spatially-distributed cost-effectiveness analysis framework for controlling water pollution. Environ. Model. Softw. 41, 107–122. https://doi.org/10.1016/j.envsoft.2012.10.008

Li, H., Perez, G.A.C., Martinez, C.A., Mynett, A.E., 2013. Self-learning cellular automata for forecasting precipitation from radar images. J. Hydrol. Eng. https://doi.org/10.1061/(ASCE)HE.1943-5584.0000646

Liu, Y., Guo, T., Wang, R., Engel, B.A., Flanagan, D.C., Li, S., Pijanowski, B.C., Collingsworth, P.D., Lee, J.G., Wallace, C.W., 2019. A SWAT-based optimization tool for obtaining cost-effective strategies for agricultural conservation practice implementation at watershed scales. Sci. Total Environ. 691, 685–696. https://doi.org/10.1016/j.scitotenv.2019.07.175

Liu, Y., Shen, H., Yang, W., Yang, J., 2013. Optimization of Agricultural BMPs Using a Parallel Computing Based Multi-Objective Optimization Algorithm 1, 39–50.

Logan, T.J., 1993. Agricultural best management practices for water pollution control: current issues. Agric. Ecosyst. Environ. 46, 223–231. https://doi.org/10.1016/0167-8809(93)90026-L

Maharjan, G.R., Prescher, A.K., Nendel, C., Ewert, F., Mboh, C.M., Gaiser, T., Seidel, S.J., 2018. Approaches to model the impact of tillage implements on soil physical and nutrient properties in different agro-ecosystem models. Soil Tillage Res. 180, 210–221. https://doi.org/10.1016/j.still.2018.03.009

Mahecha, L., Escobar, J.P., Suárez, J.F., Restrepo, L.F., 2007. Tithonia diversifolia (hemsl.) Gray (botón de oro) como suplemento forrajero de vacas F1 (Holstein por Cebú). Livest. Res. Rural Dev. 19.

Maringanti, C., Chaubey, I., Arabi, M., Engel, B., 2011. Application of a multi-objective optimization method to provide least cost alternatives for NPS pollution control. Environ. Manage. 48, 448–461. https://doi.org/10.1007/s00267-011-9696-2

Maringanti, C., Chaubey, I., Popp, J., 2009. Development of a multiobjective optimization tool for the selection and placement of best management practices for nonpoint source pollution control. Water Resour. Res. 45. https://doi.org/10.1029/2008WR007094

Me, W., Abell, J.M., Hamilton, D.P., 2015. Effects of hydrologic conditions on SWAT model performance and parameter sensitivity for a small, mixed land use catchment in New Zealand. Hydrol. Earth Syst. Sci. 19, 4127–4147. https://doi.org/10.5194/hess-19-4127-2015

Mejia-Diaz, E., Mahecha-Ledesma, L., Angulo-Arizala, J., 2017. Consumo de materia seca en un sistema silvopastoril de Tithonia diversifolia en trópico alto. Agron. Mesoam. 28, 389–403. https://doi.org/10.15517/ma.v28i2.23561

Mejía-Díaz, E., Mahecha-ledesma, L., Angulo-Arizala, J., 2017. Tithonia diversifolia : especie para ramoneo en sistemas silvopastoriles y Tithonia diversifolia : specie for grazing in silvopastoral systems and methods for estimating consumption. Agron. Mesoam. 28, 289–302. https://doi.org/10.15517/am.v28i1.22673

Memmah, M.M., Lescourret, F., Yao, X., Lavigne, C., 2015. Metaheuristics for agricultural land use optimization. A review. Agron. Sustain. Dev. https://doi.org/10.1007/s13593-015-0303-4

Mendoza, G., Jeuken, A., Matthews, J. H., Stakhiv, E., Kucharski, J., & Gilroy, K. (2018). *Climate risk informed decision analysis (CRIDA): Collaborative water*

resources planning for an uncertain future. UNESCO Publishing.

Menzel, R.G., 1980. Enrichment ratios for water quality modeling. CREAMS: A Field-Scale Model for Chemicals, Runoff, and Erosion from Agricultural Management Systems.

Moriasi, D.N., Arnold, J.G., Van Liew, M.W., Bingner, R.L., Harmel, R.D., Veith, T.L., 2007. Model Evaluation Guidelines for Systematic Quantification of Accuracy in Watershed Simulations. Trans. ASABE 50, 885–900. https://doi.org/10.13031/2013.23153

Moriasi, D.N., Gitau, M.W., Pai, N., Daggupati, P., 2015. Hydrologic and water quality models: Performance measures and evaluation criteria. Trans. ASABE 58, 1763–1785. https://doi.org/10.13031/trans.58.10715

Morris, M.D., 1991. Factorial Sampling Plans for Prelim inary Computational Experiments. Am. Stat. Assoc. 33, 161–174.

Murgueitio, E., 2005. Silvopastoral systems in the neotropics, in: Mosquera, M.R., McAdam, J., Rigueiro, A. (Eds.), International Silvopastoral and Sustainable Land Management. CAB, Lugo, Spain, pp. 24–29.

Murgueitio, E., Barahona, R., Flores, M., Chará, J., Rivera, J., 2016. Es Posible Enfrentar el Cambio Climático y Producir más Leche y Carne con Sistemas Silvopastoriles Intensivos. Ceiba 54, 23–30. https://doi.org/10.5377/ceiba.v54i1.2774

Nair, S.S., King, K.W., Witter, J.D., Sohngen, B.L., Fausey, N.R., 2011. Importance of Crop Yield in Calibarting Watershed Water Quality Simulation Tools. J. Amercian Water Resour. Assoc. 47, 1285–1297. https://doi.org/10.1111/j.1752-1688.2011.00570.x

Nash, J.E., Sutcliffe, J. V, 1970. River Flow Forecasting Through Conceptual Models Part I-a Discussion of Principles*. J. Hydrol. 10, 282–290. https://doi.org/10.1016/0022-1694(70)90255-6

Nayeb Yazdi, M., Ketabchy, M., Sample, D.J., Scott, D., Liao, H., 2019. An evaluation of HSPF and SWMM for simulating streamflow regimes in an urban watershed. Environ. Model. Softw. 118, 211–225. https://doi.org/10.1016/j.envsoft.2019.05.008

Neitsch, S.., Arnold, J.., Kiniry, J.., Williams, J.., 2011. Soil & Water Assessment Tool Theoretical Documentation Version 2009. Texas Water Resour. Inst. 1–647. https://doi.org/10.1016/j.scitotenv.2015.11.063

Nielsen, A.H., Kristensen, I.S., 2005. Nitrogen and phosphorus surpluses on Danish dairy and pig farms in relation to farm characteristics. Livest. Prod. Sci. 96, 97–107. https://doi.org/10.1016/j.livprodsci.2005.05.012

Ólafsson, S., 2006. Chapter 21 Metaheuristics. Handbooks Oper. Res. Manag. Sci. 13, 633–654. https://doi.org/10.1016/S0927-0507(06)13021-2

Organización de las Naciones Unidas para la Alimentación y la Agricultura (FAO), Ministerio de Ambiente y Desarrollo Sostenible (MADS), 2018. Guía de buenas prácticas para la gestión y uso sostenible de los suelos en áreas rurales. Bogotá, D.C.

Osorio, J.D., Uribe, N., García-tavera, L.M., Bustamante, A.E., 2019. Optimización de uso del suelo acorde con restricciones ambientales y sociales : caso cuenca de

Riogrande II. Semest. Económico 22, 19–48.

Panagopoulos, Y., Makropoulos, C., Mimikou, M., 2013. Multi-objective optimization for diffuse pollution control at zero cost. Soil Use Manag. 29, 83–93. https://doi.org/10.1111/sum.12012

Panagopoulos, Y., Makropoulos, C., Mimikou, M., 2011. Reducing surface water pollution through the assessment of the cost-effectiveness of BMPs at different spatial scales. J. Environ. Manage. 92, 2823–2835. https://doi.org/10.1016/j.jenvman.2011.06.035

Park, J.Y., Yu, Y.S., Hwang, S.J., Kim, C., Kim, S.J., 2014. SWAT modeling of best management practices for Chungju dam watershed in South Korea under future climate change scenarios. Paddy Water Environ. 12, 65–75. https://doi.org/10.1007/s10333-014-0424-4

Piemonti, A. D., Babbar-Sebens, M., & Jane Luzar, E. (2013). Optimizing conservation practices in watersheds: Do community preferences matter?. Water Resources Research, 49(10), 6425-6449.

Portafolio, 2014. La papa vive su mejor época gracias a los precios.

Poveda, G., Jaramillo, L., Vallejo, L.F., 2014. Seasonal precipitation patterns along pathways of South American low-level jets and aerial rivers. Water Resour. Res. 50, 98–118. https://doi.org/10.1002/2013WR014087

Qin, C.Z., Gao, H.R., Zhu, L.J., Zhu, A.X., Liu, J.Z., Wu, H., 2018. Spatial optimization of watershed best management practices based on slope position units. J. Soil Water Conserv. 73, 504–517. https://doi.org/10.2489/jswc.73.5.504

Quintero, M., 2014. Mixed crop-livestock systems and conservation tillage: Farm profitability, adoption potential, and environmental impacts. University of Florida.

Quintero, M., 2009. Effects of conservation tillage in soil carbon sequestration and net revenues of potato-based rotations in the Colombian Andes.

Quintero, M., Comerford, N., 2013. Effects of conservation tillage on total and aggregated soil organic carbon in the Andes. Open J. Soil Sci. 2013, 361–373. https://doi.org/http://dx.doi.org/10.4236/OJSS.2013.38042

Quintero, M., Otero, W., 2006. Mecanismo de financiación para promover Agricultura de Conserva- ción con pequeños productores de la cuenca de la laguna de Fúquene. Su diseño, aplicación y beneficios.

Rabotyagov, S., Campbell, T., Valcu, A., Gassman, P., Jha, M., Schilling, K., Wolter, C., Kling, C., 2012. Spatial Multiobjective Optimization of Agricultural Conservation Practices using a SWAT Model and an Evolutionary Algorithm. J. Vis. Exp. 1–11. https://doi.org/10.3791/4009

Ram, G., Prescher, A., Nendel, C., Ewert, F., Miltin, C., Gaiser, T., Seidel, S.J., 2018. Soil & Tillage Research Approaches to model the impact of tillage implements on soil physical and nutrient properties in di ff erent agro-ecosystem models. Soil Tillage Res. 180, 210–221. https://doi.org/10.1016/j.still.2018.03.009

Ramírez-Restrepo, J.J., Meneses-S., V., Vergara-C., A., 2015. Estudio autecológico de schroederia setigera en el embalse tropical Riogrande II, Antioquia, Colombia.

Caldasia 37, 359–379. https://doi.org/10.15446/caldasia.v37n2.53558

Ramírez, C.D., 2014. Determinantes Espacialmente Explícitos de Transiciones en Coberturas Terrestres con Significativo Impacto para la Provisión de Servicios Ecosistémicos: Análisis Temporal y Espacial, 1986-2012 Master thesis in Environment and Development. Universidad Nacional de Colombia, Sede Medellin.

Rasouli, S., Whalen, J.K., Madramootoo, C.A., 2014. Review : Reducing residual soil nitrogen losses from agroecosystems for surface water protection in Quebec and Ontario , Canada : Best management practices , policies and perspectives. Can. J. Soil Sci. 94, 109–127. https://doi.org/10.4141/CJSS2013-015

Restrepo, E.M., Rosales, R.B., Xochilt, M., Estrada, F., David, J., Orozco, C., Rivera, E., 2016. Es Posible Enfrentar el Cambio Climático y Producir más Leche y Carne con Sistemas Silvopastoriles Intensivos. Ceiba 54, 23–30. https://doi.org/10.5377/ceiba.v54i1.2774

Ritchie, J.T., 1972. Model for predicting evaporation from a row crop with incomplete cover. Water Resour. Res. 8, 1204–1213. https://doi.org/10.1029/WR008i005p01204

Ritter, W.F., Shirmohammadi, A., 2001. Agricultural Nonpoint Source Pollution, 2001 by CR. ed, Agricultural nonpoint source pollution : watershed management and hydrology.

Roberts, T.L., 2007. Right product, right rate, right time and right place ... the foundation of best management practices for fertilizer, Fertilizer Best Management Practies. General Principles, Strategy for their Adoption and Voluntary Initiatives vs Regulations.

Rodriguez, G., Soto, G., 1999. Fertilizacion de hortalizas orgánicas, in: Xl Congreso Nacional Agronómico / III Congreso Nacional de Suelos 1999. pp. 267–275.

Romagnoli, M., Portapila, M., Rigalli, A., Maydana, G., Burgués, M., García, C.M., 2017. Assessment of the SWAT model to simulate a watershed with limited available data in the Pampas region, Argentina. Sci. Total Environ. 596–597, 437–450. https://doi.org/10.1016/j.scitotenv.2017.01.041

Rubiano, J., Quintero, M., Estrada, R.D., Moreno, A., 2006a. Multiscale analysis for promoting integrated watershed management. Water Int. 31, 398–411. https://doi.org/10.1080/02508060608691941

Rubiano, J., Soto, V., Suárez, L.A., Girón, E., Pernett, X., 2006b. Identifying the sources of nitrate and phosphate contamination in Lake Fuquene using natural stable isotopes, Springs.

Salazar, A., 2016. Ordenación de la cuenca Río Ubaté-Laguna de Fúquene en Colombia. Universitat Politécnica de Valéncia.

Sarkar, S., Pressey, R.L., Faith, D.P., Margules, C.R., Fuller, T., Stoms, D.M., Moffett, A., Wilson, K.A., Williams, K.J., Williams, P.H., Andelman, S., 2006. Biodiversity conservation planning tools: Present status and challenges for the future. Annu. Rev. Ecol. Evol. Syst. 31, 123–159. https://doi.org/10.1146/annurev.energy.31.042606.085844

Sedano, K., Carvajal, Y., Ávila, Á., 2013. Variabilidad climática, cambio climático y gestión integrada del riesgo de inundaciones en Colombia. Rev. Semillas 47–53.

Shen, Z., Hou, X., Li, W., Aini, G., Chen, L., Gong, Y., 2015. Impact of landscape pattern at multiple spatial scales on water quality: A case study in a typical urbanised watershed in China. Ecol. Indic. 48, 417–427. https://doi.org/10.1016/j.ecolind.2014.08.019

Singirankabo, U. A., Ertsen, M. W., & van de Giesen, N. (2022). The relations between farmers' land tenure security and agriculture production. An assessment in the perspective of smallholder farmers in Rwanda. Land Use Policy, 118, 106122.

Sinnathamby, S., Douglas-Mankin, K.R., Craige, C., 2017. Field-scale calibration of crop-yield parameters in the Soil and Water Assessment Tool (SWAT). Agric. Water Manag. 180, 61–69. https://doi.org/10.1016/j.agwat.2016.10.024

Smarzyńska, K., Miatkowski, Z., 2016. Calibration and validation of SWAT model for estimating water balance and nitrogen losses in a small agricultural watershed in central Poland. J. Water L. Dev. 29, 31–47. https://doi.org/10.1515/jwld-2016-0010

Soane, B.D., 1990. The role of organic matter in soil compactibility: A review of some practical aspects. Soil Tillage Res. 16, 179–201. https://doi.org/10.1016/0167-1987(90)90029-D

Solomatine, D.P., Wagener, T., 2011. Hydrological Modelling, in: Elsevier (Ed.), Treatise on Water Science. pp. 435–457.

Stewart, B.A., Lal, R., 1994. Soil processes and water quality. CRC Press LLC.

Suescún, D., Villegas, J.C., León, J.D., Flórez, C.P., García-Leoz, V., Correa-Londono, G.A., 2017. Vegetation cover and rainfall seasonality impact nutrient loss via runoff and erosion in the Colombian Andes. Reg. Environ. Chang. 17, 827–839.

Tessema, S.M., Lyon, S.W., Setegn, S.G., 2014. Effects of Different Retention Parameter Estimation Methods on the Prediction of Surface Runoff Using the SCS Curve Number Method. Water Resour. Manag. 28, 3241–3254. https://doi.org/10.1007/s11269-014-0674-3

Tuppad, P., Santhi, C., Wang, X., Williams, J.R., Srinivasan, R., Gowda, P.H., 2010. Simulation of conservation practices using the APEX model. Appl. Eng. Agric. 26, 779–794.

Tuppad, P., Srinivasan, R., 2008. Bosque River Environmental Infrastructure Improvement Plan: Phase II BMP Modeling Report.

Urbano, D., 1997. Efecto de la fertilización nitrogenada sobre el rendimiento y calidad de tres gramíneas tropicales. Rev. la Fac. Agron. 14, 129–139.

Uribe, N., Corzo, G., Quintero, M., van Griensven, A., Solomatine, D., 2018. Impact of conservation tillage on nitrogen and phosphorus runoff losses in a potato crop system in Fuquene watershed, Colombia. Agric. Water Manag. 209, 62–72. https://doi.org/10.1016/j.agwat.2018.07.006

Uribe, N., Srinivasan, R., Corzo, G., Arango, D., Solomatine, D., 2020. Spatio-temporal critical source area patterns of runoff pollution from agricultural practices in the Colombian Andes. Ecol. Eng. 149, 105810. https://doi.org/10.1016/j.ecoleng.2020.105810

Van Horn, H.H., Wilkie, A.C., Powers, W.J., Nordstedt, R.A., 1994. Components of

Dairy Manure Management Systems. J. Dairy Sci. 77, 2008–2030. https://doi.org/10.3168/jds.S0022-0302(94)77147-2

Villamil, M.B., Nafziger, E.D., 2015. Geoderma Corn residue , tillage , and nitrogen rate effects on soil carbon and nutrient stocks in Illinois. Geoderma 253–254, 61–66. https://doi.org/10.1016/j.geoderma.2015.04.002

Wang, X., Zhou, B., Sun, X., Yue, Y., Ma, W., Zhao, M., 2015. Soil Tillage Management Affects Maize Grain Yield by Regulating Spatial Distribution Coordination of Roots , Soil Moisture and Nitrogen Status 1–19. https://doi.org/10.1371/journal.pone.0129231

Williams, 1995. Singh, V. P. (Ed.). (1995). Computer models of watershed hydrology (Vol. 1130). Highlands Ranch, CO: Water Resources Publications.

Winchell, M., Manager, P., Meals, D., Folle, S., Moore, J., Braun, D., Deleo, C., Budreski, K., Environmental, S., 2011. Identification of Critical Source Areas of Phosphorus Within the Vermont Sector of the Missisquoi Bay Basin. Montpelier. https://doi.org/092156-G

Yang, G., Best, E.P.H., 2015. Spatial optimization of watershed management practices for nitrogen load reduction using a modeling-optimization framework. J. Environ. Manage. 161, 252–260. https://doi.org/10.1016/j.jenvman.2015.06.052

Yazdi, M.N., Sample, D.J., Scott, D., Owen, J.S., Ketabchy, M., Alamdari, N., 2019. Water quality characterization of storm and irrigation runoff from a container nursery. Sci. Total Environ. 667, 166–178. https://doi.org/10.1016/j.scitotenv.2019.02.326

Yijie, S., Gongzhang, S., 2008. Improved NSGA-II Multi-objective Genetic Algorithm Based on Hybridization-encouraged Mechanism. Chinese J. Aeronaut. 21, 540–549. https://doi.org/10.1016/s1000-9361(08)60172-7

Yu, S., Xu, Z., Wu, W., Zuo, D., 2015. Effect of land use on the seasonal variation of streamwater quality in the Wei River basin, China. Proc. Int. Assoc. Hydrol. Sci. 368, 454–459. https://doi.org/10.5194/piahs-368-454-2015

Zebarth, B., Rosen, C., 2007. Research perspective on nitrogen BMP development for potato. Am. J. Potato Res. 3–18.

Zhai, T., Johnson, K.D., von Kiparski, G.R., Gillespie, A.R., Neary, M., Mohtar, R.H., 2006. Modeling forage growth in a Midwest USA silvopastoral system. Agrofor. Syst. 67, 243–257. https://doi.org/10.1007/s10457-005-3823-0

Zhang, S., Liu, Y., Wang, T., 2014. How land use change contributes to reducing soil erosion in the Jialing River Basin, China. Agric. Water Manag. 133, 65–73. https://doi.org/10.1016/j.agwat.2013.10.016

Zhou, P., Huang, J., Pontius, R.G., Hong, H., 2016. New insight into the correlations between land use and water quality in a coastal watershed of China: Does point source pollution weaken it? Sci. Total Environ. 543, 591–600. https://doi.org/10.1016/j.scitotenv.2015.11.063

Zhu, L.J., Qin, C.Z., Zhu, A.X., Liu, J., Wu, H., 2019. Effects of different spatial configuration units for the spatial optimization of watershed best management practice scenarios. Water (Switzerland) 11. https://doi.org/10.3390/w11020262

Zuluaga, A.F., Rivera, J.E., 2013. Los sistemas silvopastoriles (SSPi) en el trópico de

altura son una herramienta para la adaptación de la lechería al cambio climático. Infortambo Andin. 58–61.

LIST OF ACRONYMS

ACO	Ant Colony Optimization
AET	Actual evapotranspiration
Ag-BMPs	Agricultural Best Management Practices
Ag-BMPs	Agricultural best management practices
AnnAGNPS	Agricultural Nonpoint Source
ARS	Agricultural Research Service
CAR	Regional Environmental Authority of Cundinamarca
CBMIGA	Case Based Micro Interactive Genetic Algorithm
CIAT	The International Center for Tropical Agriculture
CN	Curve Number
CSAs	Critical Source Areas
CT-BMP	Conservation tillage best management practices
CY	Crop Yield
DE	Differential Evolution
DEM	Digital Elevation Model
DSS	Decision support systems
DST	Decision support tool
EAs	Evolutionary Algorithms
EAs	Evolutionary Algorithms
EPM	Medellin's Public Service Company
FAO	The Food and Agriculture Organization
GA	Genetic Algorithm
GIS	Geographic Information Systems

HRUs	Hydrological Response Units
IDEAM	Institute of Hydrology, Meteorology and Environmental Studies
IGAC	Agustin Codazzi Geographic Institute
IPCC	Intergovernmental Panel on Climate Change
IPNI	The International Plant Nutrition Institute
IT	Intensive tillage
LPUAI	Load per Unit Area Index
MAE	Mean absolute error
NO_3^-N	Nitrate-N
NPGA	Niched Pareto genetic algorithm
NPS	Non-Point Source
NR	Nitrate Reduction
NSE	Nash–Sutcliffe efficiency index
NSGA-II	Non-dominated Sorting Genetic Algorithm
PAN	Food and Nutrition National Plan
PET	Potential evapotranspiration
RMSE	Root mean square error
SI	Swarm Intelligence
SPEA 2	Strength Pareto evolutionary algorithm 2
ST-CSAs	Spatio-temporal critical source areas
SWAT	Soil and Water Assessment Tool
SWAT	Soil Water Assessment Tool
TN	Total Nitrogen
TP	Total phosphorus
USDA	United States Department of Agriculture

UT-GRA	Temporary Union of Environmental Risk Management
WEPP	Water Erosion Prediction

LIST OF TABLES

LIST OF FIGURES

ABOUT THE AUTHOR

Natalia Uribe was born in Medellin (Colombia) in June 1982. She graduated from University of Valle, in Cali, Colombia, in October 2005. She holds two MSc degrees. MSc in Environmental Science, specialization Environmental Science and Technology from UNESCO-IHE in 2015. And, MSc in Engineering, specialization in Sanitary and Environmental engineering at the University of Valle. Currently, Ms. Uribe is a PhD candidate at IHE-Delft Institute for Water Education under the Department o Delft, The Netherlands.

Personal email: nauriribera@gmail.com

Journals publications

- Uribe, N., Srinivasan, R., Corzo, G., Arango, D., & Solomatine, D. (2020) Spatio-temporal critical source areas patterns of runoff pollution from agricultural practices in the Colombian Andes., Ecological Engineering, 149, 105810. https://doi.org/10.1016/j.ecoleng.2020.105810.
- Múnera, J. D. O., Rivera, N. U., García-Tavera, L. M., & Ochoa, E. A. B. (2019) Optimización de uso del suelo acorde con restricciones ambientales y sociales: caso cuenca de Riogrande II, Semestre Económico, 22(52), 19-48. https://revistas.udem.edu.co/index.php/economico/article/view/3038.
- Uribe, N., Corzo, G., Quintero, M., van Griensven, A., & Solomatine, D. (2018) Impact of conservation tillage on nitrogen and phosphorus runoff losses in a potato crop system in Fuquene watershed, Colombia., Agricultural Water Management, 209, 62-72. https://www.sciencedirect.com/science/article/pii/S037837741831000X.
- Francesconi W., Uribe N., Valencia J., & Quintero M. (2018) Andean Hydrology. Chapter four. Modeling for Management: A Case Study of the Cañete Watershed, Peru., CRC Press. ISBN 9781498788403. https://www.crcpress.com/AndeanHydrology/Rivera-Godoy-Faundez-Saavedra/p/book/9781498788403.
- Tapasco, J., M. Quintero, N. Uribe, J. Valencia, G. Romero. (2015) Impactos Económicos del Cambio Climático en Colombia., BID Monografía No. 258, Washington D.C., https://publications.iadb.org/handle/11319/7218.
- Uribe, N., Quintero, M., & Valencia, J. (2013) Aplicación del Modelo Hidrológico SWAT (Soil and Water Assessment Tool) a la Cuenca del Río Cañete (SWAT).,

Centro Internacional de Agricultura Tropical (CIAT). 46 p., https://hdl.handle.net/10568/107463.

- Quintero, M., Estrada, RD., Burbano, J., Tapasco, J., Uribe, N., Escobar, G., Beland, Valencia, J. (2013) Panorama para la distribución de los beneficios de los servicios ambientales hidrológicos de la cuenca del río Quijos, Ecuador., CIAT Work document No. 224., http://dapa.ciat.cgiar.org/publications-2013/.
- Uribe N. (2010) Spanish version of the Soil and water assessment tool user manual SWAT 2005.

IHE DELFT
Institute for Water Education
under the auspices of UNESCO

TU Delft Delft University of Technology

In an effort to meet the global growing food demand, nutrient pollutants in runoff have also increased due to intensified agricultural practices. For this reason, stakeholders have tried to shift from conventional agricultural practices to best management practices (BMPs). However, the selection and allocation of agricultural BMPs (Ag-BMPs) at a watershed scale, in practice, is very complex. Optimization approaches for selecting and allocating Ag-BMPs have been used, with limitations on the inclusion of temporal and dynamic spatial aspects. To address this issue, the dissertation's main objective is to build a spatio-temporal multi-objective optimization modelling framework that provides new insights to improve the selection and allocation of Ag-BMPs in a watershed. To achieve the objective, the optimization framework has been developed, and it allows for incorporation of a greater number of crops and Ag-BMPs scenarios in the optimization model, as well as contemplating the space and time variations to allocate Ag-BMPs. In this framework, the SWAT hydrological model is coupled with the multi-objective optimization algorithm (NSGA-II). Minimization of nitrate (NO_3^-N) losses and maximization of crop yields at field level were the objective functions. The developed framework and experience with it on the considered case study in Latin America is seen as a useful hydroinformatics tool for supporting management decisions in agriculture.

This book is printed on paper from sustainably managed forests and controlled sources

9 789073 445482